



Kingdom of Saudi Arabia
King Abdulaziz City For
Science and Technology
General Directorate Of
Research Grants Programs

ARP-15-5

FINAL REPORT

**AN INVESTIGATION OF THE GEOPHYSICAL
AND HYDROGEOLOGICAL
CHARACTERISTICS OF THE
NORTHWESTERN PART OF AL-MADINAH
AREA (WADI MALAL)**

Dr. Omar A. Al-Harbi
Dr. Abdulrahman I. Al-Abdula'aly
Dr. Abdullah M. Al-Amri
Dr. Abdulaziz S. Al-Turbak
Dr. Kamel M. Skeikho

KING ABDULAZIZ CITY FOR SCIENCE AND TECHNOLOGY

1998G.

GDRGP@KACST.EDU.SA - بريد إلكتروني - فاكس ٤٨١٣٨٧٨ - هاتف ٤٨٨٣٥٥٥-٤٨٨٣٤٤٤ - ١١٤٤٢ - الرياض ١١٤٤٢ - ١١٤٤٢ - ١١٤٤٢

**NORTHWESTERN PART OF AL-MADINAH
AREA (WADI MALAL)**

Dr. Omar A. Al-Harbi
Dr. Abdulrahman I. Al-Abdula'aly

AR-15-05

**AN INVESTIGATION OF THE GEOPHYSICAL AND HYDRO-
GEOLOGICAL CHARACTERISTICS OF THE NORTHWESTERN
PART OF AL-MADINAH AREA (WADI MALAL)**

FINAL REPORT

(Revised)

Dr. Omar A. Al-Harbi - KACST

Dr. Abdullah M. S. Al-Amri - KSU

Dr. Abdulaziz S. Al-Turbak - KSU

Dr. Kamel M. Skeikho - KACST

Dr. Abdulrahman I. Al-Abdula'aly - KACST

**Submitted to
General Directorate of Research Grants Programs,
King Abdulaziz City for Science and Technology (KACST)**

September, 1998

TABLE OF CONTENT

ABSTRACT (ARABIC)	I
ABSTRACT (ENGLISH)	III
CHAPTER ONE: INTRODUCTION	1
CHAPTER TWO: LITERATURE REVIEW	4
2.1 Introduction	4
2.2 Geological setting of Al Madinah area	4
2.2.1 Hulayfah Group	5
2.2.2 Al Ays Group	5
2.2.3 Furayh Group	8
2.2.4 Tertiary and Quaternary Basalt	11
2.2.5 Quaternary sediments	12
2.3 Structural geology of Al Madinah area	12
2.4 Applications of resistivity methods in groundwater investigations	13
2.5 Application of remote sensing in groundwater studies	15
2.6 Hydrological, hydrogeological and water quality studies	16
CHAPTER THREE: GEOLOGY OF THE AREA	22
3.1 Introduction	22
3.2 Regional tectonism	23
3.3 Geology of down-stream area	24
3.4 Geomorphology	24
CHAPTER FOUR: DETECTION OF LINEAMENTS AND DRAINAGE SYSTEM OF WADI MALAL USING SATELLITE DATA	27
4.1 Introduction	27
4.2 Data selection	27
4.3 Digital image processing	28
4.3.1 Contrast stretch	28
4.3.2 Spatial image filtration	29
4.3.3 Principal component	29

4.3.4. Intensity Hue Saturation (IHS)	30
4.4 Interpretation of digitally enhanced outputs for groundwater study	30
4.4.1 Lineament detection	30
4.4.2 Drainage pattern	31
4.5 Recommendation	30
CHAPTER FIVE: GEOPHYSICAL SURVEYING	41
5.1 Introduction	41
5.2 Field work and data treatment	41
5.2.1 Resistivity surveying procedure	42
5.2.2 Magnetic surveying procedure	44
5.3 Data analysis and interpretation	45
5.3.1 Vertical Electrical Sounding (VES)	45
5.3.2 Horizontal Electrical Profiling (HEP)	47
5.3.3 Magnetic surveying	48
5.4 Recommendation	45
CHAPTER SIX: DRILLING AND SEDIMENTOLOGY	76
6.1 Introduction	76
6.2 Stratigraphy of wells	76
6.3 Sedimentological studies of Wadi Malal	80
6.3.1 Method	81
6.3.2 Grain size parameters	81
6.4 Conclusion	86
CHAPTER SEVEN: EVALUATION OF WATER RESOURCES	100
7.1 Surface water	101
7.1.1 Precipitation in the study area	101
7.1.2 Data on surface runoff	101
7.1.3 Wadi Mali soil physical characteristics	102
7.1.4 Flood frequency for Wadi Malal	103
7.1.5 Volume of rainfall and its contribution to groundwater recharge	105
7.2 Groundwater	105

7.2.1 Previous studies	105
7.2.2 Estimation of groundwater storage	106
7.2.3 Results of drilling samples	108
7.2.4 Discussion	109
7.3 Quality of groundwater	109
7.3.1 Samples collection	109
7.3.2 Samples analysis	109
7.3.3. Results and discussion	110
7.3.4 Suitability of Wadi Malal wells water for irrigation	112
CHAPTER EIGHT: CONCLUSION AND RECOMMENDATION	134
CHAPTER NINE: REFERENCES	137
APPENDIX 5A	143
APPENDIX 5B	200
APPENDIX 5C	215

ملخص

لقد أدى النمو الحضري السريع في منطقة المدينة المنورة إلى زيادة كبيرة في استخراج المياه الجوفية المحلية وقد أدت هذه الزيادة الكبيرة مع النقص في التغذية الطبيعية إلى هبوط مناسيب المياه وتدهور نوعيتها .

ويعتمد سكان المدينة المنورة وسكان منطقة الدراسة الواقعة بين خطي عرض ٢٤° - ٢٤° ٤٠' شمالاً وخطي طول ٣٩° و ٣٩° ٢٥' على المياه الجوفية لأغراض الشرب والزراعة ومن أهم الوديان في منطقة المدينة المنورة وادي الحمض ويمثل وادي ملل أهم روافده .

وتحتوي الصور الفضائية المأخوذة من الأقمار الصناعية على معلومات مفيدة لدراسات المياه الجوفية وقد اختيرت بعض هذه المعلومات لتحليلها لهذه الدراسة حيث تم استكمال صور لاندسات في كل فروع الدراسة أما صور سبوت فقد استعملت للتأكد من المواقع وربطها بالخرائط الأرضية . وقد تمت الاستفادة من الصور الفضائية المختلفة في دراسة طوبوغرافية منطقة الدراسة وخاصة ما يتعلق منها بتحديد مسارات الأودية الفرعية والظواهر الجيولوجية المختلفة واختيار المواقع المناسبة للدراسة الجيوفيزيائية ومواقع حفر الآبار وقد تم تحليل جميع الصور الفضائية الخاصة بالدراسة باستخدام نظم التحليل المتطورة المتوفرة لدى المركز السعودي للاستشعار عن بعد بمدينة الملك عبدالعزيز للعلوم والتقنية .

ويمكن تصنيف الصخور في منطقة وادي ملل إلى مجموعتين من الصخور :
صخور القاعدة والتي تحتوي على مجموعة العيس وفوقها مجموعة الفريخ من حقب ما قبل الكامبري وتغطي الوادي رواسب وديانية حديثة وتتراوح سماكته بين ٤٠ و ٨٠ متر وتتكون من رمال ورمال طينية وطين وبعض الحصى أما التكوين الماسني في منطقة الدراسة فهو تكوين غير محصور ويكون الوادي جاف معظم أيام السنة .

ولمعرفة الطبقات التحت سطحية بشكل مفصل في منطقة الدراسة فقد تم إجراء ٨ مقاطع جيوفيزيائية ولمعرفة تفاصيل مقاطع التكوين فقد استعملت طرق المقاومة الكهربائية (الجس الكهربائي العمودي والمقطع الأفقي) والمسح المغناطيسي لدراسة تغير المقاومة الكهربائية مع العمق عند مواقع الجسات وربط ذلك مع المعلومات الجيولوجية المتوفرة وقد بينت المعلومات الجيوفيزيائية (الكهربائية المغناطيسية) عمق صخور القاعدة ونوعية الطبقات المختلفة و إمكانية تواجد المياه الجوفية بشكل جيد في أسفل وادي ملل ، وباستعمال نتائج الدراسة الجيوفيزيائية والاستشعار عن بعد فقد اختيرت ست مواقع لحفر الآبار ، وتم تحليل ١٨٤ عينة واختيرت من أعماق مختلفة .

لقد تم استخدام طرق مختلفة لدراسة رواسب الوادي بالاعتماد على طرق إحصائية مختلفة لمعرفة متوسط حجم الحبيبات وذلك لاجل التوصل إلى خصائص الرواسب ، حيث دلت أن معظم الرواسب في المنطقة المشبعة خشنة وذات تصنيف جيد وعالية الاستدارة أما عينات الآبار فقد تم تحليلها لمعرفة الخصائص الهيدرولوجية مثل معامل النفاذية والكثافة النوعية ونسبة الفراغات ونسبة الرمل والطين والطيني في كل عينة حيث يتبين أن قيمة الكثافة النوعية ثابتة تقريبا أما العوامل الأخرى فتتغير حسب نوع التربة .

وقد جمعت المعلومات المناخية عن مناطق الدراسة من وزارة الزراعة والمياه حيث توجد ثلاث محطات لقياس السيول وهي المحطات M401 , M402 , M403 وتعطي كل منها معدل التدفق الشهري للسيول .

أما دراسة نوعية المياه في وادي ملل فقد أعتمد فيها على جمع ٣٣ عينة من الآبار الموزعة على منطقة البحث (عينتين في الجزء العلوي من الوادي ، ١٦ عينة في منتصف الوادي و ١٥ عينة في أسفل الوادي) ويتراوح عمق هذه الآبار بين ٣٠ و ٨٠ متر و درجة معدل الحرارة من ٣٠ - ٣٥ م° وقد حظلت هذه العينات لمعرفة الخصائص الطبيعية والكيميائية المختلفة لهذه المياه ومناسبتها للري وعلى ضوء هذه النتائج فقد تم تصنيف مياه هذه الآبار على حسب جودتها وملاءمتها للاستخدامات الزراعية المختلفة .

ABSTRACT

Rapid urbanization of the city of Madinah Al-Munawwarah and its suburbs has resulted in a phenomenal increase in the exploitation of local ground water resources. The increased abstraction coupled with decreased recharge has led to decline in water levels as well as chemical quality.

The population of Al-Madinah area in general and study area Wadi Malal (24° 05' N and 24° 40' N: 39° 00' E and 39° 25' E) in particular relies heavily on ground water for drinking purposes and agriculture needs. The possibility of ground water is more because many tributaries join the Wadi Malal in the region and it is also the main tributary of Wadi Al-Hamd, which is one of the main source of the ground water in the region.

The landsat -5 thematic mapper (TM) and SPOT satellite often contains information that can be useful for ground water studies. Therefore, these data have been selected for analysis in this study. Landsat (TM) data has been used throughout the analysis, while SPOT data use only for field checking and ground truth. The Landsat 5 thematic mapper sensor (TM) provides excellent geological information. The TM scanner record 6 bands of the reflected visible and infrared spectrum, with image elements dimensions of 30 x30 m on the ground, and one thermal infrared band with image element dimension of 20 x 120 m on the ground. Spectral characteristics of 7 TM bands are discussed.

The geologic setting around Wadi Malal can generally be classified into two groups of rock units. The basement including both Al Ays group and overlying Furayh group of Precambrian age. Almost the entire wadi covered by the recent alluvium deposits. The thickness of this formation ranges from 40-80 m. This is made up of mainly sands, sandy clays, Clay and occasional gravel zones. The wadi aquifer is unconfined. The main wadi and its tributaries remain dry throughout most of the year.

In order to fully understand the subsurface hydrogeologic conditions, eight geophysical profiles with the help of remote sensing data have been selected.

To delineate the geometry of the aquifers and to determine the subsurface geological and hydrological conditions, the resistivity method was carried out applying two different

electrode spacing arrangements, namely Schlumberger and Wenner to create vertical electrical sounding (VES) and horizontal electrical profiling (HEP) respectively. In addition to that, ground magnetic surveying also carried out in the same location of VES. The object of VES is to deduce the variation of resistivity with depth and correlate it with the geological information in order to infer the depth and the resistivities of the layers present. The integration of various geophysical data (VES, HEP, and magnetic) that the ground water potentiality occurs in the down stream of the wadi. On the basis of remote sensing and geophysical survey 6 boreholes points were selected at downward in the wadi. The 184 borehole samples were physically identified

During the sedimentological study, different methods have been used by different workers but more common is the graphic plot method (Folk and Ward 1957) used in this study, and most of the samples in saturation zone are coarse, well rounded and well sorted. The borehole samples were also analyzed in the light of hydrological characteristics such as specific gravity, density, void ratio, and coefficient of permeability, porosity, and the weight percentage of gravel, sand, silt and clay. The averages for specific gravity and density for all the samples do not vary. The void ratio and porosity show variation of their values as though upstream consistent with the changing in gravel sand and fine sediments percentage.

The hydroclimatological study of the Wadi Malal area, which included in this study, is based on observations collected by the Ministry of Agriculture and Water. Three runoff-measuring stations are close to the study area. They are M401, M402, and M403. These stations give their mean monthly runoff.

Thirty-three samples were collected from the study area, which comprises 2 upstream wells, 16 middle stream wells and 15 downstream wells. The locations of these wells with their respective depths have been presented. All these wells were shallow and the depths of the wells vary between 30-80 m., where as average temperatures ranges from 30° - 35°C and were located in the agricultural area of Wadi Malal.

CHAPTER ONE

INTRODUCTION

The population of Al Madinah area in general and study area Wadi Malal (24°05' N and 24°40' N; 39°00' E and 39°25' E) in particular relies heavily on groundwater for drinking purposes and agriculture needs. Area is laying on an arid region that has no perennial rivers, infiltration during the period of precipitation is the only source of recharge to these wadi aquifers. The study area, Wadi Malal selected, keeping in mind that this wadi is the main tributary of Wadi Al-Hamd, which is the only source of natural water in the area and has great agricultural potentialities.

Earlier studies indicate that agriculture was the main source for the people of the area. The agriculture of the area has tended to decline steadily in recent years, for many reasons, apparently the most important thing will be the reduced amount of water available for irrigation.

Groundwater resources assessment of any area requires detailed investigation including the topography, morphology, climate patterns, surface structural geological features all of which provide preliminary basic information concerning availability of water storage, and natural recharge possibilities. These informations can be collected by the geophysical survey, which gives the following information:

- A- Depth, thickness and lateral extent of aquifers in sedimentary formation.
- B- Thickness of weathered and fractured zones and depth of massive basement rocks, delineation of solution cavities in hard rocks.
- C- Depth to water table.
- D- Structural and stratigraphic conditions controlling groundwater occurrence.

The geophysical methods used in this investigation include resistivity VES, HEP and magnetic. The vertical electrical sounding (VES) method is one of the most widely used surface methods for measuring earth resistivity. In this method, keeping the place of observation constant, sets of apparent-resistivity values are obtained successively for different

electrode spacing. The value of apparent resistivity is plotted as a function of electrode spacing on log-log paper. The curve is referred as an electrical sounding curve. The vertical distribution of resistivities within a given volume of rock is called a geoelectric section. This method is very useful in locating aquifer by taking advantage of contrast in geophysical properties between water bearing and non- water bearing formations.

The Wenner arrangement was used in HEP to detect lateral variations in the resistivity and to make the structures with near vertical boundaries, such as faults, dikes and fractures.

We also employed magnetic method survey. In magnetic method of survey, variations in the magnetic field of the earth in relation to subsurface geology is detected and measured. To select the geophysical survey points a preliminary map was required. For the preparation of preliminary lineament and drainage map the various remote sensing techniques were adopted. Geomorphic features and associated sediment having groundwater potentiality recognized on the basis of their spectral features present in satellite imagery. The classification of different geomorphic features was done on the basis of total contrast, texture, shape, size, and drainage configuration. The prepared preliminary lineament maps which was based on the remote sensing data, have been used in the selection of eight (M1, M2, M3, M4, M5, M6, M7, M8) geophysical profile which cover the whole wadi.

The two main groups Al Ays and overlying Furayh of Precambrian age covered the whole wadi. These are Precambrian layered metasedimentary and metavolcanic rocks. Almost the entire wadi is covered with recent alluvium deposits that lie between mountain ranges. Alluvium, which is covered the wadi consists of gravel, sand, silt and clay derived from adjacent rocks. The width of the wadi sediments ranges from few meters to several hundred of meters. The thickness of the sediments, vary from place to place it depends upon the configuration of the basement rocks. Being close to the source rocks, the sediments are generally heterogeneous and less porous than those deposited in alluvial plains. However, because of their coarse texture, they have high permeability.

Based on remote sensing and geophysical survey data, six drilling sites have been selected at down stream of the wadi. Textural and hydrological attributes have been analyzed from the borehole cutting. Climatological study of the wadi area which, included in this study is based on observation collected by Ministry of Agriculture and Water (MAW). Three

runoff-measuring stations that are close to the study area were taken into consideration. They are M401, M402, and M403. These stations give mean monthly runoff.

Quality and quantity are relative terms that depend on the purpose for which water is intended to be supplied. Samples were collected from upper, middle, and lower stream of the wadi. All samples were analyzed for temperature, pH, turbidity, conductivity, total dissolved solids, total hardness, Ca, Mg, total alkalinity, Fe, Na, K, F, Cl, NO_3 and SO_4 using standard methods. Temperature, pH, turbidity, and conductivity were measured in the field.

The main objective of this investigation is to locate aquifers capable of yielding water of suitable quality for drinking and irrigation purposes.

CHAPTER TWO

LITERATURE REVIEW

2.1 Introduction

The geologic work in the Al Madinah area was started in 1960, by the Directorate General of Mineral Resources. Several geologic investigators including Brown and Jackson (1960) who presented a general study of the Arabian Shield. Bhutta (1961a, b) and Brown et al, (1963) evaluated the reported mineral prospects of the area. A geographic map of the northeastern area was published by Brown and Jackson (1958). The same map revised and published in (1968) on the scales 1:50,000. Geologic detail mapping of the area was prepared by Hummel (1967). Study of Harrat Rahat basalt plateau for hydrologic point of view by Daessle and Durozoy (1972) and Daessle (1973). The detail geologic mapping for western Saudi Arabia and Al Madinah area were prepared by Pellaton (1981) and results of mineral exploration in the same area were published by Brosset (1976). The earlier significant fieldwork in the area was done by Kahr (1961), whose report served as the basis for the later investigation of the ultramafic rock by the Bureau de Recherches Geologique et Minières (BRGM). The occurrence of ultramafic rock in the northwest of the quadrangle was also noted in short report by Bhutta (1960). Apart from some reconnaissance field work Johnson and Trent (1966) and Petot (1972) with geologic work in the area is shown on 1: 100 000 scale map resulting from field work between 1970 and 1977 by BRGM, Pellaton and Dhellemmes (1978) and Hadley (1974). Bokhari, 1988 and 1993 has used LANDSAT images to generate drainage pattern in Al Madinah area.

2.2 Geological setting of Al Madinah area

Al Madinah quadrangle, located in the Arabian Shield between latitude 24° and 25° N and longitude 39° and 40° E, covering an area around 16550 Km².

The area is covered for almost 75 percent by the basalt of Harrat Rahat. The other 25 percent is made of Precambrian basement rock occupying the west edge and northeast corner of the area and represented by distinct units. The quadrangle is underlain by Precambrian metasedimentary, metavolcanic and igneous rocks, sandstone belongs to the Cambro-Ordovician age, Quaternary and Tertiary basaltic flows and surficial deposits (Pellaton, 1981), (Fig. 2.1).

The upper Proterozoic of Precambrian age sub-divided in to three groups: Hulayfah Group, Al Ays Group and Furayh Group (Table 2.1).

2.2.1 Hulayfah Group

Hulayfah Group, which lies in the northeastern corner of the quadrangle and consists of volcanic pyroclastic and sedimentary rocks of Nuqrah Formation, is separated by Tertiary basalt. The rocks look like as it those of Urayfi Formation of the Al Ays Group, but the field correlation is not possible at any part of the quadrangle. In the Al Madinah area, rocks of upper Proterozoic age are generally represented by two main groups: Al Ays and Furayh Groups separated by slight angular unconformity.

2.2.2 Al Ays Group

The Al Ays Group is well defined by Kemp (1980) and Pellaton (1981) in the Wadi of Al Ays (Latitude 25° N and Longitude 38° E).

The Al Ays Group, which is predominantly composed of mafic to silicic volcanic, epiclastic and detrital sedimentary deposits, cover the northern half and southwest of the quadrangle. The various igneous intrusions cut the rock and overlain by Furayh Group. The Al Ays Group constitutes three different formation: Farshah Formation of andesitic lava and pyroclastic rocks, Urayfi Formation, rhyolitic sedimentary, forming the upper part, Difayrah Formation, volcanic-sedimentary, it is equivalent to the upper part of the Urayfi Formation.

Farshah Formation

Farshah Formation consists of andesitic lava and pyroclastic rocks. The formation is several thousand meters thick overlain by Urayfi Formation, which transacts the entire width of its outcrop in the northern part of the quadrangle.

In the lower part of the Farshah Formation, dark gray or violet andesite and basalt of pyroclastic lava were rarely amygdaloidal are present, while at the upper part, the well defined flow, where the amygdaloidal lava are present, with amygdules of quartz, chlorite and epidote. The thin intercalation of green and dark-gray dacite occurs. The tuffs are common, but heterogeneous towards the top. Presences of several rhyolite layers are interbedded, which indicate the significant petrological changes of the silicic rock of the overlying Urayfi Formation.

Urayfi Formation

The formation is characterized of silicic volcanic and detrital sedimentary rocks lying in the north and northeast of Al Madinah where different facies of alternatively present, well defined formation of epiclastic volcanic breccia, sandstone and pyroclastic rocks are clearly formed with the layers of rhyolite, ignimbrite, rhyolite tuffs and dacite in the northeast of the quadrangle. A detrital sedimentary member has been also identified in the Wadi Altammah area in the north west of the quadrangle. At the top of the Farshah Formation, gradational changes from andesitic tuffs to heterogeneous tuffs are present.

The epiclastic volcanic rocks and rhyolite tuffs remarkably represent the upward changes from mafic to silicic. The composition is variable in the different part of the quadrangle. In the southwest, it is characterized with flow textured rhyolite, is partly spherulitic and in some places, prismatic columnar jointing. In the north at the base of the formation interbedded tuff, rhyolite, and andesite are overlain by rhyolite, dacite, ignimbrite, welded tuff, and rhyolite tuff and rhyolite breccia tuff in alternating and commonly repeated layers

Detrital Sedimentary Member.

A thick detrital sedimentary member forms inliers in the Quaternary age cover and contact with the Urayfi Formation in the northwest (Wadi Altammah). These rocks lenticular intercalation of all sizes, composition of the rock is greenish-gray, fine grained, well-bedded sandstone, with rounded volcanic grains in throughout the formation. It shows several sedimentary structures, graded bedding, crossbedding and slumping. Graywacke and siltstone are present, conglomerate and breccia, with pebbles and angular fragments of volcanic material can be seen.

Difayrah Formation.

It covers a small area on the western side of the quadrangle. This formation lies at the top of the Al Ays Group and correlation with upper part of the Urayfi Formation. It consists of alternating rhyolitic volcanic rocks, and intercalated with fine-grained detrital rocks were deposited under water. The sedimentary rocks comprise, fine grained gray wacke, siltstone epiclastic sandstone, with thin layers of chert and marble.

The Deposition of the Al Ays Group resulted from submergence at the end of a long period uplift and erosion (Kemp, 1980).

Intrusions in the Al Ays Group

It was believed that the intrusions are younger than Al Ays Group in Al Madinah quadrangle. The Difayrah Formation is cut by gabbro in Musayjid complex, which is composed of granite, granodiorite and diorite. The deposit spread out among the quaternary deposits of Wadi Rahqan in southwest of quadrangle. On its west, the Urayfi Formation is intruded by metamorphosed volcanic rocks. In the south of quadrangle, homogenous intrusions were recognized in Urayfi Formation. In the northern part of Jabal Warqan, peralkalic granite is considered the post Furayh age.

Northeast of the quadrangle, mesocratic granodiorite intruded the Nuqrah Formation, which is identified as equivalent of Al Ays Group intrusions and assigned to correlate with

neighboring northern quadrangle. Regarded that all the intrusions are younger than Al Ays Group but older than Furayh Group in the northwest and southwest of the quadrangle.

2.2.3 Furayh Group

Furayh Group is covering southern half of the quadrangle. This group generally forms low hills surrounded by Quaternary cover. It unconformably overlies the Al Ays Group, the contact is only identifiable by the presence of volcanic dikes in the Urayfi Formation. The group comprises; Murayr Formation of discontinuous conglomeratic, Qidirah Formation of mafic volcanic rock of various thicknesses. Dawnak Formation: Sandstone

The unconformity between the Furayh Group and Al Ays Group is not clear every where.

Murayr Formation

It occurs at the base of Furayh Group in the eastern margin of the quadrangle. Where an anticline exposes several hundred meters of polymictic conglomerate and sandstone overlain by Qidirah Formation. The conglomerate composed of pebbles and boulders of rhyolite, andesite, and granite. Interbeds of lithic sandstone with clear bedding occur. The colour of sandstone is green, purplish brown.

On the western part of quadrangle, the Murayr Formation overlies the Urayfi Formation which consist of poorly rounded and poorly sorted boulders and composed of rhyolite and ignimbrite of the same type occur in the underlying Urayfi Formation. The conglomerate is overlain by green or purple well bedded sand stone the sedimentary structure are present such as ripples marks and very clear graded bedding in the sandstone. Overlying the sandstone are andesitic and basaltic flows.

Qidirah Formation

Qidirah Formation is located in the east of Harrat Rahat which consist of mafic volcanic rock, but most of the outcrop is in the west of Harrat Rahat where the distinctly thick layers of detrital sedimentary rocks are interbedded and have been identified as a separate member. The composition of the Qidirah Formation is andesite and dark-gray to

green amygdaloidal basalt containing chlorite and epidote pillow lava also, occur at the top of the formation and rarely at the base, at the top of the formation layering occur in the amygdaloidal lava, the structure of the lava is massive.

Detrital Sedimentary Member

The detrital sedimentary form three outcrop zone, interstratified in the Qidirah Formation at the east of Jabal al Hinu and Jabal Asqaf The layers are covered by Quaternary deposits and Tertiary basalt flow to the west are bounded by faults. The detrital sedimentary member consists of polymictic conglomerate with rounded boulder, coarse grained and fine grained sandstone, sedimentary structures are ripple marks, cross bedding, microslumping, indication of shallow water deposition. The mudflakes, mud cracks and local unconformities that indicate periodic emergence.

Dawnak Formation

It consists of sandstone with conglomerate, tuff and marble constitute in the southern part of the quadrangle, and more restricted to north and west of Harrat Rahat. In the east of Al Madinah airport the sedimentary rocks are bounded to Harrat Rahat and lithologically is similar to Furayh Group. The outcrops show an alternation of amygdaloidal basalt and tuff, which regarded as Qidirah Formation. It is also believed that the intrusions represented by batholiths and plutonic calc-alkalic granite are considered younger than Furayh Group. The southeast of the area is represented by a thick sequence of several rocks, including graywacke, siltstone, lithic sandstone, sandstone and conglomerate.

Intrusions in the Furayh Group

All the Proterozoic Formations with the exception of peralkalic granite cut by the dikes and occur particularly in the western area of the quadrangle. A dike cutting the Urayfi Formation between Mahattat Muhit and Wadi Al Aqiq (Al Hamd) comprises diorite, microdiorite, microgabbro and andesite.

The dikes are various thickness ranging from decimeter to several meters, at some places it occupies almost the 70 percent of total rock volume, the host rocks look like fragmented blocks which have undergone no rotation in relation to one another. In the west of area, the Difayrah Formation mafic and felsic dike, strike N 70°- 80° W.

North of Al Madinah, numerous composite dikes of microgranite, rhyolite, diorite and gabbro intrude the granite along two directions one N 45° W and Parallel to the faults which affect the granite, and other orthogonal to the first at N 45° E. They do not cut across the host rock.

Two intrusions of alkalic to peralkalic granite crop out in the quadrangle. The largest is the circular pluton at Jabal al Byda, north west of Al Madinah, which has a diameter around 12 km and is composed of pink medium - grained granite containing abundant, and in some places subhedral quartz crystals. The feldspar is mainly potassic and perthitic, and mafic minerals are irregularly represented.

The second dike crops out on the southern margin of the quadrangle at Jabal Warqan. It cuts both post - Al Ays granite and Furayh Calc-alkalic granite containing perthitic potassic feldspar and sodic mafic minerals.

Intrusions of monzonite, diorite, gabbro occur as dikes, sills and stocks in the east and south east of the quadrangle. A horizontal sheet was crops out over an area of 20 x15 km, and it is 50-70m thick and intrudes the Urayfi Formation with a discordance of as much as 40° occur near Bir al Harr area, north east of the Al Madinah. The dikes are composed of fine grained quartz diorite containing andesite, amphibole, biotite, quartz and gabbro containing pyroxene and amphibole. Al Jabal Mudayba southeast, an intrusion of gabbro is differentiated to monzonite at the center. In the west of the quadrangle at Jabal as Asfa and Jabal Malah, diorite, intrusive in the Qidirah Formation but cut by posts Furayh Calc-alkalic granite. It is described by Brosset (1976) as being either a heterogeneous intrusion of fine grained equigranular diorite and quartz diorite, or a heterogeneous intrusion of heterogranular diorite, quartz diorite and granodiorite containing unassimilated inclusions of host rock.

The whole Al Madinah area covered by granite, adamellite and granodiorite from several large syntectonic inclusions in the scattered form. The major one are the Jabal al

Dar'a, Jabal al Arajib and Jabal al Jizl batholiths in the south-west, the As Sahwah batholith in the North. The batholith is composed of coarse-grained equigranular mesocratic granodiorite containing oligoclase, rare potassic feldspar, quartz, biotite, and green amphibole. The periphery of the batholith has a slightly more alkalic composition with coarse grained or microgranular. Batholith near the Jabal al Jizl is composed of calc-alkalic granite displaying two principal facies; one with more abundant potassic feldspar and relatively coarse grained, the other containing large quantities of plagioclase, finer grained and relatively enriched in mafic minerals.

In the north-west and south-west of Al Madinah several intrusions of microgranite have been crop out, is composed of salmon-pink or red leucocratic microgranite with either a porphyritic texture showing euhedral oligoclase in a micropegmatic matrix of quartz and feldspar.

Rhyolite, granophyre and microgranite, crop out in a small area in the north south aligned stocks intrusive in the Qidirah Formation. The stocks composed of well-crystallized rhyolite. In some places, flow textured which contains small euhedral crystals of quartz and feldspar in a pale matrix with abundant opaque minerals, Salmon pink or red microgranite containing small crystals feldspar and amphiboles.

Salmon pink aphyric granophyre, all stages of transition between the various rock types can be seen.

2.2.4 Tertiary and Quaternary basalt

Tertiary and Quaternary basalt, consisting of flows that have been extruded from several craters lying along fractures boarding the fault graben of the Red Sea. These basalt were originated during extensive volcanic activity that started at the end of Tertiary and continued during the Quaternary to historical times (ITALCONSULT, 1975).

The western part of the Arabian Shield where the Tertiary and Quaternary basalt in Al Madinah forms the north-south alignment of basalt plateau which lies between latitude 22° and 27° N. Harrat Rahat Craters and volcanic domes which are extending from north to northwest axial with an elevation of 1360 meters in south of quadrangle. The bore hole data

shows that basalt overlies continental clay, clayey sandstone and marls are intercalated and gravelly is identified lying directly on Precambrian basement, and is considered probably of Oligocene age. Five basaltic flows are marked from numerous volcanoes of the central axis. The younger dominates the topography while the oldest have eroded. In the west of Al Madinah, on the top of buttes perched basalt extruded prior to the subsidence of trough within which Harrat Rahat and Harrat Khaybar were formed.

2.2.5 Quaternary sediments

Unconsolidated deposits ranging from silt to boulders occur through out the area with in the wadi. These alluvial deposits lie between mountain ranges or between exposures of hard rocks. Coarse materials comprising sand, gravels and pebbles form the bulk of the wadi deposits, which are among the most productive of aquifers. The most extensive such deposits occupy the floor of the Jizl trough from the north to the north east and east west of the area. The central part of the trough, which the main waters, courses pass. Typically, the deposits are characterized by basal gravel and pebbles, succeeded upwards by fine materials.

The wadi alluvium and broad lateral braided stream deposits occur in the main wadis, the latter occupying wadi pediment slope in many places, with feldspathic sand being particularly well developed. The sedimentation may be cyclic with repetition of the gravel-sand-clay sequence. The nature of deposits, size, sorting and shape of grains and their mineralogical composition depends on the Physiographic features and geological history of the source rocks and maturity of the stream carrying the sediments. The thickness of the wadi deposit varies widely, depending on the configuration of the basal rocks and land surface profile.

2.3 Structural geology of Al Madinah area

The basement complex rocks show sign of very old folding and faulting, ascribable to various tectogenetic phases - mostly compressive which occurred repeatedly in Precambrian times (ITALCONSULT, 1975).

The Shield was displaced left laterally more than 250 km (Brown, 1971), mostly along the three major north-west trending faults zones, each of 5 to 10 km wide.

This major large fault movement on the Najd fault system is in a region 300 km wide by 1100 km long, but the effects of the Najd stress can be found throughout the shield. The folding occur in the Al Ays Group with the axial planes of the folds generally trending north. Dips are in places very steep and even over turned, but generally ranging between 30° and 40° N. In the north, Urayfi Formation is contained in isoclinal structure with numerous secondary folds, plunging slightly to the east-south east.

Folding occurs during which the Murayr and Qidirah Formations behaved in rigid manner, but the less compact Dawnak Formation was affected by multiple small amplitude folds with vertical axial planes.

A Northwest-trending, left lateral, trans-current fault system prevailed over the conjugate north east trending right lateral trans-current fracturing (Brown and Jackson, 1960, Moore, 1979).

East-west fractures belonging to another fault system, probably later than the Najd, (Pellaton, 1981) occur in the Jabal al Arajib granite batholith and in the Jabal Bayda' alkalic granite.

In the Qidirah Formation near the Jabal al Rabd and Jabal Ghurab, due to deformation intense schistosity are developed, where the rocks are transformed to schist. A layered gabbro complex has cropped out in a shear zone, at Jabal al Musayjid.

2.4 Applications of geophysical methods in groundwater investigations

Resistivity surveys are usually restricted to relatively small-scale applications because of the labor involved in physically planting the electrodes prior to each measurement. For this reason, resistivity method is not commonly used in reconnaissance exploration.

The most widely employed use of resistivity survey is in hydrogeological investigations, as important information can be provided on geological structure, lithologies and subsurface water resources without the large cost of an extensive drilling, which might be unattainable by other geophysical methods (Zohdy et al. 1984). For example, electrical

methods are unique in furnishing information concerning the depth of the fresh salt-water interface. A thick clay layer separating two aquifers can be detected easily on a sounding curve but the same clay bed may be a low velocity layer in seismic refraction and cause erroneous depth estimates.

Deppermann and Homilus (1965) investigated the geoelectric conditions where the water table can be detected on an electrical sounding curve. Whenever the water table is overlain and underlain by several layers of different resistivities, its detection on a sounding curve may be impossible. Under favorable conditions the water table can be detected on a sounding curve as a conductive layer (Zohdy et al. 1984).

However, Kearey and Brooks (1991) indicate that the depth of penetration obtained by this method is limited by the maximum electrical power that can be introduced into the ground and by the practical difficulties of laying out long lengths of cable.

Zohdy and Jackson (1969) carried out several deep electrical sounding on the Island of Hawaii to determine the depth to low resistivity layers that may represent basaltic lava saturated with water. They concluded that the minimum depth to such layer is of the order of 900 m.

In the San Juan area, California, several buried stream channels were discovered by Zohdy in 1965 and by Page in 1968, using the combined techniques of horizontal profiling (HEP) using the Wenner array and electrical sounding using the Schlumberger and Wenner arrays.

Geological techniques, coupled with hydrogeological investigations have been used in evaluating groundwater resources. Adam (1981) has mentioned that geophysical investigations have proved the presence of a sub-basaltic drainage system in a study area south of Al Madinah. Al Muttair et al. (1989) have shown how geophysical techniques can be used in evaluating the flow in an unconfined aquifer in central Saudi Arabia. Geophysical results were combined with observations wells data and information on the aquifer to estimate the flow across certain locations in the aquifer down stream from a recharge dam. Bayumi (1992) studied the groundwater resources of the northern part of Harrat Rahat south of Al

Madinah area. Major factors affecting both quantity and quality of groundwater in the study area were investigated.

In main resistivity surveys, a commuted direct current or very low frequency current is introduced into the ground via two current electrodes (C1 & C2).

The potential difference is measured between a second pair of electrodes (P1 & P2) (Fig. 2.2).

According to the electrodes arrangements, the methodology applied will have special treatment. In this study, Schlumberger and Wenner arrangements will be applied to VES and HEP respectively. The Wenner uses an equal spacing between adjacent electrodes whereas the Schlumberger arrangement retain symmetry about a center point but it uses much smaller spacing than Wenner for the potential electrodes. Details of such arrangements will be given in the next phase.

For VES, Schlumberger arrangement is recommended for two reasons:

- 1- Schlumberger is less sensitive to undetected lateral variations in resistivity and provides a means to recognize such effects and to partially correct for them.
- 2- Schlumberger is slightly faster in field operation since only the current electrodes must be moved between readings.

If the ground is comprised of horizontal, homogeneous, and isotopic layers, electrical sounding data represent only the variation of resistivity with depth. In practice, however, VES data are influence by both vertical and horizontal heterogeneties. Therefore, the interpretation and presentation of sounding data should be such that horizontal variations in resistivity can be distinguished easily from vertical ones (Zohdy et al, 1984).

2.5 Application of remote sensing in groundwater studies

Remote sensing techniques have proved to be an effective method for tracing potential groundwater occurrence and have become a standard practice in hydrogeological reconnaissance surveys. In areas with a little hydrogeological information, remote sensing provides basic information on physiography, vegetation and geology. In areas where basic

information is already available, remote sensing may gather this information on a regional scale (satellite images) or, to enhance details, on a local scale (aerial photographs).

LANDSAT AND SPOT satellite images often contain information that can be useful for assessment of groundwater resources. Images are often displayed in colour, using information from three different channels or spectral wavelength bands. Tonal variations in these so-called multispectral images are reflecting ground characteristics of rock, soil and vegetation types. The reflectance value of a certain ground feature often varies in the three images channels. This is utilized by remote sensing technology. We can identify and delineate different ground features relevant to groundwater occurrence, such as geological structures and fracture (lineament) and drainage patterns. By using various image-processing techniques, we can improve the hydrogeological assessment by enhancing small tonal and texture variations that may present in the raw data. Image processing can be applied starting with simple and quick methods, subsequently introducing can be applied starting with simple and quick methods, subsequently introducing more complex transforms.

Remote sensing can provide good information for groundwater exploration or investigation, which can be supplemented and verified by others field techniques (geophysical study, drilling, etc.). In fact, the integrated satellite images with geophysical and or drilling has been used for groundwater exploration (Voute 1986; Krol, et al, 1986, Mohan, et al, 1987, Deutsch and Heydt, 1987, Feder, 1987, Van and Seevers, 1988, Usha, et al, 1989, Aberra and Wihuri, 1989, Das, 1991, Teme and Oni, 1991, Andersson, et al, 1992, Krishnamurthy, et al, 1992, Ob"Yedkov, 1992, Rao, et al, 1993, Bokhari, 1993, Minor, et al, 1994, Shivakumar and Gulhane, 1994, Knapp, et al, 1994, Alwash and Zilger, 1994).

2.6 Hydrological, hydrogeological and water quality

Due to the absence of regular climatological stations in the study area, reliable records of climatological variables are difficult to obtain further processing. Precipitation in the area is irregular, unpredictable and long and dry periods are common. The annual rainfall in wadi not exceeds 100 mm. The available records of annual precipitation and evaporation of a

station located nearby the area collected from the hydrology department in the Ministry of Agriculture and water. These records show, that the amount of rainfall reached its highest value in 100 mm/year, where as in the same year the evaporation losses were less compared with the previous years (ITALCONSULT, 1979).

Despite the fact that the area is close to the Holy City of the Al Madinah, the information related to water study in this area was meagre. The study of Bokhari 1988, of wadi sediment on Al Madinah taking into considerations the wadi aquifer is unconfined and characterized by typical alluvial valley fill deposits. The main wadi and its tributaries remain dry throughout most of the year but during seasonal rainfall when some precipitation infiltrates down through the alluvial sediment.

The saturated part of the valley fill acts as a groundwater artery transmitting, within its narrow confines, a greater abundance of water than in basement rocks. Being close to the source rocks, the sediments are generally heterogeneous and less porous than those deposited in alluvial plains. However, because of their coarse texture, they have high permeability.

Wedge-shaped aquifers are common in these sediments. The lateral extent of the aquifer being limited due to truncations against basement rocks, barrier boundary conditions are encountered.

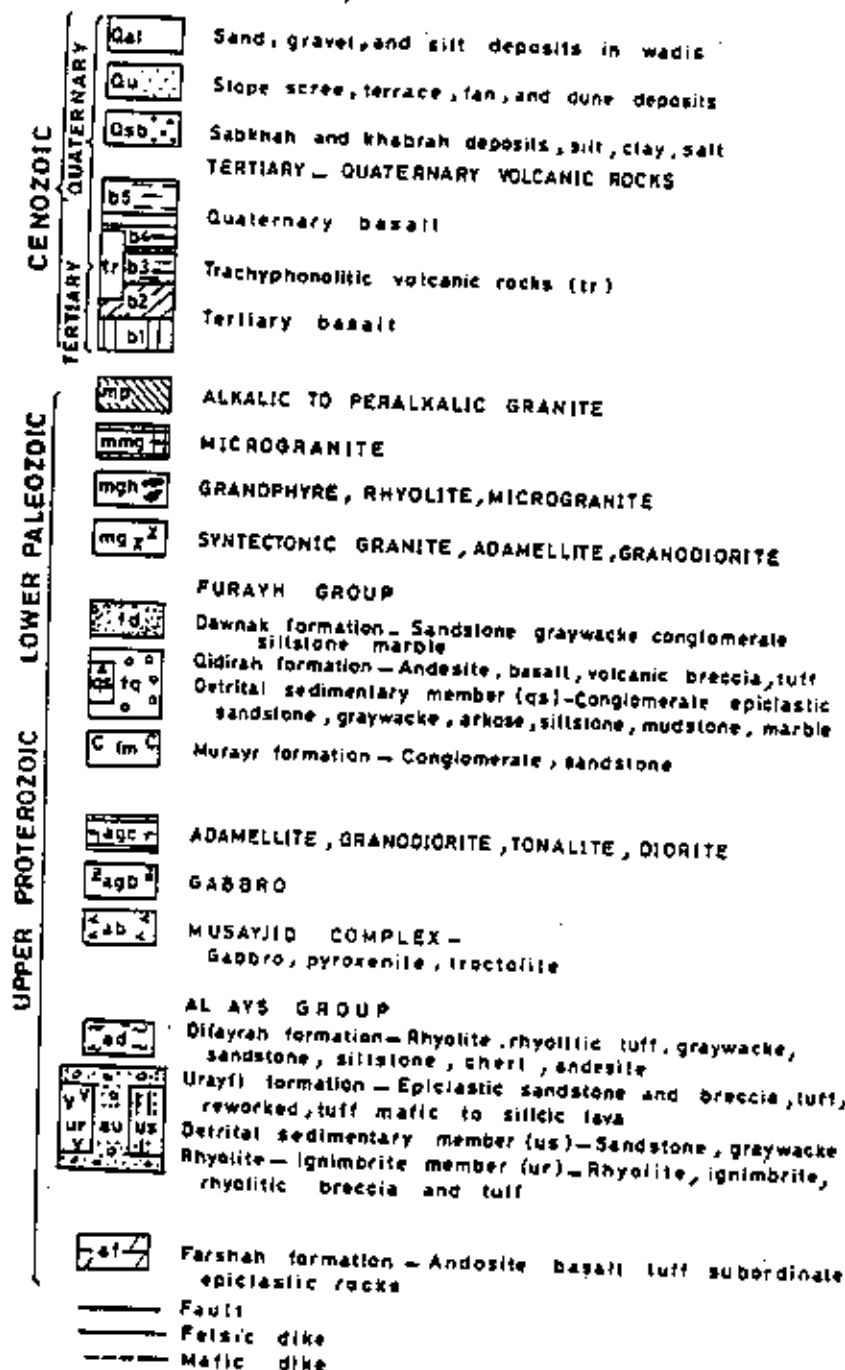
In many groundwater assessment studies, evaluation of the quality of ground water is as important as the quantity, in as much as the usability of ground water available is determined by its chemical, physical and bacteriological properties. The study of the quality of ground water envisages field observation regarding the source and environment of ground water occurrence, sources of pollution and other related aspects having a bearing on the quality of groundwater.

Informations on wells water quality of the study area are meagre. A paper published by Bokhari and Khan (1992) is considered the only work that gave some information on the quality of the water around the Al Madinah area. The paper was not based to give detailed information regarding the quality of wells water but rather develop easier deterministic empirical relationships for the use in determining the groundwater composition, quality and suitability for domestic purposes. Even though the workers collected samples from 105 wells

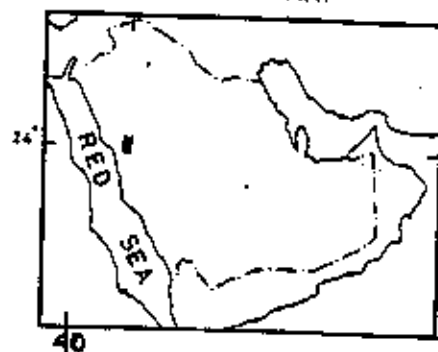
around the Al Madinah area (24°00'25°00' longitudes and 39°00'-39°45' latitudes) which were analyzed for pH, temperature, Ca, Mg, Na, K, SO_4^{2-} , Cl^- , bicarbonates, and electrical conductivity (EC), however, only the latter values were reported. Results of other parameters were used to report such as $\text{SO}_4^{2-}/\text{Cl}^-$ and the relationships of (Na + K) or EC versus other ions. The workers reached the following conclusions:

- (I) The value of EC increases with distance from upstream indicating poorer quality.
- (II) The ratio of $\text{SO}_4^{2-}/\text{Cl}^-$ decreases with distance from upstream.
- (III) The relationship of EC with hydraulic gradient and the number of joining tributaries are poor.
- (IV) The water quality of Al Madinah area is good mainly composed of chloride and sulphates of Ca^{++} and Mg^{++} .

LEGEND



LOCATION MAP



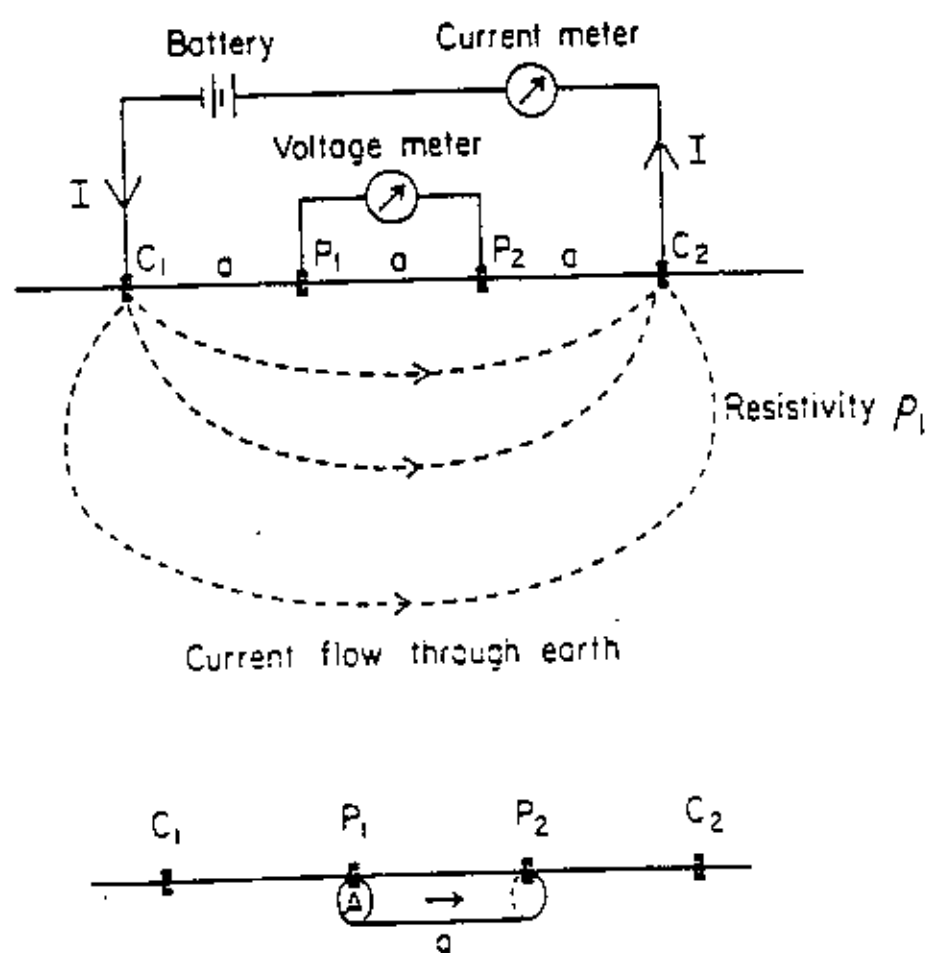


Fig. 2.2 Resistivitymeter instrument connected to 4-electrodes (C_1 , P_1 , P_2 and C_2)

Table 2.1 Generalized lithostratigraphic divisions of Al-Madinah area (Pellaton, 1981)

Era	Age (in m.y.)	Units		Lithology	Intrusive rocks
		Group	Formation		
CENOZOIC	0 to 40			Basalt flows Trachyphonolytic extrusions	
			Unconformity		
PALEOZOIC	Cambro-Ordovician			Sandstone	
			Unconformity		
UPPER PROTEROZOIC	561 to 673	FURAYH	Murayr	Conglomerate	Microgranite; Granophyre Peralkalic granite Granite; Granodiorite
			Qidirah	Mafic volcanic	
			Dawnak	Sandstones	
			Unconformity		
	742	AL AYS	Difayrah	Volcanic-sedimentary	Granodiorite; Tonallite; Diorite; Gabbro
			Urayfi	Rhyolitic-sedimentary	
			Farshah	Andesitic	

CHAPTER THREE

GEOLOGY OF THE AREA

3.1 Introduction

During the geological field work outcrops of Al Ays and Furayh Groups were studied along the Wadi Malal, only the few scattered formations of Al Ays and Furayh Groups were covered the whole wadi.

The Urayfi Formation of Al Ays Group covered the northeastern part of the study area, which consists of silicic volcanic rock and derivative epiclastic. The upper part of the Urayfi Formation consists of heterogeneous tuff with interbedded lava showing upward progression from mafic to silicic. Furayh Group dominated the southern part of the study area. It forms low hills surrounded by Quaternary cover, it unconformably overlies the Al Ays Group. The group comprises discontinuous conglomeratic, mafic volcanic rock of various thickness and sand stone. The Qidirah Formation forms middle part of the Furayh Group and covers the southern part of the study area from Jabal al Asfa to Jabal Kashbon towards the upstream of Wadi Malal. It consists of andesite and dark gray to green amygdaloidal basalt containing chlorite and epidote. The amygdaloidal lava generally occurs at the top and base of the formation. The amygdules vary in size from one mm. to several mm. Pillow lava generally occurs at the top of the formation and seen at the various places at the base. At the top of the formation, layering occurs in the amygdaloidal lava, some places few meter thick flows are identified (Pellaton, 1981).

Intrusions in Qidirah Formation are mainly represented by batholiths and plutons of calcalkalic, alkalic and peralkalic granite. These are syn- or late Kinematic, and were preceded by small intrusions of diorite. Intrusions are generally younger than Furayh Group.

Diorite, intrusive in the Qidirah Formation cut by post - Furayh Calc-alkalic granite, lies in the west of the area at Jabal Asfa and Jabal Malah. It is either a homogeneous intrusion of fine grained equigranular diorite or quartz diorite.

Most of the study area is covered by the scattered granite, adamellite and granodiorite form several large syntectonic intrusions. The major one is near Jabal Jizl batholiths in the west. The batholith is composed of calc-alkalic granite displaying two principal facies: More abundant potassic feldspar and relatively coarse grained, the other containing greater quantities of plagioclase, finer grained and relatively enriched in mafic minerals. All the formations in the area are cut by the dikes and crops out in the western part of the study area. The dikes are varying in thickness several decimeters to several meters. In some places, it occupies more than 50 percent of the total rock volume, the host rock appears as fragmented and direction of dikes is generally E-W (Pellaton, 1981).

3.2 Regional tectonism

The tectonic features of the study area are extremely complex. The basement complex rocks show sign of very old folding and faulting, ascribable to various tectogenetic phases- mostly compressive which occurred repeatedly in Precambrian times.

Qidirah Formation have been affected by a major phase of folding with north - northwest trending axial planes. The major phase of folding was followed by a minor phase during which the Qidirah Formation behaved in a rigid fashion, where as the less compact of other formation was affected by multiple small amplitude folds with vertical axial planes.

The faults of the area can be divided into two main groups. The first belongs to the Najd Fault system and characterizes the southwest of the area, the main fault strike west - north west. In the north, they intersect the other formations, producing left lateral displacement. The second, much more recent, corresponds to fractures which gave rise to the volcanic emission centers during the tertiary and Quaternary, these emission centers are largely grouped along a north-south trending median axis (Pellaton, 1981).

3.3 Geology of downstream area

The present study is largely confined to the down stream of Wadi Malal ($24^{\circ} 30' 00''$ and $24^{\circ} 45' 00''$ N, $39^{\circ} 10' 00''$ and $39^{\circ} 25' 00''$ E). The possibility of the groundwater is more because many tributaries join the Wadi Malal in the region.

Near the confluence of Wadi Malal and Wadi Malhah, a patch of Urayfi Formation of Al-Ays Group is occupied in the east of the wadi. The rocks are epiclastic sandstone and breccia, tuff mafic to silicic lava. Many dikes, generally mafic in nature, cut all the proceeding formation, they were formed a confused structure particularly east and north east of the wadi. The general strikes of the dikes are northwest and east west. The dikes are mainly of porphyritic andesite, microdiorite, and diorite. In the west of wadi (Jabal Jilzi), many felsic dikes are noted, consist of porphyritic rhyolite and strike east-west direction. In this particular area, only one fault occurs near the Jabal al Munaywir. The strike of the fault is northwest (Fig. 3.1).

The wadi sediment consists of sands, sandy clays and sand with occasional pebbles and gravel. The wadi is surrounded by volcanic rocks of basalt, rhyolite and tuff. Commonly they consist of several successive flows of variable thickness and lateral extent. A typical flow unit consists of dense and massive horizon, passing upward into a vesicular, amygdaloidal or jointed horizon. The significant geohydrological characteristics of these rocks are primarily porosity in the form of vesicles, lava tubes and occasional tunnels formed due to escape of gases. Secondary porosity is also developed due to fracturing during the cooling of the lavas, tectonic disturbances and weathering. In the studied area, the vesicular porosity of basalt is considerably reduced by filling up minerals like zeolites and silica to form amygdales. The successive flows nature of the basalt being more susceptible to weathering, but in this area little weathering is pronounced.

Igneous rocks occur as intrusive amidst large bodies or plutons. The plutonic rocks generally in the form of dikes include such coarse textured igneous rocks as granite, diorite and pyroxenite, ranging in composition from acidic to basic depending on the silica content. The igneous and metamorphic rocks usually have porosities less than 1%, the void being minute, generally isolated and in consequential form a practical viewpoint.

3.4 Geomorphology

Al Madinah area is bound by the Harrat Rahat in the west with deep valleys and in the east by peneplain of Cambrian age. The drainage patterns of the area are controlled by the geological features in the outcrop. The drainage pattern of Harrat Rahat which consist of

basalt have a dendritic drainage pattern, controlled by the slopes of the basalt cover (ITALCONSULT, 1975). The valleys in the north flow in dendritic drainage system. The region having number of catchment area which drain to Red Sea. The basement consists of two main groups of rock units separated by a slight angular unconformity. Al Ays Group and overlying Furayh Group. Bokhari (1993) suggested on the basis of remote sensing data and by the help of a model, that the rocks of the two groups were affected by N-S folding and fracturing took place in an East-West direction, along the fractures erosion have been taken place and development of the main valleys like Wadi Al Aqiq, Wadi Malal and Wadi Furaysh. The main tributaries to these valleys run perpendicular or sub-perpendicularly to this direction. The drainage of the area is also follow the joints and less eroded fracturing.

The Wadi Malal in the study area (Latitudes 24° 05' N and 24° 40' N, Longitudes 39° 00' E and 39° 25' E), is about 65 Km long, flowing from South to Northwest. The Wadi Malal is generally enclosed between rock walls, having crop out in deep valley in the mountainous terrains. It is one of the main tributaries of Wadi Al Aqiq (Al Hamd), which is an important source of natural water in the Al Madinah area. The Wadi Malal is wide at the upstream end, with part of the wadi covered by basalts; the down stream reaches however are evolved in the Precambrian basement rocks as passages. In the upper part of the stream, many tributaries like ad Dabwah, Hulayqah and Furaysh join the main wadi. At the confluence of these wadis, the width of Wadi Malal varies from 0.5 to 2 km. In general, the width of wadi varies from place to place and on average the width is slightly more than one kilometer. The number of tributaries joining from the western side is more than those joining from eastern flanks of the wadi.

This area is a part of Hijaz range and elevations in general are between 1000 and 1500 m. The highest point is 602-m (Jabal Jamirah) in south West of the wadi and towards the West, at the middle length of the wadi 683-m (Jabal Umm).

The region has an arid climate with hot dry summers and cold winters, and evaporation rates are very high.

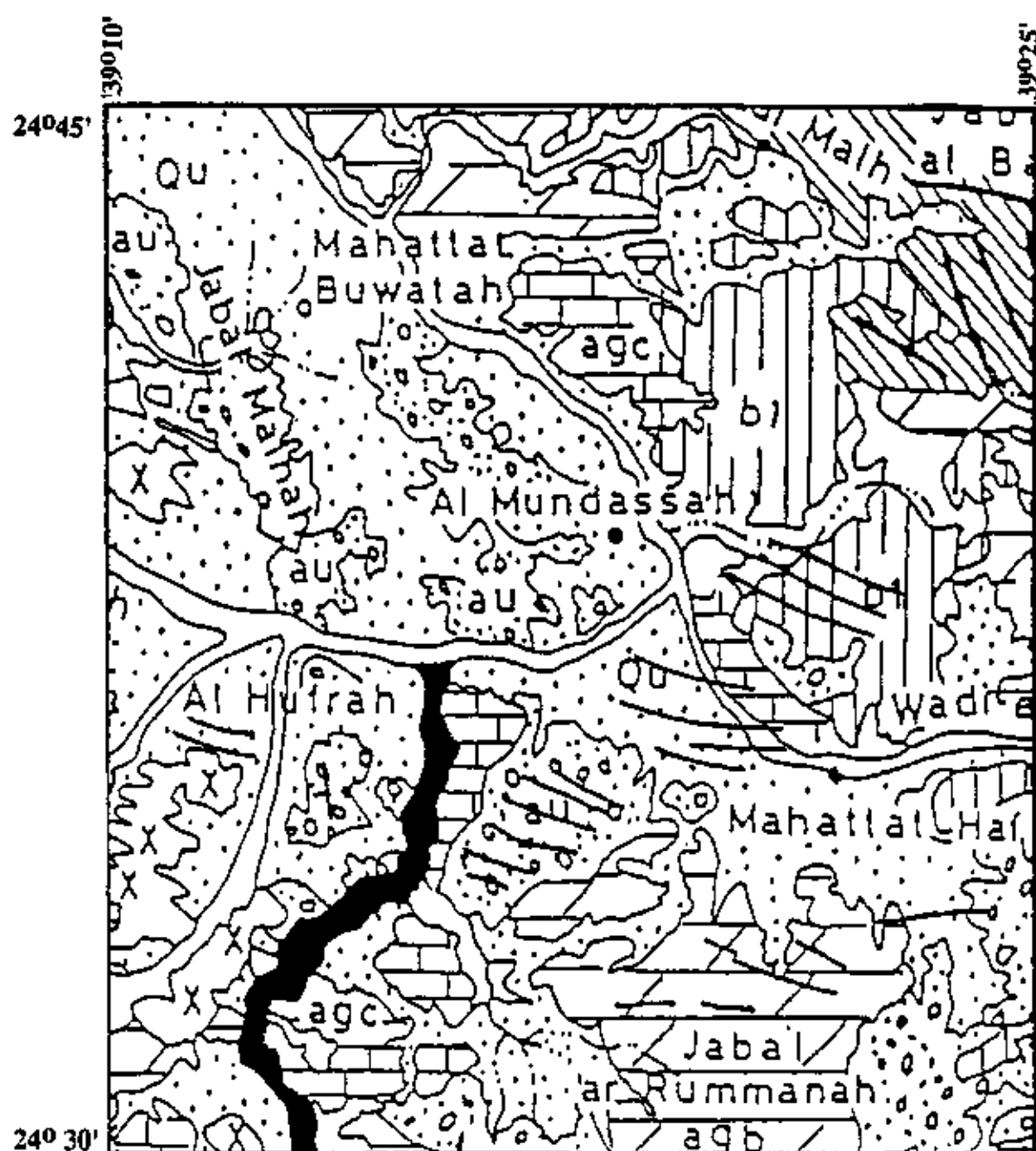


Fig. 3.1 Geological map of down-stream of wadi Malal (Pellaton, 1981)

(for legend see fig. 2.1).

CHAPTER FOUR

DETECTION OF LINEAMENTS AND DRAINAGE SYSTEM OF WADI MALAL USING SATELLITE DATA

4.1 Introduction

Geomorphological and geological features, namely landforms, rock units and geological structures, have a definite relationship with the occurrence and movement of groundwater in hard-rock crystalline formations.

These indicators can be grouped into two categories:

- 1- Direct indicators ground parameters that are directly related to groundwater occurrence (e.g. lakes, canals, rivers, etc.)
- 2- Indirect indicators (hydrogeological parameters which are regionally affect groundwater (e.g. drainage patterns, fractures system or lineament, soil, rock types, structure, landforms and vegetation)

Satellite remote sensing provides information on geology and geomorphology relevant to groundwater exploration. Large areas can be evaluated quickly from satellite data and possible locations for groundwater zones identified for further detailed study (such as geophysical and hydrological studies). Therefor, remote sensing investigation only for supporting the other investigations.

Digital enhancement techniques remotely sensed data help in the extracting specific features that act as groundwater indicators and ultimately lead to the preparation of maps indicating groundwater prospective zones.

4.2 Data selection

The LANDSAT-5 thematic Mapper (TM) and SPOT satellite often contains information that can be useful for groundwater studies. Therefore, these data have been selected for analysis in this project. LANDSAT TM data has been used in all the analysis, while SPOT data used only for field checking and ground truth. The LANDSAT 5 have

Thematic Mapper sensors (TM) which provide excellent geological information. The TM scanner record six bands of the reflected visible and infrared spectrum, with image element dimensions of 30 by 30 meters on the ground, and one thermal infrared band with image element dimensions of 20 by 120 meters on the ground. Spectral characteristics of seven TM bands are discussed in table (4.1). The TM data path 170 row 43 acquired in the winter period (where low sun elevation angles, enhance the visibility of topographic variation, and help in lineament detection and interpretation. However, lineaments or topographic feature running parallel to the sun azimuth on the acquired date, will be hard to detect). All the image data were atmospherically corrected.

The digital image analysis was carried out using image processing system at the Saudi Center for Remote Sensing (SCRS), which is configured around a VAX 4300 computer system along with MERIDIAN image processing software.

4.3 Digital image processing

Digital image processing is extremely broad, and it often involves procedures, which can be mathematically complex. However, in this study only few techniques were used (contrast stretch, edge enhancement, principal component analysis, false color composite, intensity Hue saturation) to detect lineaments and the drainage patterns. The definitions of these techniques in brief are followed: -

4.3.1 Contrast stretch

In general, it so happens that the number of actually recorded intensity levels in a scene is rather low and the fully dynamic range of the digital image is not utilized. Reallocation of gray levels could also be done to improve the contrast between some specific types of ground objects. Contrast stretching is a typical point operation. Contrast stretch was done interactively to obtain the best possible image for the current application. The linearly contrast stretch of TM bands 7m 4 and 2 in red green and blue (R, G, B) can clearly show some the drainage pattern and the lineaments (Fig. 4.1).

4.3.2 Spatial image filtration

Lineament in an image can usually be identified by visual interpretation using tone, texture, pattern, association etc. However, many lineaments are not clear and require image-processing enhancement. Spatial filtration techniques have been the most common method of enhancement lineament.

Image filtration techniques when applied to digital image, are designed to enhance different scales of tonal or digital value "roughness" (i.e., different spatial frequencies). Spatial filtering depends, not only upon the value of pixel being processed, but also on the pixel values surrounding it. In this regard, spatial filtering is an area operation. Spatial filters can be, either to emphasize or de-emphasize the abrupt changes in pixel digital numbers (DN's), there by altering an image's textural appearance (Lillesand and Kiefer, 1987).

The image filtration involves two procedures: -

1. A moving window is established which has an array of coefficients or weighting factors (the array are referred to as the filters or kernels).
2. The kernel starts from the top left corner of the image. Each coefficient factor is multiplied by the corresponding pixel value (DN), and the result stored in an output image (Lilliesand and Kiefer, 1987).

This technique is applied to the satellite data in order to detect the lineaments or fractures in the study area (Fig. 4. 2).

4.3.3 Principal component

Principal component (PC) transformation used to decrease amount of correlation between bands of data and maximize the differences between bands. This transformation can be performed on any number of bands, and will generate axes in N-space where the N axes correspond to the number of input bands. Generally speaking, the first principal component contains brightness information of the image. In this study, PC applied to bands 7,4 and 2 produce 3 component. Only first component used for visual interpretation (Figure 4.3)

4.3.4. Intensity Hue Saturation (IHS)

The intensity, Hue and Saturation transformation takes an image from the familiar red-green-blue color space to a new system of Intensity, Hue and saturation. Intensity is a function of brightness; Hue represents the color of the object; and saturation is the purity of the color. An image is first transformed in IHS space, where the intensity, Hue and saturation components are individually stretched. They then transformed back to the original R, G, and B color space. In this study this transformation were applied to TM bands 7,4, and 2 (Figures 4.4 - 4.5). These images (IHS saturation image) used in this study only to show the drainage patterns specially the channels.

4.4 Interpretation of digitally enhanced outputs for groundwater study.

Visual interpretation of various outputs generated through digital data enhancement technique was carried out using standard interpretation keys, such as tone, texture or both. In such dry area the interpretation must find out the indirect indicators for groundwater (hydrogeological parameters which regionally affect groundwater) (e.g., drainage patterns, fracture systems or lineament, soil, rock types, structure, landforms and vegetation). Therefore, lineament and drainage patterns according to the lineament map and the field visit it has been found most of the producing water wells lie within the major faults in the area.

4.4.1 Lineament detection

Lineaments are generally straight alignments that run over a variety of local geological features and the majority of them extend nearly vertical with depth. It is generally believed that lineament represents the surface expressions of deep-seated crust fractures propagated upward through overlaying consolidated and unconsolidated materials or downward to great depths lineaments may be continuous or discontinuous. Continuous lineaments are the continuous straight lines. In discontinuous lineaments the separate features are aligned in a consistent direction and are relatively closely spaced.

According to the literature review, lineaments may be distinguished on LANDSAT satellite images by one or more of the following indicators: -

- a) Alignment of topographic forms often emphasized by shadowing.

- b) Alignment of drainage patterns.
- c) Band of variable widths, which contrast in tone to the immediately adjacent areas.
- d) Lines of variable length, straightens and continuity as set apart by tonal contrasts in the image.
- e) Co-alignment of cultural features, e.g. farms, road patterns, etc. with underlying structural and/or surrounding topographic control.

Complementary survey in selected areas for verification of the interpretation, to study the surface geology to obtain additional information and to conduct geophysical studies. In study area, the major trending of lineaments are running northwest and the minor is northeast. All the agriculture activities are located within Wadi Malal itself. Figures 4.6 and 4.7 shows the major lineaments in the study area.

The lineament mapped for this investigation can be used with independently collected geologic and hydrologic data to interpret the groundwater flows system in Wadi Malal or in regional extensive aquifers.

4.4.2 Drainage pattern

Bokhari (1988, 1991, and 1993) studied the drainage system around Al Madinah using LANDSAT TM data. He found the drainage system can generally be divided into two groups as follows:

- (1) The drainage in the basement rocks is mainly tectonically controlled by N-S faulting and hence fracturing in E-W and others directions. Wadi Malal is an example and most of the drainage follows the lineaments direction.
- (2) The Harrat Rahat basalt plateau drainage system.

In order to detect the drainage pattern two different image processing techniques were applied to the satellite images. The first, IHS transformation, second is the principal component (Figures 4.3 to 4.5). In those images, it is very easy to locate the major and minor channels. Those images used in this study for the hydrological study and for locating the best area for further geophysical investigations.

4.4.2 Drainage pattern

Bokhari (1988, 1991, and 1993) studied the drainage system around Al Madinah using LANDSAT TM data. He found the drainage system can generally be divided into two groups as follows:

- (1) The drainage in the basement rocks is mainly tectonically controlled by N-S faulting and hence fracturing in E-W and others directions. Wadi Malal is an example and

4.5 Recommendation

The most prospective area selected on the basis of lineaments and drainage pattern maps (Figs 4.1-4.7) and confirmed by field visit has been recommended for geophysical investigation.



Fig. 4.1 Linearly stretch false colour composite of TM bands, 7.4 and 2 in red, green and blue cover, wadi Malal.



Fig. 4.2 High pass filtered of TM band image for wadi Malal.

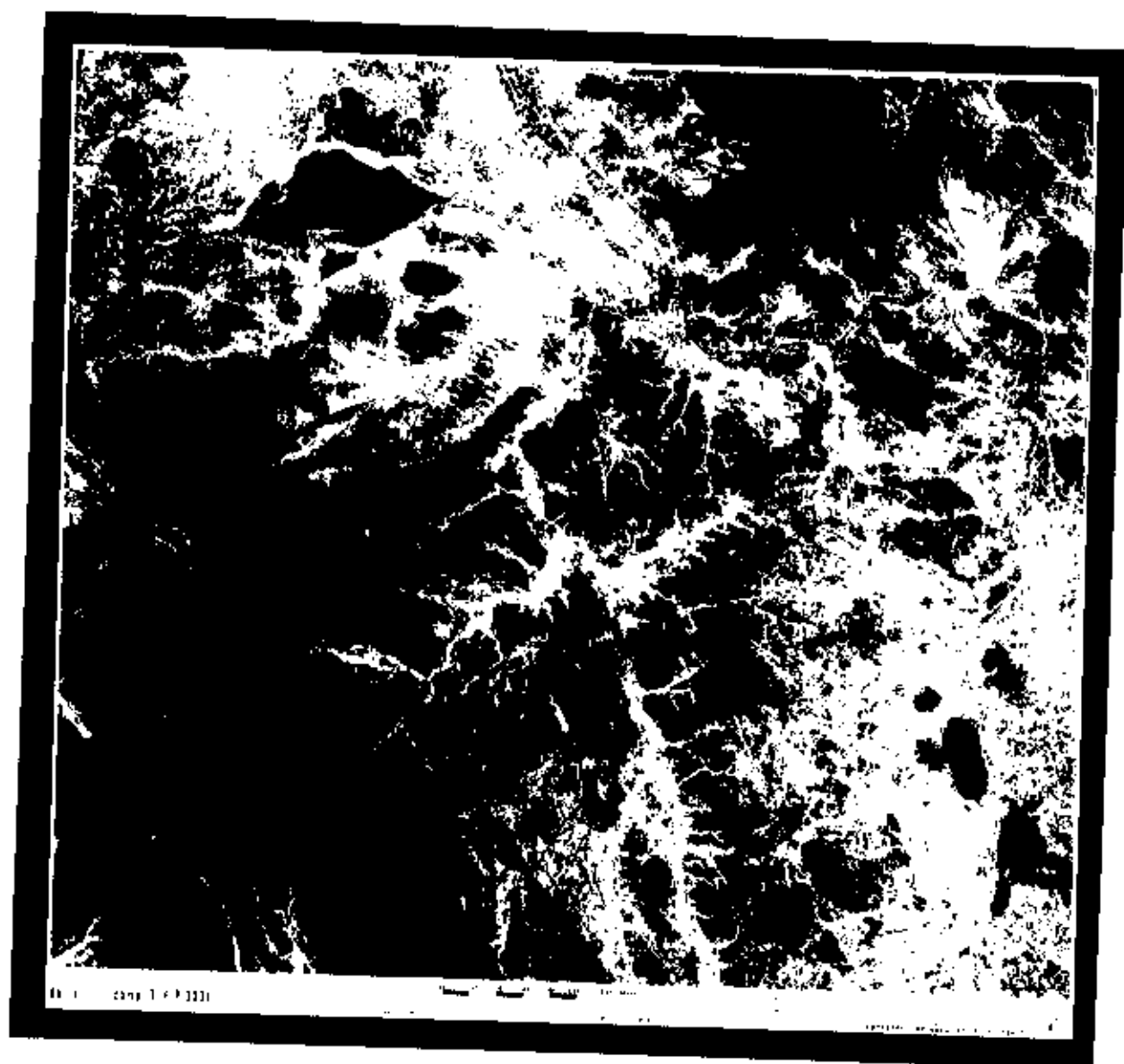


Fig. 4.3 Filtered image (3x3) for third component 1 of principal component (band 7, 4, 2). Showing the drainage pattern of wadi Malal.

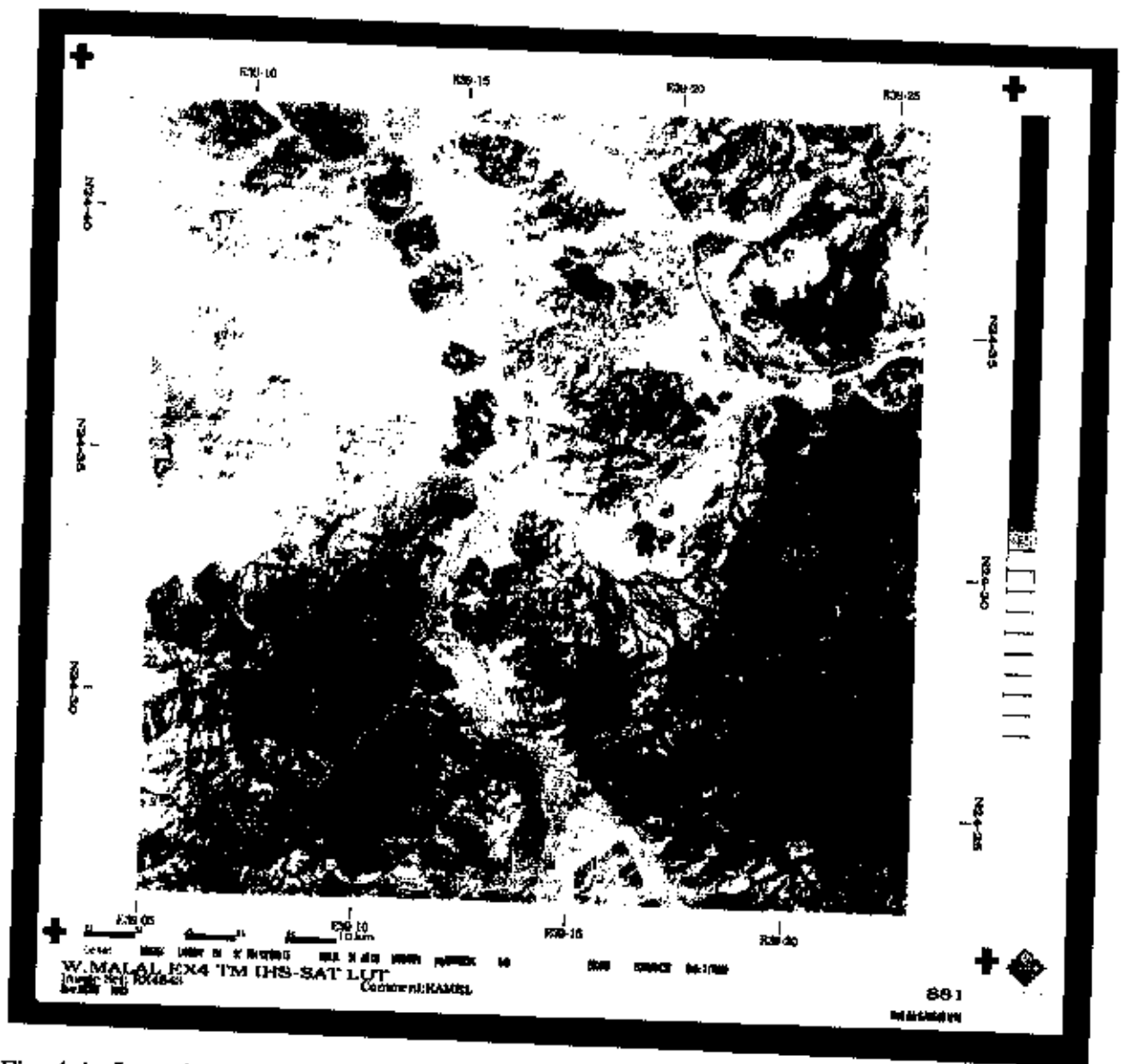


Fig. 4.4 Intensity Hue Saturation (IHS) processed image for wadi Malal (northern part).
Showing the drainage channels.

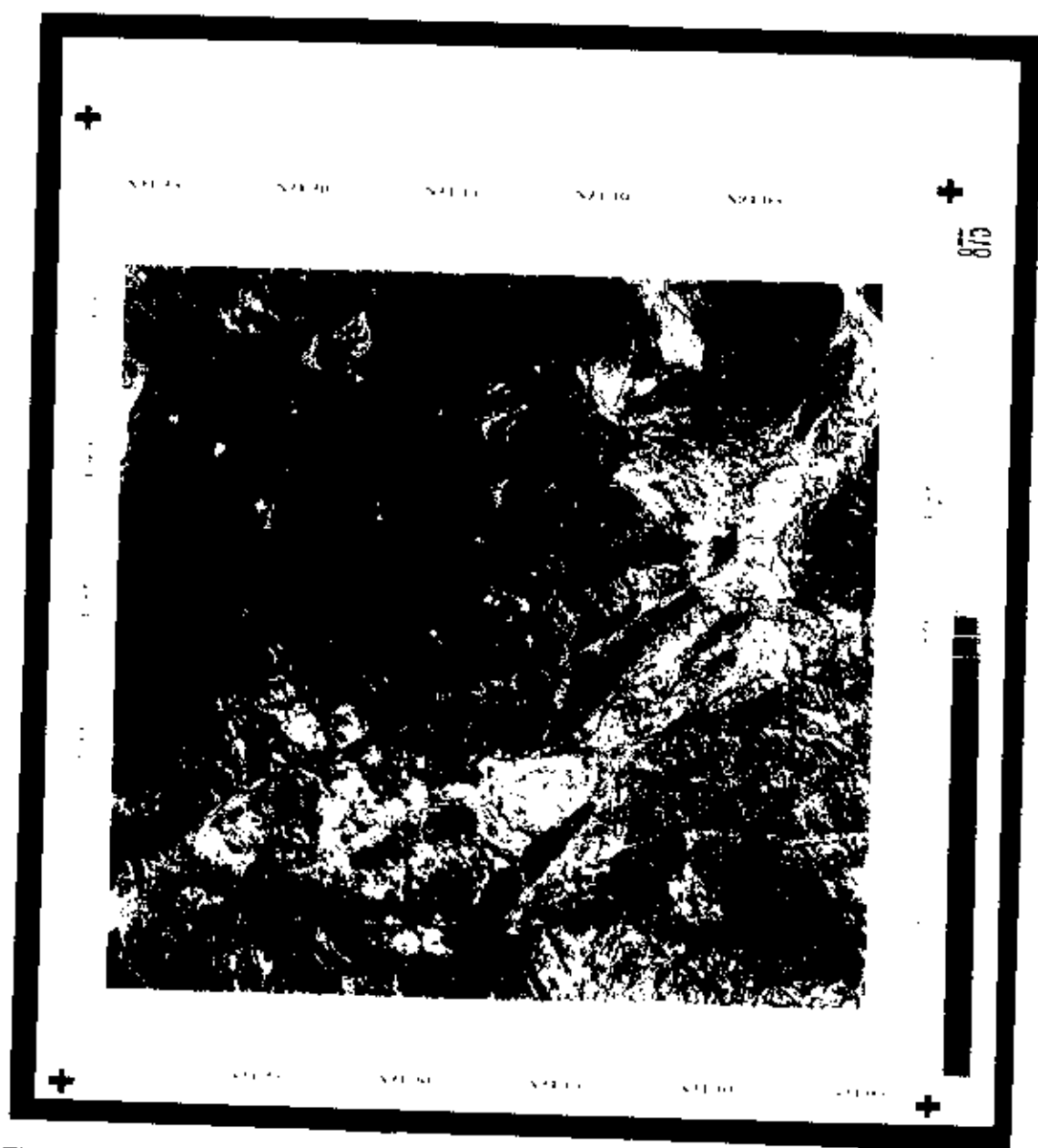


Fig. 4.5 Intensity Hue Saturation (IHS) processed image for wadi Malal (southern part).
Showing the drainage channels.

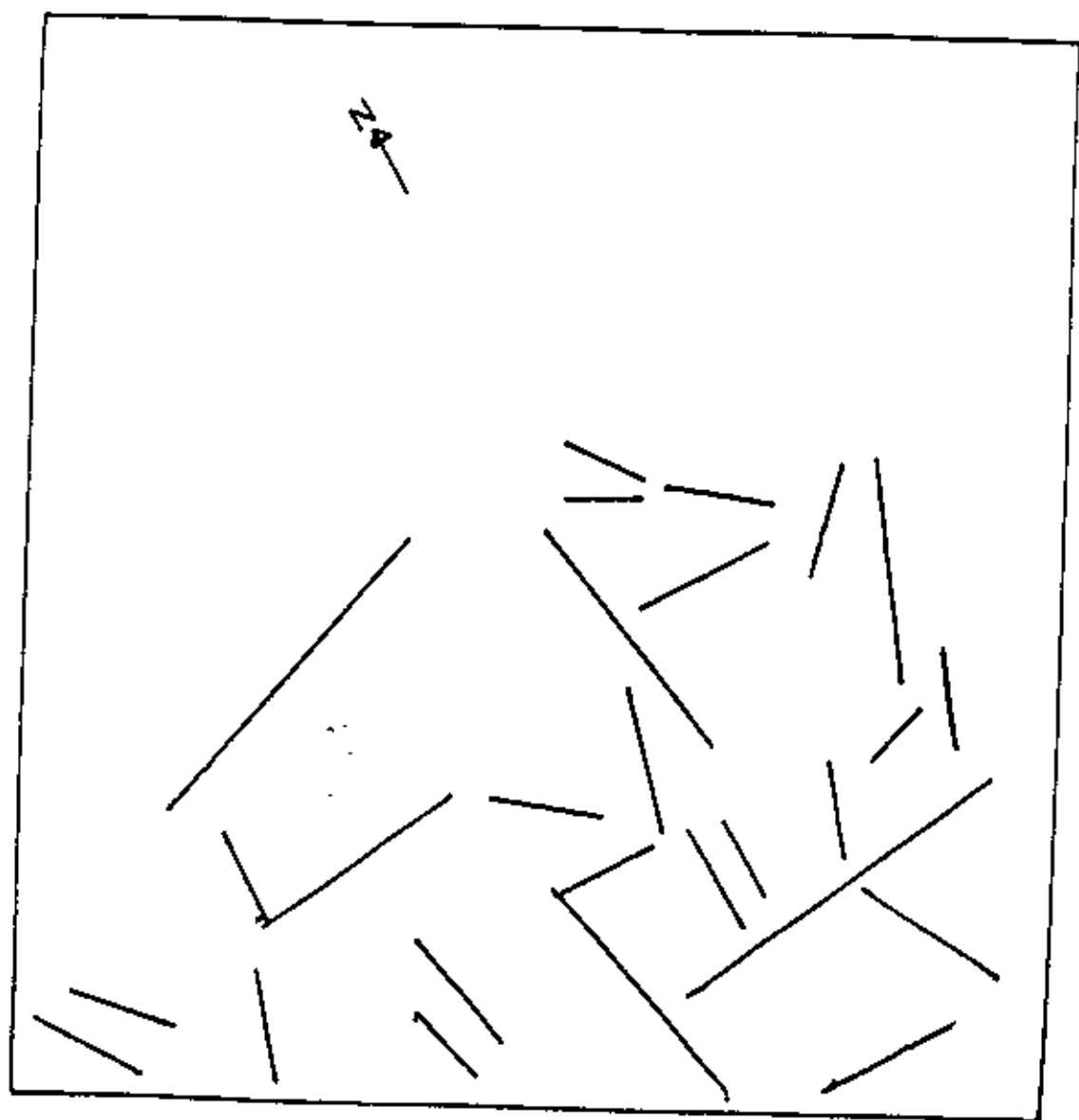


Fig. 4.6 Preliminary lineaments map for northern part of wadi Malal.

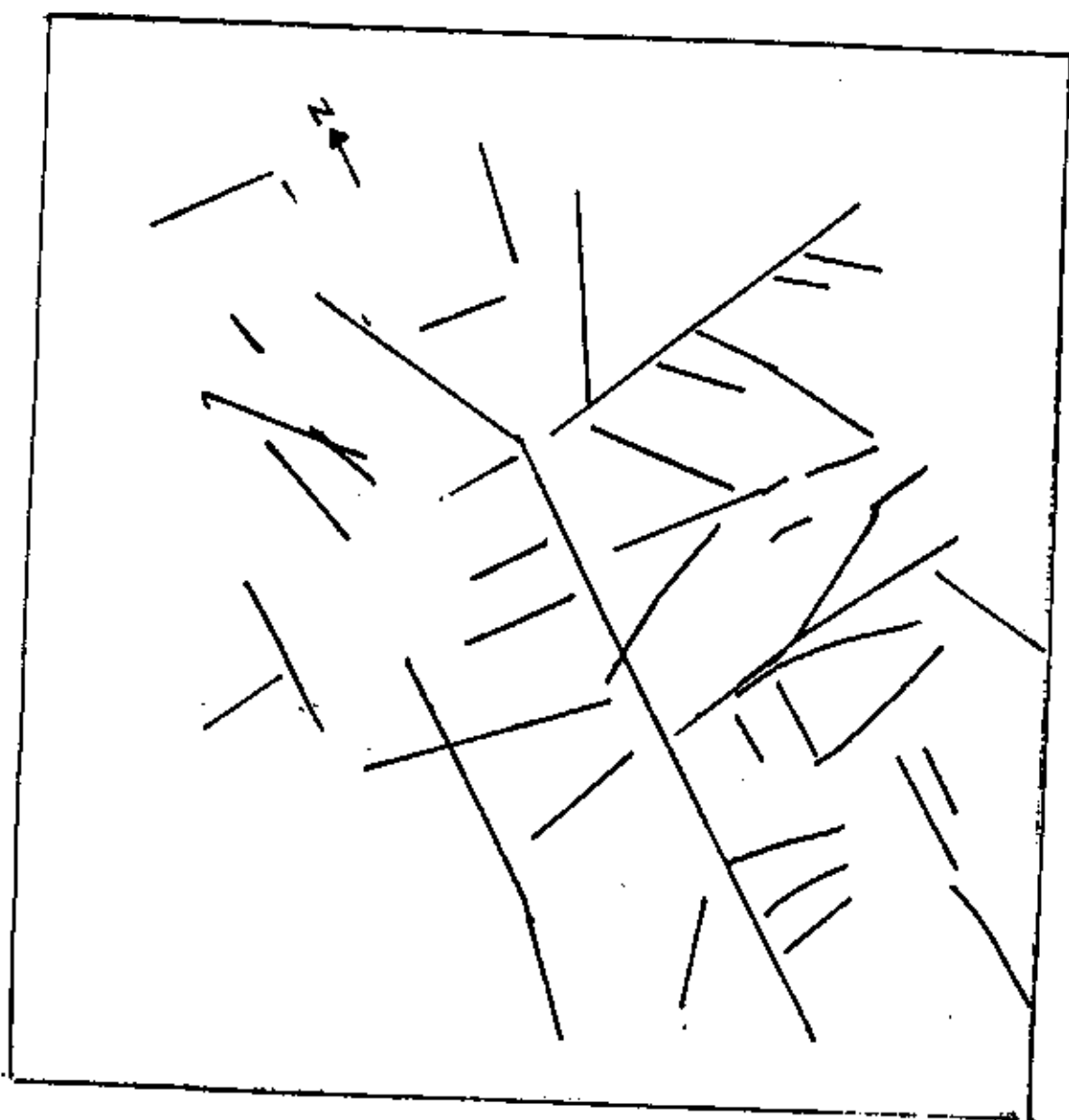


Fig. 4.7 Preliminary lineaments map for southern part of wadi Malal.

Table 4.1 Thematic Mapper Spectral Bands (From Lillesand and Keifer, 1987).

BAND	WAVE LENGTH (m)	NOMINAL SPECTRAL LOCATION	PRINCIPAL APPLICATION
1	0.45 - 0.52	Blue	Designed for water body penetration, making it useful for coastal water mapping. Also useful for soil/vegetation discrimination, forest type mapping, and cultural feature identification.
2	0.52 - 0.60	Green	Designed to measure green reflectance peak of vegetation for vegetation discrimination and vigor assessment. Also useful for cultural feature identification.
3	0.63 - 0.69	Red	Designed to sense a chlorophyll absorption region aiding in plant species differentiation. Also useful for cultural feature identification.
4	0.76 - 0.90	Near-infrared	Useful for determining vegetation types, vigor and biomass content. For delineating water bodies, and for soil moisture discrimination.
5	1.55 - 1.75	Mid-infrared	Indicative of vegetation moisture content and soil moisture. Also useful for differentiation of snow from clouds.
6	10.4 - 12.5	Thermal - infrared	Useful in vegetation stress analysis, soil moisture discrimination and thermal mapping application.
7	2.08 - 2.35	Mid-infrared	Useful for discrimination of mineral and rock types. Also sensitive to vegetation moisture content.

GEOPHYSICAL SURVEYING OF WADI MALAL

5.1 Introduction

The hydrogeophysical investigation plays a very important role in the assessment of groundwater in Wadi Malal since there is a considerable lack of hydrogeological and hydrological information. Significant and detectable contrast in resistivity values of the lithological units have enabled the application of electrical resistivity and ground magnetic method.

In order to understand the subsurface hydrogeology conditions, the main objective of this study is to investigate the subsurface structural features obtained from the resistivity (VES & HEP) and magnetic data to delineate any potential water-bearings' fractures in the bedrock.

This study presents the applications of Zohdy and Bissorf (1989) n-layers model and layering model (Parasins 1979) to VES sounding to produces the correspondence subsurface resistivity sections. In addition, the subsurface cross section was implied to reveal more information about the subsurface lateral variations.

The results obtained from horizontal electrical profiling (HEP) in the area between M3 and M4 were also presented in this report to indicate any horizontal variations or subsurface hidden faults.

To determine the depth to the basement, for magnetic profiles were also carried out the sites of VES, namely M3, M5, M6 and M7.

5.2 Field work and data treatment

In order to delineate the geometry of the aquifer and to determine the subsurface geological and hydrological conditions, the resistivity method was carried out applying two different electrode spacing arrangements, namely Schlumberger and Wenner to create vertical electrical soundings (VES) and horizontal electrical profiling (HEP) respectively. In

addition, ground magnetic surveying was also carried out in some locations of VES (M3, M5, M6 and M7).

5.2.1 Resistivity surveying procedure

The object of VES is to deduce the variation of the resistivity with depth and correlate it with the geological information in order to infer the depth and the resistivities of the layers present.

The ground geophysical field work carried out in the wadi alluvium plain, consisted of 8 VES lines perpendicular to the trend of Wadi Malal, namely M1, M2, M3, M4, M5, M6, M7 and M8, (Figs 5.1 and 5.2). Each line consists of several soundings as indicated in the figures 5.3, 5.4, and 5.5 and in appendix 5A.

An ELREC-T was used to obtain the measurement of VES and HEP. The maximum current electrode spacing ($AB/2$). In the Schlumberger arrangements reached 300 meters, while the intensity of the measurement was about 7 reading per decade at $AB/2$ values of 1.5, 2, 3, 4, 6, 8, 10, 15, 20, 30, 40, 60, 80, 100, 150, 200 and 300 m.

Most field curves were composed of only two or three segments. The first segment obtained by expanding $AB/2$ from 3-10 m with $MN/2$ held fixed at 0.5m. The second segment expands from $AB/2$ at 10-40m and $MN/2$ at 3m. The third segment expands from $AB/2$ at 40-300m and $MN/2$ varies between 10-30m.

Some sounding curves indicated noise interference, particularly at larger $AB/2$. The main causes of the such noises could be due to the low power of the instrument used in this survey at $AB/2 > 200$ m, which can not provide sufficient signal strength to exceed the required signal to noise ratios. The noise also increases when the current passes through good conductor (e.g. clays).

The following procedures were applying to introduce the possible correction to the resistivity curves.

1. Correction of VES measurements to satisfy /Schlumberger configuration. The recovery of such measurement was achieved by testing the appropriate geometrical factor for AB and MN .

2. Rejection of distinct major noise measurements associated with extremely small $MN/2$ and large $AB/2$.
3. Careful interpolation between widely spaced points on the log-log plots, especially at small $AB/2$ values in each decade.
4. Rejection of improper overlapping measurements curves at the same $AB/2$ values when increasing $MN/2$.

The apparent resistivity values computed in the field were reduced using automated inversion computer programs (Zohdy and Bisdorf 1989; and Parasins 1979) to allow either automatic correction or user-defined corrections. The final corrected resistivity curves were redigitized for subsequent data analysis and interpretation.

The first techniques adopted by Zohdy and Bisdorf 1989, used to obtain the so called n -layers models equivalent to each of the corrected apparent resistivity sounding curves. It does not require input model to start the automatic iteration for calculating the final model. Instead the number of $AB/2$ in a sounding is considered as the number of the layers while the apparent resistivity values are considered as the equivalent input resistivity for each layer. The resistivity values and sampling intervals on the curves were used automatically to create the first approximation of the corresponding multi layer model. Hence, this model has been modified in layers thicknesses and resistivities through a number iterations until the best fit between the calculated curve and the apparent resistivity curves reached (Appendix 5A).

The second technique is based on the mathematical solutions suggested by Parasins (1979) to describe the apparent resistivity curves according to the equation.

$$\rho_a(r) = r^2 \int_0^\infty T(\lambda) J_1(\lambda r) \lambda d\lambda$$

Where:

J_1 : The Bessel's function of order 1;

r : Half electrode spacing ($AB/2$)

$T(\lambda)$: The resistivity transform

ρ_a : The apparent resistivity

The application of this equation is to fit the same layer thicknesses and /or resistivities with the apparent resistivity curves through a number of layers, which described the lithology variation beneath the sounding site. The number of layers is related mainly to the geological layers that might occur beneath the sounding and not to the number of resistivity measurements in the sounding as considered in the Zohdy method. The advantage of this method is that it can be expressed directly using the lithological layering model in a straight forward manner and its interpretation does not require a high skill as does the Zohdy method.

VES curves were subjected to both techniques of sounding analysis. A multi layer and model and absolute layering model corresponding to each sounding were then obtained using advanced software (Figs. 5.3, 5.4, 5.5, and appendix 5A)

In addition, 10 HEP were also carried out using Wenner configuration in the area between M3 and M4 perpendicular and parallel to the trend of the wadi with 30m station interval along each profile. The distance between the adjacent parallel HEP was 50m. The Wenner arrangement was used in HEP to detect lateral variations in the resistivity and to mark the structures with near-vertical boundaries, such as faults, dikes and fractures.

5.2.2 Magnetic surveying procedure :

The magnetic method involves measurement of the directions, gradient or intensity of the earth's magnetic field and interpretation of variations in these quantities over the area of investigation.

There are very specific criteria that need to be considered when carrying out a magnetic survey for hydrological or environmental applications.

- a. The estimated depth at which the targets are and their nature.
- b. The precision and accuracy required of the surveys
- c. The orientation of the target

Envi-Mag instrument was used to carry out magnetic surveying profiles perpendicular to the Wadi Malal and superimposed over VES sites, namely (M3, M5, M6, and M7) with a distance interval of 5m between the two adjacent stations (Appendix 5B).

5.3 Data analysis and interpretation

5.3.1 Vertical Electrical Sounding (VES)

The general features of the interpreted resistivities in figures. 5.6 - 5.17 ranged from low ($< 20 \text{ ohm.m}$), to high ($> 150 \text{ ohm.m}$) Specifically, on the basis of typical resistivities of materials in similar geological environments, the interpreted resistivity ranges in Wadi Malal can be classified into three geoelectric layers (GEL) as follows:

GEL 1 with high resistivities of 150 to 300 ohm.m

GEL 2 with low resistivities of 10 to 30 ohm.m

GEL 3 with moderate to high resistivities of 50 to 150 ohm.m

Boundaries between geoelectric layers (GEL) were determined by the midpoint method. The boundary separating the shallow, high resistivity zones from the shallow, low resistivity zones were determined by finding the mid point between the maximum value of the first peak and the minimum value of the trough. Except for the lower limit of the deep layer, all other boundaries were determined similarly.

This procedure was used to prepare six lithological cross sections namely, M3, M4, M5, M6, M7 and M8 (Figs. 5.6, 5.8, 5.10, 5.12, 5.14, and 5.16) respectively.

Sections M3 of figures 5.6 and 5.7 consist of the results of VES M3.1-M3.8. The dry alluvium near the surface of the top of 5-20 is characterized by high resistivity values (150 to 350 ohm .m) The cross section also reveals the extent of the water bearing layers along the profile below the dry alluvium. This layer is associated with the low resistivity values (10-30 ohm.m) at depth ranging from 20 to 60 m. The clay content decreases beneath VES 4 and 5. This section also demonstrated lateral lithological variations, such as clay lenses beneath VES 1,2, and 3 at a depth ranging from 15 to 25m having an average thickness of about 10m. This clay layer is associated with the lowest resistivity values in the section ($< 20 \text{ ohm.m}$). The intermediate to high resistivity values (50 to 150 ohm.m) at depths greater than 50m are associated with the weathered bedrock which is believe to contain substantial amount of water in some fractures and joints. The results obtained from four boreholes along the profile of M3 indicate the average depth of the bedrock lies between 55 to 65m and fresh basement

of rhyolite lies beneath bedrock at 65 to 75 m depth which is in good agreement with VES results.

Sections M4 of figures 5.8 and 5.9 consist of the results of VES M4.1-4.3. These sections indicate that the upper surface layer is dry alluvium because it is associated with high resistivity values beneath M4.1 (100-250 ohm.m) and has a thickness of about 8m. The water bearing layer is distinct is obvious beneath sounding M4.2 with moderate resistivity values (20 - 50 ohm.m) reflect lower clays content and lower salinity. The sharp increase of the resistivity values beneath the entire section is probably due to the existence of the bedrock at depth grater than 50m. Cutting from borehole indicates the depth to the weathered bedrock between 60 to 62 m.

Sections M5 of figures 5.10 and 5.11 consist of the result of VES M5.1-5.7. The dry alluvium near the surface at the top of 5 m is characterized by high resistivity values (100-200 ohm.m). The cross section of figure 5.10 also reveals the extent of a water-bearing layer along the profile below the dry alluvium. This layer is associated with the lows resistivity values (10-20 ohm.m) at depths ranging from 30-40 m. The clay content decreases beneath M5.1 and M5.7. Depth to the bedrock ranges from 70-72 m. The section M6 of figures 5.12 and 5.13 consists of the results of VES M6.1 - 6.5. The dry alluvium near the surface at the top of 5 m is characterized by its high resistivity values (150-350 ohm.m). The cross section also reveals the extent of a water-bearing layer along the profile below the dry alluvium. This layer is associated with the lows resistivity values (10 - 30 ohm.m) at depth ranging from 10 - 40 m. This section also demonstrated lateral lithological variations, such as clays content decreases towards M6. This clays layer is associated with the lowest resistivity values in the section (10 ohm.m) The intermediate to high resisitvty values (50-150 ohm.m) at depths greater than 65 m are associated with the weathered bedrock which is believed to content substantial amount of water in some fracture and joints.

The cross section M7 of figures 5.14 and 5.15 consists of the results of VES 7.1-7.4. This section indicates that the upper surface of the sediment is dry alluvium because it has high resistivity values along the profile (150-300 ohm.m) and a thickness of about 20-m. The probable water bearing layers is unsaturated and the amount of water is not promising. This sharp increase in the resistivity values beneath the entire section is probably due to the

existence of the bedrock at depths greater than 60-m. The cross section M8 of figures 5.16 and 5.17 consists of the results of VES 8.1 -8.4. The dry alluvium near the surface at the top of 10 m is characterized by high resistivity values (150-300 ohm.m). This section also reveals that the amount of water is localized and the water bearing layers along the profile below the dry alluvium is unsaturated. The depth of the bedrock ranges between 50-60 m.

Generally, the three-geoelectric sections show three subsurface geologic layers. The upper most layers consist of gravel and unconsolidated dry sediments, which associated with high resistivities. The middle layer composed of clayey and silt- fine materials intermixed with gravel and water. This layer probably constitutes the water bearing rock in the wadi, especially M6 with resistivities range from 10-30 ohm.m. Evidence from these measurements indicates that the water table varies in depths between 50 - 60 m. The unconformable layer between the weathered bedrock and saturated deposit is clearly identified from the sharp contrast in resistivities values above and below it. The lower most layers may represent the weathered bedrock. Depths to the bedrock range from 55-65 m, which underlie by fresh basement layer at depths greater than 80 m.

5.3.2 Horizontal Electrical Profiling (HEP)

In addition to the eight VES curves and contour sections, HEP were completed across the study area perpendicular and parallel to the trend of Wadi Malal. The location of HEP in the area lies between M3 and M4. These profiles were plotted with distance Vs apparent resistivities (Fig. 5.18). The apparent resistivity values are also plotted at their respective stations locations and a contour map with a 5 ohm.m contouring constructed (Fig. 5.19).

The HEP contour map is characterized by a more or less homogeneous resistivity of moderate to high values (40 -300 ohm.m). It is well known in the semi arid areas that the uppermost part of the wadis is characterized by a sequence of dry alluvial deposits (high resistivity) overlying the moist alluvium which associated with a remarkable drop in the resistivities values. Profiles 3,4,6,7, and 8 of figure 5.18 may indicate a hidden fault

between 15-30 m below the surface. There is no other information can be obtained from HEP.

5.3.3 Magnetizing surveying

The two major applications of the magnetic surveys to groundwater studies have been the study of magnetic aquifers, mainly basalt and determination and the configuration of the basement rock underline the water bearing sediments. The study of the basement rock involves determining relief and depth to the surface of the basement at several points.

Interpretations of the magnetic data in terms of geologic features involve in both quantitative and qualitative analysis. The qualitative interpretations involve distinction of structure and the lithostratigraphy. The quantitative interpretation involves defining the shape, position, depth and intensity of the magnetization of the body-causing anomaly.

Theoretically, magnetic anomalies are produced by variations of intensity in the magnetization of the rocks. This magnetization (J) is the sum of induced and remnants magnetization.

$$J = R + KT$$

Where:

R : remnant magnetization

K : magnetic susceptibility

T : total magnetizing force of the earth's magnetic field.

MAGNETIC PROFILE M3:

The results obtained from total magnetic intensity profile in M3 (Fig. 5.20) indicate that the shallow fault line is passing along the strike of Wadi Malal near by station 100m. The total length of this profile is 2100 m with a distance interval of 5 m between the two adjacent stations. A deep fault line located at 1600 m.

In order to determine the precise depth to the basement, the M3 is divided into four segments (Appendix 5C) and subjected to the frequency analysis techniques. Based on magnetic susceptibility values obtained from rock type in the area, we obtained the best-fit correlation coefficient above 85 % between the observed and theoretical curves (Fig. 5.21).

At distance range from 0 - 1600 m shows low magnetic susceptibility values (< 0.002 e.m.u.) Which are indicative of acidic composition (probably granitic rocks). Whereas high magnetic susceptibility values (0.011 e.m.u.) between 1600-2100 m indicate basic to ultrabasic rocks which is believed to be gabbro. The depth to the fresh basement (not weathered) reached a maximum depth of 115 m below the ground surface. The shallowest depths to the basement 37-55 m were located near the flanks of the wadi. This may be the extension of the basement of the outcrop. These depth values confirmed with the previous resistivity contour sections.

MAGNETIC PROFILE M5

The total intensity magnetic profile M5 of a total length of 500 m (Fig. 5.22) reveals that a fault is passing near the end of the profile covering the area at distance between 370 and 450 m. The entire profile was first subjected to the spectral analysis technique (Appendix 5c). The line was divided into two segments and depth values were 73 and 71 m. at the center of each segment.

The obtained geologic model (Fig. 5.23) indicates that the average depth to the basement is 60 m.

MAGNETIC PROFILE M6

The total length of magnetic intensity profile M6 is 1200 m (Fig 5.24). It indicates a very distinct fault at the middle of the profile. The fault zone extends from 550-680 m. Two other faults may also occur at the hills around the wadi between 0-50 m and at 1200 m.

The energy spectrum of the total intensity profile (Appendix 5C) suggests that the profile can be divided into three segments and the energy spectrum of the each magnetic segments was calculated, the calculated depth of each segments indicates that the maximum depth is attained in the fault line in the middle of the profile.

The obtained geologic model reveals a depth of the magnetic basement of about 83 m. The high intensity of magnetic response due to faulting may be attributed to the ultrabasic host rock. The poor fitting between the observe and calculated curves at the middle of the

profile (Fig. 5.25) is probably due to some remnants magnetization still existed in the host rocks.

MAGNETIC PROFILE M7

The total length of the magnetic intensity profile M7 is 600 m (Fig. 5.26). It reveals a fault line extending between 100 and 300 m.

The energy spectrum decay curve of M7 (Appendix 5C) divide the profile into three segments. The obtained indicates a depth of about 59 m to the magnetic basement. Most of the wadi deposits along the profile are underlain by fresh basement of medium magnetic susceptibility values, which are equivalent granetic rocks.

PROFILE	INCLINATIO N	DECLINATION	MAGNETIC FIELD	AZIMUTH	STRIKE
M3	35°	1°	41000 nT	75°	-5°
M5	35°	1°	41000 nT	85°	-5°
M6	30°	1°	41000 nT	60°	-30°
M7	35°	1°	41000 nT	60°	-30°

5.4 Recommendation

On the basis of interpretation of the resistivity and magnetic survey, result the profiles M3, M4 and M5 were selected for the drilling of the wells.

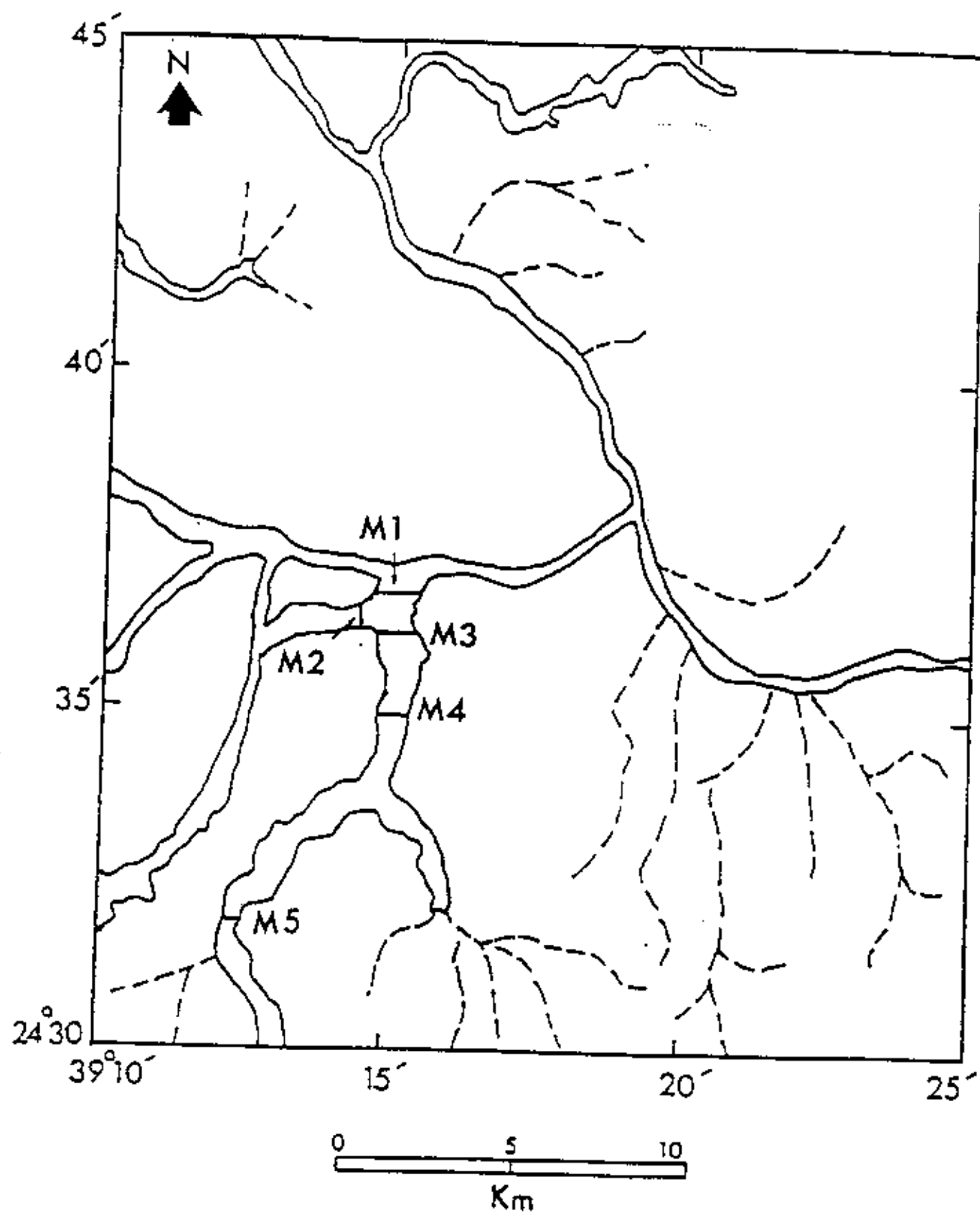


Figure 5.1 Location map of VES points in down-stream of Wadi Malal

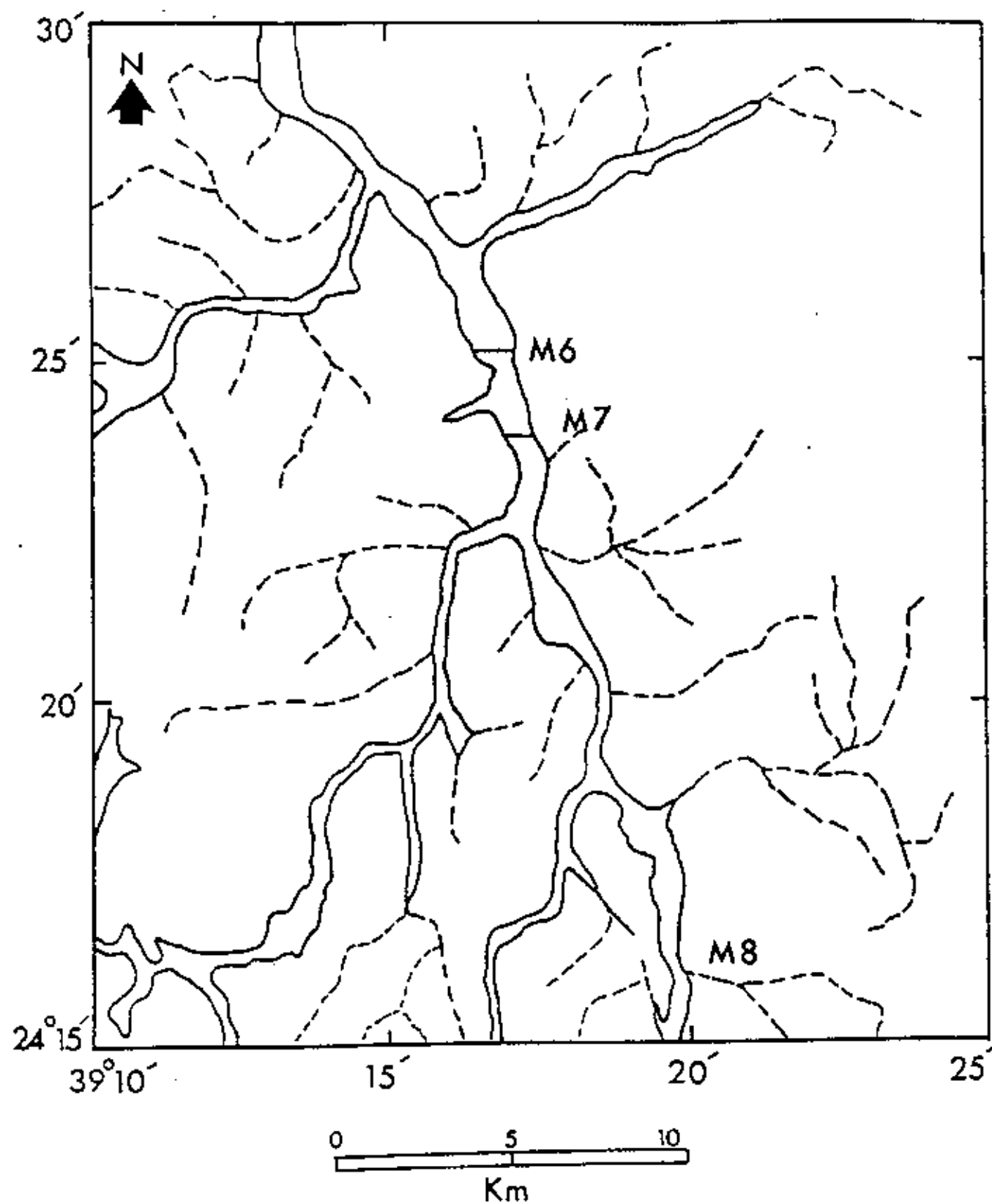
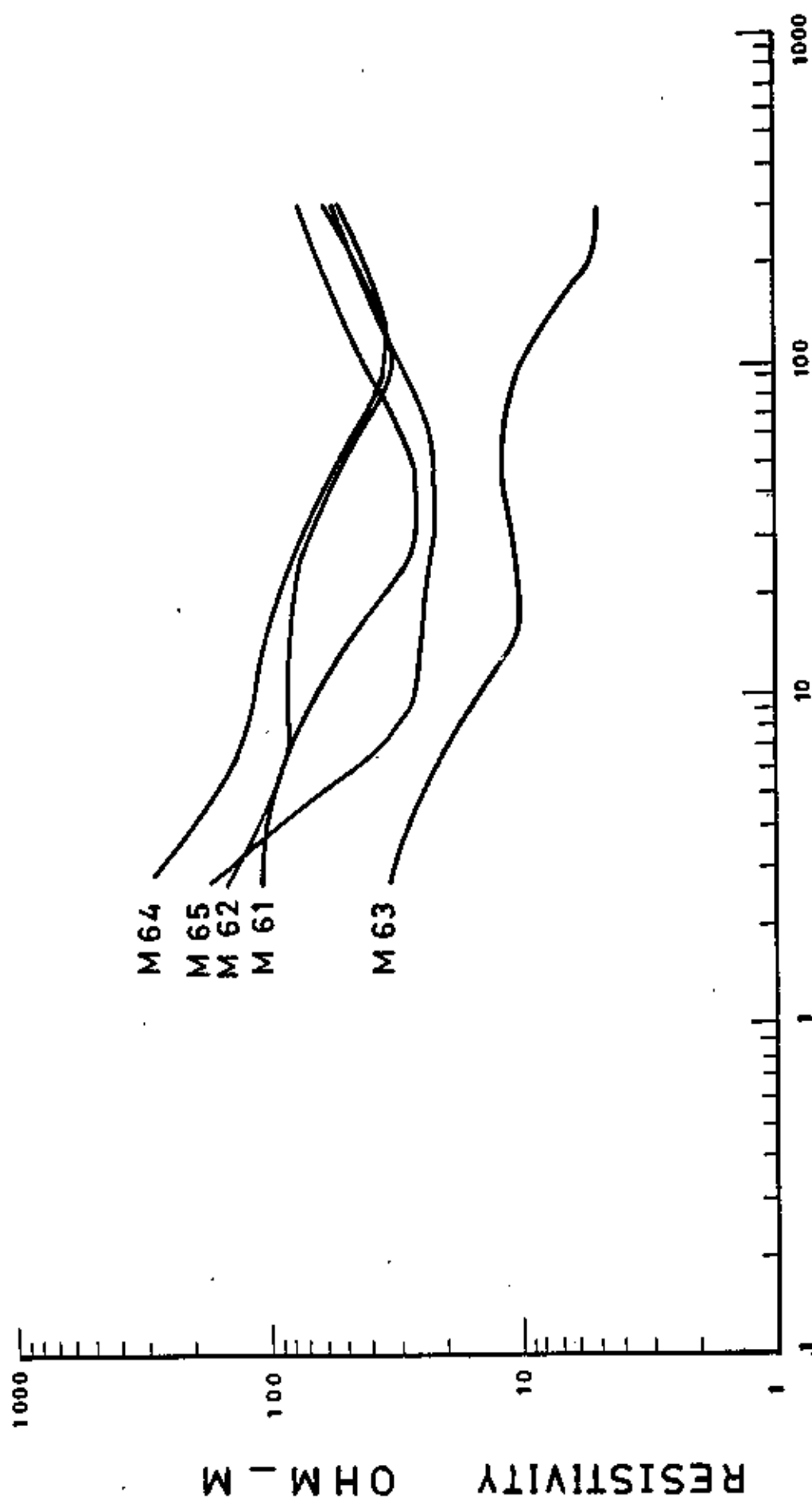


Figure 5.2 Location map of VES points in middle-stream of Wadi Malal



ELECTRODE SPACING (AB/2), OR DEPTH IN METERS

Fig. 5.3 AB/2 Vs. apparent resistivity of M6 profile showing superimposed sounding curves

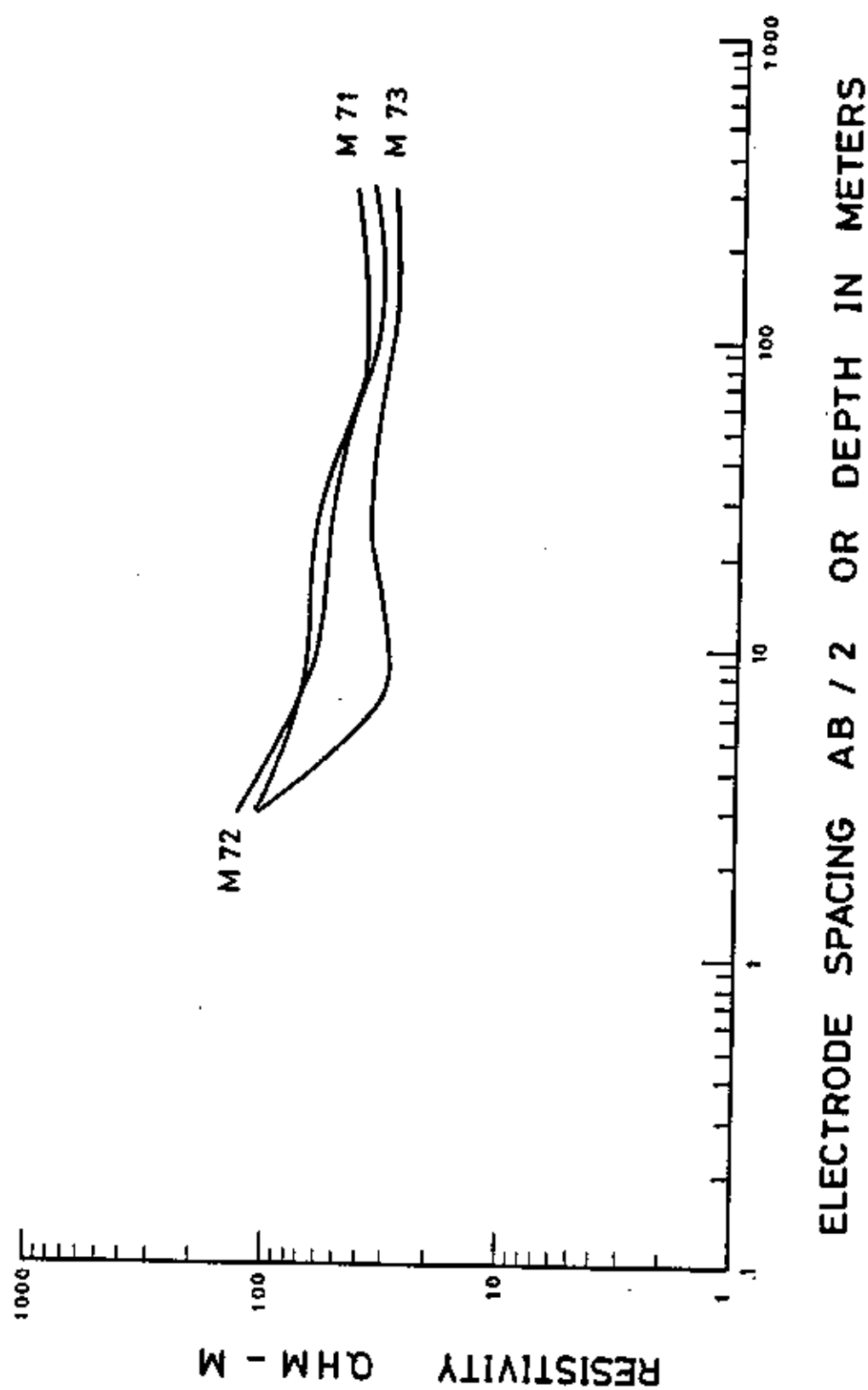


Fig. 5.4 AB/2 Vs. apparent resistivity of M₄ profile showing superimposed sounding curves.

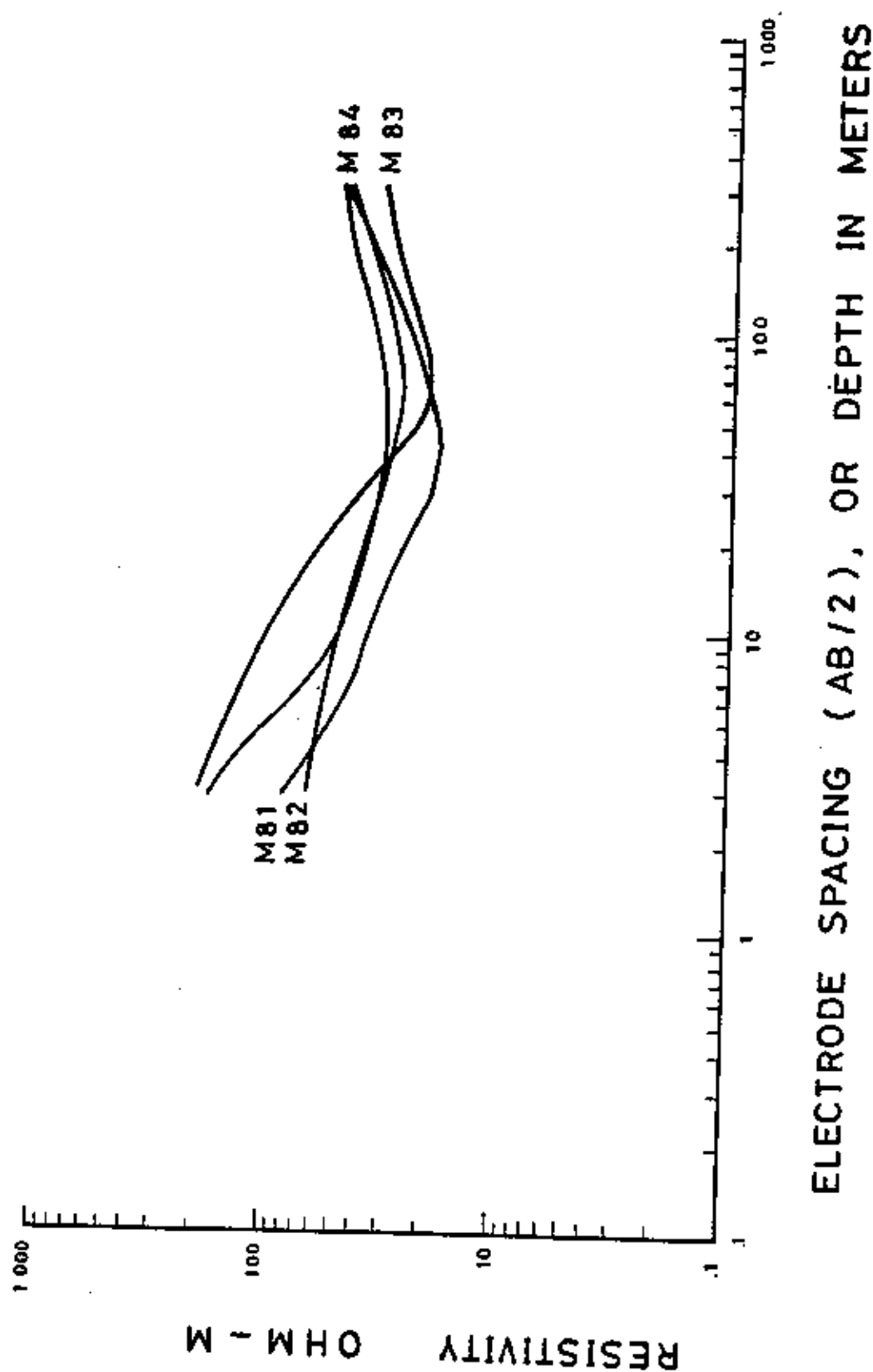


Fig. 5.5 AB/2 Vs. apparent resistivity of M8 profile showing superimposed sounding curves.

PROFILE NO. : M3

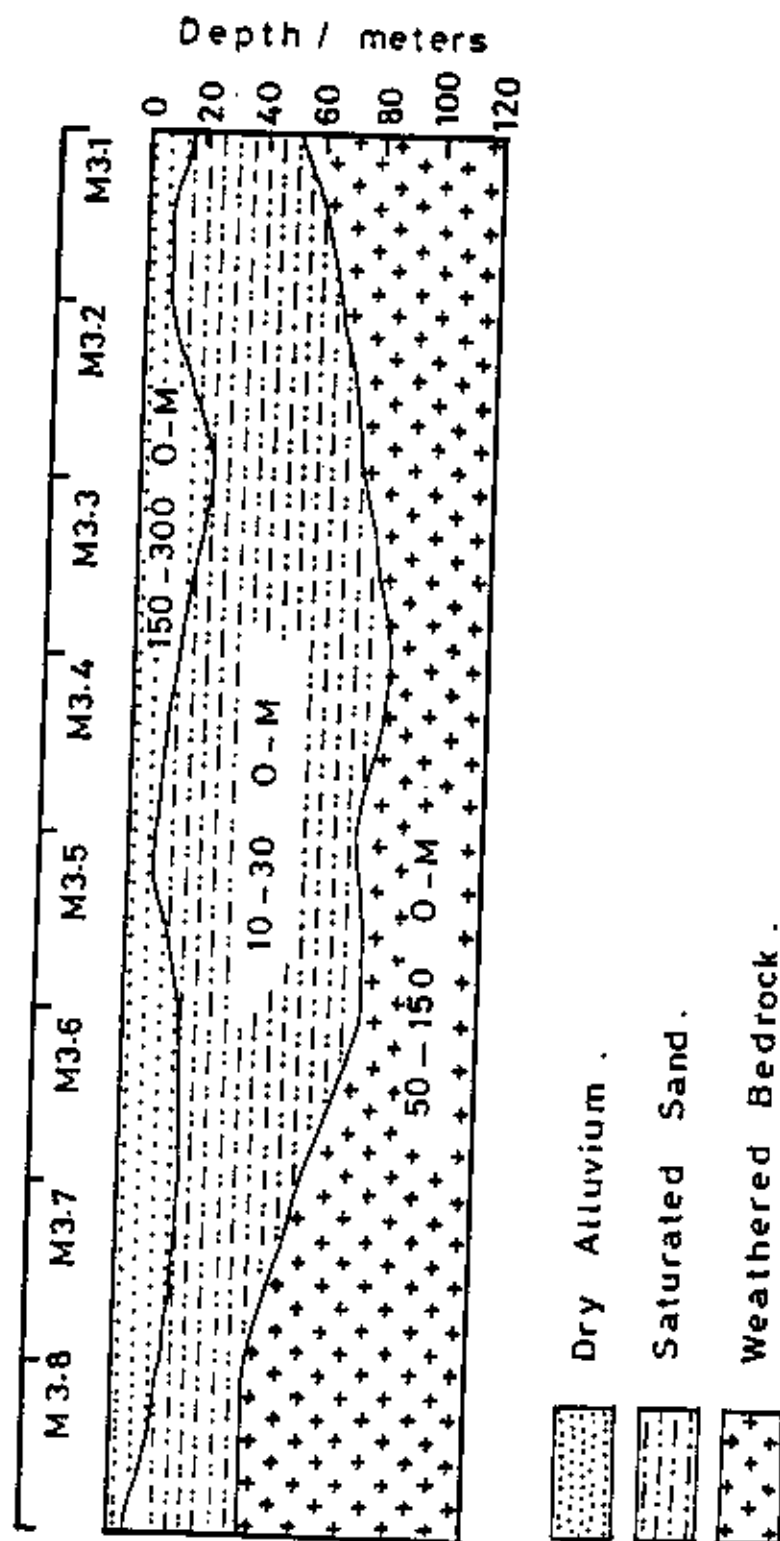


Fig. 5.6. Interpreted subsurface resistivity and equivalent geological sections along profile M3.

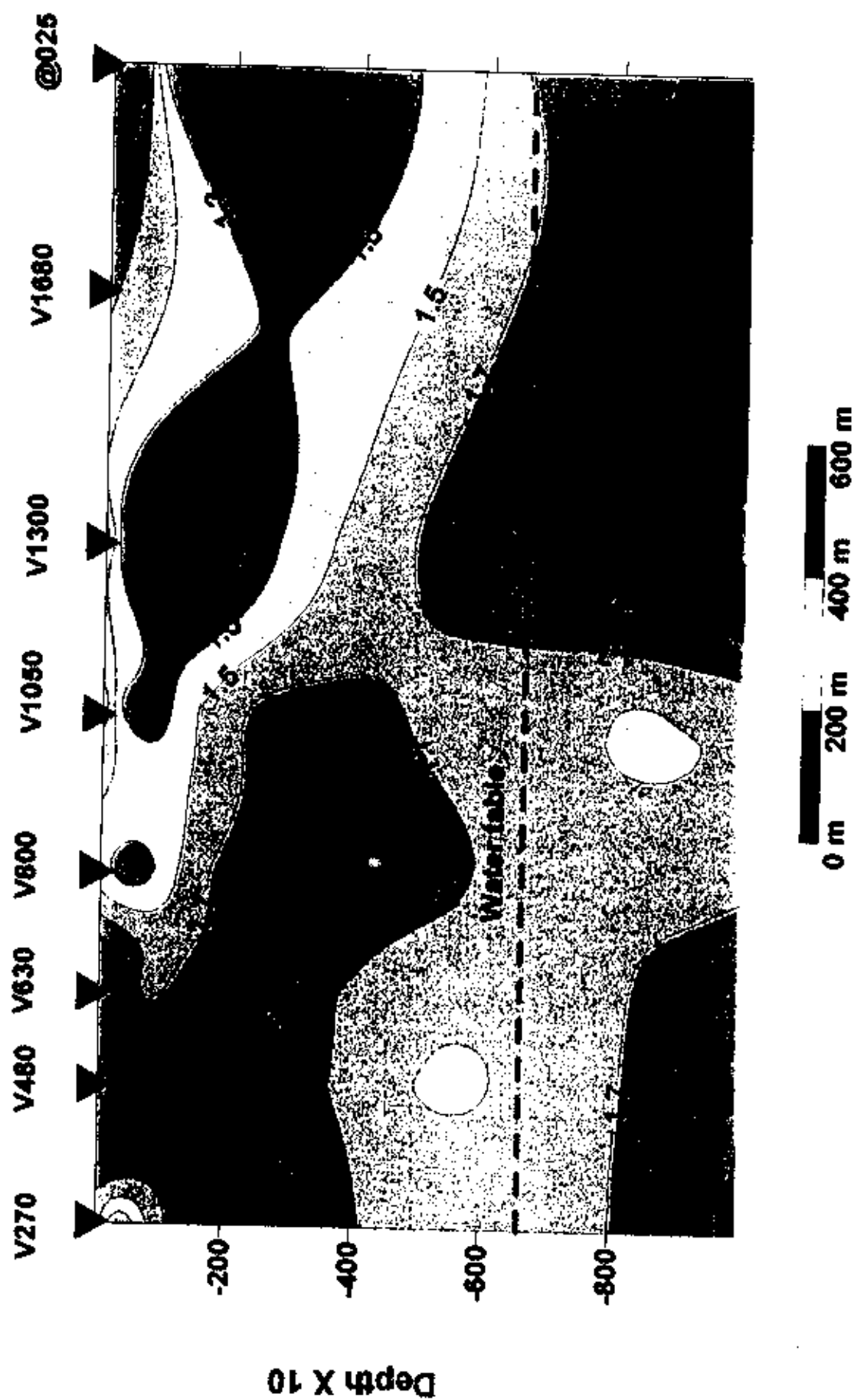
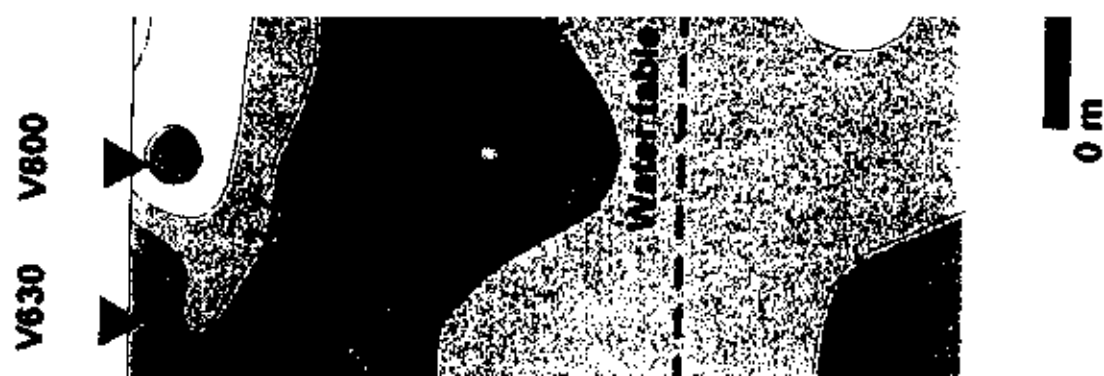


Fig. 5.7. Interpreted resistivity contour section of M3. Contour values are to the power of 10 ($10^{1.4}$, $10^{1.5}$ etc...)



Interpreted resistivity contour section of M3. Contour values are to the power of 10 ($10^{1.4}$, $10^{1.5}$ etc...)

PROFILE NO.: M4

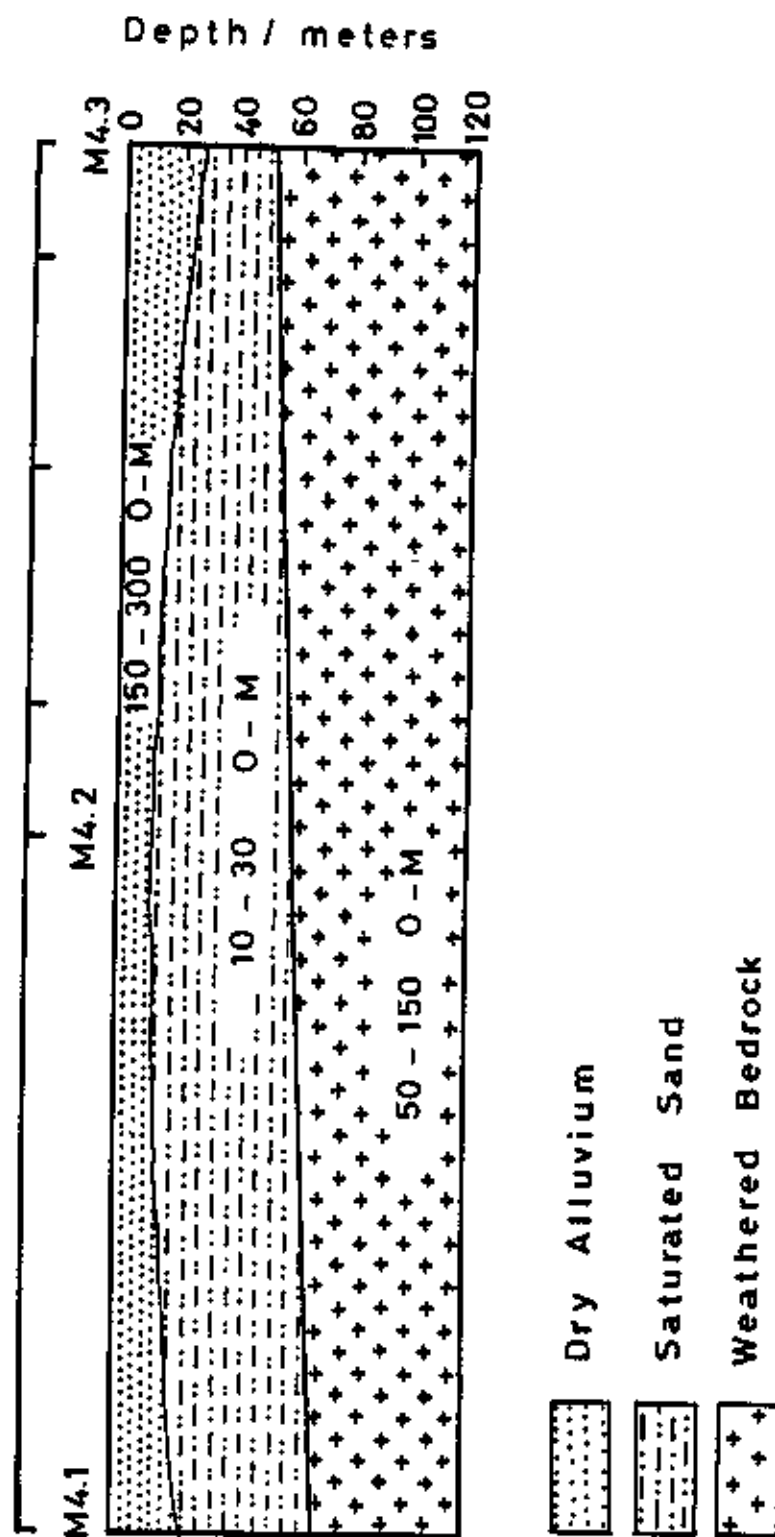


Fig. 5.8 Interpreted subsurface resistivity and equivalent geological sections along profile M4

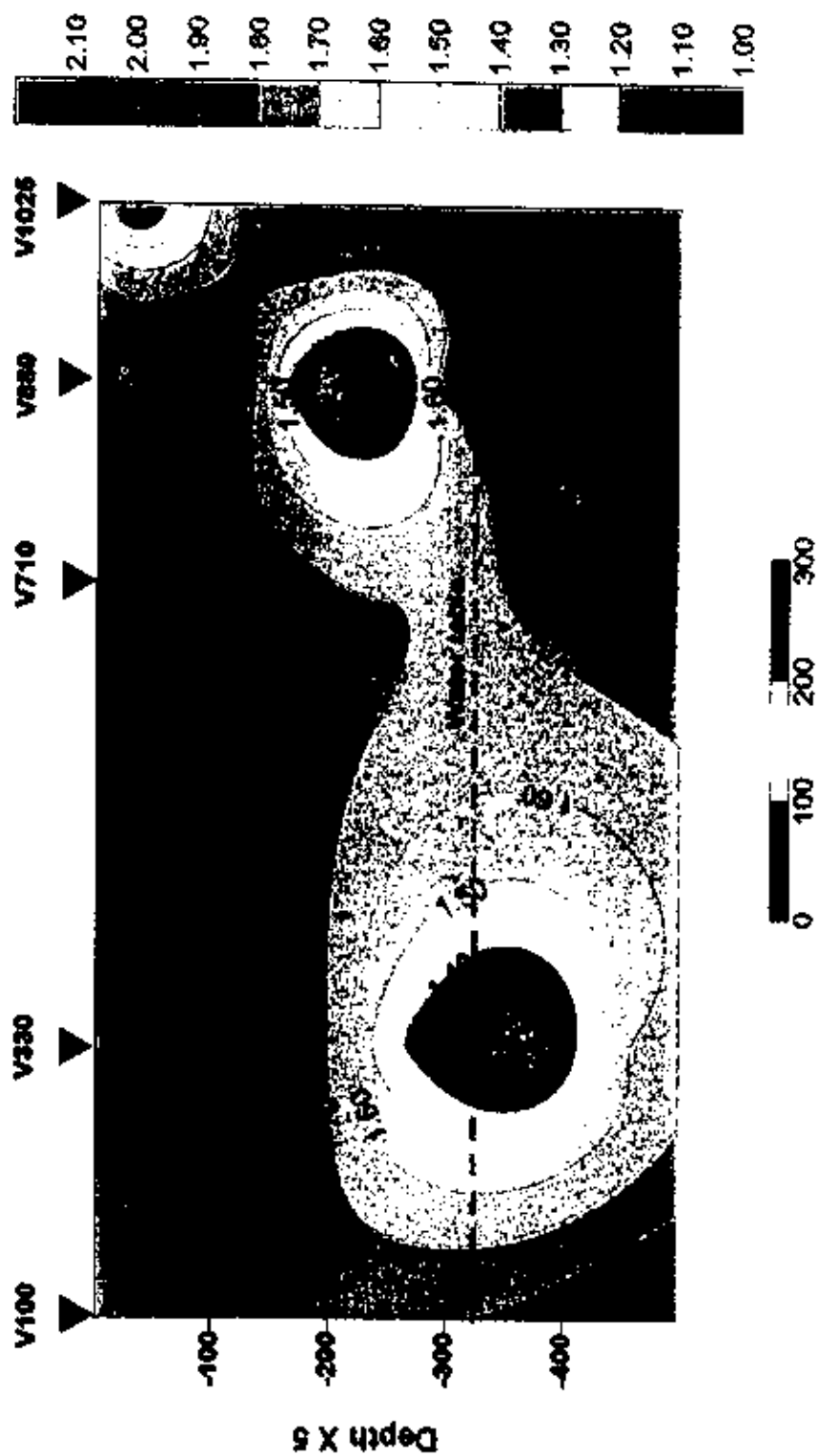


Fig. 5.9. Interpreted resistivity contour section of M4. Contour values are to the power of 10^{11} , 10^{12} , etc...

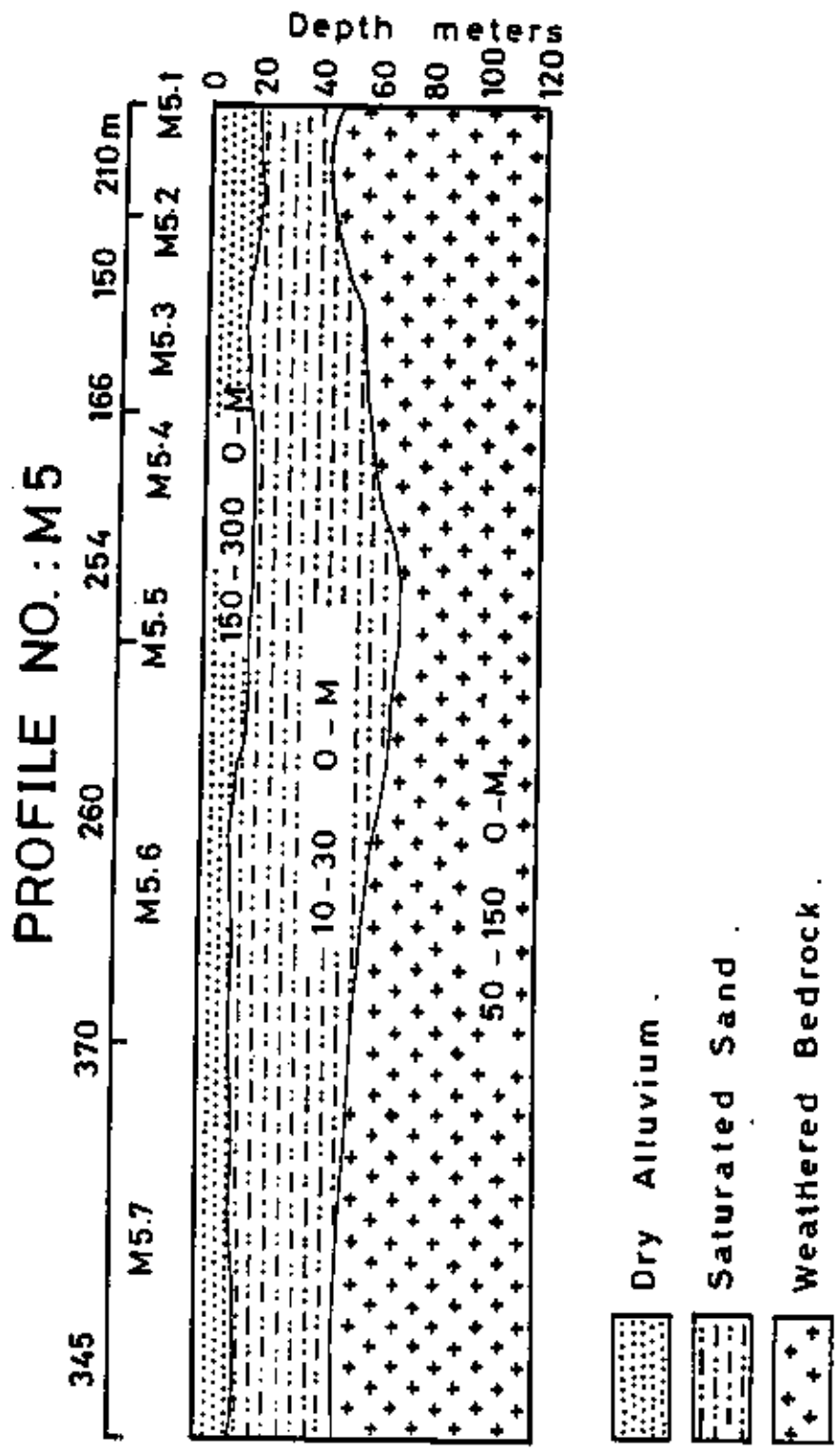


Fig. 5.10. Interpreted subsurface resistivity and equivalent geological sections along profile M5.

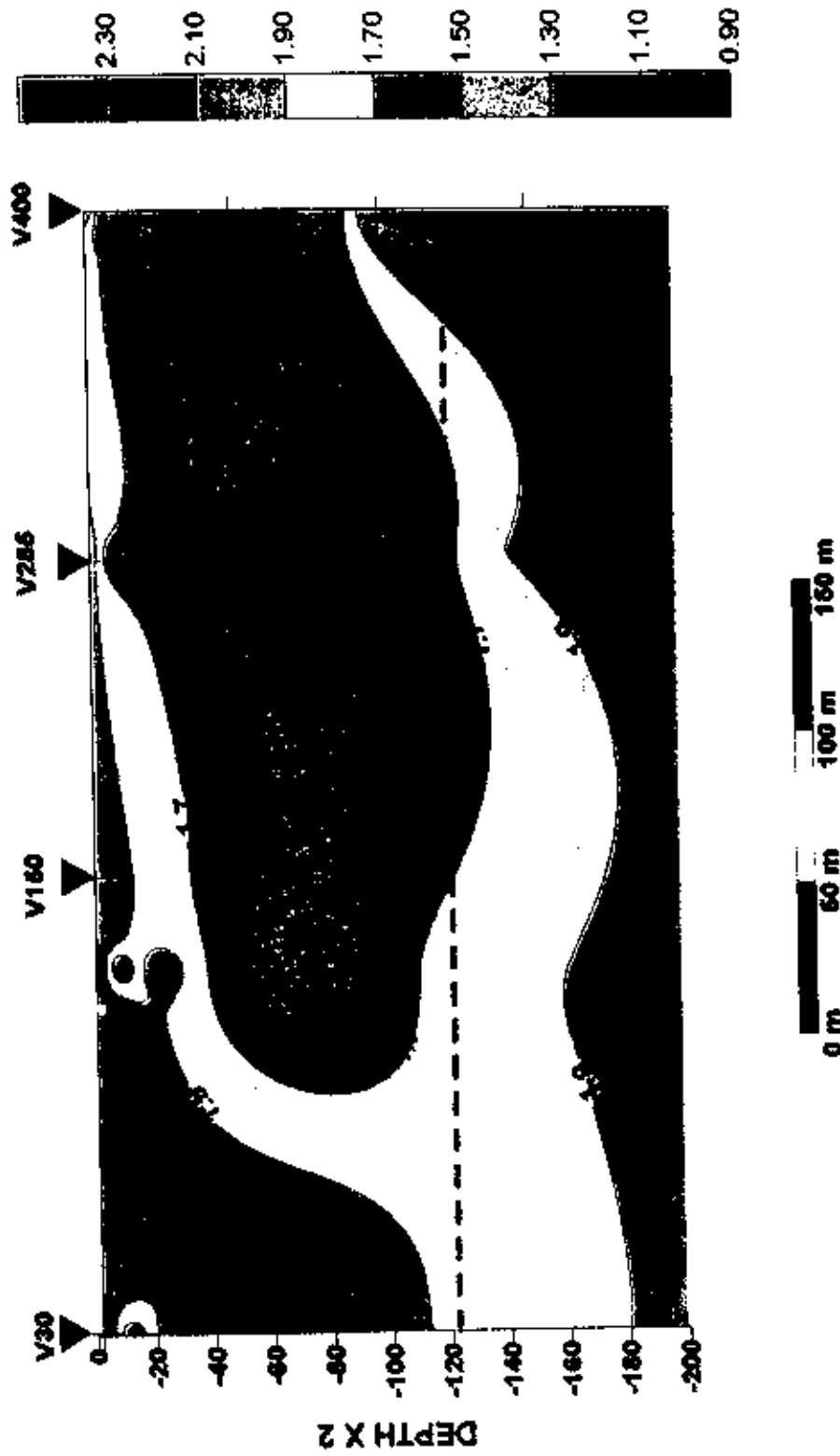


Fig. 5.11. Interpreted resistivity contour section of M5. Contour values are to the power of $10^{1.1}$, $10^{1.3}$ etc...

PROFILE NO.: M6

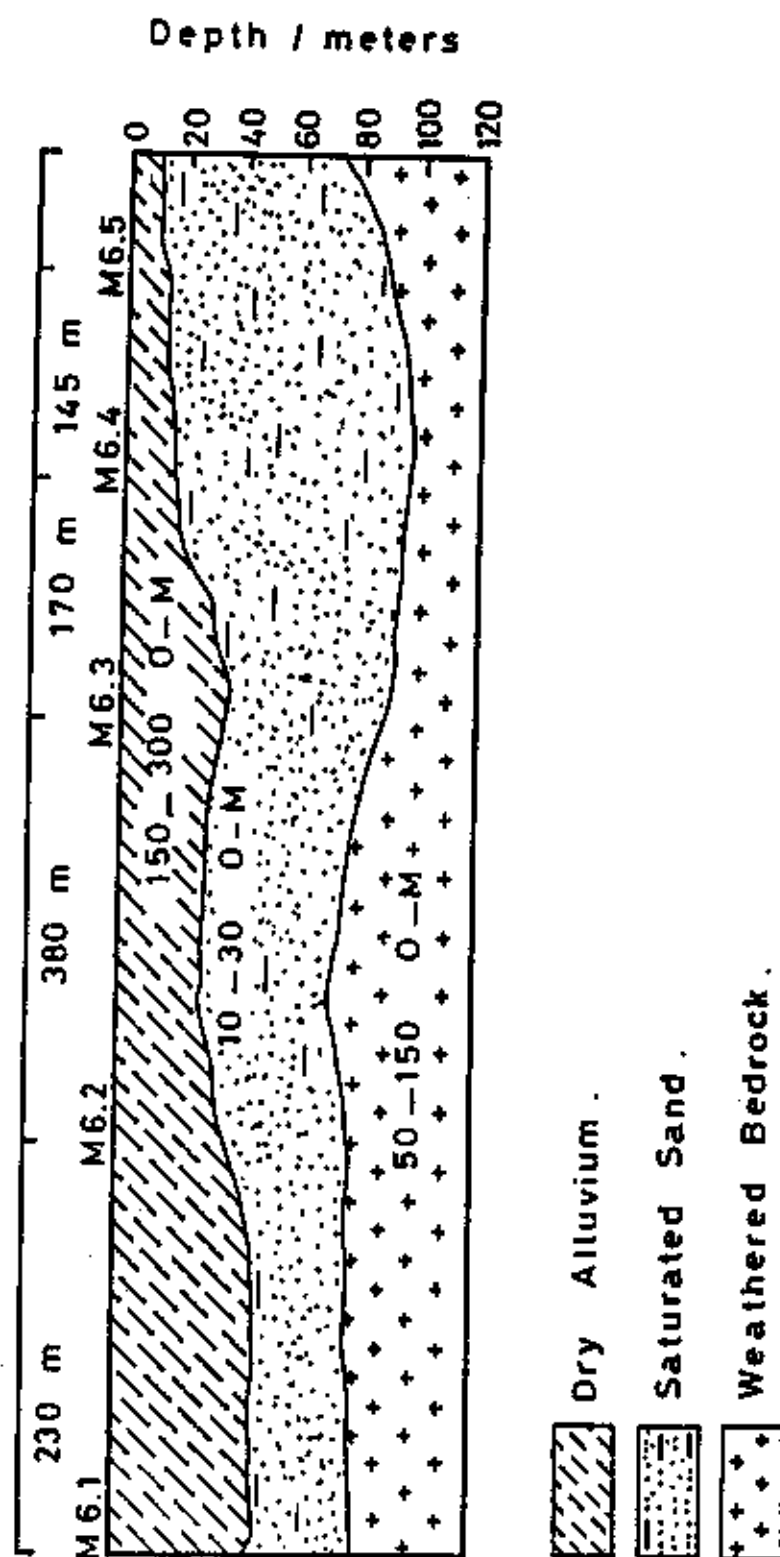


Fig. 5.12 Interpreted subsurface resistivity and equivalent geological sections along profile M6.

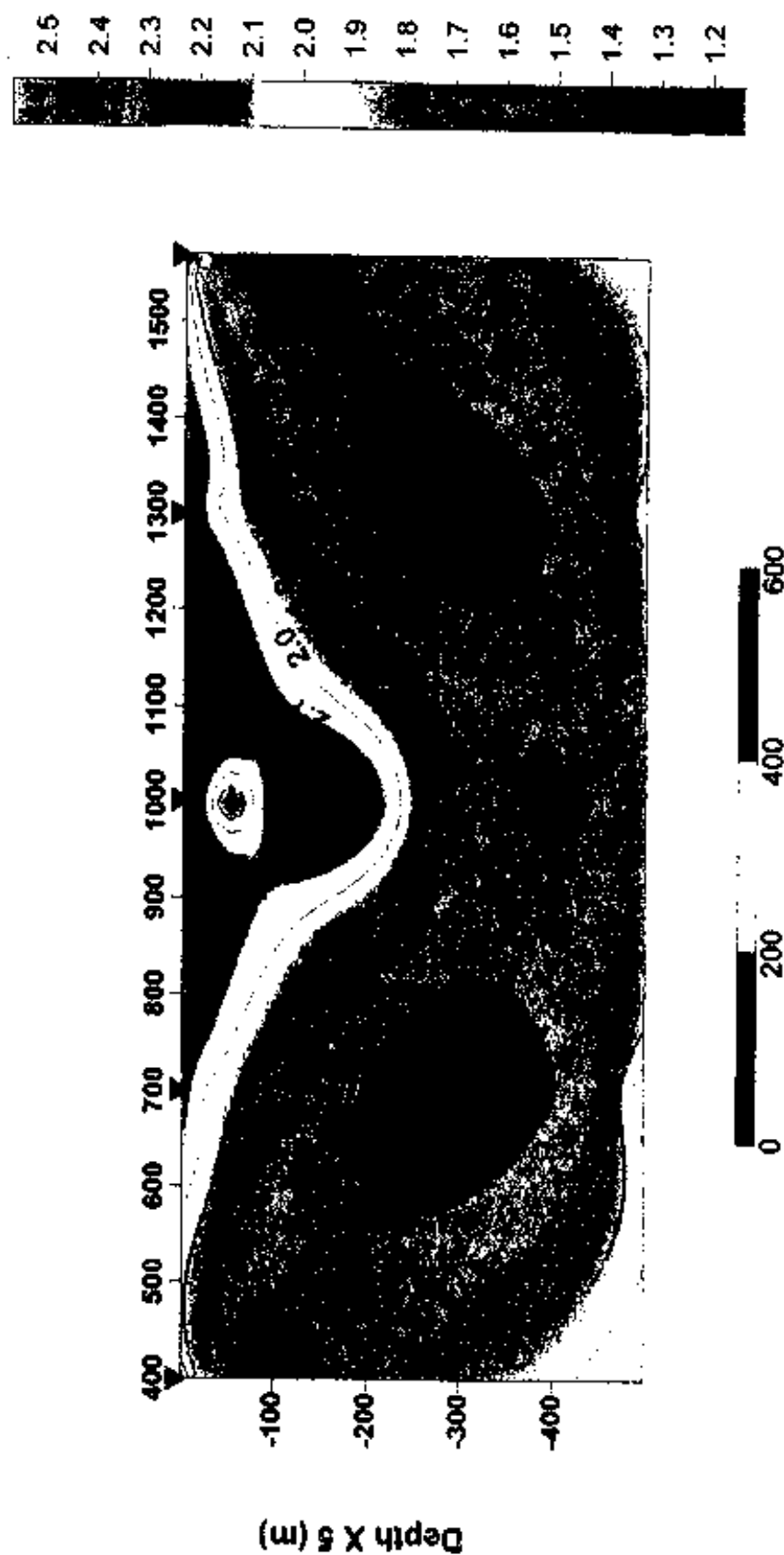


Fig. 5.13. Interpreted resistivity contour section of M6. Contour values are to the power of 10 ($10^{1.1}$, $10^{1.3}$ etc...)

PROFILE NO. : M7

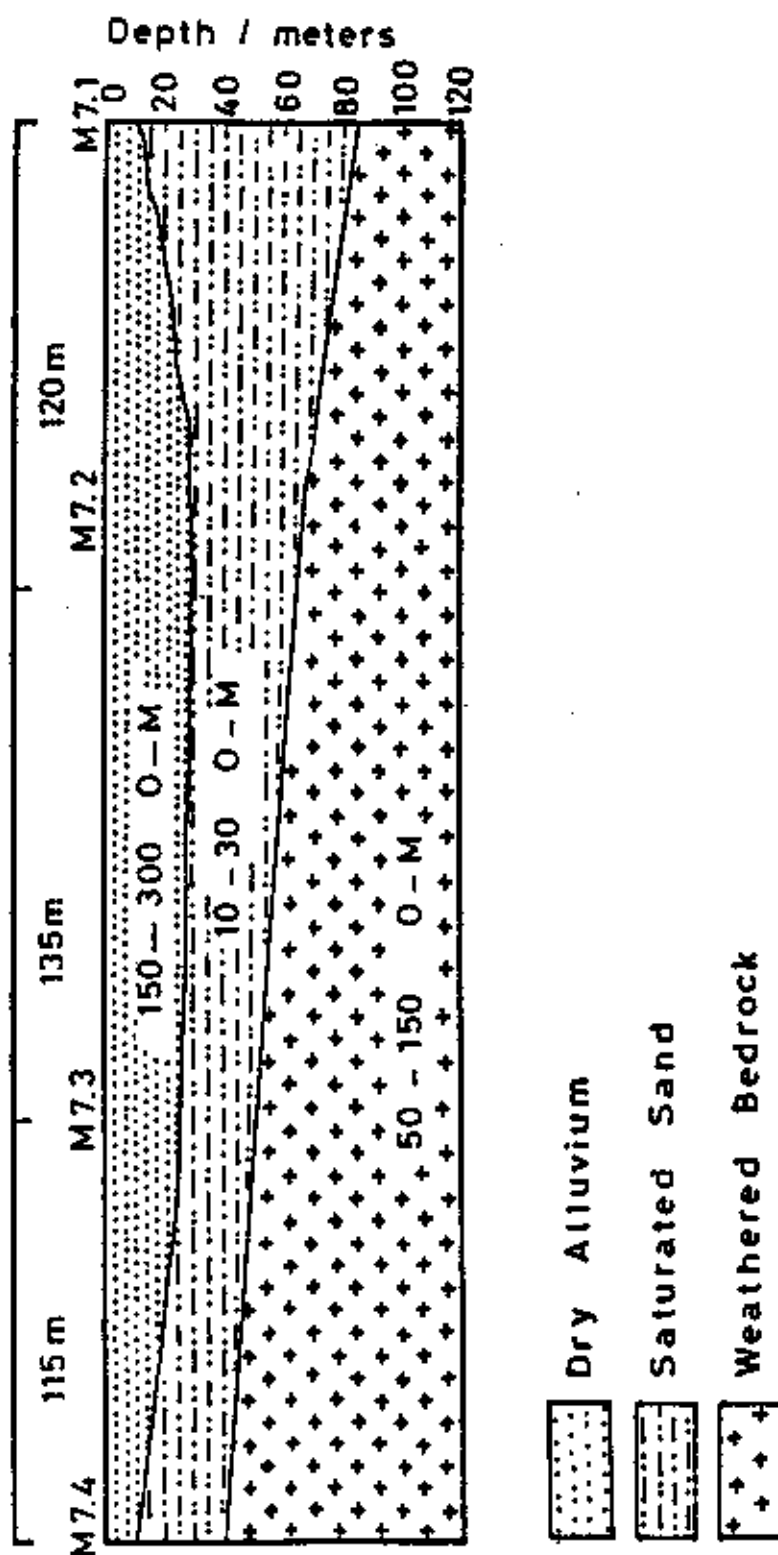


Fig. 5.14. Interpreted subsurface resistivity and equivalent geological sections along profile M7.

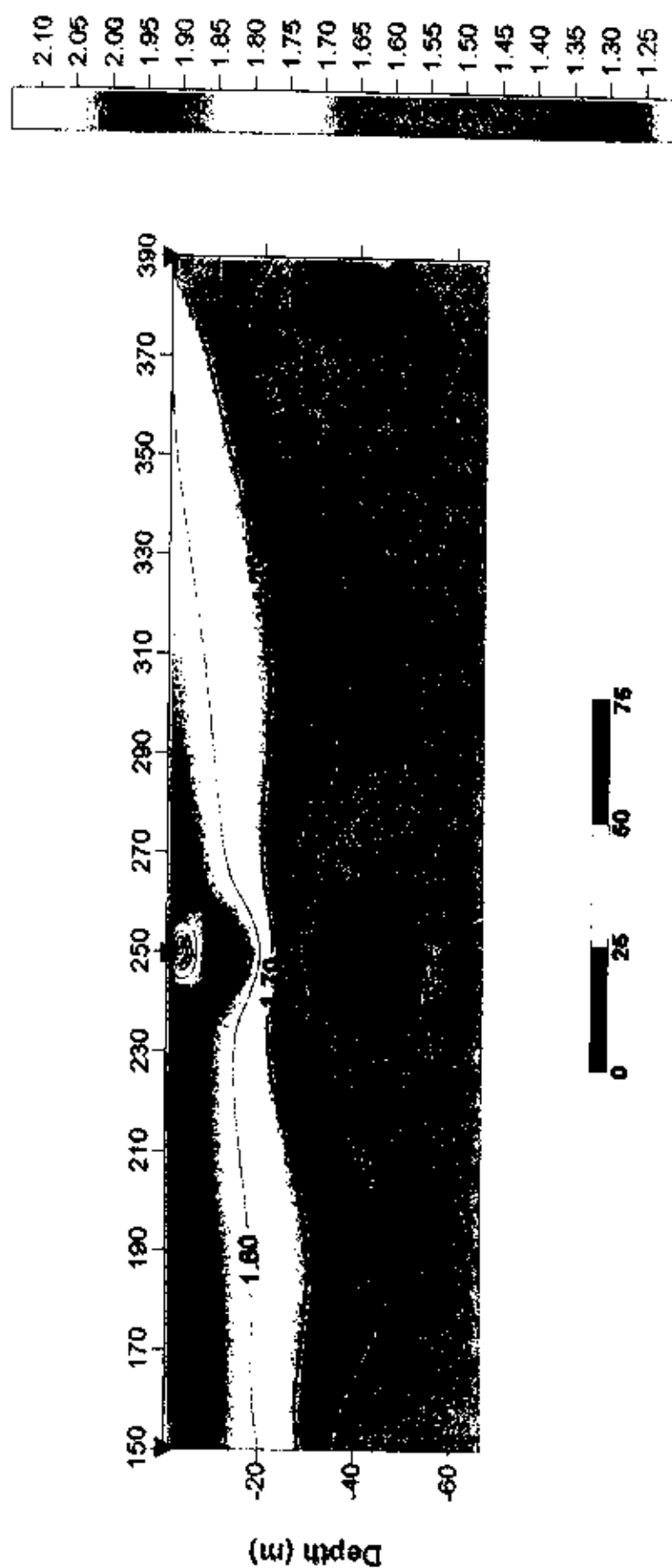


Fig. 5.15. Interpreted resistivity contour section of M7. Contour values are to the power of $10^{1.1}$, $10^{1.3}$ etc...

PROFIEE NO M8

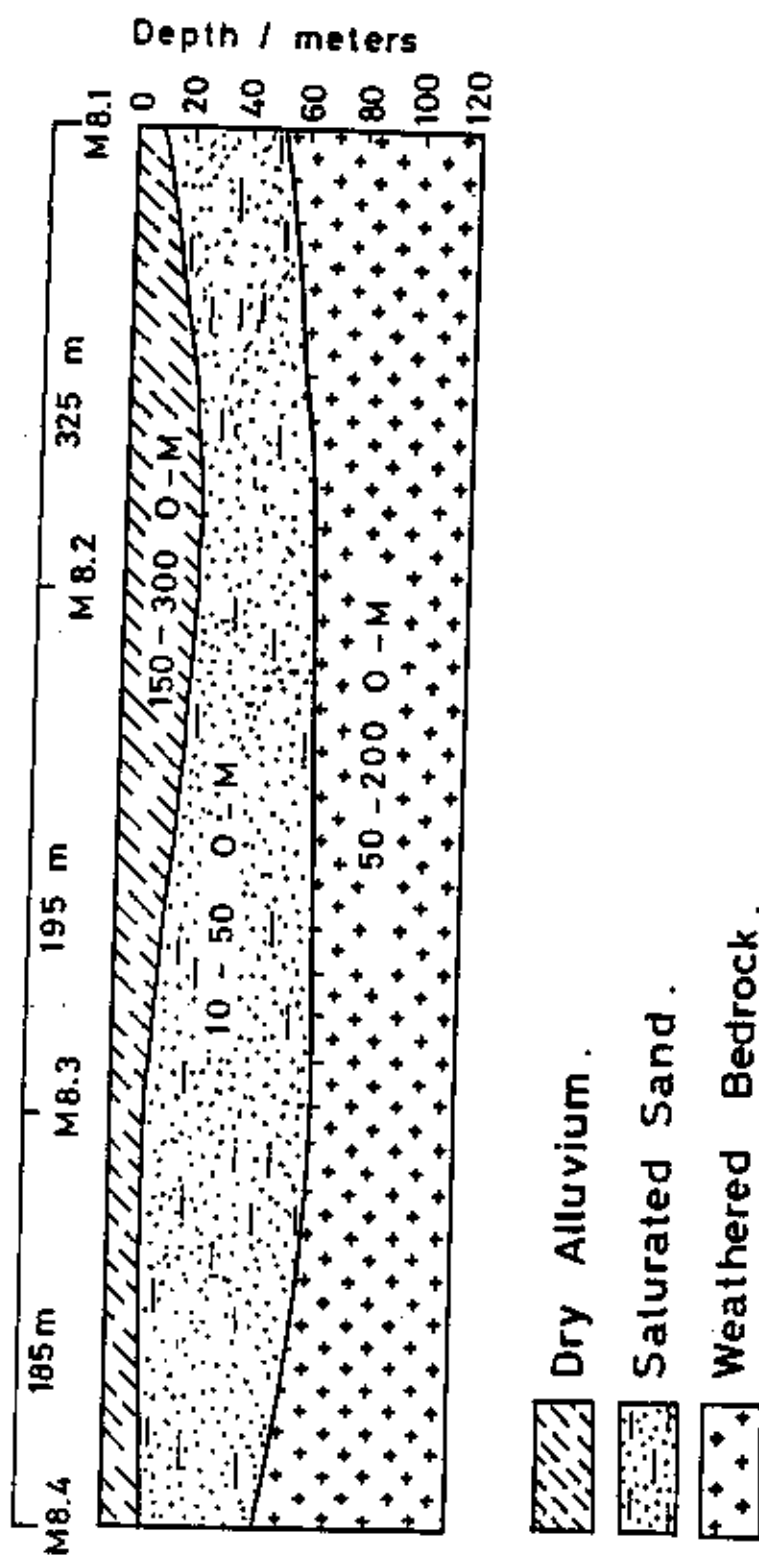


Fig. 5.16 Interpreted subsurface resistivity and equivalent geological sections along profile M8.

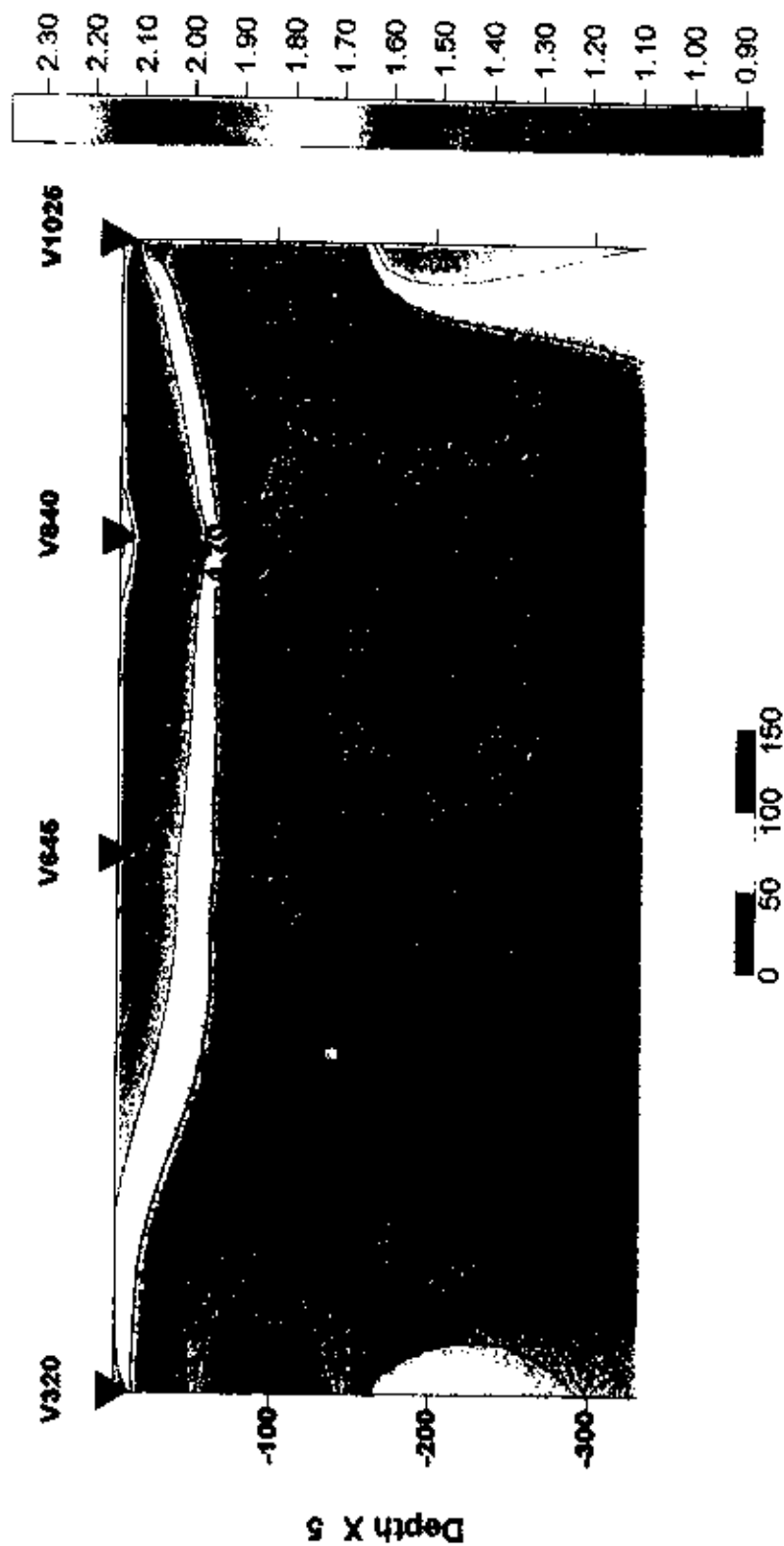


Fig. 5.17. Interpreted resistivity contour section of MB. Contour values are to the power of 10 ($10^{1.1}$, $10^{1.3}$ etc...)

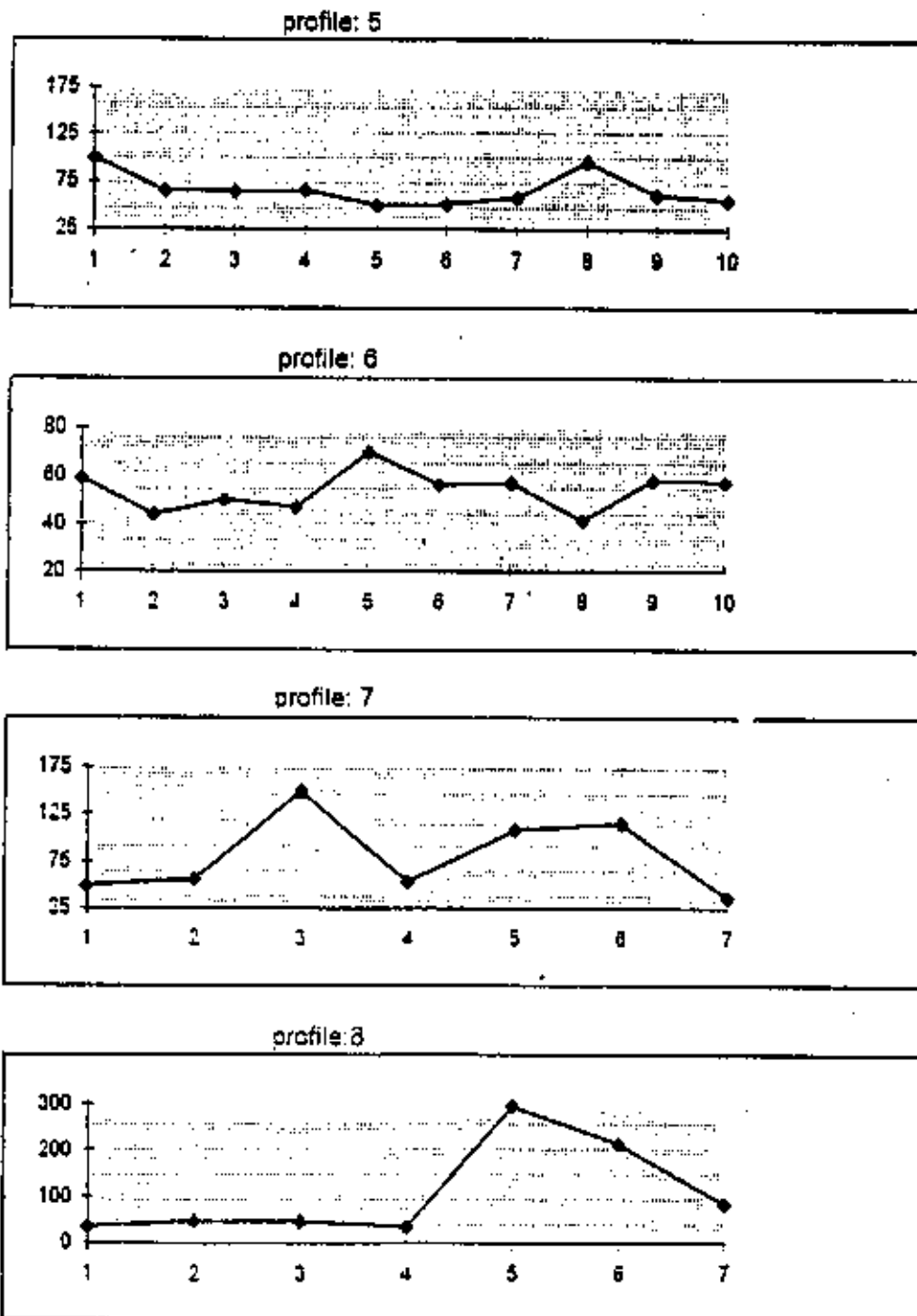
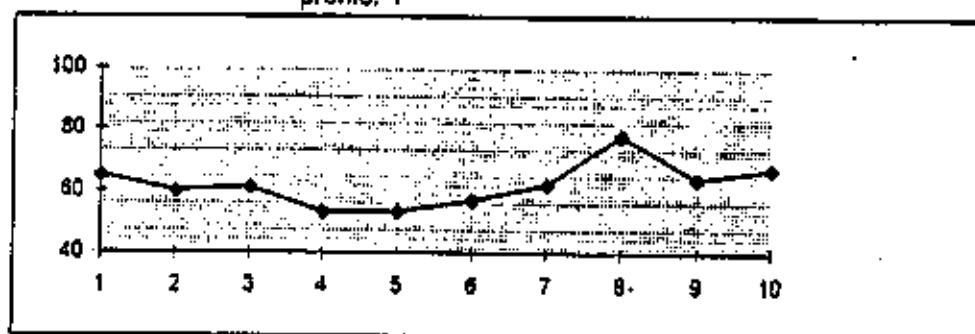
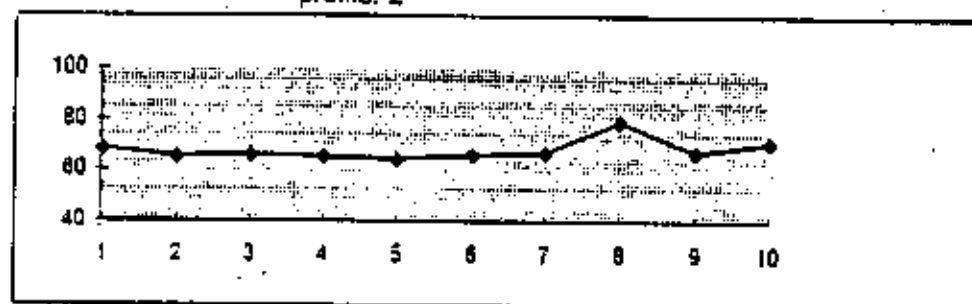


Fig. 5.18a Apparent resistivity Vs. station no. of the area between M3 and M4.

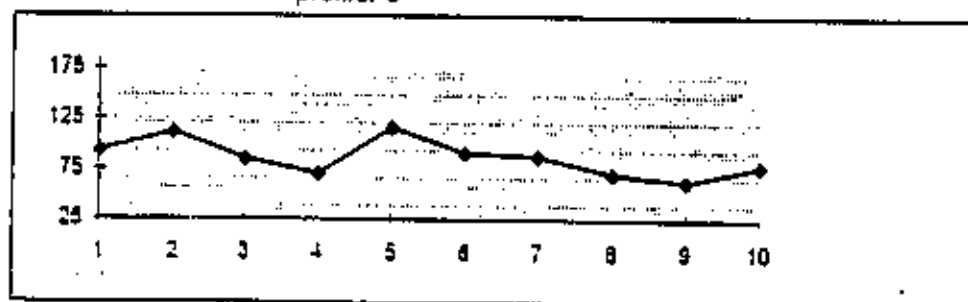
profile: 1



profile: 2



profile: 3



profile: 4

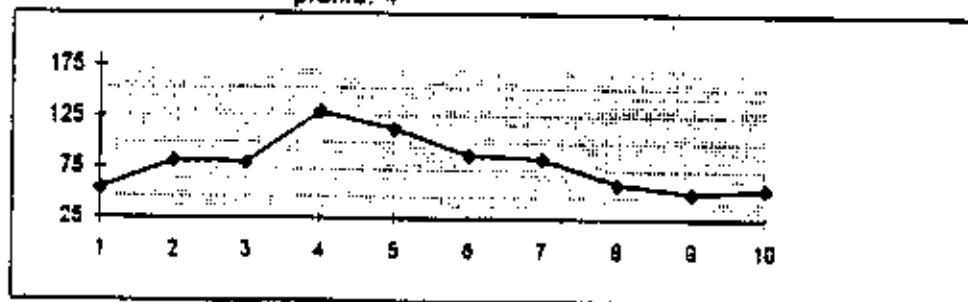


Fig. 5.18b Apparent resistivity Vs. station no. of the area between M3 and M4.

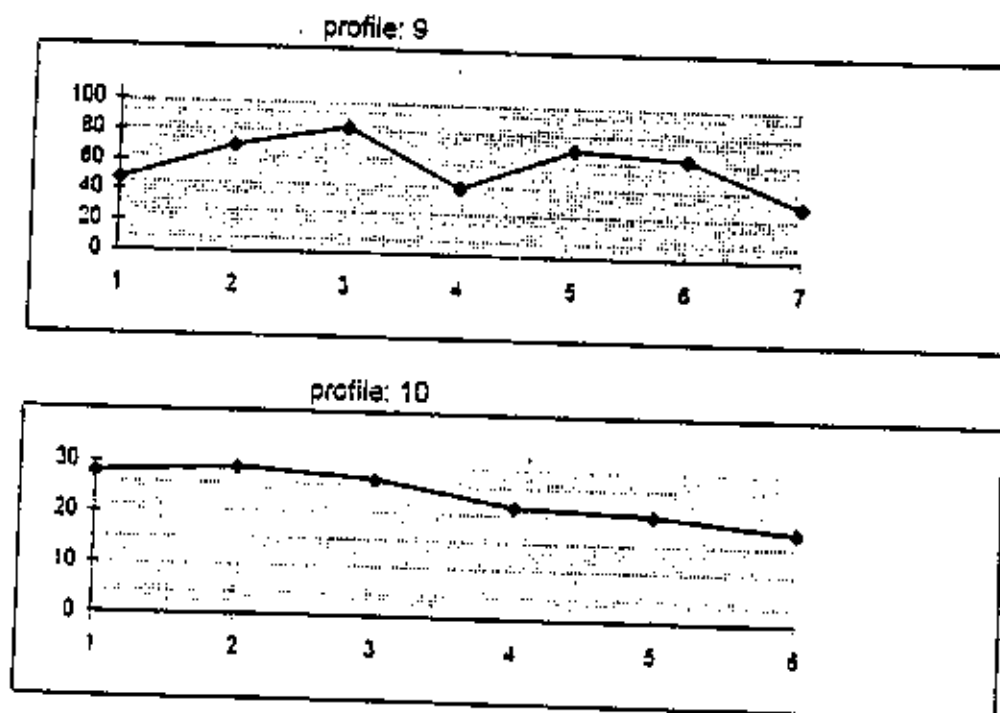


Fig. 5.18c Apparent resistivity Vs. station no. of the area between M3 and M4.

HEP RESISTIVITY CONTOUR MAP

Between M3 and M4

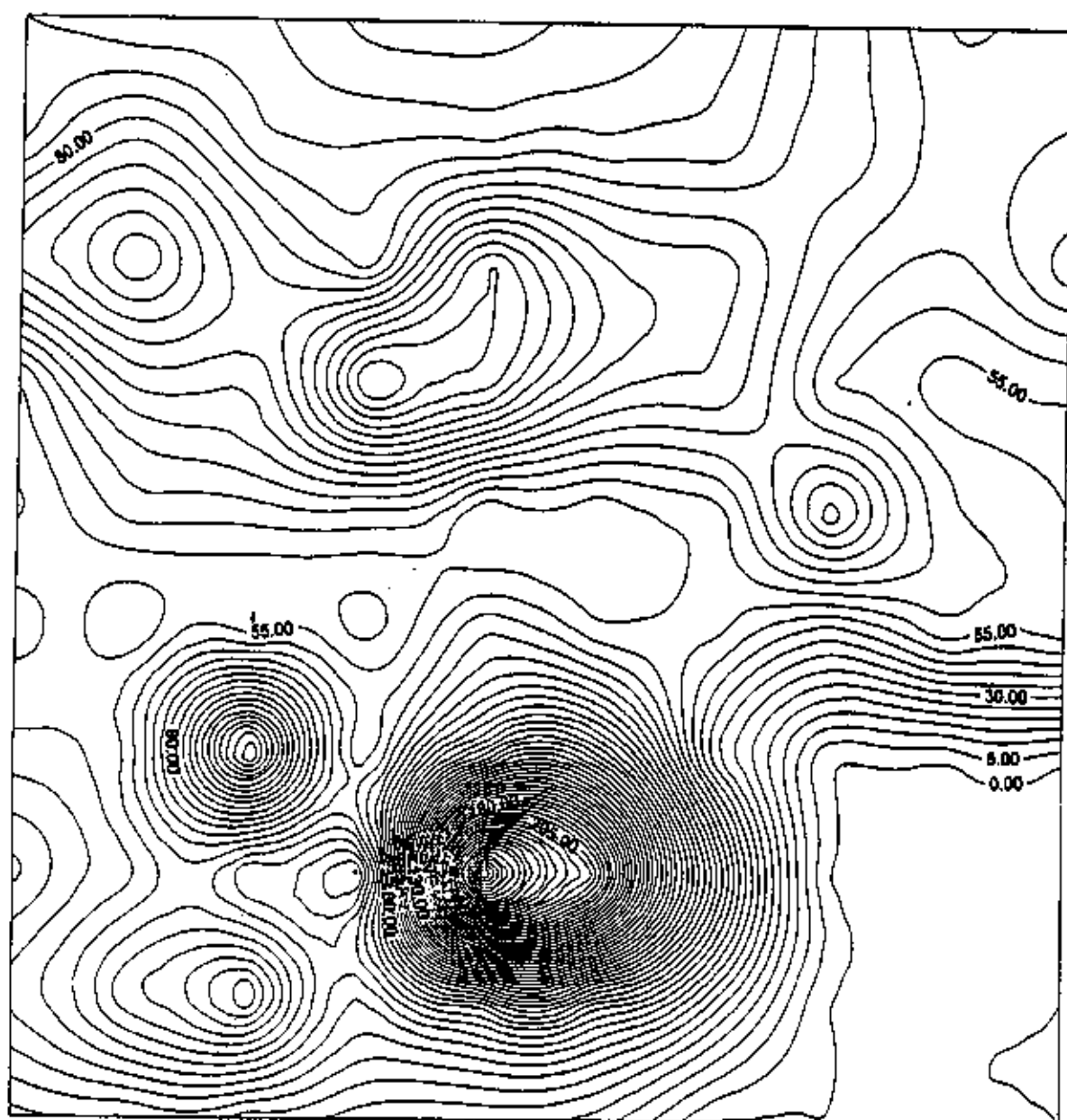


Fig. 5.19 HEP resistivity contour map of the area between M3 and M4.

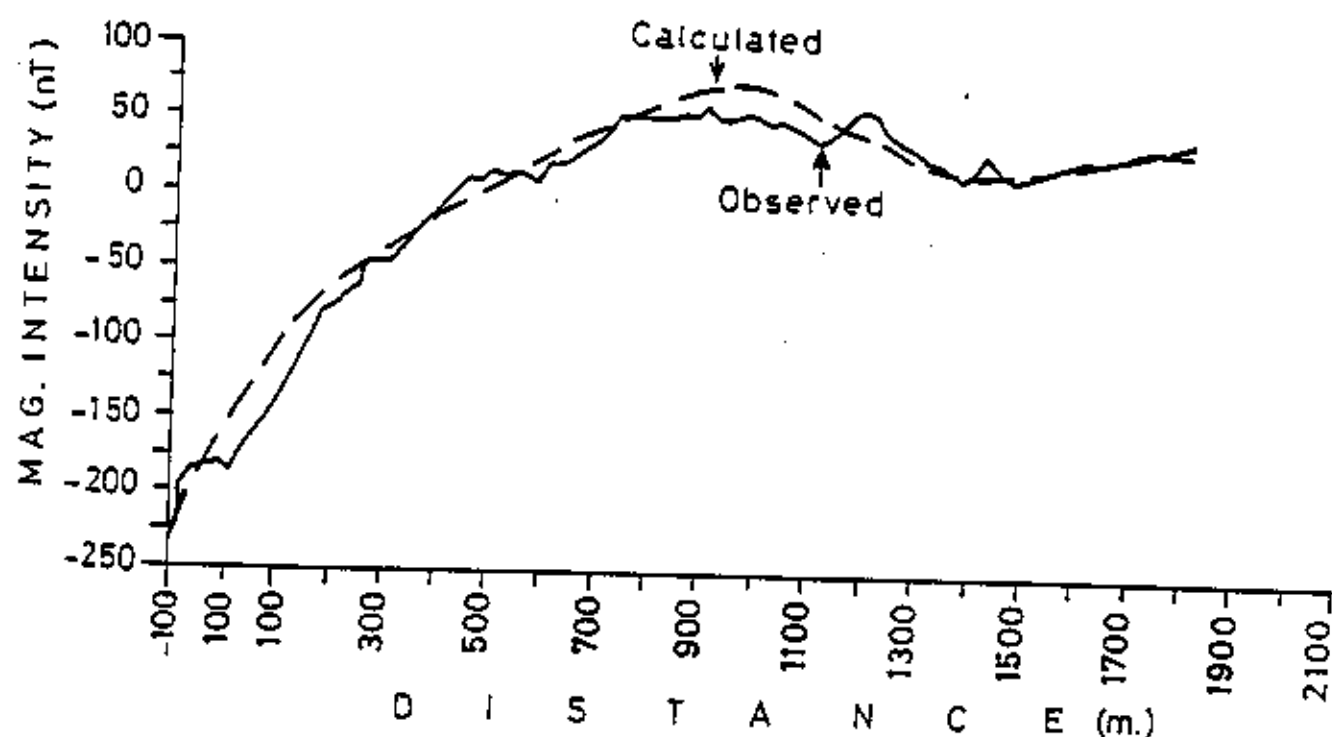
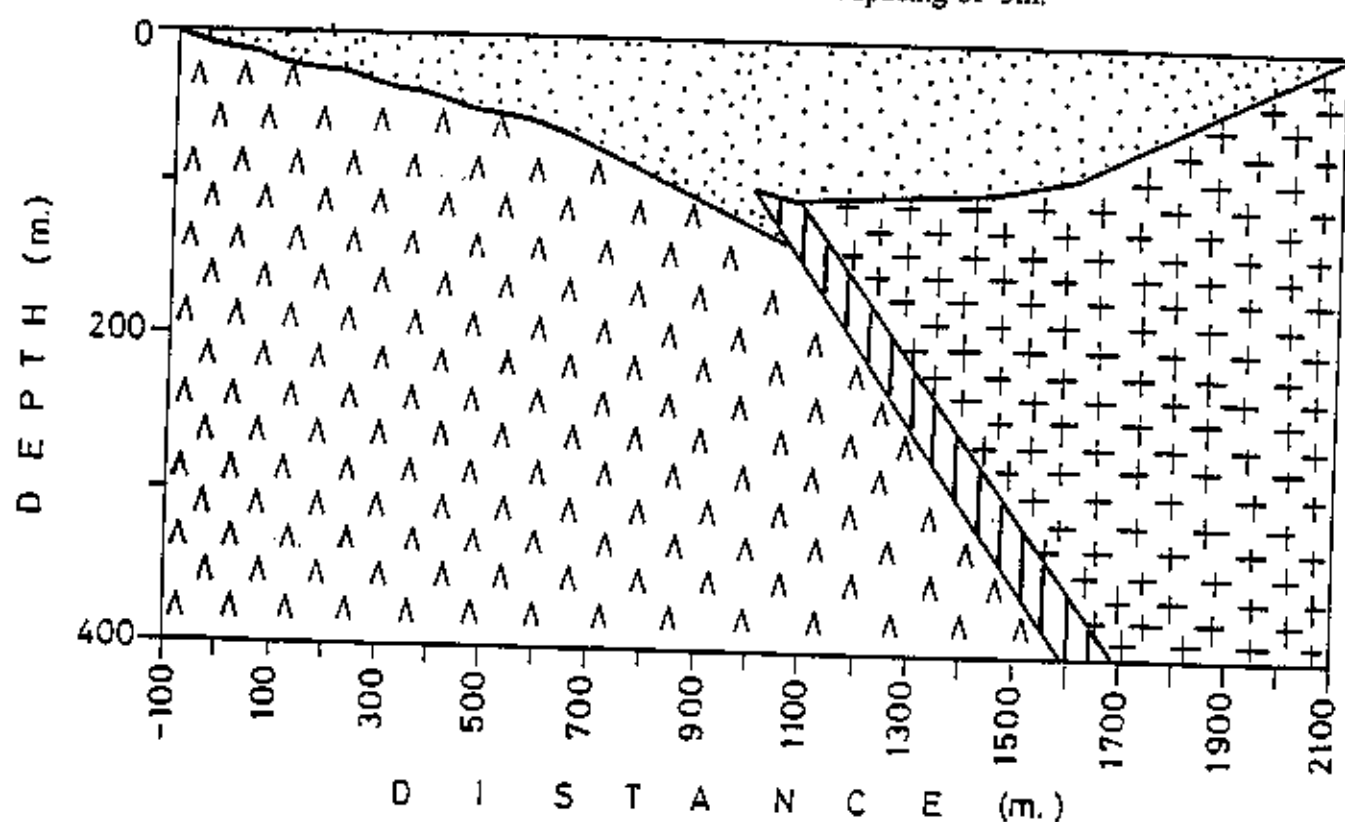


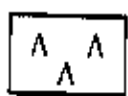
Fig. 5.20 The total intensity magnetic profile (Readings in gamma Vs. station) measured at the line of M3 with station spacing of 5m.



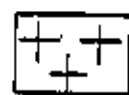
LEGEND



Wadi deposits



Older acidic rocks
(Granitic?) with low K



Basic rocks
(Gabbro?) with high K



Younger acidic rocks
with very low K

Fig. 5.31 Geological model of magnetic data with the observed and calculated curves for M3

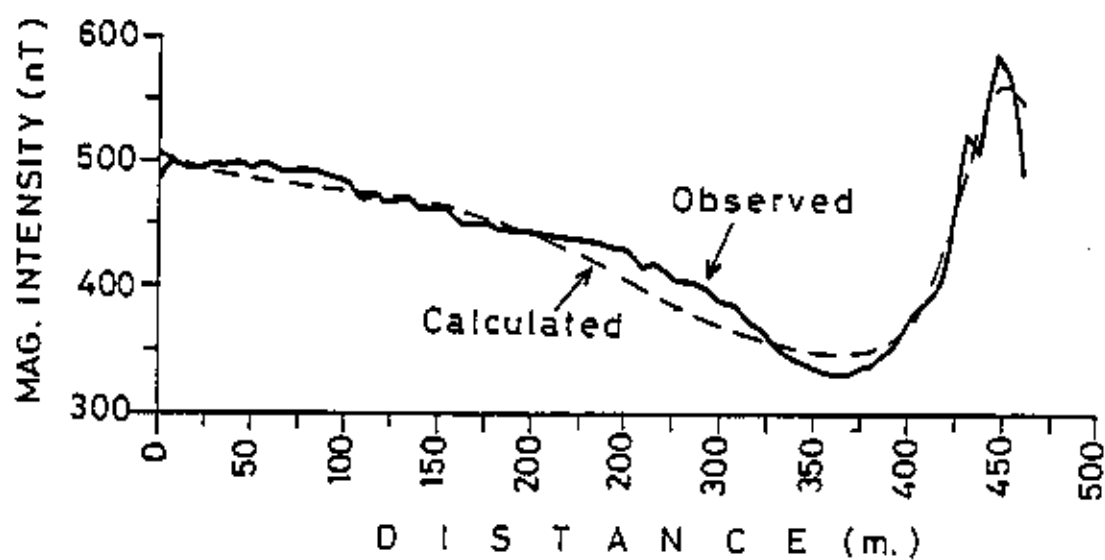


Fig. 5.22 The total intensity magnetic profile (Readings in gamma Vs. station) measured at the line of M5 with station spacing of 5m.

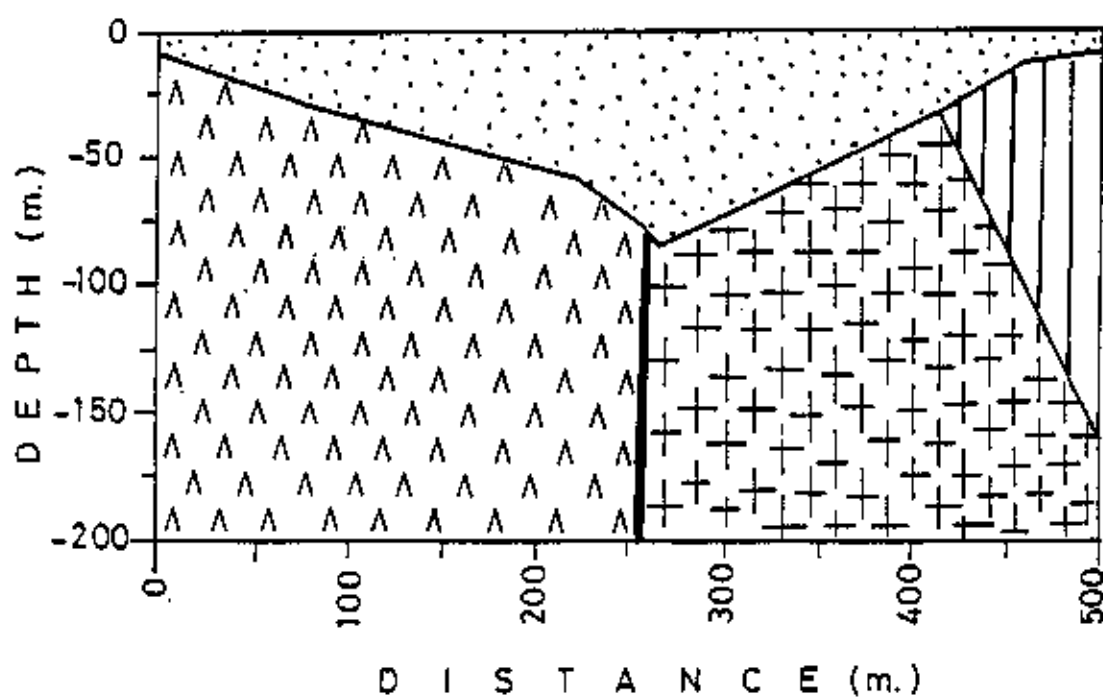


Fig. 5.23 Geological model of magnetic data with the observed and calculated curves for M5

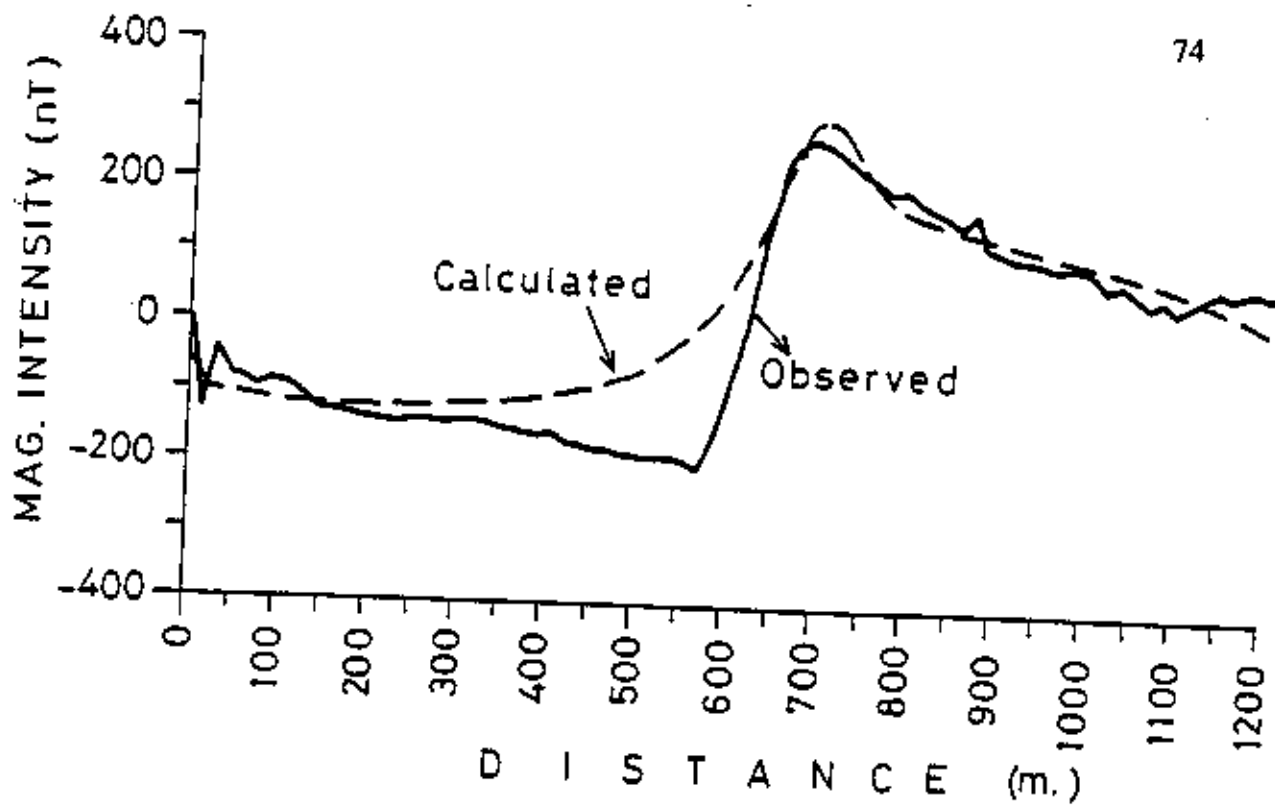


Fig. 5.24 The total intensity magnetic profile (Readings in gamma Vs. station) measured at the line of M6 with station spacing of 5m.

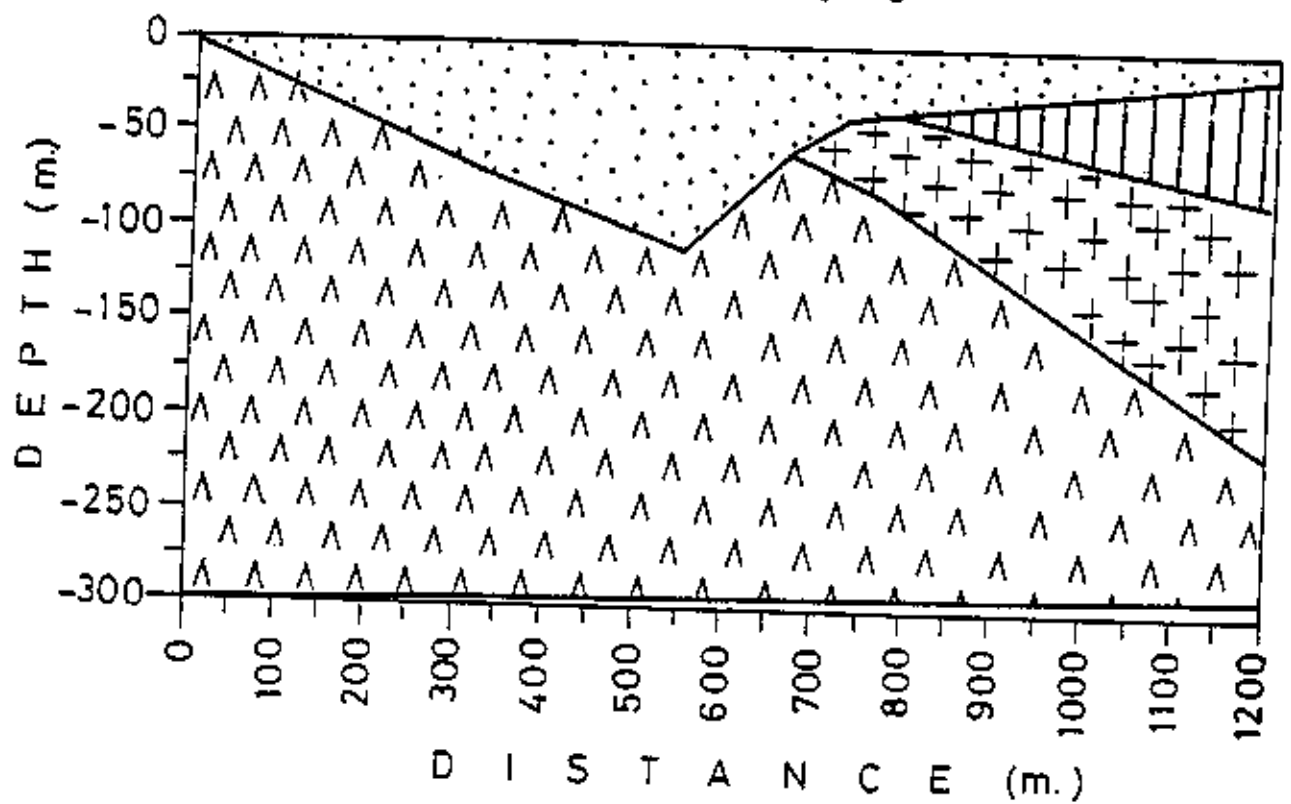


Fig. 5.25 Geological model of magnetic data with the observed and calculated curves for M6

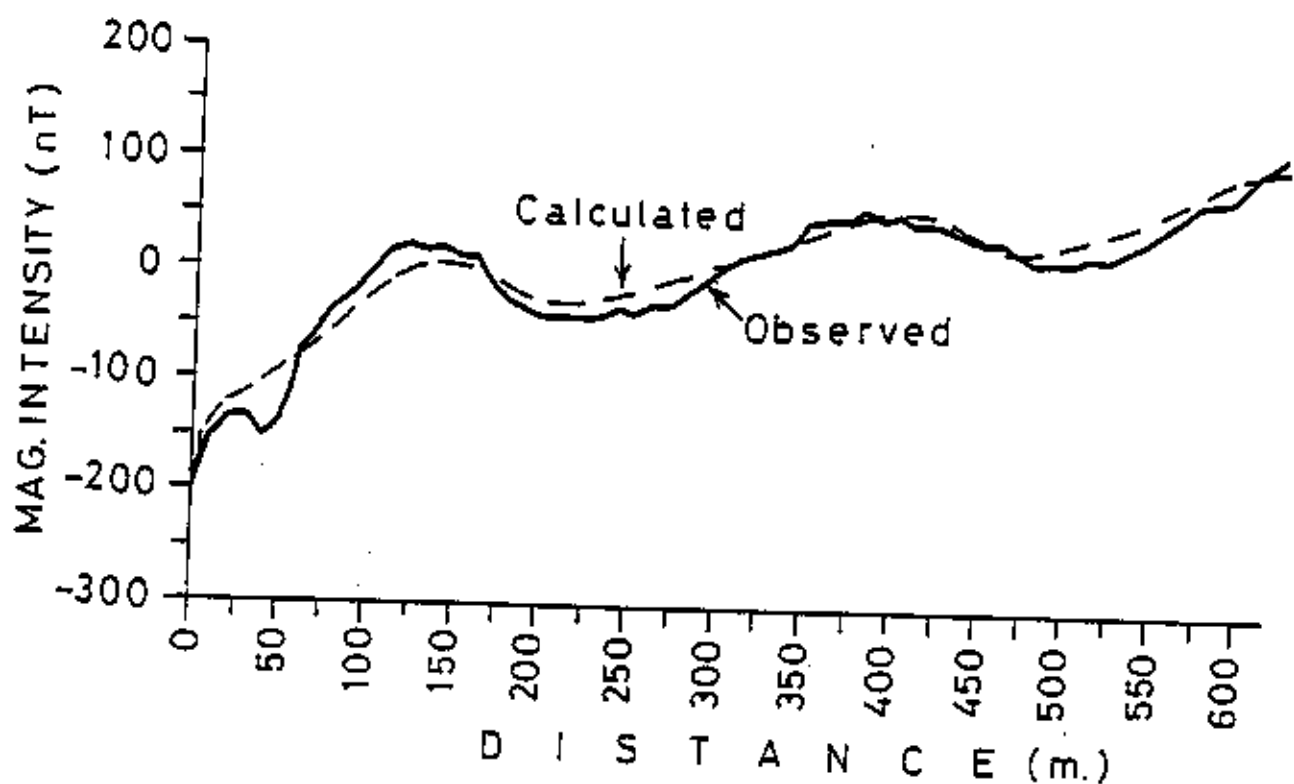


Fig. 5.26 The total intensity magnetic profile (Readings in gamma Vs. station) measured at the line of M7 with station spacing of 5m.

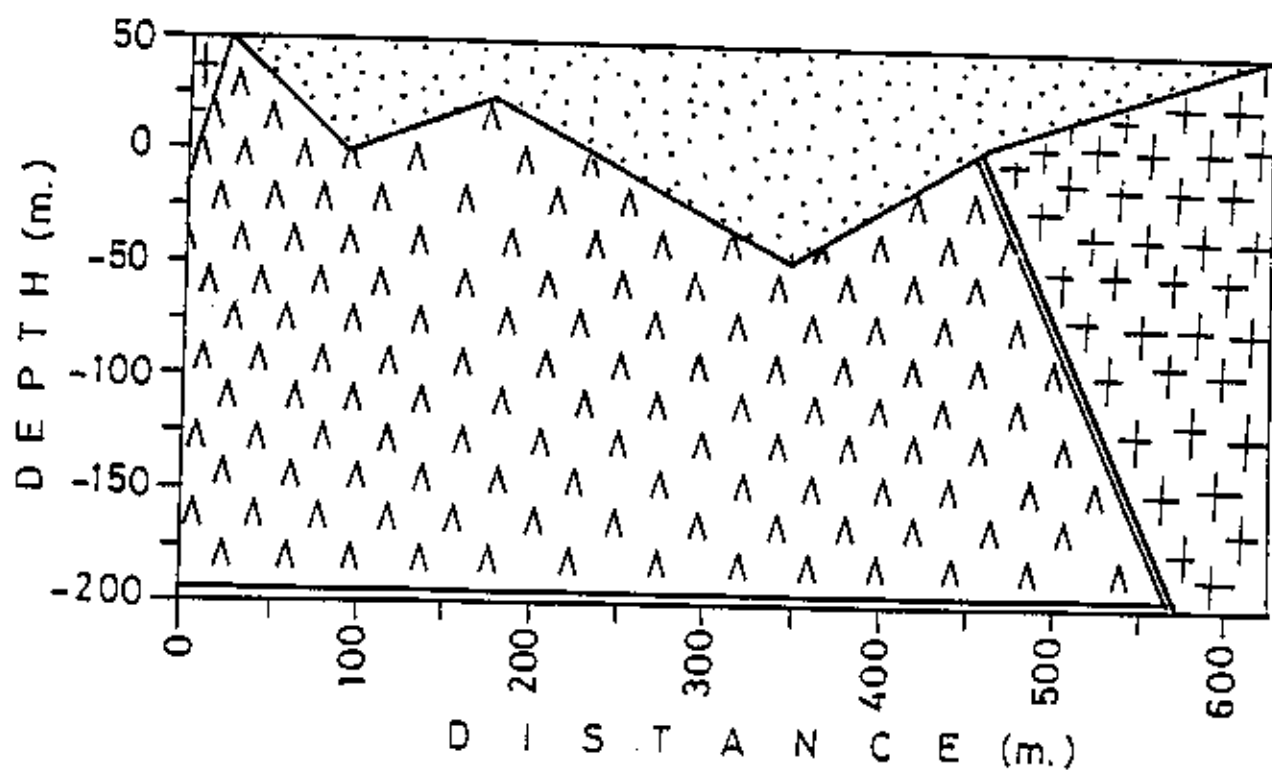


Fig. 5.27 Geological model of magnetic data with the observed and calculated curves for M7

DRILLING AND SEDIMENTOLOGY OF WADI MALAL

6.1 Introduction

Drilling sites for drinking water and agriculture purposes are selected on the basis of Geophysical, hydrogeologic and geological aspects taking into consideration. The localized features such as fault and gravel lenses have been pinpoint during the well selection (Fig. 6.1).

Geologic logs are made to correlate the strata to indicate the thickness and extent of aquifers and confining layers, and the configuration of the bed-rock topography. In this study, the soft material in the form of silt and clay tends to form sludge with water and makes the study more complicated. However, driller has been instructed to take samples at 2m regular intervals and whenever a change in formation is noticed. The samples are laid out on a plank for drying and the depth intervals of each are immediately and clearly marked. All the samples has been collected on the site and noted their preliminary description together with the other information received from the driller. Finally, the samples collected from the sites were brought to laboratory for further analysis to determine their sedimentological and hydrologic properties.

6.2 Stratigraphy of the wells

WELL NUMBER ONE (M3.1)

- 0-20 m. Alluvium, the dominated grains size of the units are ranges from fine to pebbles. The most of the grains are subangular to rounded. The grains are black, light green, pink and white. The lower part of the unit comprises high percentage of sticky and soft clays. The pebbles are varies in size and colour as well as roundness (Fig 6.2).
- 20-32 m. The majority of the grains are ranges from fine to granules sizes. The grains are subangular to rounded in shape. The grains comprise by varies colour such as black, pink, gray, light green and white. The soft clays occur in small amount. The granules are different size, shape and colour.

- 32-44 m. Fine to very coarse sand/granules size occurs in this unit. The grains are subangular to subrounded. The grains are black, pink, light green and white. The soft clays occur in small ratio in relation to sand.
- 44-48 m. Fine to pebbles size the grains are angular to subrounded. Most of the grains are black, pink, and glassy white. The percentages of clays are low in comparison to sand. The high percentages of granules and pebbles are dominated the unit.
- 48-58 m. The most of the grains ranges from fine to granules size and angular to rounded shape. The colour of the grains is black, pink, and light green and glassy white. The granules are dominated most of the units. The percentage of soft and sticky clays is low in comparison to sand.
- 58-62 m. Fine to granular size and subangular to subrounded shape. The grains are black, pink, light green and white. However, black colors are dominated. The clay percentage is low in this unit.
- 62-68 m. Bed rocks (weathered and massive rhyolite).

WELL NUMBER TWO (M3.2)

- 0-8 m. Alluvium, the grains are fine to pebbles size. Most of the grains are subangular to rounded. The grains are black pink, brown and white. The soft clay percentage is less. Some of the pebbles size is more than centimeter (Fig 6.3).
- 8-16 m. Fine to pebbles size and subrounded to rounded shaped grains. The grains are black, pink and white in colour. The 50% of the unit dominated by soft clays.
- 16-38 m. Most of the grains are fine to granules size and subangular to subrounded in shape. The grains are gray, pink, brown, black and white. The ratio between clay and sand are about 40:60.
- 38-44 m. Fine to granules size and most of the grains are subangular. The sediments are dominated by pink color grains followed by black and white. The clays are less in percentage in compare to above unit.

- 44-50 m. The grains are fine to pebbles size and subangular to subrounded in shape. The sediments are dominated by black colour followed by pink and light green (especially in fine grains and clays). The ratio between clays and sand is 25:75.
- 50-76 m. Fine to pebbles size grains, subangular to rounded. The unit is dominated by pebbles of various size shape and colour. The most of the grains are black followed by pink and white. The soft and sticky clays are present in lesser percentage.
- 76-80 m. Bedrocks, the unit is dominated by pink colour chips (unweathered rhyolite).

WELL NUMBER FOUR (M3.3)

- 0-20 m. Alluvial, majority of the grains is ranges from fine to very coarse grained, subangular to rounded and brown, pink, black and white colour. The unit is dominated by soft clays (Fig 6.4).
- 20-50 m. This unit is dominated by sticky and soft clays. A small percentage of fine to coarse grained occurs. Most of the grains are subangular to subrounded. The common colors of the grains are varies at different depth.
- 50-52 m. Fine to granular size grains. The grains are subangular to well rounded, Pink, brown, gray and white colour are common. The clays percentage are less than above unit.
- 52-54 m. Weathered and fractured rocks.
- 54-56 m. Bedrocks.

WELL NUMBER THREE (M3.4)

- 0-20 m. Alluvium, majority of the grains are fine to very coarse grained and subangular to rounded. The colors of the grains are pink, black, gray and white. The percentage of the clays is less than sand. The granules and pebbles are present and form about 5% of the total grain size (Fig 6.5).

- 20-22m. The average grain size is fine to granule size with some pebbles. Grains are angular to subrounded. The colour of the grains is pink, brown and white. The soft clays are present in small amount.
- 22-38 m. Most of the grains are fine to pebbled size and pebbles are well rounded, but rest of the grains are subangular to subrounded. The grains are black, brown, light green pink and white in colour. The percentage of clays is higher than sand.
- 38-41 m. Weathered and fractured rhyolite bed
- 41-43m Massive rhyolite (Bedrock)

WELL NUMBER FIVE (M4)

- 0-16 m. Fine to very coarse grained, subrounded to rounded shaped. The grains are brown, black, white and light green. The percentage of clays is higher as compared to sand, especially in the lower part of the unit (Fig 6.6).
- 16-30 m. Majority of the grains is ranges from fine to pebble size and subangular to subrounded. The color of the grains is pink, gray, white, black and brown. The ratio between clays and sand are 30:70.
- 30-50 m. The average grain size ranges from fine to pebble size and angular to subrounded. The colour of the grains is black, white, pink and brown. The ratio between clays and sand are 30:70.
- 50-60 m. The average grain size ranges from fine to granule size and subangular to rounded shaped. The grains are pink, black, gray, white and brown colour. The ratio between clays and sand are 70:30.
- 60-62 m. Weathered bedrocks.

WELL NUMBER SIX (M5)

- 0-20 m. Alluvium, majority of the grains are ranges from fine to pebbles size and angular to subrounded. The grains are black and dark brown colour. Few grains are cherty in nature. The ratio between clays and sand are 20:80 (Fig 6.7).

- 20-40 m. Most of the grains are ranges from fine to granule size and angular to subrounded. The grains are black, light green, brown and white colour. The much variation in grain size. The ratio between clays and sands are 25:75.
- 40-52 m. Fine to pebbles size grains. The grains are subangular to subrounded. The colour of the grains is black, brown, light green pink. The percentage of clay is very high as compared to sand to upper unit
- 52-65m The size of grains ranges from fine to granules size and angular to subangular grain shaped. The grains are black, brown pink and gray colour. The ratio between clays and sand are 20:80.
- 65-70 m. Fine to pebbles size and subangular to subrounded, some pebbles are well rounded. The colour of the grains is black, brown, and pink. The ratio between clays and sand are 30:70.
- 70-72 m. Bedrocks.

The results of drilled wells are in agreement with the results of geophysical survey. The thickness of the saturation zones varies from 20 to 60m. The samples from the drilled wells needed further sedimentological studies because it plays a very important role in the evaluation of aquifer characteristics.

6.3 Sedimentological studies of Wadi Malal

Grain size parameters and their relationship with depositional processes in general reviewed by Folk (1966), Visher (1969) and Friedman (1979). These reviews are highly informative as they are based on a large volume of literature on grain size contributed by a large number of workers. Different methods have been used by different workers but more common is the graphic plot method (Folk and Ward, 1957), all these methods focus attention on mean grain size, standard deviation, skewness and kurtosis of the distribution. The degree of sorting and sizes of grains of sediment are of considerable importance in ground water studies. These are determined by mechanical analysis, which consist of separation of grains of various size groups by passing through a set of standard sieves.

The data obtained can be plotted as a histogram simple frequency curve, or cumulative frequency curve. For most purposes in ground water studies, however, cumulative curves are more useful.

6.3.1 Method:

The 183 boreholes samples have been collected from six wells among 71 representative samples selected for the study and grain size analysis were carried out with a Ro-tap sieve shaker. A 0.5 ϕ interval employed to provide maximum accuracy. The weight of the various fractions is determined and the percentage weight of each fraction with respect to the total is calculated.

Grain size parameters (Graphic mean, inclusive standard deviation, inclusive graphic skewness and kurtosis), as defined by Folk & Ward, (1957) were obtained from values intercepted at specific percentiles.

The data of grain-size analysis was plotted as cumulative curves on probability paper by plotting cumulative percentage versus grain size in phi (ϕ) intervals to ensure maximum accuracy in determines grain-size parameters by graphic methods.

6.3.2 Grain size parameters:

Graphic Mean Size (Mz)

It is the best measure for determining the average grain size, and given by the formula:

$$M_z = (\phi 16 + \phi 50 + \phi 84) / 3$$

Inclusive graphic standard deviation

The inclusive graphic standard deviation is a measure of the sorting of the grain size distribution and includes 90 percent of the size frequency distribution. Sorting also shows the constancy in the energy level of the depositing agent and thus reflects the presence or absence of coarse and fine grained fractions, and is given by the formula:

$$\sigma_I = (\phi 84 - \phi 16) / 4 + (\phi 95 - \phi 5) / 6.6$$

Inclusive graphic skewness (SKI)

Skewness is a measure of the symmetry of the grain-size distribution. If there is more material in the coarse tail (coarse skewed), the skewness is referred to as being negative and if there is more material in fine tail (fine skewed) it is positive.

Inclusive graphic skewness is given by the formula

$$SKI = (\phi 16 + \phi 84 - 2 \phi 50) / 2(\phi 84 - \phi 16) + (\phi 5 + \phi 95 - 2 \phi 50) / 2(\phi 95 - \phi 5)$$

Graphic kurtosis (KG)

Kurtosis measures the ratio between the sorting in the tails of the distribution and sorting in the central portion of the distribution. If the central portion is better sorted than the tail to be excessively peaked or leptokurtic. If the tails are better sorted than the central portion, the curve is to be peaked or platykurtic.

Kurtosis may be measured by the following formula

$$KG = (\phi 95 - \phi 5) / (2.44(\phi 75 - \phi 25))$$

The computed grain size parameters of the Wadi Malal sand included graphic mean size, inclusive graphic standard deviation, inclusive graphic skewness, and graphic kurtosis, are summarized in tables 6.1 to 6.6.

Well number one (M3.1)

The graphic mean size values ranges between 1.13 ϕ to -0.95 ϕ (Medium to very coarse sand) on the average, the sands consist of very coarse sand (46.0 percent), coarse sand (38.0 percent) and medium sand (16.0 percent).

Inclusive graphic standard deviation values ranges between 1.83 ϕ to 2.29 ϕ (poorly sorted to very poorly sorted) most sands are very poorly sorted (69.0 percent) and poorly sorted (31.0 percent).

Inclusive graphic skewness values range from 0.330 to -0.191 (strongly fine skewed to coarse skewed). Majority of the samples shows strongly fine skewed (46.0 percent), fine skewed (39.0 percent) and coarse skewed (15.0 percent).

Graphic kurtosis values of the sand range from 0.659 to 1.165 (very platykurtic to Leptokurtic). Platykurtic samples are dominant (84.0 percent) followed by very platykurtic (8.0 percent) and Leptokurtic (8.0 percent).

The weight percentage of gravel ranges from 18.0 to 70.0 percent, on the average 44%. The percentage of sand range from 29.0 to 79.0 percent and an average 52% and the percentage of clay range from 1-9% percent, on the average 4%.

Well number two (M3.2)

The graphic mean size values ranges between 1.36 ϕ to -1.260 ϕ (Medium to Granule) on the average, the sands consist of very coarse sand (54.0 percent), coarse sand (20.0 percent), medium sand (13.0 percent) and Granule (13.0 percent).

Inclusive graphic standard deviation values ranges between 1.14 ϕ to 2.38 ϕ (poorly sorted to very poorly sorted), most sands are poorly sorted (60.0 percent), followed by (27.0 percent) and moderately sorted (13.0 percent).

Inclusive graphic skewness range from 0.484 to -0.327 (strongly fine skewed to strongly coarse skewed). Majority of the samples shows fine skewed (54.0 percent) strongly fine skewed (13.0 percent), nearsymmetrical (13.0 percent), strongly coarse skewed (13.0 percent) and coarse skewed (7.0 percent).

Graphic kurtosis values of the sand ranges from 0.538 to 2.062 (very platykurtic to very leptokurtic), platykurtic samples are dominant (47.0 percent), Leptokurtic (20.0 percent), Mesokurtic (13.0 percent), very Leptokurtic (13.0 percent) and very platykurtic (7.0 percent).

The weight percentage of gravel ranges from 12 to 78 percent on averages 45%. The percentage of sand range from 24 to 76 percent, on average 53% and clay percentages range from 0 to 6 percent, an average 2.0 percent.

percent) and moderately sorted (13.0 percent).

Inclusive graphic skewness range from 0.484 to -0.327 (strongly fine skewed to strongly coarse skewed). Majority of the samples shows fine skewed (54.0 percent) strongly fine skewed (13.0 percent), nearsymmetrical (13.0 percent), strongly coarse skewed (13.0 percent) and coarse skewed (7.0 percent).

Graphic kurtosis values of the sand ranges from 0.538 to 2.062 (very platykurtic to very

Well number three (M3.3)

The graphic mean size values ranges between -0.22ϕ to 1.99ϕ (very coarse to medium sand) on the average, the sands consist of very coarse sand (11.0 percent) coarse sand (33.0 percent and medium sand (56.0 percent).

Inclusive graphic standard deviation values ranges between 1.88ϕ to 2.38ϕ (poorly to very poorly sorted) most sand are very poorly sorted (67.0 percent) and poorly sorted (33.0 percent).

Inclusive graphic skewness values range from -0.40 to 0.27 (strongly coarse to fine skewed). Majority of the samples shows nearsymmetrical (46.0 percent) fine skewed (22.0 percent and strongly coarse skewed (22.0 percent).

Graphic kurtosis values of sand range from 0.609 to 0.751 (very platykurtic to Leptokurtic), platykurtic samples are dominant (67.0 percent) and Leptokurtic (33.0 percent).

The weight percentage of gravel ranges from 13.0 to 47.0 percent, on the average 26%. The percentage of sand ranges from 57.0 to 80.0 percent, and on the average 66.0 and the percentage of clay range from 1-12 percent, on the average 8.0 percent.

Well number four (M3.4)

The graphic mean size values ranges between -0.298ϕ to 2.26ϕ (very coarse to medium sand) on the average, the sands consist of very coarse sand (10.0 percent) coarse sand (30.0 percent and medium sand (50.0 percent) and fine sand (10.0 percent).

Inclusive graphic standard deviation values ranges between 1.91ϕ to 2.40ϕ (poorly to very poorly sorted) most sand are very poorly sorted (50.0 percent) and poorly sorted (50.0 percent).

Inclusive graphic skewness values range from -0.269 to 0.538 (strongly coarse to fine skewed). On the average; the sands consists of strongly coarse skewed (10.0 percent), coarse skewed (20.0 percent), nearsymmetrical (30.0 percent) and Fine skewed (40.0 percent).

The Graphic kurtosis values of sand range from 0.897 to 0.560 (very platykurtic to Leptokurtic), platykurtic samples are dominant (60.0 percent) followed by very platykurtic (40.0 percent).

The weight percentage of gravel ranges from 11.0 to 50.0 percent, on the average 25%. The percentage of sand ranges from 47.0 to 80.0 percent, and on the average 68.0 and the percentage of clay range from 2-10 percent, and on the average 7.0 percent.

Well number five (M4)

The graphic mean size values ranges from 0.50 ϕ to -0.616 ϕ (coarse to granule) on the average, the sands consist of granule (8.0 percent), very coarse sand (84.0 percent) and coarse sand (8.0 percent).

Inclusive graphic standard deviation values ranges between 1.62 ϕ to 2.14 ϕ (poorly to very poorly sorted). The majority of the samples are poorly sorted (83.0 percent), followed by very poorly sorted 17.0 percent).

The inclusive graphic skewness values ranges from 0.126 to 0.812 (Fine skewed to strongly fine skewed). Majority of the samples show strongly fine skewed 96.0 percent) followed by fine skewed (3.0 percent).

The graphic kurtosis values of the sand ranges from 0.635 to 1.091 (very platykurtic to mesokurtic). Majorities of the samples are platykurtic (58.0 percent), very platykurtic (25.0 percent) and Mesokurtic (17.0).

The Weight percentage of gravel ranges from 30 to 68.0 percent, on average (52.0 percent). The percentage of sand ranges form 31-69.0 percent on the average (47.0 percent). and the percentage of clay range from 1-2.0 percent, an average (1.0 percent).

Well number six (M5)

The graphic mean size values ranges between 0.048 ϕ to -1.202 ϕ (coarse to granule sand), on the average the sand consists of granule (8.0 percent)m very coarse sand (75.0 percent) and coarse sand (17.0 percent).

Inclusive graphic standard deviation values ranges between 1.10 ϕ to 2.14 ϕ (poorly to very poorly sorted), most sands are poorly sorted 83.0 percent) followed by poorly sorted (17.0 percent).

The Inclusive graphic skewness values ranges from 0.055 to 0.500 (Near symmetrical to strongly fine skewed). Majority of the samples shows strongly fine skewed (67.0 percent), fine skewed (25.0 percent) and nearsymmetrical (8.0 percent).

The Graphic kurtosis values of the sand range from 1.030 to 0.660 (Mesokurtic to very platykurtic). Majorities of the samples are platykurtic (67.0 percent) very platykurtic (17.0 percent), Mesokurtic (8.0 percent) and Leptokurtic (8.0 percent).

The weight percentage of gravel ranges from 43 to 69.0 percent, on average (53.0 percent). The percentage of sand ranges from 30 to 61.0 percent, on the average (46.0 percent), and the percentage of clay ranges from 1-2.0 percent, on average (1.0 percent).

6.4 Conclusion

The sedimentological studies indicate that grains in the saturation zones are coarse, well rounded and well sorted. The percentage of clays generally ranges between 1-10 percent. The percentage of sand and grovels ranges from 24-80 % and 11-78% respectively.

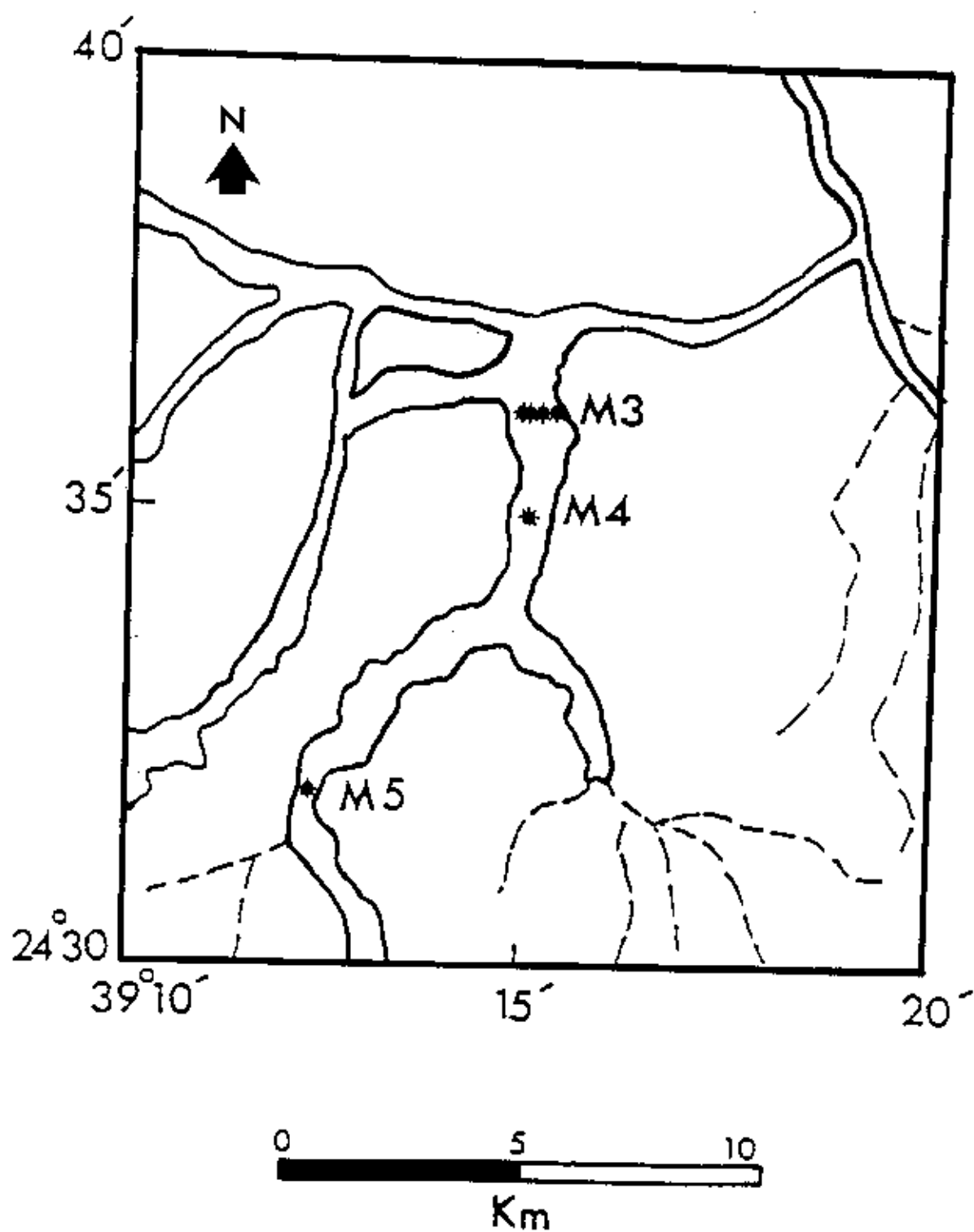


Fig. 6-1 Location map of well points in down-stream of wadi Malal.

Fig. 6.2 Geological section of well number one (M3.1)

Age	Scale (m)	Lithology	Description
Quaternary	5		Sand - fine to coarse Clay - soft and sticky Pebbles - well rounded
	10		
	15		
	20		
	25		Sand - fine to coarse clay - soft Granule - different sizes
	30		
	35		Sand - fine to very coarse clay - soft
	40		
	45		Pebbly fine to coarse sand
	50		Sand - fine to very coarse, granules
	55		Sand - fine to very coarse, soft clay, granular
	60		Bedrocks(basement), weathered Rhyolite
	65		

Fig. 6.3 Geological section of well number two (M3.2)

Age	Scale (m)	Lithology	Description
Quaternary	5		Sand - fine to very coarse Pebbles
	10		Sand - fine to very coarse
	15		Clay - soft 50%
	20		Sand - Fine to coarsr Clay 40% Granule
	25		
	30		
	35		
	40		Sand - fine to coarse Clay 15%
	45		Sand - fine to coarse Clay 25%
	50		Sand - fine to coarse Clay 10%
	55		
	60		
	65		
	70		
	75		Bedrocks-unweathered Rholite

Fig. 6.4 Geological section of well number three (M3.3)

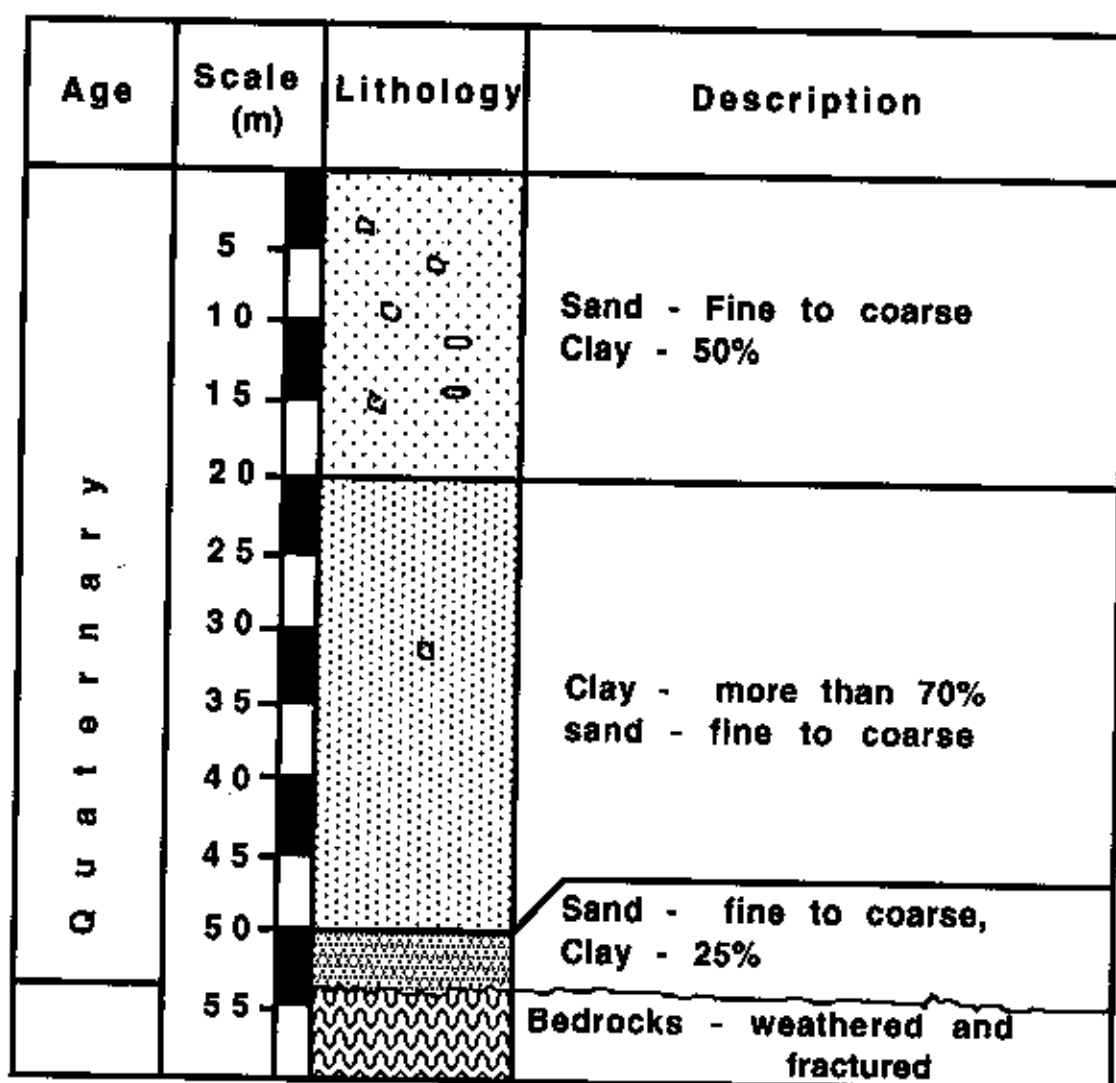


Fig. 6.5 Geological section of well number four (M3.4)



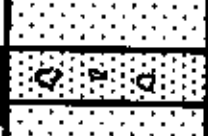

Age	Scale (m)	Lithology	Description
Quaternary	5		Sand - fine to very coarse Clay - 30%
	10		
	15		Sand - fine to coarse Clay - 10 % Granule
	20		
	25		Sand - fine to very coarse Pebbly Clay - 60%
	30		
	35		
	40		Bedrocks - weathered, fractured
	45		

Fig. 6.6 Geological section of well number five (M4)

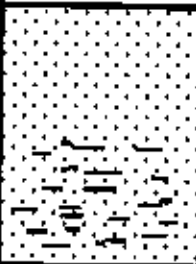

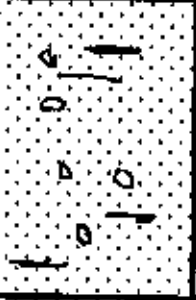
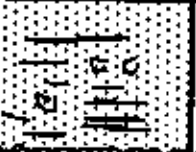

Age	Scale (m)	Lithology	Description
Quaternary	5		Sand - Fine to very coarse Clay - more than 50% in lower part
	10		
	15		
	20		Sand - fine to coarse, pebbly Clay - 30%
	25		
Quaternary	30		Sand - fine to very coarse, pebbly Clay - 15%
	35		
	40		
	45		Sand - fine to very coarse. granule Clay - 70%
	50		
Quaternary	55		Bedrocks - weahered
	60		
	65		

Fig. 6.7 Geological section of well number six (M5)

Age	Scale (m)	Lithology	Description
Quaternary	5		Sand - fine to coarse, 50% Pebbles - 30% Clay - 20%
	10		
	15		
	20		
	25		Sand - fine to very coarse, 50% Granule - 25% Clay - 25%
	30		
	35		
	40		
	45		Sand - fine to coarse, 40% Pebbles - 40% Clay - 20%
	50		
	55		
	60		Sand - fine to very coarse, 40% Granule - 30% Clay - 30%
	65		
	70		
			Bedrocks, weathered

Table 6.1 Textural attributes and percentage of gravel, sand and clay in drilled samples of wadi Malal (Well No. 1).

DEPTH OF SAMPLE (M)	MEAN SIZE		SORTING		SKEWNESS		KURTOSIS		Gravel wt. %	Sand wt. %	Silt & Clay wt. %
	Value (Phi)	Verbal Scale	Value (Phi)	Verbal Scale	Value (Phi)	Verbal Scale	Value (Phi)	Verbal Scale			
2	0.34	CS	1.97	PS	0.317	SFS	0.855	PK	37.00	60.00	3.00
8	-0.01	VCS	2.20	VPS	0.330	SFS	0.687	P	49.00	47.00	4.00
14	0.126	CS	2.22	VPS	0.264	FS	0.684	P	43.00	52.00	5.00
18	-0.86	VCS	1.96	PS	0.845	SFS	0.843	P	60.00	37.00	3.00
22	-0.95	VCS	1.92	PS	0.861	SFS	1.165	L	70.00	29.00	1.00
28	-0.11	VCS	2.29	VPS	0.539	SFS	0.659	VP	50.00	44.00	6.00
32	-0.18	VCS	2.02	VPS	0.221	FS	0.719	P	45.00	51.00	4.00
36	1.360	MS	2.21	VPS	-0.124	CS	0.767	P	24.00	67.00	9.00
42	1.130	MS	1.83	PS	-0.191	CS	0.768	P	18.00	79.00	3.00
46	0.040	CS	2.15	VPS	0.296	FS	0.839	P	45.00	51.00	4.00
52	0.120	CS	2.18	VPS	0.244	FS	0.794	P	42.00	54.00	4.00
56	-0.020	VCS	2.16	VPS	0.306	SFS	0.708	P	47.00	49.00	4.00
60	0.210	CS	2.15	VPS	0.242	FS	0.815	P	35.00	61.00	4.00

VCS (Very coarse sand); CS (Coarse sand); MS (Medium sand); FS (Fine sand); G (Gravel);

MS (Moderately sorted); PS (Poorly sorted); VPS (Very poorly sorted).

SFS (Strongly fine skewed); FS (Fine skewed); NS (Near symmetrical); CS (Coarse skewed); SCS (Strongly coarse skewed)

VP (Very platykurtic); P (Platykurtic); M (Mesokurtic); L (Leptokurtic); VL (Very leptokurtic).

Table 6.2 Textural attributes and percentage of gravel, sand and clay in drilled samples of wadi Malal (Well No. 2).

DEPTH OF SAMPLE (M)	MEAN SIZE		SORTING		SKEWNESS		KURTOSIS		Gravel wt. %	Sand wt. %	Silt & Clay wt. %
	Value (Phi)	Verbal Scale	Value (Phi)	Verbal Scale	Value (Phi)	Verbal Scale	Value (Phi)	Verbal Scale			
2	1.15	MS	2.41	VPS	-0.327	SCS	0.538	VP	30.00	69.00	1.00
6	-0.19	VCS	1.96	PS	0.203	FS	0.717	P	43.00	55.00	2.00
14	-0.53	VCS	1.99	PS	0.531	SFS	0.819	P	56.00	41.00	3.00
22	0.48	CS	2.38	VPS	0.264	FS	0.817	P	36.00	58.00	6.00
28	-0.10	VCS	1.97	PS	0.11	FS	0.807	P	38.00	59.00	3.00
36	0.81	CS	1.90	PS	0.019	NS	1.068	M	21.00	76.00	3.00
40	-0.18	VCS	1.90	PS	0.151	FS	0.812	P	42.00	57.00	1.00
48	0.10	CS	2.19	VPS	0.275	FS	0.680	P	43.00	54.00	3.00
52	-0.93	VCS	1.69	PS	0.484	SFS	1.275	L	66.00	32.00	2.00
58	1.36	MS	1.82	PS	0.277	FS	0.714	P	12.00	84.00	4.00
64	-0.63	VCS	0.83	MS	0.243	CS	1.136	L	47.00	53.00	0.00
70	-1.19	G	0.94	MS	0.168	FS	2.858	VL	76.00	24.00	0.00
74	-0.02	VCS	1.50	PS	0.264	FS	1.001	M	40.00	59.00	1.00
76	-1.26	G	0.79	MS	0.004	NS	2.062	VL	78.00	22.00	0.00
80	-0.38	VCS	1.14	PS	0.108	FS	1.311	L	48.00	52.00	0.00

P

Table 6.3 Textural attributes and percentage of gravel, sand and clay in drilled samples of wadi Malat (Well No. 3).

DEPTH OF SAMPLE (m)	MEAN SIZE		SORTING		SKEWNESS		KURTOSIS		Gravel wt. %	Sand wt. %	Silt & Clay wt. %
	Value (Phi)	Verbal Scale	Value (Phi)	Verbal Scale	Value (Phi)	Verbal Scale	Value (Phi)	Verbal Scale			
2	1.99	MS	1.95	PS	-0.400	SCS	0.751	P	15.00	75.00	10.00
6	1.67	MS	1.96	PS	-0.014	NS	0.63	VP	15.00	73.00	12.00
12	0.41	CS	2.26	VPS	0.021	NS	0.667	VP	38.00	57.00	5.00
16	0.78	CS	2.37	VPS	0.011	NS	0.68	P	31.00	63.00	6.00
22	1.17	MS	2.29	VPS	0.055	NS	0.676	P	23.00	65.00	12.00
26	1.98	MS	2.08	VPS	-0.408	SCS	0.685	P	16.00	72.00	12.00
32	1.82	MS	1.88	PS	-0.164	CS	0.740	P	13.00	80.00	7.00
36	0.44	CS	2.38	VPS	0.278	FS	0.609	VP	40.00	59.00	1.00
40	-0.21	VCS	1.99	PS	0.263	FS	0.735	P	47.00	49.00	4.00

Table 6.4 Textural attributes and percentage of gravel, sand and clay in drilled samples of wadi Malal (Well No. 4).

DEPTH OF SAMPLE (m)	MEAN SIZE		SORTING		SKEWNESS		KURTOSIS		Gravel wt. %	Sand wt. %	Silt & Clay wt. %
	Value (Phi)	Verbal Scale	Value (Phi)	Verbal Scale	Value (Phi)	Verbal Scale	Value (Phi)	Verbal Scale			
2	0.53	CS	2.20	VPS	-0.128	CS	0.754	P	30.00	68.00	2.00
8	1.03	MS	2.25	VPS	0.126	FS	0.560	VP	30.00	64.00	6.00
14	1.15	MS	2.23	VPS	0.147	FS	0.646	VP	22.00	68.00	10.00
20	0.23	CS	2.18	VPS	0.231	FS	0.825	P	37.00	59.00	4.00
26	2.26	FS	1.95	PS	-0.538	SCS	0.897	P	11.00	80.00	9.00
32	0.75	CS	2.40	VPS	0.090	NS	0.682	P	32.00	60.00	8.00
38	1.73	MS	1.94	PS	-0.103	CS	0.604	VP	16.00	74.00	10.00
44	1.74	MS	1.91	PS	-0.043	NS	0.629	VP	11.00	79.00	10.00
48	1.63	MS	1.98	PS	-0.076	NS	0.867	P	15.00	77.00	8.00
52	-0.29	VCS	1.93	PS	0.269	FS	0.897	P	50.00	47.00	3.00

Table 6.5 Textural attributes and percentage of gravel, sand and clay in drilled samples of wadi Malal (Well No. 5).

DEPTH OF SAMPLE (m)	MEAN SIZE		SORTING		SKEWNESS		KURTOSIS		Gravel wt. %	Sand wt. %	Silt & Clay wt. %
	Value (Phi)	Verbal Scale	Value (Phi)	Verbal Scale	Value (Phi)	Verbal Scale	Value (Phi)	Verbal Scale			
2	0.50	CS	2.14	VPS	-0.134	CS	0.786	P	30.00	69.00	1.0
6	-0.21	VCS	2.00	VPS	0.208	FS	0.656	VP	46.00	52.00	2.0
12	-0.07	VCS	1.94	PS	0.126	FS	0.805	P	36.00	63.00	1.0
18	-0.54	VCS	1.96	PS	0.547	SFS	0.635	VP	55.00	44.00	1.0
24	-0.54	VCS	1.96	PS	0.546	SFS	0.801	P	56.00	43.00	1.0
30	-0.52	VCS	1.96	PS	0.525	SFS	0.830	P	56.00	43.00	1.0
34	-0.57	VCS	1.98	PS	0.527	SFS	0.862	P	57.00	41.00	2.0
40	-0.27	VCS	1.95	PS	0.227	FS	0.662	VP	48.00	51.00	1.0
44	-1.13	G	1.95	PS	0.812	SFS	0.960	M	63.00	36.00	1.0
48	-0.61	VCS	1.62	PS	0.539	SFS	0.861	P	58.00	40.00	2.0
54	-0.48	VCS	1.93	PS	0.480	SFS	0.678	P	51.00	48.00	1.0
60	-0.99	VCS	1.95	PS	0.473	SFS	1.091	M	68.00	31.00	1.0

Table 6.6 Textural attributes and percentage of gravel, sand and clay in drilled samples of wadi Malal (Well No. 6).

DEPTH OF SAMPLE (m)	MEAN SIZE		SORTING		SKEWNESS		KURTOSIS		Gravel wt. %	Sand wt. %	Silt & Clay wt. %
	Value (Phi)	Verbal Scale	Value (Phi)	Verbal Scale	Value (Phi)	Verbal Scale	Value (Phi)	Verbal Scale			
2	0.048	CS	2.16	VPS	0.229	FS	0.660	VP	43.00	55.00	2.00
8	-0.55	VCS	1.93	PS	0.498	SFS	0.805	P	54.00	45.00	1.00
12	-0.80	VCS	1.59	PS	0.389	SFS	0.796	P	55.00	44.00	1.00
20	-0.49	VCS	1.95	PS	0.459	SFS	0.811	P	50.00	48.00	2.00
26	-0.85	VCS	1.62	PS	0.432	SFS	0.796	P	58.00	41.00	1.00
38	-0.61	VCS	1.88	PS	0.500	SFS	0.872	P	56.00	42.00	2.00
44	0.05	CS	2.14	VPS	0.233	FS	0.670	VP	43.00	56.00	1.00
52	-0.25	VCS	1.82	PS	0.135	FS	0.737	P	44.00	54.00	2.00
56	-1.20	G	1.59	PS	0.837	SFS	1.030	M	69.00	30.00	1.00
62	-0.97	VCS	1.45	PS	0.468	SFS	0.866	P	67.00	32.00	1.00
66	-0.54	VCS	1.91	PS	0.487	SFS	0.853	P	54.00	45.00	1.00
70	-0.34	VCS	1.10	PS	0.055	NS	1.351	L	39.00	61.00	0.00

CHAPTER SEVEN

EVALUATION OF WATER RESOURCES

The evaluation of surface and groundwater potential are of the main objectives of this study.

The data available on meteorological and hydrological variables were collected from the Ministry of Agriculture and Water. The collected information includes the following:

- A- Data from the two major meteorological stations in Al Madinah area. These are M001 and M004. The data includes all major meteorological variables such as air temperature, pan evaporation, wind data and precipitation.
- B- Data concerning other precipitation recorders station of J223, M214 and M215. This data includes only monthly precipitation for these stations for few years.
- C- Summary of data from the runoff station around Al Madinah area. These include monthly and annual discharge in million cubic meters for runoff stations J408, M401, M402, M403, M404, M407, M408 and M409.
- D- Observation Wells Data: Data from five observation wells around Al Madinah area were also made available. These include MU-T2 (Al-Musayjid), ME-T4 and ME-T5 (Harrat Rahat), KHA-T3 (Harrat Khayber) and SA-T3 (Wadi Al Safra).

On the basis of data obtain from the MAW, the following information was observed:

- 1- All the records from the meteorological and runoff data are given only up to 1986 or 1987 at best. This well be checked with the MAW to see if, for some locations at least, there is more data to be collected.
- 2- Unfortunately there is no runoff station or observation well located within the study area itself. The two meteorological station areas located in Al Madinah itself (M001) and at Hanakiyah (M004). However, the meteorological data will be useful for the whole region of Al Madinah including the study area. With regard to the runoff station, data from similar catchment in Al Madinah area were used. The closest

observation well to the study area is the one located at Al-Musayjid. Data from wells within the study area was not available.

7.1 Surface water

7.1.1 Precipitation in the study area

Rainfall is the original source of all water resources. Therefore, the analysis of precipitation data within the study area is very important for the evaluation of its water resources.

Precipitation in Al Madinah area is generally low to very low. ITALCONSULT (1979) has estimated rainfall for the whole Madinah area to be between 50 and 100 mm/year. They also suggested that a large part of it occurs in a few rainfall events and that it can be of great intensity. Data from all the stations having precipitation records close to the study area were collected from the Hydrology department in the Ministry of Agriculture and Water. Table 7.1 shows basic information that was either collected or calculated for these stations. Fig. 7.1 shows the locations of four of the meteorological stations that are close to the study area. The mean annual precipitation for Wadi Malal area was estimated by the average of the four stations shown in Fig. 7.1. This resulted in 61.6 mm as an average annual rainfall distributed throughout the year in similar manner as the four stations. The rainfall starts from October to May with the greatest amounts occurring in March and April. The summer months June through September are all much drier than the rest of the year. This is a typical distribution of rainfall in the whole interior regions of Saudi Arabia.

7.1.2 Data on surface runoff

There are eight runoffs measuring stations in the whole region of Al Madinah. The data from these stations were collected from the Hydrology department in the MAW. Three of them are close to the study area. They are M401, M402 and M403. Table 7.2 gives basic information on these three stations while Table 7.3 gives their mean monthly runoff in m³/s (Al-Ahmadi, 1994).

The runoff values given in Table 7.3 show the following:

1. Surface runoff can be expected from the months of Nov. through May for any medium or large size catchment areas like those for the stations M401 and M402. Wadi Malal is almost the size of the catchment for M402.
2. During the months June through October, runoff is not expected in these areas. Rainfall may occur in October but since the condition of the soil will be too dry after a long and dry summer it is expected that runoff is not generated. Most of the water will simply infiltrate.

7.1.3 Wadi Malal soil physical characteristics

Soil samples were collected from Wadi Malal at different sections M3, M4, M5, M6, M7 and M8. These sections are located across Wadi Malal flood plane as we move from the downstream to the upstream part of the wadi.

Two sets of samples were taken close to the surface (0 -50 cm depths) and at different locations along the sections M3 to M8. The results of the analyses of the first set of samples were presented and discussed in details in chapter three. They represent the statistical evaluation of grain size distribution (texture) of the soil in the study area. The second set of samples is presented and discussed in this chapter. They are directed toward evaluation of basic soil physical characteristics.

Table 7.4 shows the sampling stations, wadi flood plain width and the main channel width at the different locations across the wadi. From the values presented in this table, the average width of the floodplain and the average main channel width were calculated. They are 975 m and 216.7 m, respectively

Table 7.5 shows the summary of the test results of the second group of soil samples. In this table specific gravity (G_s) Dry density (γ^d) in cm/sec, void ratio (e), coefficient of permeability or saturated hydraulic conductivity (K) in gr/sec., porosity (n) and grain size analysis for the 24 samples is given. There were six samples at station M3 with the first M3-SS-1 taken in the main channel while the rest were taken along the section at different locations. Similarly, at the other stations one sample is within the main channel while the

rest are along the section. For the stations M4 to M8, the samples located in the main channel are M4-SS-5, M5-SS-3, M6-SS-1, M7-SS-3 and M8-SS-3, respectively.

The average specific gravity, dry density, void ratio and porosity for the locations were calculated from the test results. They are presented in Table 7.6. The averages for specific gravity and dry density for all the locations do not vary too much as expected. The void ratio and porosities show variations of their values as we move upstream that are generally consistent with the change in soil grain size distribution.

The values of the coefficient of permeability in cm/sec. given in table 7.5 show clearly low values of this important parameter outside the main channel due to impermeability of the soil. However, the values of K in m/sec. are all high within the main channel, which is expected. Since the value of the saturated hydraulic conductivity is very important in the estimation of flow within the wadi bed, the values of K were calculated at different stations in m/day and they are presented as given in table 7.7

7.1.4 Flood frequency for Wadi Malal

There are no rainfall or runoff stations within the catchment of Wadi Malal. The estimation of the flood frequency can be estimated by using regression equations that were developed by Al-Turbak and Quraishi (1987) for different regions of Saudi Arabia. The basic equation used is the following:

$$Q_t = a (DA)^b (AP)^c (CL)^d (CS)^e$$

Where Q_t is the peak discharge (m^3/s) for the recurrence interval, t years.

DA = Drainage Area, Km^2

AP = Mean annual precipitation, mm

CL = Main channel length, Km

CS = Main channel average slopes m/m

a , b , c , d and e are regression coefficients given by Al-Turbak and Quraishi (1987) for $t = 5, 10, 25, 50$ and 100 years recurrence intervals.

For Wadi Malal, the following were used in the application of the flood frequency equation:

$$DA = 3200 \text{ Km}^2$$

$$AP = 61.6 \text{ mm}$$

$$CL = 65 \text{ Km}$$

$$CS = 0.0062 \text{ m/m}$$

The average slope of the main channel CS was calculated from difference of elevation between the two ends of the main wadi channel divided by channel length (CL). The values of the coefficients a, b, c, d and e for $t = 5$ years is shown below as an example. These are taken from Al-Turbak and Quraishi (1987):

$$a = 9.44 \times 10^{-7}$$

$$b = 0.0389$$

$$c = 2.5285$$

$$d = 0.2693$$

$$e = -0.9335$$

Using the values of wadi parameters and the regression coefficients, the peak discharge for $t = 5$ years was calculated and found to be $Q_5 = 15.3 \text{ m}^3/\text{s}$.

In a similar fashion, the peak discharge for the return periods $t=10, 25, 50$ and 100 years was calculated and the results are given as:

t, years	Qt, (m³/s)
5	15.3
10	22.8
25	30.5
50	37.2
100	43.2

The small values for Q_t even for 100 years flood is normal for the very dry conditions of the study area.

7.1.5 Volume of rainfall and its contribution to groundwater recharge

The volume of the mean annual rainfall (m^3) was estimated for Wadi Malal area. The total volume is estimated to be:

$$VR = 3200 (1000)^2 (61.6 \text{ mm})$$

Or $197,120,000 \text{ m}^3$. Only 2-4% of this volume, however, recharges the local aquifer. This was estimated by previous studies. Based on this, the volume of surface water contributing directly to groundwater recharge is between 3,942,400 and 7,884,800 m^3 with an average annual value of 5,913,600 m^3 . This means that on the average 5,913,600 m^3 of water will recharge the local aquifer in Wadi Malal. The source of this recharge is surface water, flowing in wadi channels and infiltrating to the water table.

7.2 Groundwater

7.2.1 Previous studies

ITALCONSULT (1979) presented general reports on all aspects of development of the Al Madinah area including general survey of groundwater. The main conclusions of ITALCONSULT study with regard to groundwater in Al Madinah area are:

- 1- Total saturated volume of the aquifer complex was estimated to be $15200 \times 10^6 \text{ m}^3$.
This will give maximum groundwater storage of about $750 \times 10^6 \text{ m}^3$ in the whole Al Madinah area, assuming an average specific yield of 5%.
- 2- A total of 1302 wells (dug and drilled) were inventoried in the whole Al Madinah area, 10 - 15 % drilled wells and almost all of them completed in the sub-basaltic alluvial aquifer.
- 3- Total annual volume of water extracted for irrigation was about $30 \times 10^6 \text{ m}^3$
- 4- Total annual volume of water extracted for domestic use was about $10 \times 10^6 \text{ m}^3$
- 5- The transmissivity of the whole Al Madinah area can be estimated to be $3 - 5 \times 10^{-3} \text{ m}^2/\text{s}$ and the specific yield is $5 - 8 \times 10^{-2}$.
- 6- The percentage of rainfall which reaches to the aquifer is 2 - 4 %.

The ITALCONSULT study was good in the sense it has surveyed all aspects of water in Al Madinah area. However, none of the details were carried out in Wadi Malal.

7.2.2 Estimation of groundwater storage.

The ground water in storage in the aquifer in Wadi Malal was estimated by finding the volume of the saturated zone and multiplying it by the average specific yield of the aquifer.

The volume of the saturated zone in the study area was calculated using the results of the geophysical part of the study. To estimate the groundwater in storage in Wadi Malal area, it is necessary to first estimate the cross sectional areas of the saturated alluvium at the different stations. The part of the saturated volume of the aquifer between M3 and M4, for example, can be estimated by multiplying the average of the cross sectional areas at the two stations by the distance between them.

The cross sectional area of the saturated sand at M3 profile, for example was calculated using the following procedure:

- 1- The area is divided into parts each part represents an incremental cross-sectional area of the saturated medium between vertical lines.
- 2- The depth of the saturated sand at each vertical location is estimated from the profile using the scale of the profile.
- 3- The incremental cross-sectional area is then calculated by multiplying the average of the depths of the saturated sand by the distance between the vertical locations.
- 4- The incremental cross-sectional areas are added to obtain the total cross-sectional area of the saturated sand at the profile location.
- 5- This procedure was used in all the calculations of the cross-sectional areas for all the profiles.

Using the profiles No. 3 and 4, the cross sectional areas for saturated sand are estimated as follows:

$$\text{at M3, } A = 64190 \text{ m}^2$$

$$\text{at M4, } A = 33479 \text{ m}^2$$

The distance between M3 and M4 is estimated to be 2.25 km. The volume of saturated sand between M3 and M4 was then estimated as:

$$V_{3-4} = \frac{(64190 + 33479)}{2} (2250)$$

$$V_{3-4} = 109,877,625 \text{ m}^3$$

The volume of water in storage between M3 and M4 can be found by multiplying V_{3-4} by the average specific yield (S_y). For Al Madinah area, S_y is within the range $(5-8) \times 10^{-2}$. If the value $S_y = 5 \times 10^{-2}$ is used, the volume of groundwater in storage between the two stations M3 and M4 in Wadi Malal is calculated as:

$$V_I = 109,877,625 (5 \times 10^{-2})$$

$$V_I = 5,493,881 \text{ m}^3$$

In a similar manner, the volume of water in storage between M4 and M5 in Wadi Malal was estimated as follows:

First, the cross sectional areas of the saturated zones are found (from geophysical profiles)

$$\text{at M4, } A = 33479 \text{ m}^2$$

$$\text{at M5, } A = 18346 \text{ m}^2$$

The distance between the two stations M4 and M5 is about 7.5 km. The volume of saturated zone between M4 and M5 is calculated as

$$V_{4-5} = \frac{(33479 + 18346)}{2} (7500)$$

$$V_{4-5} = 194,343,750 \text{ m}^3$$

Similarly, the volume of groundwater in storage between the two stations M4 and M5 in Wadi Malal is calculated as follows:

$$V_{II} = 194,343,750 (5 \times 10^{-2})$$

$$V_{II} = 9,717,188 \text{ m}^3$$

Table 7.8 shows the results of groundwater in storage in Wadi Malal. The total groundwater storage given in the table is 62,335,000 m³. This represents the groundwater in storage in the local aquifer extending under the main channel only. It does not include the last part of the catchment (upstream of profile No. 8) and it does not include the parts of the aquifer away from the flood plain of the main wadi channel. Based on the areas not covered, it is estimated that about 30% should be added to the found volume to make it representing the whole area.

It is therefore, estimated that the total groundwater in storage in Wadi Malal is about 81 million cubic meter.

7.2.3 Results of drilling samples

Tables 7.9-7.14 shows the results of the analysis carried out on samples taken during the drilling of the six wells explained in chapter three. These results include specific gravity, dry density, void ratio, porosity and the hydraulic conductivity (coefficient of permeability) for the samples taken at the shown depths.

The values of the specific gravity and dry density vary slightly and are all within the expected ranges. Void ratio and porosity value variations depend mainly on soil type of the samples. The lithology of the wells is given in chapter three and the description given for each layer explains the variation in the void ratio and porosity. The hydraulic conductivity also varies with soil type. It is noted for example that at well no. M3.1 the hydraulic conductivity is low to medium except after the 42 m depth, which is consistent with the description given in chapter three.

7.2.4 Discussion

ITALOCUNSLT has estimated that the total groundwater in storage in Al Madinah area was about 750 million cubic meters. The result of this study has shown that groundwater in storage in Wadi Malal was about 81 million cubic meters. The catchment area of Wadi Malal is 3200 km² while the catchment for the Al Madinah area in ITALOCUNSLT study about 10 times as much. Therefore, the estimate of groundwater in storage in the study area is reasonable.

It was also estimated by this study that the mean annual recharge to the aquifer in Wadi Malal catchment is about 5.9 million cubic meters. To be able to see if the groundwater in the study area is being depleted, it is necessary to estimate the annual pumpage and compare it to the annual recharge. If the water being pumped annually is more than the estimated mean annual recharge, then the aquifer is being depleted.

It is suspected that the annual pumping in the study area is higher than the mean annual recharge. This means that the aquifer in Wadi Malal catchment, like almost all aquifer in the area, is being depleted. Water is being replaced which will result in declining water levels. The evidence of this is clear since so many farms have recently been started in the downstream area of the much Wadi Malal and in some of its tributaries.

7.3 Quality of groundwater

7.3.1 Samples collection

A total of 33 wells were sampled covering the study area as follows (Figs. 7.2, 7.3, 7.4):

- 2 upstream wells
- 16 middle stream wells
- 15 down stream wells

Table 7.15 lists the wells numbers, locations and depths.

7.3.2 Samples analysis

All collected samples were analyzed in duplicate for the following constituents: temperature, pH, EC, turbidity, total dissolved solids (TDS), total hardness, alkalinity, Ca,

Mg, Na, K, Fe, Mn, Cl^- , SO_4^{2-} , NO_3^- , and F. The first four parameters were measured in the field during samples collection time whereas the remaining parameters were measured in the laboratory by following the Standard Methods for Water and Wastewater Examination. Table 7.16 gives details about the methods of analysis and the equipment used.

7.3.3 Results and discussion

Thirty-three samples were collected from the study area, which included 2 upstream wells, 16 middle stream wells and 15 down stream wells. The locations of these wells with their respective depths have been presented in Table 7.15. Wells were shallow and the depths of the wells varied between 30 and 80 meters. All of the wells were located in the agricultural areas of Wadi Malal in Al Madinah area. Samples were analyzed for temperature, pH, turbidity, conductivity, dissolved solids, total hardness, Ca, Mg, total alkalinity, Fe, Na, K, F, Cl, NO_3 and SO_4 using Standard Methods. Temperature, pH, turbidity and conductivity were measured in the field.

Considering the physico-chemical characteristics of all well waters (Tables 7.17, 7.18, and 7.19) average temperature varied between 30 and 35°C for upstream, middle stream and down stream. The average pH for upstream, middle stream and down stream well samples was 7.1, 6.9 and 6.98 respectively, whereas average turbidity for upstream, middle stream, and down stream wells was 0.79, 1.0 and 0.82 NTU respectively. The average dissolved solids (TDS) were 1283, 1148 and 1323 mg/L respectively for upstream, middle stream and downstream wells. Average calcium (as CaCO_3) and magnesium (as MgCO_3) for upstream, middle stream and down stream wells were 370.8, 470.1, 470.1 mg/L and 139.1, 133.4, 133.8 mg/L respectively, whereas average sodium and potassium were 211, 163.5, 181.0 mg/L and 2.2, 3.6 and 3.5 mg/L respectively. Fluoride concentrations were found in low concentrations and varied between 0.63 and 0.95 mg/L. Average chloride concentrations were 343, 328.4 and 277.5 mg/L respectively, for upstream, middle stream and down stream wells. Nitrate was present in considerably high concentrations in all wells. Average nitrate levels of 60.5, 131.7 and 198.8 mg/L were found for upstream, middle stream and down

stream wells respectively. Average SO₄ values for upstream, middle stream and down stream wells were 252.5, 202 and 251.8 mg/L respectively. The average alkalinity was 209, 192.7 and 174 mg/L for upstream, middle stream and down stream wells respectively.

The results showed that there was very little variation for average pH from upstream wells to the down stream wells. It was true for the average turbidity values. Average dissolved solids increased in the down stream wells. Average calcium was also found to increase in the down stream samples as compared to the upstream wells. Small variation was observed for average magnesium and potassium from upstream wells to downstream wells. Average sodium decreased in the middle stream wells but increased in the downstream wells. The same trend was observed for sulphate also. Average fluoride decreased from upstream wells to down stream wells. The most dramatic change was observed for nitrates. Nitrate jumped from its average value of 60.5 mg/L in the upstream wells to 198.8 mg/L in the downstream wells. The high levels of nitrate in all samples may be attributed to the fact the area in which the sampling was carried out is a predominantly agriculture area and the use of nitrogen based fertilizers in the fields may have increased nitrates in the shallow aquifers from which the wells are connected. Also, an increase from upstream to down stream wells shown a movement of nitrates from upstream to the down stream.

Upstream Wells:

Only two wells were sampled in this group of wells. Conductivity dissolved solids and several ions like Ca, Mg, Na, K, F, Cl and SO₄ were higher in well 31 than well 32 (Table 7.17). It may be mentioned that well 31 is down stream to well 32 and is deeper (58 M) than well 32 (51 M) and therefore, ionic movement from well 32 to well 31 may not be ruled out.

Middle Stream Wells:

16 wells were sampled in this group of wells. The well depths varied between 30 and 65 meters. Maximum conductivity, dissolved solids and various cations and anions were found in well 30 which is a shallow well with 35 meter depth, whereas minimum levels of different parameters were found in well 18 which has a depth of 65 meter (Table 7.18).

Down Stream Wells:

15 wells were sampled in this group of wells. The well depths varied between 55 and 80 meters. In fact, these wells were much deeper than the upstream and middle stream wells. The maximum ionic concentrations were found in well two and the minimum in well 13 (Table 7.19).

7.3.4 Suitability of Wadi Malal well waters for irrigation:

The suitability of water for irrigation is judged mainly from the following characteristics:

- a. Total concentration of soluble salts (TDS)
- b. Relative proportion of sodium to other cations.
- c. Chlorides and sulphates.
- d. Bicarbonates.
- e. Concentrations of potentially toxic elements present in water.
- f. Bacterial contamination.

However, the suitability of irrigation water is very much influenced by the constituents of the soil, which is to be irrigated. A particular water may be harmful for irrigation on a particular soil but the same water may be tolerable or even useful for irrigation on some other soil. Values for different grades of irrigation water are shown in Table 7.20.

The evaluation of Wadi Malal well waters showed that considerable concentration of Ca, Mg, Na and K were present in most of the well waters. It is known that salts of Ca, Mg, Na and K present in irrigation water may prove injurious to plants. When present in excessive quantities, they reduce the osmotic activities of plants and may prevent adequate aeration.

The sodicity of the irrigation water is the extent to which it can possibly influence the exchangeable sodium content of the soil and cause infiltration and permeability problems affecting the plant growth. The criteria used to evaluate irrigation waters from sodicity point of view are percentage of Sodium and Sodium Absorption Ratio. The percentage of Sodium

for both the upstream well waters was above 40% making these waters Grade B irrigation water. However, 62% well waters in the middle stream were of Grade A quality, with respect to percentage of Sodium whereas the rest belonged to Grade B. In down stream wells 47% well waters belonged to Grade A of irrigation water whereas the rest belonged to Grade B.

The evaluation of Wadi Malal well waters with respect to chloride showed that in upstream wells, one well belonged to Grade B (W 32) and the other (W 31) belonged to Grade C of irrigation water. In middle stream wells, 62% met the Grade B quality of water whereas the rest were of Grade C quality. In downstream wells, 80% wells were of Grade B quality whereas the rest were of Grade C quality. Considering Sulphates, all well waters from upstream to downstream wells were of Grade B quality of irrigation water.

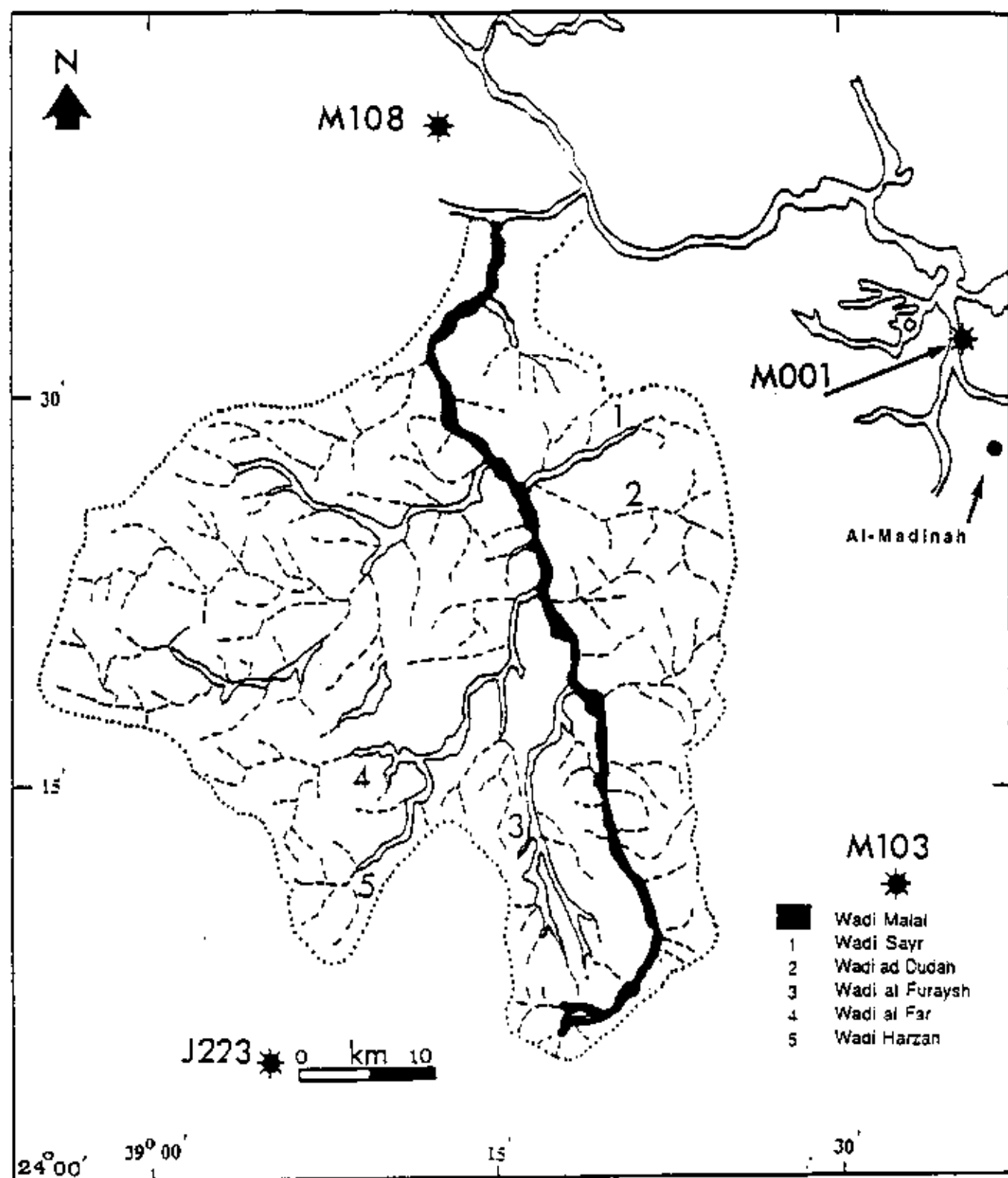


Fig. 7.1 Meteorological stations around wadi Malal

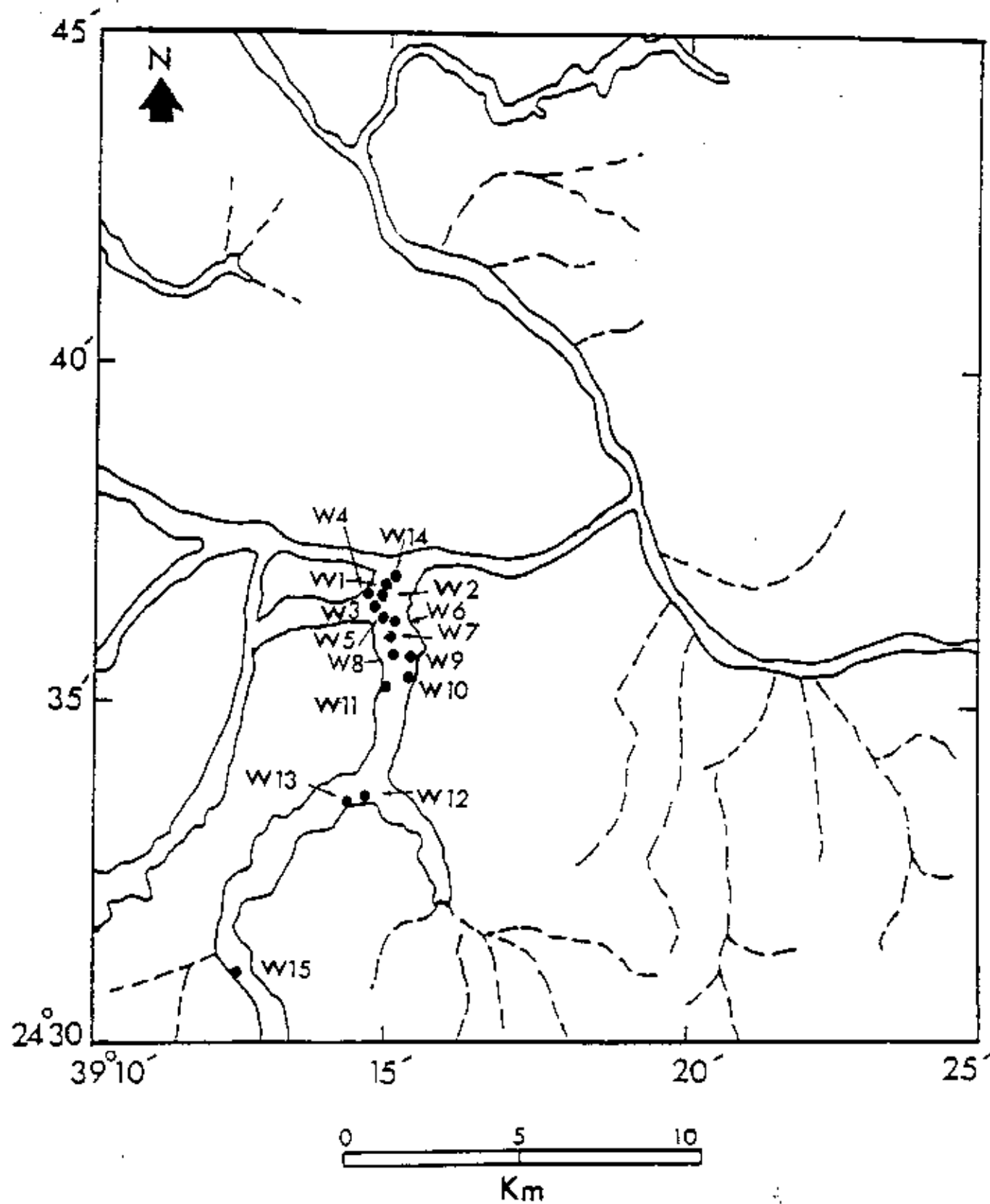


Fig. 7.2 Wells locations in down-stream, wadi Malal

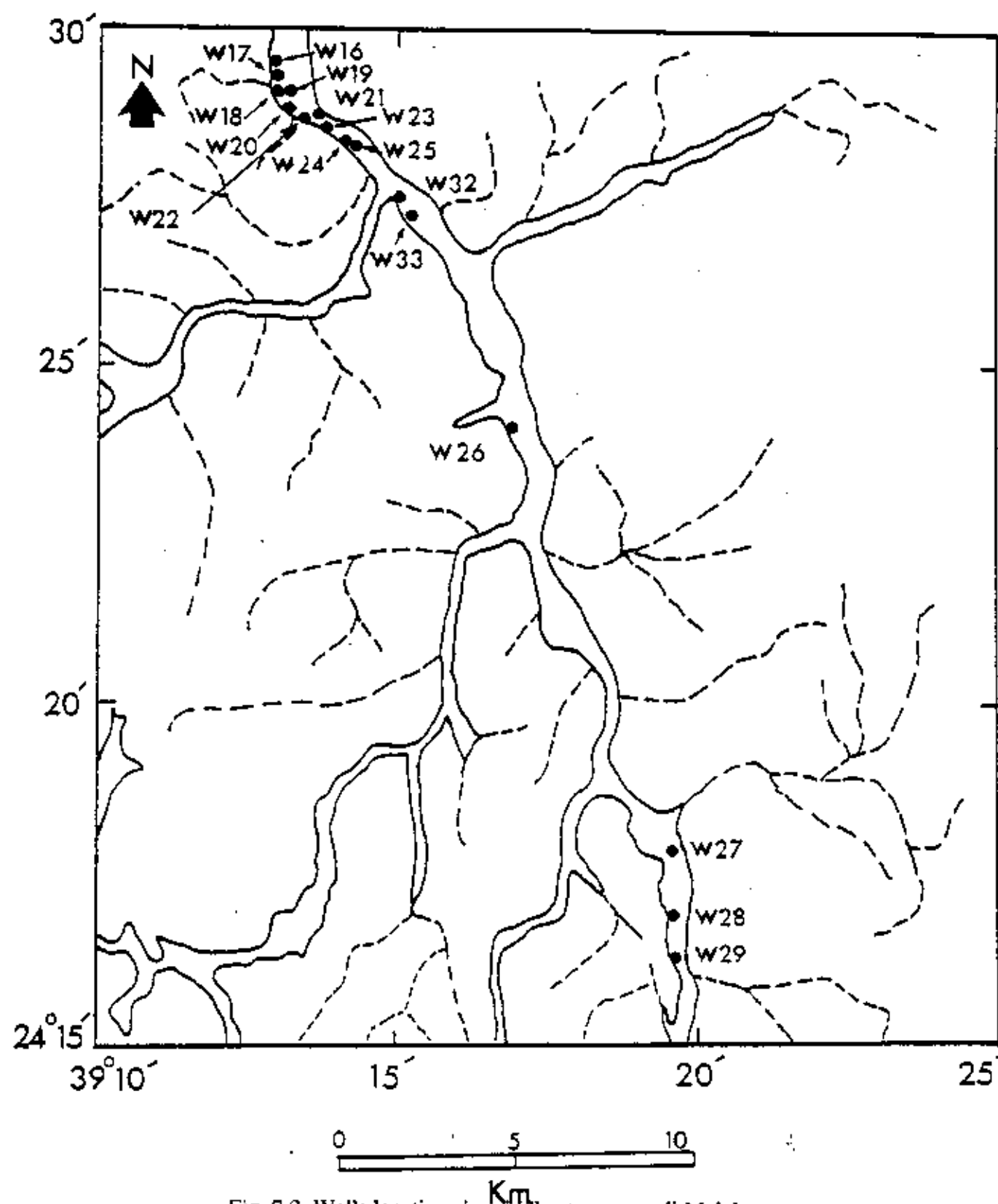


Fig. 7.3 Wells locations in middle-stream; wadi Malal

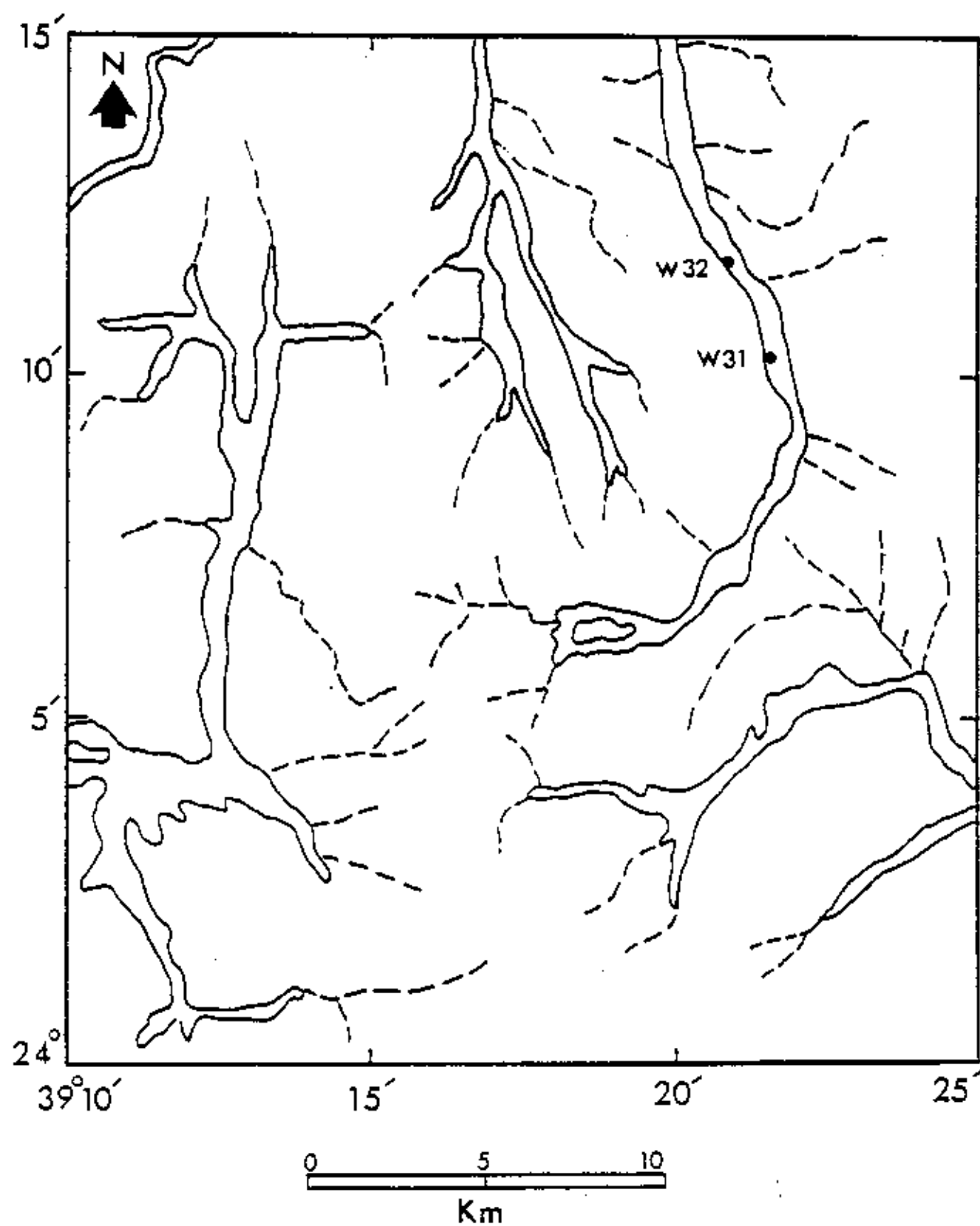


Fig. 7.4 Wells locations in upper-stream, wadi Malal

Table 7.1 Precipitation stations

NAME AND COORDINATES	YEARS OF RECORDS	MEAN ANNUAL PRECIPITATION (mm)
Madinah Farm (M001) Lat. 24° 31' N. ; Long. 39° 35' E.	25	59
Hanakiyah (M004) Lat. 24° 50' N. ; Long. 40° 31' E.	25	62.1
Bir Mashī (M103) Lat. 24° 11' N. ; Long. 39° 32' E.	20	42.3
Meleileh (M108) Lat. 24° 40' N. ; Long. 39° 13' E.	20	53.1
Mosyjid (J223) Lat. 24° 05' N. ; Long. 39° 05' E.	15	92.2

Table 7.2 Basic parameters of three runoff stations

STATION NAME, NO. AND YEARS OF RECORDS	CATCHMENT AREA (KM ²)	COORDINATES	ELEVATION (m)
Wadi Aqūl at the Dam (M401), 18 years	33,000	Lat. 24° 30' N. Long. 39° 44' E.	625
Wadi Aqiq at Arwa Dam (M402), 17 years	3100	Lat. 24° 27' N. Long. 39° 35' E.	620
Wadi Awali at Bathān DAM (M403), 17 years	16	Lat. 24° 27' N. Long. 39° 36' E.	630

Table 7.3 Mean monthly runoff (m³/s) for three runoff stations

MONTH	M401	M402	M403
JANUARY	5.2	3.5	0.7
FEBRUARY	1.0	0.0	0.0
MARCH	6.5	7.4	0.0
APRIL	61.2	14.0	2.1
MAY	6.8	1.1	0.1
JUNE	0.0	0.0	0.0
JULY	0.0	0.0	0.0
AUGUST	0.0	0.0	0.0
SEPTEMBER	0.0	0.0	0.0
OCTOBER	0.0	0.0	0.0
NOVEMBER	34.5	1.1	0.1
DECEMBER	6.7	1.8	0.1

Table 7.4 Approximate flood plain and main channel widths, Wadi Malal

Station	Flood plain width (m)	Main channel width (m)
M3	2100	425
M4	820	180
M5	460	190
M6	1300	200
M7	620	155
M8	550	150

Table 7.5 Soil samples test results

Sample No.	Sp. gr. G_s	Density γ_d gm/cm ³	Void ratio "e"	Coeff. of Perme. "k"	Porosity "n"	Gravel %	Sand %	Silt %	Clay %
M3-SS-1	2.71	1.73	0.56	145.7	0.36	5	90.3	4.7	-
M3-SS-2	2.71	1.89	0.43	8.142	0.30	8.3	81.1	8.9	1.7
M3-SS-3	2.71	1.89	0.43	0.132	0.30	22.5	53.5	13.5	10.5
M3-SS-4	2.72	1.74	0.55	8.17	0.35	5.8	78.5	11.7	4.5
M3-SS-5	2.719	1.67	0.62	11.54	0.38	7.5	77.5	11.0	4.0
M3-SS-6	2.71	1.82	0.49	13.93	0.32	10.2	79.2	8.0	2.6
M4-SS-1	2.70	1.88	0.43	20.0	0.30	16.7	74.2	9.1	-
M4-SS-2	2.71	1.70	0.59	17.7	0.37	0.8	90.1	9.1	-
M4-SS-3	2.716	1.81	0.49	16.3	0.33	10.0	78.3	8.1	3.6
M4-SS-4	2.71	1.67	0.61	22.3	0.38	18.1	69.7	8.9	3.3
M4-SS-5	2.72	1.74	0.56	42.1	0.36	1.0	89.3	9.7	-
M5-SS-1	2.71	1.78	0.52	59.94	0.33	11.3	81.8	6.9	-
M5-SS-2	2.70	1.79	0.51	41.77	0.33	15.8	76.5	7.7	-
M5-SS-3	2.68	1.84	0.45	331.0	0.312	26.7	70.5	2.8	-
M6-SS-1	2.70	1.9	0.42	206.6	0.29	23.7	72.9	3.4	-
M6-SS-2	2.71	1.85	0.45	7.98	0.313	20.1	68.8	8.9	2.2
M6-SS-3	2.71	1.92	0.41	12.91	0.29	17.3	74.0	8.7	-
M6-SS-4	2.72	1.89	0.44	3.33	0.30	7.9	71.4	16.4	4.3
M7-SS-1	2.71	1.83	0.48	13.12	0.32	4.5	82.5	9.7	3.3
M7-SS-2	2.72	1.78	0.52	11.91	0.34	3.5	80.6	13.0	2.9
M7-SS-3	2.71	1.67	0.62	174.3	0.38	1.0	93.8	5.2	-
M8-SS-1	2.71	1.99	0.35	0.61	0.26	22.3	60.5	14.3	2.9
M8-SS-2	2.70	2.07	0.31	6.95	0.23	25.0	66.2	8.8	-
M8-SS-3	2.69	1.92	0.40	198.0	0.28	28.0	69.3	2.7	-

Table 7.6 Average values of basic soil characteristic

STATION	G _s	d	e	n
M3	2.716	1.795	0.512	0.339
M4	2.715	1.764	0.542	0.350
M5	2.702	1.809	0.497	0.328
M6	2.708	1.892	0.432	0.301
M7	2.719	1.762	0.545	0.352
M8	2.701	1.995	0.355	0.261

Table 7.7 Main channel K

STATION	cm/sec. $\times 10^{-4}$	m/d
M3	145.7	12.59
M4	42.1	3.64
M5	331.0	28.60
M6	206.7	17.86
M7	174.3	15.06
M8	198	17.11

with the average value of K for the whole main channel being 15.81 m/day.

Table 7.8 Calculation of groundwater in storage, wadi Malal.

PROFILE NO.	SATURATED AREA, m ²	DISTANCE BETWEEN PROFILES(Km)	VOLUME OF SATURATED ZONE, $\times 10^6$ (m ³)	VOLUME OF STORED WATER $\times 10^6$ (m ³)
3	64190	2.25	109.9	5.495
4	33479	7.50	194.3	9.715
5	18346	14.17	534.2	26.71
6	56921	2.26	79.9	3.995
7	13891	14.52	328.4	16.42
8	31346			
TOTAL				62.335

Table 7.9 Results for drilling samples well number one (M3.1)

Depth (m)	Specific Gravity, G_s	Dry Density (g/cm^3)	Void Ratio (e)	Porosity (n), %	Coefficient of Permeability k_{20} , (cm/sec.)
2	2.753	1.851	0.6675	40.03	2.848×10^{-4}
8	2.752	1.727	0.5935	37.25	2.1×10^{-4}
14	2.738	1.907	0.4358	30.35	7.404×10^{-5}
18	2.738	1.745	0.5691	36.27	2.063×10^{-4}
22	2.718	1.884	0.4427	30.68	2.341×10^{-4}
28	2.703	1.74	0.5534	35.83	1.834×10^{-4}
32	2.738	1.678	0.6317	38.71	5.305×10^{-5}
36	2.721	1.636	0.6632	39.88	2.645×10^{-5}
42	2.74	1.56	0.7584	43.07	1.981×10^{-4}
46	2.7	1.743	0.5491	35.44	1.032×10^{-3}
52	2.829	1.645	0.7198	41.85	1.813×10^{-3}
56	2.71	1.598	0.7065	41.40	2.582×10^{-4}
60	2.71	1.711	0.6639	38.86	7.11×10^{-4}

Table 7.10 Results for drilling samples well number two (M3.2)

Depth (m)	Specific Gravity, G _s	Dry Density (g/cm ³)	Void Ratio (e)	Porosity (n), %	Coefficient of Permeability k ₂₀ (cm/sec.)
2	2.773	1.675	0.6555	39.60	1.358 *10 ⁻⁶
6	2.761	1.744	0.5831	36.83	9.913* 10 ⁻⁵
14	2.721	1.871	0.4543	31.24	5.509*10 ⁻⁴
22	2.7	1.653	0.6334	38.78	1.903*10 ⁻³
28	2.69	1.675	0.6060	37.73	0.0478
26	2.719	1.623	0.6753	40.31	2.558* 10 ⁻⁴
40	2.71	1.659	0.6335	38.78	1.722* 10 ⁻⁴
48	2.708	1.677	0.6148	38.07	1.033* 10 ⁻⁴
52	2.703	1.891	0.4294	30.04	1.18* 10 ⁻³
58	2.8	2.056	0.3619	26.57	3.227* 10 ⁻⁵
64	2.808	1.693	0.6586	39.71	0.0557
70	2.81	1.755	0.6011	37.54	0.0637
74	2.81	1.848	0.5206	34.23	0.0254
76	2.81	1.623	0.7314	42.24	0.0243
78-80	2.81	1.707	0.6462	39.25	0.102

Table 7.11 Results for drilling samples well number three (M3.3)

Depth (m)	Specific Gravity, Gs	Dry Density (g/cm ³)	Void Ratio (e)	Porosity (n), %	Coefficient of Permeability k ₂₀ , (cm/sec.)
2	2.727	1.554	0.7548	43.01	5.763* 10 ⁻⁵
6	2.715	1.573	0.7280	42.06	1.966* 10 ⁻⁶
10	2.737	1.507	0.8162	44.94	4.93* 10 ⁻⁵
12	2.7	1.853	0.4571	31.37	1.008* 10 ⁻³
16	2.739	1.765	0.5518	35.56	4.045* 10 ⁻⁵
22	2.73	1.568	0.7411	42.56	3.213* 10 ⁻⁵
26	2.73	1.474	0.8521	46.01	5.536* 10 ⁻⁵
32	2.73	1.426	0.9144	47.77	3.353* 10 ⁻⁵
34	2.682	1.473	0.8208	45.08	2.639* 10 ⁻⁶
36	2.756	1.363	1.0220	50.54	1.0658* 10 ⁻⁶
40-41	2.711	1.734	0.5634	36.04	5.906* 10 ⁻³

Table 7.12 Results for drilling samples well number four (M3.4)

Depth (m)	Specific Gravity, Gs	Dry Density (g/cm ³)	Void Ratio (e)	Porosity (n), %	Coefficient of Permeability k ₂₀ , (cm/sec.)
2	2.69	1.818	0.4796	32.42	1.565* 10 ⁻⁴
8	2.7	1.602	0.6854	40.67	3.154* 10 ⁻⁵
12	2.72	1.558	0.7458	42.72	1.790* 10 ⁻⁴
14	2.73	1.646	0.6586	39.71	4.271* 10 ⁻⁵
20	2.7	1.615	0.6718	40.19	1.254* 10 ⁻⁴
22	2.77	1.4	0.9786	49.46	7.35* 10 ⁻⁶
26	2.715	1.354	1.0052	50.13	1.672* 10 ⁻⁴
32	2.723	1.51	0.8033	44.55	1.447* 10 ⁻⁵
34	2.71	1.456	0.8613	46.27	2.372* 10 ⁻⁵
38	2.716	1.352	1.0089	50.22	2.715* 10 ⁻⁵
44	2.78	1.281	1.1702	53.92	7.624* 10 ⁻⁶
48	2.72	1.448	0.8785	46.76	1.256* 10 ⁻⁵
52	2.7	1.667	0.6197	38.26	1.990* 10 ⁻³

Table 7.13 Results for drilling samples well number five (M4)

Depth (m)	Specific Gravity, G _s	Dry Density (g/cm ³)	Void Ratio (e)	Porosity (n), %	Coefficient of Permeability k ₂₀ , (cm/sec.)
2	2.731	1.416	0.9287	48.15	8.72* 10 ⁻⁵
6	2.71	1.765	0.5354	34.87	2.531* 10 ⁻⁴
8	2.72	1.75	0.5543	35.66	2.233* 10 ⁻⁴
12	2.718	1.813	0.4992	33.30	2.001* 10 ⁻⁴
16	2.72	1.861	0.4616	31.58	1.984* 10 ⁻⁴
18	2.7	1.818	0.4851	32.67	1.931* 10 ⁻⁴
24	2.699	1.827	0.4773	32.31	2.143* 10 ⁻³
30	2.71	1.823	0.4866	32.73	4.132* 10 ⁻⁴
34	2.71	1.82	0.4890	32.84	4.891* 10 ⁻⁴
40	2.71	1.81	0.4972	33.21	3.912* 10 ⁻⁴
42	2.7	1.981	0.3629	28.63	6.121* 10 ⁻³
44	2.702	2.003	0.3490	25.87	5.600* 10 ⁻³
48	2.715	1.8	0.5083	33.70	4.912* 10 ⁻⁴
52	2.723	1.781	0.5289	34.59	5.213* 10 ⁻⁴
54	2.73	1.769	0.5432	35.20	5.559* 10 ⁻⁴
60	2.73	1.778	0.5354	34.87	5.031* 10 ⁻⁴

Table 7.14 Results for drilling samples well number six (M5)

Depth (m)	Specific Gravity, Gs	Dry Density (g/cm ³)	Void Ratio (e)	Porosity (n), %	Coefficient of Permeability k ₂₀ (cm/sec.)
2	2.713	1.919	0.4138	29.27	2.390* 10 ⁻⁴
8	2.712	1.826	0.4852	32.67	2.106* 10 ⁻⁴
12	2.711	1.574	0.7224	41.94	6.432* 10 ⁻⁴
16	2.71	1.619	0.6739	40.26	7.623* 10 ⁻⁴
20	2.7	1.835	0.4714	32.04	2.522* 10 ⁻³
26	2.702	1.705	0.5848	36.90	1.952* 10 ⁻³
30	2.7	1.679	0.6081	37.81	2.511* 10 ⁻³
34	2.71	1.426	0.9004	47.38	4.384* 10 ⁻⁴
38	2.7	1.751	0.5420	35.15	1.912* 10 ⁻³
44	2.7	1.763	0.5315	34.70	1.851* 10 ⁻³
48	2.711	1.539	0.7615	43.23	5.131* 10 ⁻⁴
52	2.71	1.376	0.9695	49.23	6.078* 10 ⁻⁴
54	2.713	1.512	0.7943	44.27	5.22* 10 ⁻⁴
56	2.7	1.826	0.4786	32.37	4.368* 10 ⁻³
60	2.702	1.795	0.5053	33.57	6.157* 10 ⁻⁴
66	2.708	1.676	0.6158	38.11	9.47* 10 ⁻⁴

Table 7.15 Sample well, their locations and depth.

WELL NO.	SAMPLE NO.	LOCATION	DEPTH (m)
W1	1	Lat. 24° 36' 52" N Long. 39° 15' 03" E	75
W2	2	Lat. 24° 36' 45" N Long. 39° 14' 53" E	80
W3	3	Lat. 24° 36' 38" N Long. 39° 14' 51" E	70
W4	4	Lat. 24° 36' 26" N Long. 39° 15' 27" E	80
W5	5	Lat. 24° 36' 12" N Long. 39° 15' 00" E	65
W6	6	Lat. 24° 36' 8" N Long. 39° 15' 03" E	65
W7	7	Lat. 24° 35' 40" N Long. 39° 15' 04" E	60
W8	8	Lat. 24° 35' 28" N Long. 39° 15' 08" E	70
W9	9	Lat. 24° 35' 29" N Long. 39° 15' 15" E	60
W10	10	Lat. 24° 35' 20" N Long. 39° 15' 15" E	55
W11	11	Lat. 24° 35' 03" N Long. 39° 14' 58" E	57
W12	12	Lat. 24° 33' 45" N Long. 39° 14' 52" E	50
W13	13	Lat. 24° 33' 39" N Long. 39° 14' 44" E	60
W14	14	Lat. 24° 36' 53" N Long. 39° 15' 10" E	80
W15	15	Lat. 24° 30' 50" N Long. 39° 12' 35" E	55
W16	16	Lat. 24° 29' 33" N Long. 39° 13' 03" E	50

Cont. Table 7.15

W17	17	Lat. 24° 29' 28" N Long. 39° 13' 02" E	65
W18	18	Lat. 24° 29' 09" N Long. 39° 12' 55" E	65
W19	19	Lat. 24° 29' 10" N Long. 39° 13' 08" E	55
W20	20	Lat. 24° 28' 47" N Long. 39° 13' 19" E	60
W21	21	Lat. 24° 28' 31" N Long. 39° 13' 43" E	60
W22	22	Lat. 24° 28' 31" N Long. 39° 13' 25" E	55
W23	23	Lat. 24° 28' 32" N Long. 39° 13' 57" E	45
W24	24	Lat. 24° 28' 31" N Long. 39° 14' 12" E	50
W25	25	Lat. 24° 28' 31" N Long. 39° 14' 17" E	60
W26	26	Lat. 24° 24' 02" N Long. 39° 17' 03" E	47
W27	27	Lat. 24° 17' 53" N Long. 39° 19' 40" E	30
W28	28	Lat. 24° 16' 52" N Long. 39° 19' 37" E	32
W29	29	Lat. 24° 16' 13" N Long. 39° 19' 39" E	47
W30	30	Lat. 24° 12' 01" N Long. 39° 20' 39" E	35
W31	31	Lat. 24° 10' 33" N Long. 39° 21' 28" E	58
W32	32	Lat. 24° 27' 28" N Long. 39° 15' 16" E	51
W33	33	Lat. 24° 27' 25" N Long. 39° 15' 16" E	57

Table 7.16 Used methods and equipments for sample analysis

PARAMETER	METHOD / EQUIPMENT
Temperature	HACH Temperature Tester (Cat. No. 44450)
pH	Fisher Scientific Equipment Model 50 pH meter.
Electrical conductivity	HACH Model 8391-5 Turbidity test kit
TDS	Gravimetric
Alkalinity	Titration
Ca	Ion-Chromatograph
Mg	Ion-Chromatograph
Total hardness	By calculation
Fe	HACH Spectrophotometer DR/3000
Mn	HACH Spectrophotometer DR/3000
K	Ion-Chromatograph
Na	Ion-Chromatograph
Cl	Ion-Chromatograph
SO ₄	Ion-Chromatograph
NO ₄	Ion-Chromatograph
F	Ion-Chromatograph

Table 7.18 : Quality of Middle Stream Well Waters

Well No.	Temp. °C	pH	Turbi. (NTU)	Conduc. μ S/cm	TDS*	Total** hardness	Ca**	Mg**	Alkali- nity**	Fe*	Na*	K*	F*	Cl*	NO ₃ *	SO ₄ *	% Na	SAR
W16	33	6.90	0.99	1.37	914	466	372	94	176	0.05	105	3.5	0.44	212	126	115	32.6	2.4
W17	34	6.80	0.68	2.51	1804	1002	799	202.6	140	0.05	161	4.7	0.80	501	313	267	25.8	2.2
W18	35	6.80	0.86	1.03	710	393	314.6	78.2	188	0.14	98	3.4	0.37	156	75.9	106	34.9	2.1
W19	35	6.90	0.49	2.22	1642	939	749.1	190.2	152	0.06	140	4.5	0.73	409	279.8	275	24.3	1.9
W20	34	7.00	0.48	1.84	1234	733	581.8	150.7	192	0.05	120	4.5	0.59	333	160.9	196	26.1	1.9
W21	31	6.70	0.60	1.66	1164	609	479.4	129.3	240	0.04	128	4.6	0.48	288	105.4	169	31.1	2.2
W22	32	6.80	0.80	1.53	1102	527	414.5	112.4	204	0.04	126	4.2	0.49	258	95.4	150	34.0	3.8
W23	32	6.80	0.13	1.32	926	463	364.5	98.0	208	0.05	130	4.3	0.47	229	93.0	135	37.6	2.6
W24	34	7.00	0.57	1.45	1030	505	399.5	105.8	208	0.07	131	4.3	0.49	246	93.0	144	35.8	2.5
W24	35	7.10	0.48	1.46	993	452	354.5	97.1	212	0.03	134	4.4	0.48	238	94.6	138	38.9	2.7
W25	27	7.20	1.23	1.66	1124	465	342.3	122.3	192	0.17	172	1.8	0.96	311	51.3	190.5	44.5	3.4
W26	31	6.70	0.45	1.95	1306	508	409.5	98.4	164	0.06	238	3.0	1.0	396	112	230	50.3	4.6
W27	29	7.00	0.54	2.35	1688	713	531.8	182.4	188	0.06	252	2.6	1.0	458	168	309	43.3	4.1
W29	28	6.90	7.50	2.24	1622	678	504.3	173.3	192	0.83	241	2.4	0.96	453	131	280	43.4	4.0
W30	27	6.80	0.80	2.58	1920	817	616.7	200.1	220	0.10	267	3.4	1.3	502	153	270	41.4	4.0
W33	31	7.00	0.42	1.50	976	387	287.1	100.0	208	0.13	173	1.7	0.90	265	56.5	158	49.1	3.8
Min.	27	6.7	0.13	1.03	710	452	287.1	78.2	140	0.03	98	1.7	0.37	156	51.3	106	24.3	1.9
Max.	35	7.2	7.5	2.58	1920	1002	799.0	202.6	240	0.83	267	4.7	1.3	502	313	370	50.3	4.6
Avg.	32	6.9	1.0	1.79	1148	603.5	470.1	133.4	192.7	0.12	163.5	3.6	0.72	328.4	131.7	202.0	37.1	3.05

* mg/L

** mg/L as CaCO₃

SAR = Sodium Absorption Ratio

Table 7.19 : Quality of Middle Stream Well Waters

Well No.	Temp. °C	pH	Turbi. (NTU)	Conduc. μ S/cm	TDS*	Total** hardness	Ca**	Mg**
W16	33	6.90	0.99	1.37	914	466	372	94
W17	34	6.80	0.68	2.51	1804	1002	799	202.6
W18	35	6.80	0.86	1.03	710	393	314.6	78.2
W19	35	6.90	0.49	2.22	1642	939	749.1	190.2
W20	34	7.00	0.48	1.84	1234	733	581.8	150.7
W21	31	6.70	0.60	1.66	1164	609	479.4	129.3
W22	32	6.80	0.80	1.53	1102	527	414.5	112.4
W23	32	6.80	0.13	1.32	926	463	364.5	98.0
W24	34	7.00	0.57	1.45	1030	505	399.5	105.8
W24	35	7.10	0.48	1.46	993	452	354.5	97.1
W25	27	7.20	1.23	1.66	1124	465	342.3	122.3
W26	31	6.70	0.45	1.95	1306	508	409.5	98.4
W27	29	7.00	0.54	2.35	1688	713	531.8	182.4
W29	28	6.90	7.50	2.24	1622	678	504.3	173.3
W30	27	6.80	0.80	2.58	1920	817	616.7	200.1
W33	31	7.00	0.42	1.50	976	387	287.1	100.0
Min.	27	6.7	0.13	1.03	710	452	287.1	78.2
Max.	35	7.2	7.5	2.58	1920	1002	799.0	202.6
Avg.	32	6.9	1.0	1.79	1148	603.5	470.1	133.4

Table 7.19 : Quality of Down Stream Well Waters

Well No.	Temp. °C	pH	Turb. (NTU)	Conduc. msc/cm	TDS*	Total** hardness	Ca**	Mg**	Alkali-nity**	Fe*	Na*	K*	F*	Cl*	NO ₃ *	SO ₄ *	% Na	SAR
W1	33	6.90	0.52	1.67	1312	578	451.9	126.4	172	0.07	164	3.9	0.32	250	208	253	37.9	2.9
W2	35	7.00	1.01	4.32	3624	1877	1450.7	426.6	144	0.11	410	5.9	3.5	790	840	809	32.1	4.1
W3	37	6.20	1.02	2.64	2050	911	709.1	202.1	152	0.12	291	5.4	1.0	419	370	440	40.8	4.2
W4	37	7.20	0.66	1.40	1012	428	329.6	98.4	184	0.07	161	2.8	0.4	261	43.4	193	45.0	3.4
W5	34	7.00	0.62	1.73	1256	590	456.9	133.0	164	0.04	155	3.9	0.28	249	211	215	36.2	2.7
W6	35	7.00	0.54	1.35	932	398	309.6	88.1	180	0.06	142	3.5	0.16	186	100	159	43.4	3.1
W7	34	7.00	0.60	1.22	842	339	269.6	69.5	188	0.07	145	3.2	0.22	178	66.2	146	47.9	3.4
W8	33	7.10	0.48	1.41	1098	485	372.0	102.9	184	0.03	164	3.5	0.25	235	122	199	42.7	3.2
W9	34	6.90	2.5	1.52	1082	405	377.0	107.4	176	0.05	144	3.6	0.25	228	129	189	39.0	2.8
W10	34	7.00	0.82	1.60	1172	556	434.0	121.4	172	0.07	143	3.3	0.67	224	182	198	35.7	2.6
W11	35	6.90	0.58	1.32	892	412	322.1	89.7	184	0.11	125	2.9	0.56	172	94.7	160	39.5	2.6
W12	33	7.00	0.95	1.19	802	346	269.4	76.5	188	0.12	134	2.7	0.29	165	56.7	143	45.5	3.1
W13	34	7.30	0.42	0.98	692	281	221.4	59.2	180	0.06	104	3.1	0.29	126	52.7	104	44.2	2.7
W14	34	7.00	0.77	2.90	2306	1085	841.4	243.7	160	0.10	301	3.5	1.0	518	458	450	37.5	3.9
W15	36	7.20	0.92	1.28	780	297	235.9	61.3	184	0.07	133	2.7	0.35	161	47.9	120	49.0	3.3
Min.	33	6.2	0.42	0.98	692	281	221.4	59.2	144	0.03	104	2.7	0.16	126	43.4	104	32.1	2.6
Max.	37	7.3	2.5	4.32	3624	1877	1450.7	426.6	188	0.12	410	5.9	1.0	790	840	809	49.0	4.2
Avg.	35	6.98	0.82	1.77	1323	603.8	470.1	133.8	174	0.07	181.0	3.5	0.63	277.5	198.8	251.8	41.13	3.2

* mg/L

** mg/L as CaCO₃

SAR = Sodium Absorption Ratio

Table 7.20: Irrigation Water Grades

Irrigation quality parameters	Grading (in decreasing quality order)		
	A	B	C
pH	6.6 - 7.5	5.6 - 6.5 & 7.6 - 9.0	Less than 5.6 & more than 9.0
% Sodium	Less than 40	41 - 65	More than 65
Chloride, mg/L	Less than 100	100 - 350	More than 350
Sulphate, mg/L	Less than 100	100 - 1000	More than 1000

CHAPTER EIGHT

CONCLUSION AND RECOMMENDATION

To conclude the results of the project reports, the major conclusions can be summarized as follows:

- 1- For the preparation of preliminary lineaments maps following remote sensing techniques were used:
 - (a) It has been observed that the FCC generated using bands 7,4 and 2 in red, green and blue (Fig. 4.1) with linear contrast stretching is more useful in extracting geological and structural details than all FCC's examined in this work.
 - (b) Linearly stretched filtered band 5 (black and white) imagery; showed all the rock boundary and lineament (Fig. 4.2).
 - (c) The intensity component of intensity Hue saturation transformation (IHS) (Figs. 4.4-4.5).
- 2- The preliminary lineament maps (Figs. 4.5 &4.6) have been used before and during the field trip in order to choose the best area for geophysical investigations and the drilling sites.
- 3- The integration of VES, HEP and spectral analysis of magnetic data indicates that the ground water potentiality occurs mostly in the down stream area of the Wadi Malal. Because of its low clay content and highly fractured rock underline the wadi alluvium, particularly M3 and M6, the ground water aquifers occupied the saturated part of the alluvium and weathered part of the bedrock.
- 4- The results obtained from magnetic data indicate that the depth to the basement varies across the study area. The extents of the gradients on the magnetic high indicate an elevation of the top of the magnetic mass consistent with the elevation of the basement surface inferred from VES and drilling at M3 profile. The contrasting character of magnetic anomalies may suggest a difference in magnetic properties of the rock producing the anomalies. Although all the anomalies are produced by intrusive rocks.

The magnetic low near the center of profile is produced by the steeply dipping interface, probably a fault.

- 5- Based on the recommendation of remote sensing and geophysical survey, six sites were selected for drilling in the down stream of the wadi.
 - a- The drilled wells at location are in the downstream (M3, M4 and M5), and their depth vary between 43-80m. Whereas the upper part of the drilled wells are dry, the drying of zone depths vary upto level of 20m. Based on the lithologies of the wells, the saturation zone varies from 20 to 60m.
 - b- The resistivity (VES) methods indicates relatively good agreement in predicting depth to bed rock, with one to three meters difference when compared with lithologic data.
 - c- Coarse materials comprising sand, gravel and pebbles from the bulk of wadi deposits, which are among the most productive aquifers.
 - d- It is difficult to extend the application of stratigraphic correlation between profiles M3, M4 and M5, but a positive stratigraphic correlation has been observed between M3.1, M3.2, M3.5 and M3.8.
- 6- The mean annual precipitation for the study was estimated to be about 61.6 mm. Runoff occurs in the area but it is infrequent but some storms may come serious flooding.
- 7- Recharge to the aquifer in the area was estimated to be 5.9 million cubic meters per year (on the average).
- 8- The amount of groundwater in storage was calculated to be 81 million cubic meters.
- 9- Due to the many wells drilled for agricultural purposes in recent years, it is expected that present water being pumped in the study area is grater than natural recharge. This will cause water levels to decline.
- 10- Most of the upstream, middle and down stream well waters are rich in minerals and some of them (like W 30, W 2, W 3 and W 14) have considerably high ionic concentrations. These wells are mainly used for irrigational purposes.
- 11- At the time of this study, water quality in Wadi Malal is acceptable for irrigation use.

Finally, here are some recommendations for implementation:

- 1- Carry out a detailed study on Wadi Malal and another wadis in Al Madinah area to evaluate their conditions using the results of this project.
- 2- Apply isotopes techniques to estimate the recharge to Wadi Malal.
- 3- In the wake of the knowledge that the study area has a history of water potential, it is purposed that the check dams may be constructed in the wadi in order to trap the runoff. This provides infiltration over prolonged period of time, which will result in the increase in recharge of the aquifers.
- 4- To provide a database of the current status of water potential, hydrometeorological station may commissioned in order to promote and ensure further hydrogeological studies.
- 5 A continued and prolonged use of the present water for irrigation purpose may increase substantially the salt concentration in soil. This is likely to be a potential threat to the plant growth in future.

CHAPTER NINE

REFERENCES

- Abera, T. and Whiuri, H., 1989. Conventional Method and Digitally Enhanced LANDSAT Imagery for Groundwater Exploration in the Main Rift Valley of Ethiopia. In: Proceeding of 28th International Geological Congress, Washington, D.C., United States. p. 473-487.
- Adam, E.G. 1981. Groundwater Potential in the South of Al Madina Al Munawara, MSc Thesis King Abdulaziz university, Jeddah.
- Al-Ahmadi, F. S., 1994 "Data on some Runoff Stations in Al-Madina Al-Munawara Area".
- Al-Amri. A. M. 1994. The application of geoelectrical surveys in delineating groundwater in semiarid terrain - case history from central Arabian Shield. M.E.R.C., Ain Shams University, Earth Sci., 10, 41-52.
- Al-Muttair, F. F. , Al-Turbak, A. S. and Sendil, U., 1989. Management of water stored behind recharge dams in central Saudi Arabia, Final Report prepared for KACST, Riyadh, Saudi Arabia.
- Al-Turbak, A. S. and A. A. Quraishi, 1987. Regional flood frequency analysis for some selected basins in Saudi Arabia. Proc. of International Symp. On Flood Frequency and Risk Analysis, Louisiana State Univ. U.S.A., pp 27-34.
- Alwash, M. A., And Zilger, J., 1994. Remote Sensing Based Geological Mapping of the Area West of Al Madinah, Saudi Arabia. International Remote Sensing, Volume 15 Part I. p. 163-172.
- Andersson, C., Bystrom J., Oberg, M., and Ben abderrahmane, A., 1992. Remote Sensing as a Tool in Groundwater Assessment-Example of Tamanrasset Region Algeria. Hydrogeologies (Orleans). p. 93-99.
- Bayumi, T. H., 1992 Groundwater resources of the Northern part of the Harra Rahat Plateau. Ph.D. Thesis King Abdulaziz university, Jeddah.
- Bhutta, M. A., 1960. General Geology and Economic possibilities of the Jabal al Wark area: Saudi Arabian Directorate General of Mineral Resources open-file Report 3/204/1328.

- Bhutta, M. A., 1961a. Preliminary evaluation of the general water potentialities around the Al-Madinah Al Munawwara airport: Saudi Arabian Directorate General of Mineral Resources open-file Report 119, 8p., 1.
- Bhutta, M. A., 1961b. Hydrogeology of the Qeba area, Al Madinah Al Munawwara: Saudi Arabia Directorate of Mineral Resources open file Report 122m 24P.
- Bokhari, A. Y. and Khan, M. Z. A. 1992. Deterministic Modeling of Al-Madina Al-Munwarah Groundwater Quality Using Lumped Parameter Approach, J. KAU Earth Sci, 5, 89-107.
- Bokhari, A. Y., 1988. Hydrological investigation in western Al-Madinah quadrangle/Kingdom of Saudi Arabia on the basis of Land Thematic Mapper Data. J. Berliner Geowiss. Abh, 10, 114-135.
- Bokhari, A. Y., 1993. The drainage system around Al-Madinah Al-Munawwarh, Saudi Arabia as viewed from satellite data. J. KAU Earth Sci, 4, 123-137.
- Bokhari, A. Y., 1991. Hydrological investigation east of Al-Madinah, Saudi Arabia on the basis of LANDSAT thematic mapper data, Berliner geowiss. Abh. (C) band, 10, pp. 113-135.
- Brosset R., 1976. Geology and Mineral Exploration of the Al Madinah Quadrangle, 24/39D.
- Brown, G. F., 1971. Tectonic map of the Arabian Peninsula: Saudi Arabian Directorate General of Mineral Resources, Arabian Peninsula map AP - 22, scale 1:4,000,000.
- Brown, G. F., and Jackson, R. O., 1958. Geology of the Tihamat ash Sham quadrangle, Kingdom of Saudi Arabia: U. S. Geological Survey Miscellaneous Geologic Investigations Map 1-216A, Scale 1:50,000.
- Brown, G. F., and Jackson, R. O., 1968. Geology of the Tihamat ash Sham quadrangle, Kingdom of Saudi Arabia: U. S. Geological Survey Miscellaneous Geologic Investigations Map 1-216A, Scale 1:50,000.
- Brown, G. F., and Jackson, R. O., 1960. The Arabian Shield: International Geological Congress, 21st, Copenhagen, Proceedings, pt. 9, pp. 69 - 77.
- Brown, G. F., Layne, N., Goudarzi, G. H., and Maclean, W. H., 1963. Geologic map of the North Eastern Hajar quadrangle, Kingdom of Saudi Arabia: U. S. Geological Survey Miscellaneous Geologic Investigations Map 1-205 A, scale 1:500,000.

- Daessle, M., 1973, Jabal Sayid Water supply, hydrogeological study of the Harrat Rahat basalt (Adh Dhumariyah district): French Bureau de Recherches Geologiques et Minieres Technical Record 73 - JED - 9, 49 P, 16 figs., 8 tables, 2 maps, 1 cross section, 4 logs.
- Daessle, M., and Durozny, G., 1972. Jabal Sayid Water Supply, the Harrat Rahat basalt: French Bureau de Recherches Geologiques et Minieres Technical Record 72 - JED - 2, 21 P., 1 app., 1 map, 1 cross section.
- Das, D., 1991. Extraction Through Satellite Remote Sensing in an Around the Wichita Mountains, Oklahoma. In: Proceeding of 8th Thematic Conference on Geologic Remote Sensing, Denver, Colorado, U.S.A. p. 171-180.
- Depperman, K. and Homilius, J. 1965 Interpretation Geolektrischer Soundings - Kurven bei Tiefligender Grundwasserober flache: Geologisches Jahrbuch, V. 83, P. 563 - 573.
- Deutsch, M., and Heydt, H. L., 1987. Spectral Enhancement of LANDSAT, MSS, and TM Imagery Applied to Groundwater Investigations in Kenya. ASPRS-ACSM Annual Convention, Baltimore, MD, March 29-April 3, 1987. p. 412-419.
- Feder, A.M., 1987. Advanced Remote Sensing Approaches in Groundwater Exploration. In: Proceeding of Symposium on Water Resources Related to Mining and Energy; Preparation for Future, Utah. p. 13-38.
- Folk, R. L. and Ward, W. C. 1957. Brazos Rivers bar: A study in the significance of grain size parameters: J. Sediment. Petrol., 27, 3-27.
- Folk, R. L. 1966. A review of grain size parameters. Sedimentary, 6, 73-93.
- Friedman, G. M. 1979. Address of retiring president of the international association of sedimentologist: Difference in size distribution of populations of particles among sands of various origins. Sedimentology, 26, 3-32.
- Hadley, D. G., 1974. Geologic map of the Wayban quadrangle, Kingdom of Saudi Arabia: Saudi Arabian Directorate General of Mineral Resources Geologic Map GM-7, Scale 1:100,000.
- Hummel, C. L., 1967. Geology and Mineral deposits of the wadi an Nuqumi quadrangle, Kingdom of Saudi Arabia: U. S. Geological Survey Technical Letter 82, 18 P.

- ITAICONSLT, 1975. Detailed investigations of Madinah Region. Program of work and budget report. Kingdom of Saudi Arabia, Ministry of Agriculture and Water. 89p.
- ITAICONSLT, 1979 "Detailed Investigations of the Madinah Region" Final Report, No. 2 Hydrological and meteorological studies.
- Johnson, R., and Trent, V., 1966. Mineral reconnaissance of the wadi Al Ays quadrangle: U. S. Geological Survey Technical Letter No. 45.
- Kahr, V. P., 1961. General geologic report on field trips to the area north of Yanbu a Bahr: Saudi Arabian Directorate General of Mineral Resources Open-File Report, DGMR - 126, 213P. 289 figs. 3 pls.
- Kearey, P. and Brooks, M., 1991. An introduction to geophysical exploration. Blackwell Scientific publications. Second Edition.
- Kemp, J. 1980. Geologic map of the wadi Al Ays quadrangle, sheet 25c, Kingdom of Saudi Arabia. Saudi Arabian Deputy Ministry for Mineral Resources, Geoscience Map GM-53, scale 1:25,000.
- Knapp, K. R, Morgan, K. M., Donovan, N., Busbey, A., and Kresic, N., 1994. Using SPOT and TM to Map Fractures Related to Groundwater Resources in the Slick Hills of Oklahoma. 10th Thematic Conference on Geologic Remote Sensing, San Antonio, TX. USA. p. I 155-I 159.
- Krishnamurthy, J., Saivasan V., and Manavalan, P., 1992. Application of Digital Enhancement Techniques for Groundwater Exploration in a Hard-Rock Terrain. International Journal Remote Sensing. p. 2925-2942.
- Krol, G. J., de Sonnevile, J., and Vasak, L., 1986. Application of Remote Sensing for Groundwater Survey in Kenya. 20th International Symposium on Remote Sensing of Environment, Nairobi, Kenya. p. 221-234.
- Lillesand, T. M. and Kiefer, R. W. 1987. Remote sensing and image interpretation (3rd edition), John Wiley, New York.
- Minor, T. B., Carter, J. A., Chesley, M. M., Knowles, R. B., and Gustafsson, P. 1994. The Use of GIS and Remote Sensing in Groundwater Exploration for Developing Countries. 10th Thematic Conference on Geologic Remote Sensing; Exploration, Environment, and Engineering, San Antonio, TX, United States. p. I 168-I179.

- Mohan, R., Rao, G. L., and Singh, H., 1987. Groundwater Targeting Using Remote Sensing and Electrical Resistivity Methods in Parts of Saline Tracts of Agra Districts, Uttar Pradesh. *Journal Association Exploration Geophysics*. p. 99-109.
- Moore, J. M., 1979. Tectonic map of the Najd Trans current fault system, Saudi Arabia: *Journal of the Geological Society of London*, V. 136, P. 441 - 454.
- OB"Yedkov, Y. L., 1992. Remote Sensing Interpretation Keys in the Search for fresh Groundwater in Arid Regions. *Mapping Sciences and Remote Sensing*, p. 4-8.
- Page, L. M. 1968. The use of the Geoelectric Method for Investigations Geologic and Hydrologic Conditions in Santa Clara County, California, *Journal of Hydrology*, V. 7, No. 2. P. 167 - 177.
- Parasins, D. S. 1979. Principles of applied geophysics, 275p. Chapman and Hall Ltd. New York.
- Pellaton Claude, 1981. Geologic map of the Al Madinah quadrangle, sheet 24D, Kingdom of Saudi Arabia: Saudi Arabian Deputy Ministry for Mineral Resources Geologic map 6M 52-A, Scale: 250:000 with text, 19P.
- Pellaton, C., and Dhellemes, R. 1978. Geology and Mineral exploration of the Jabal Dhulay'ah quadrangle, 25/38A: French Bureau de Recherches Geologiques et Minieres Technical Record 78-JED-3 16P. 1 fig. 2 maps. 1 app.
- Petot, J., 1972. Mineral Resources and geology of the Al Ays quadrangle, zone III, sheet 89 W: French Bureau de Recherches Geologiques et Minieres in published report 15 P.
- Rao, R. S., Venkataswamy, M., Rao, C. M., and Rama Krishna, G. V. A. 1993. Identification of Overdeveloped Zones of Groundwater and the Location of Rainwater Harvesting Structures Using an Integrated Remote Sensing Based Approach. A Case Study in Part of the Anantapur District, Andhra Pradesh, India. *International Journal Remote Sensing*. p. 3231-3237.
- Shivakumar, K. S., and Gulhane, D. N., 1994. Simple Remote Sensing-Aided Method that can Drastically Reduce the use of Time Consuming Vertical Electrical Sounding to Evaluate and Locate Groundwater in karnataka Carton, India. 10th Conference on Geological Remote Sensing, San Antonio, TX, USA. p. II 174-II 183.

- Standard methods for the Analysis of Water and Waste water (1989), AWWA, APHA, WPCF.
- Teme, S. C., and Oni, S. F. 1991. Detection of Groundwater Flow in Fractured Media Through Remote Sensing Techniques-Some Nigerian Casts. *Journal of African Earth Science, the Middle East*. p. 461-466.
- Usha, K.; Ramaswamy, S. M.; and Subramanian, S. P., 1989. Fracture Pattern Modeling for Groundwater in Hard Rock Terrain; A Study Aided by Remote Sensing Technique. *International Workshop on Appropriate Methodologies for Development and Management of Groundwater Resources in Developing Countries, Hyderabad, February 28-March 4, 1989*. p. 319-328.
- Van, M. P. C. , and Seevers, P.,1988. Estimation of Groundwater Use for Irrigation in Eastern Washington Using LANDSAT Imagery. In: *Proceeding of Symposium on Water-use Data for Water Resources Management, Tucson, AZ, August 1988*. p. 667-679.
- Visher, G. A. 1969. Grain size distribution and depositional process: *J. Sediment. Petrol.*, 39, 1074-1106.
- Voute, C., 1986. Multistage Groundwater Exploration and Satellite Remote Sensing Test Area. The Kasserine Basin (Tunisia). *Elsevier Science Publishers B. V.* p. 317-326.
- Zohdy, A and Bisdorf, R. 1989. Programs for automatic processing and interpretation of Schlumberger sounding curves. Report 89-137, 64p. United States Geological Survey, Denver, Colorado, U.S.A.
- Zohdy, A. and D. Jackson 1969. Application of Deep Electrical Soundings for Groundwater Exploration in Hawaii, *Geophysics*, V. 34, 584 - 600.
- Zohdy, A., 1965. Geoelectrical and Seismic Refraction Investigations Near San Jose, California: *Groundwater*, V. 3, No. P. 41 - 48
- Zohdy, A.: Eaton, G. P., and D. R. Mabey 1984. Application of surface geophysics to groundwater investigations. *Tech. Water Resources INV.*, Book 2, chapter D1.

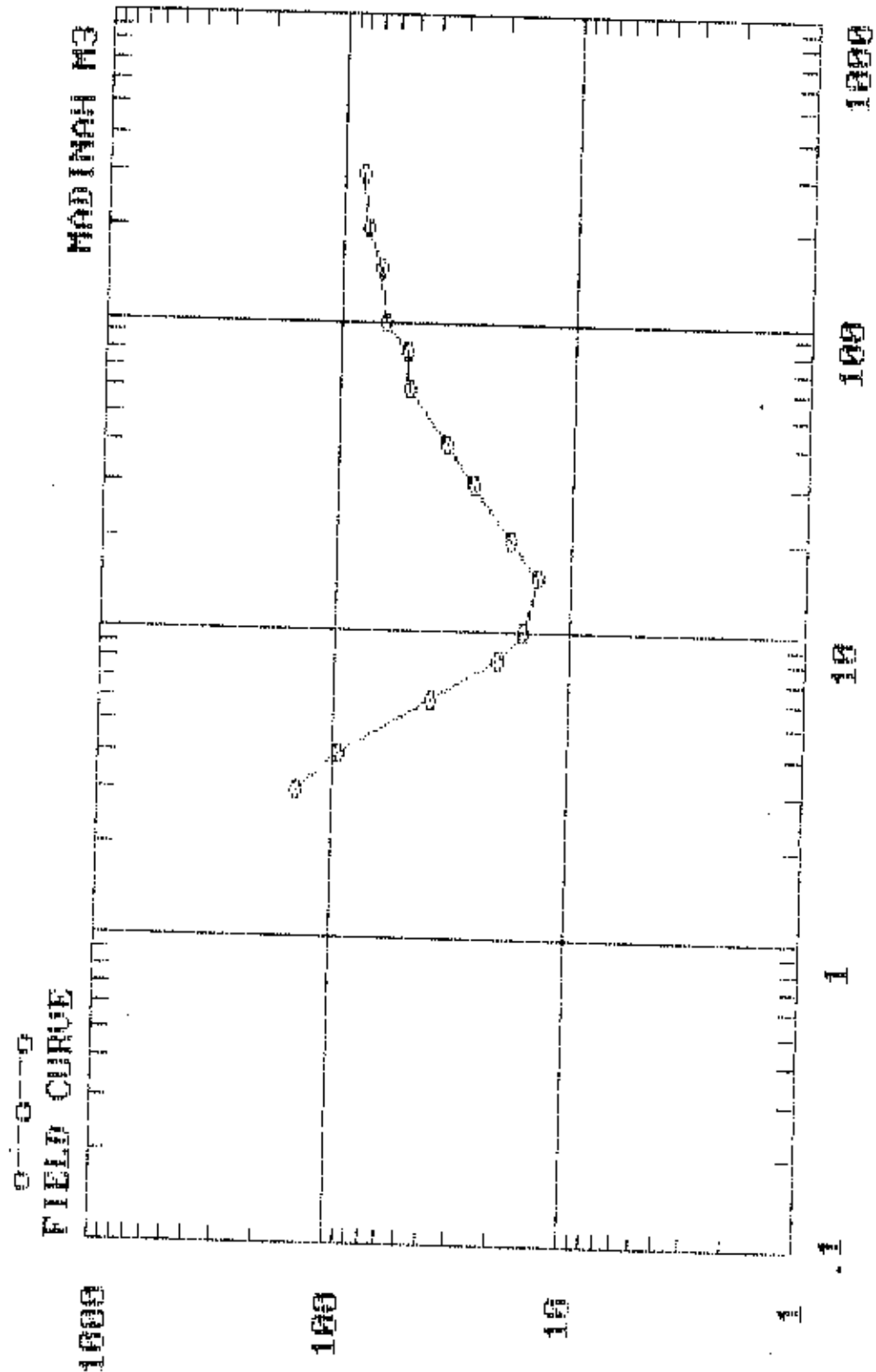
APPENDIX 5 A

**Resistivity field data and interpretation (apparent
resistivity vs. depth or $AB/2$) obtained using Zohdy (1989)
N-layer model**

M3i

MADINAH M3 (FIELD DATA)

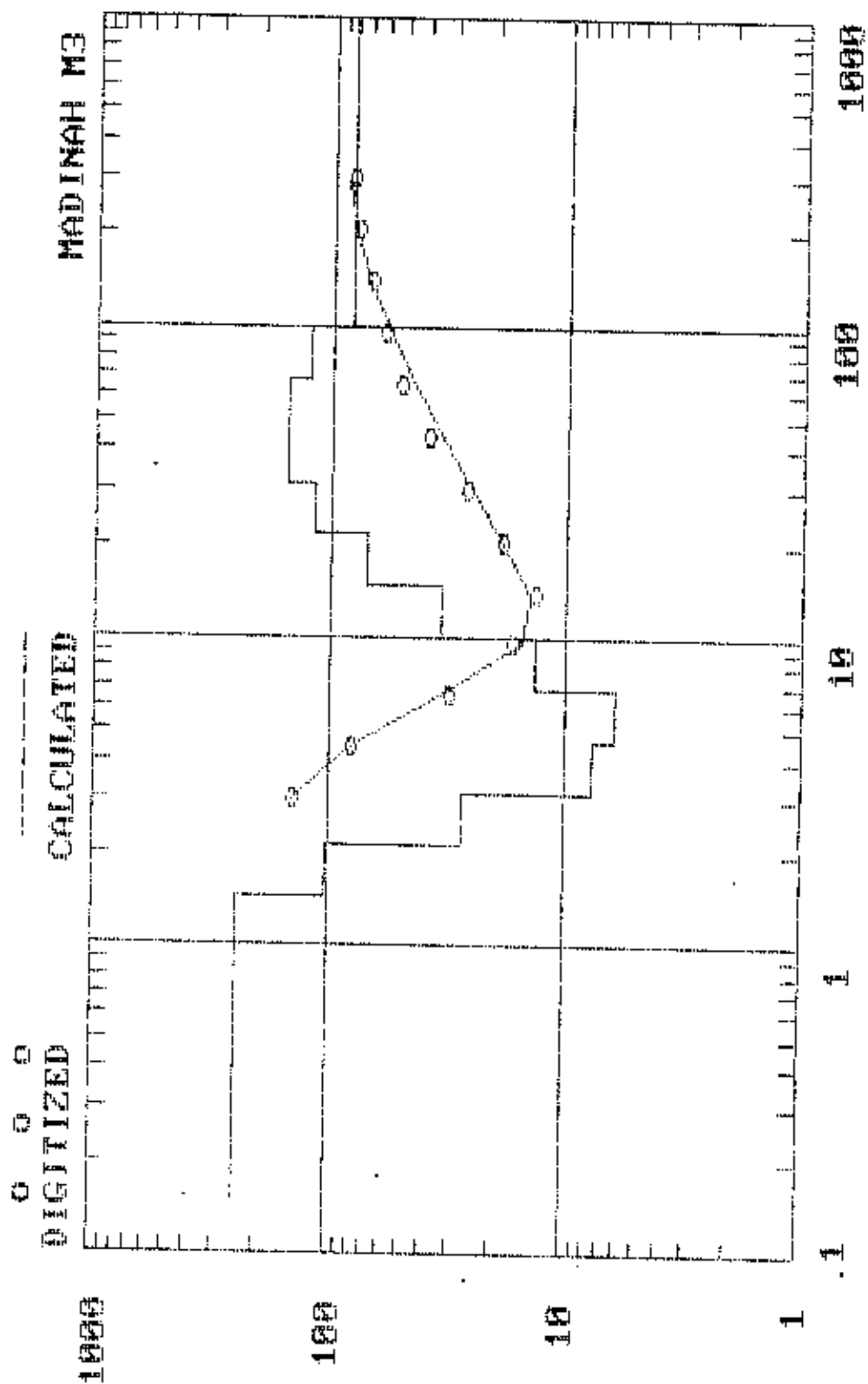
AB/2	App. Res.	AB/2	App. Res.
3	141.3	30	26.2
4	95.6	40	34.6
6	39	60	50.5
8	20.3	80	52.2
10	16	100	64
15	13.9	150	69
20	18.1	200	78
		300	83.2



M31

MADINAH M3 (INTERPRETATION)

DEPTH	RESIS.	DEPTH	RESIS.
1.458	242.6464	14.58	33.48802
2.140051	101.874	21.40052	70.46326
3.141166	26.95502	31.41167	117.4381
4.610601	7.579451	46.10602	152.18
6.767437	4.139345	67.67439	153.9591
9.93324	13.48757	99.33241	124.0455
		99999	83.13067



ELECTRODE SPACING (AB/2), OR DEPTH, IN METERS

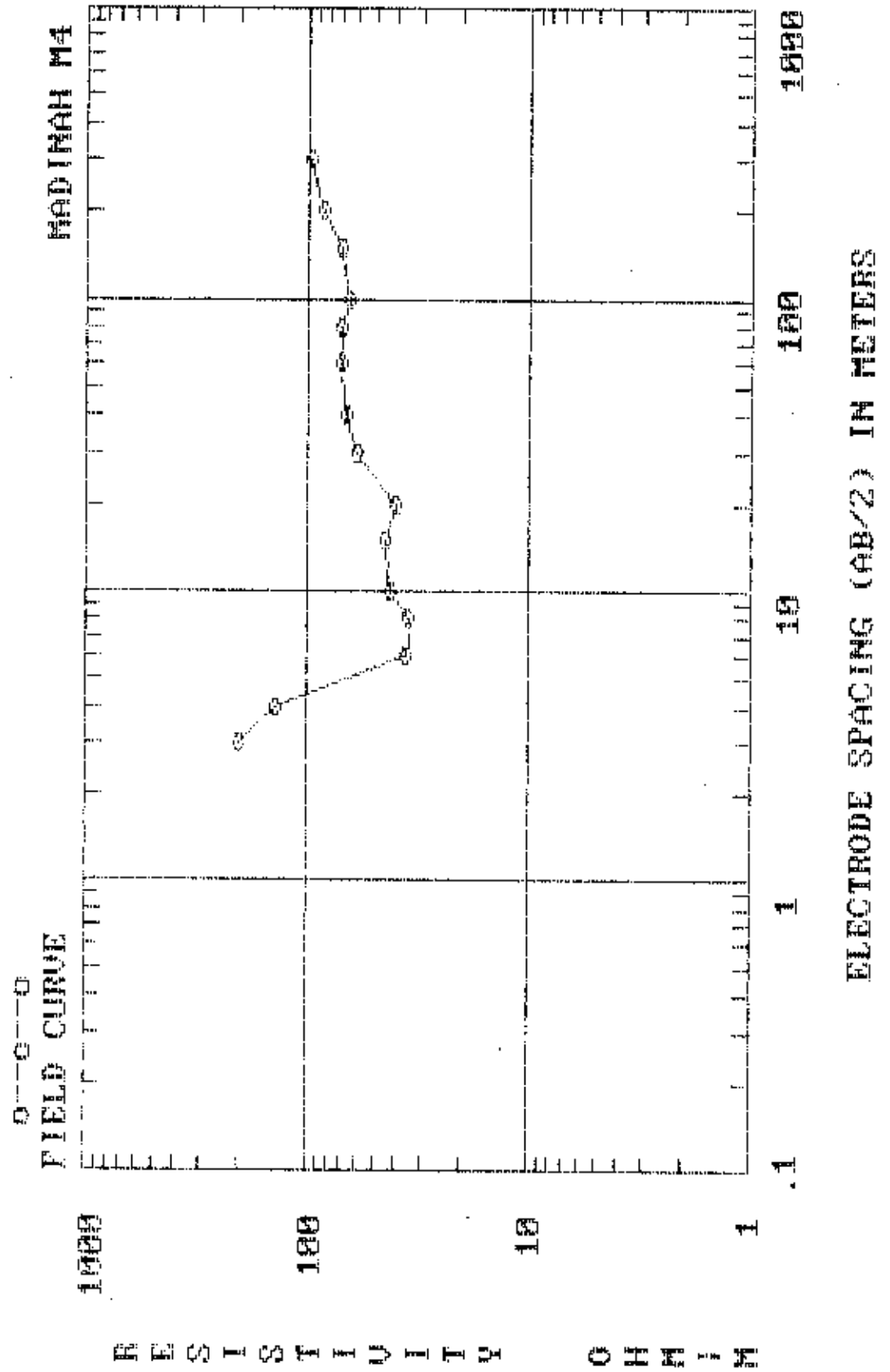
RESISTIVITY

OHM/CM

M32

WADINAH M4 (FIELD DATA)

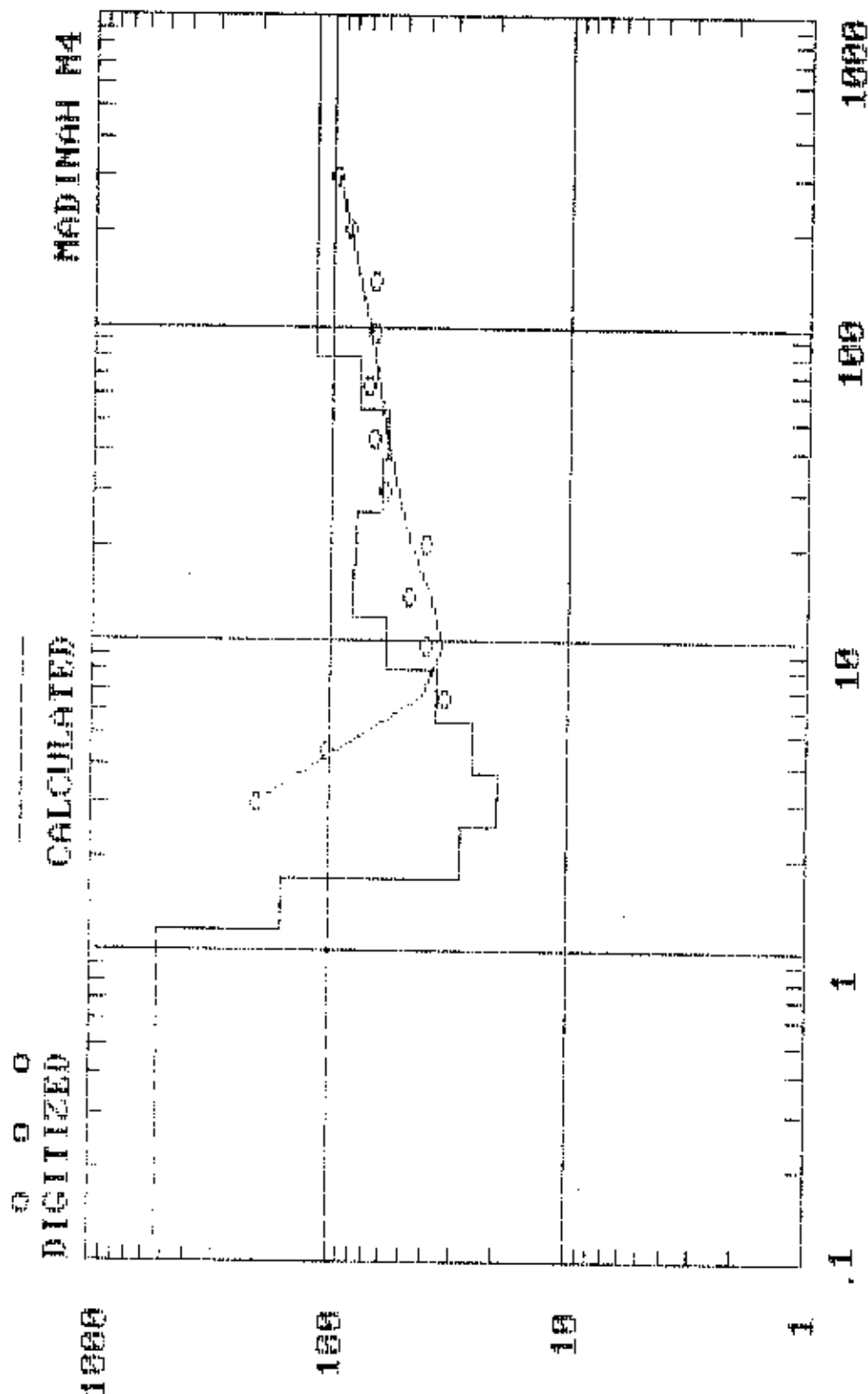
AB/2	App. Res.	AB/2	App. Res.
3	200	30	60
4	140	40	66
6	36	60	70
8	35	80	70
10	42	100	65
15	44	150	70
20	40	200	85
		300	98



M32

MADINAH M4 (INTERPRETATION)

DEPTH	RESIS.	DEPTH	RESIS.
1.18098	517.3987	11.8098	58.11336
1.733442	160.4538	17.33442	80.5859
2.544344	28.0423	25.44345	78.21984
3.734587	19.53764	37.34588	61.40932
5.481624	25.13784	54.81625	57.86353
8.045924	35.62292	80.45926	77.0732
		99999	118.5866



ELECTRODE SPACING (AB/2), OR DEPTH, IN METERS

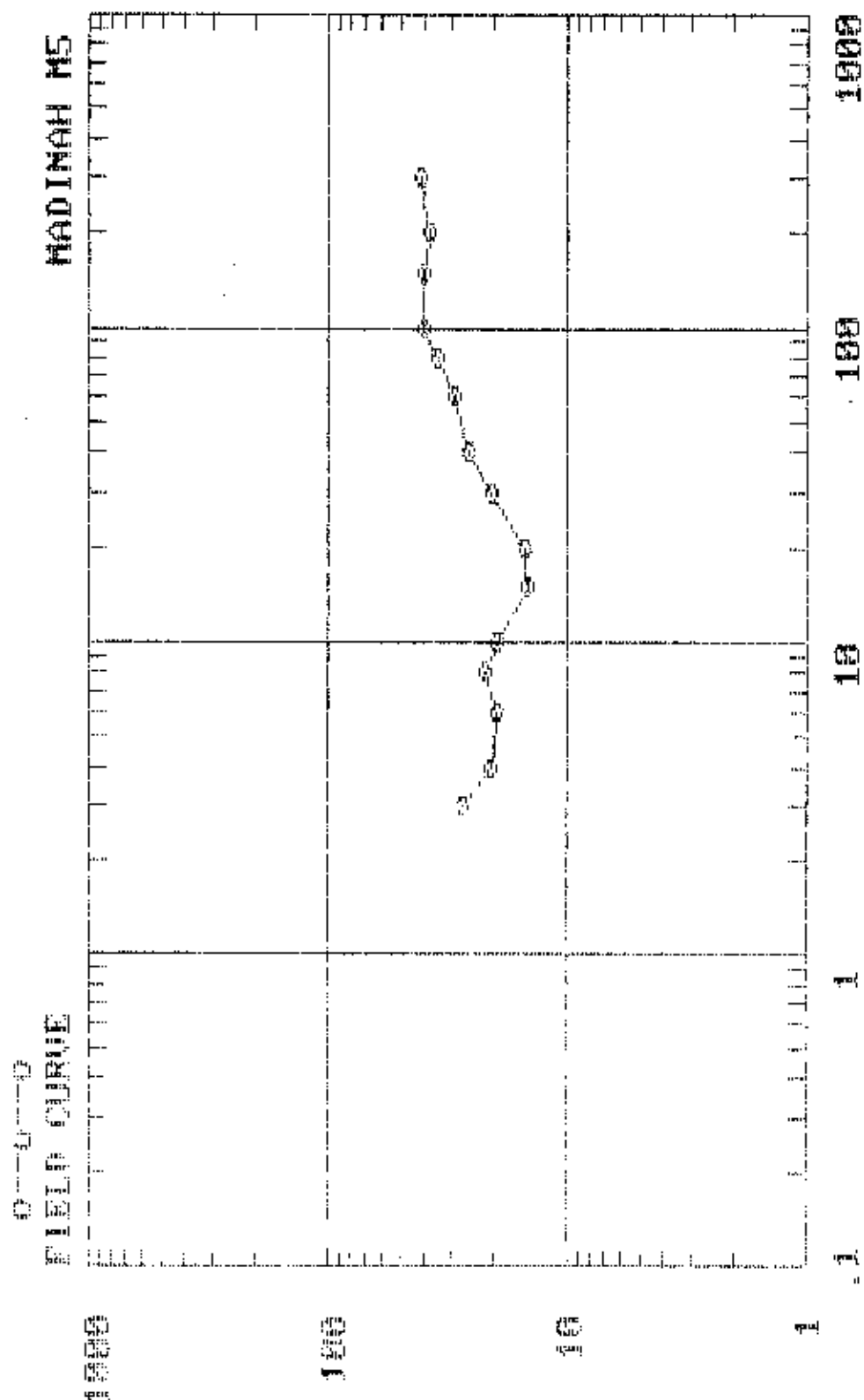
RESISTIVITY

OHM-M

M33

HADINAH M5 (FIELD DATA)

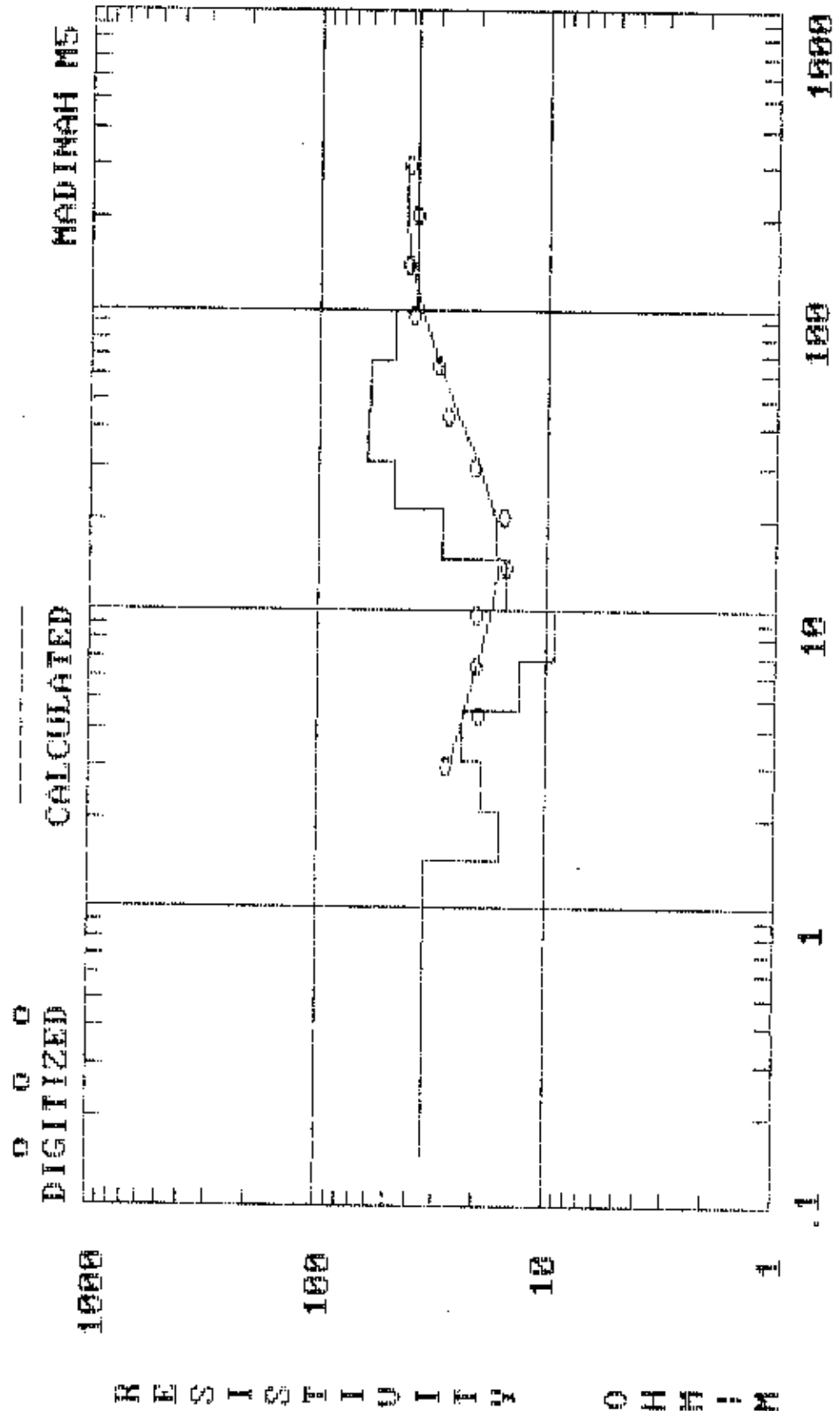
AB/2	App. Res.	AB/2	App. Res.
3	27.6	30	20.6
4	20.8	40	25.8
6	19.7	60	29.5
8	22	80	34.6
10	19.5	100	40.3
15	14.8	150	39.5
20	15.1	200	37.4
		300	41.2



M34 33

MADINAH M5 (INTERPRETATION)

DEPTH	RESIS.	DEPTH	RESIS.
1.458	34.18114	14.58	14.94403
2.140051	15.79239	21.40052	28.8304
3.141166	19.32266	31.41167	47.36193
4.610601	23.25295	46.10602	61.59016
6.767437	13.2397	67.67439	59.32469
9.93324	9.324019	99.33241	46.29095
		99999	37.95854

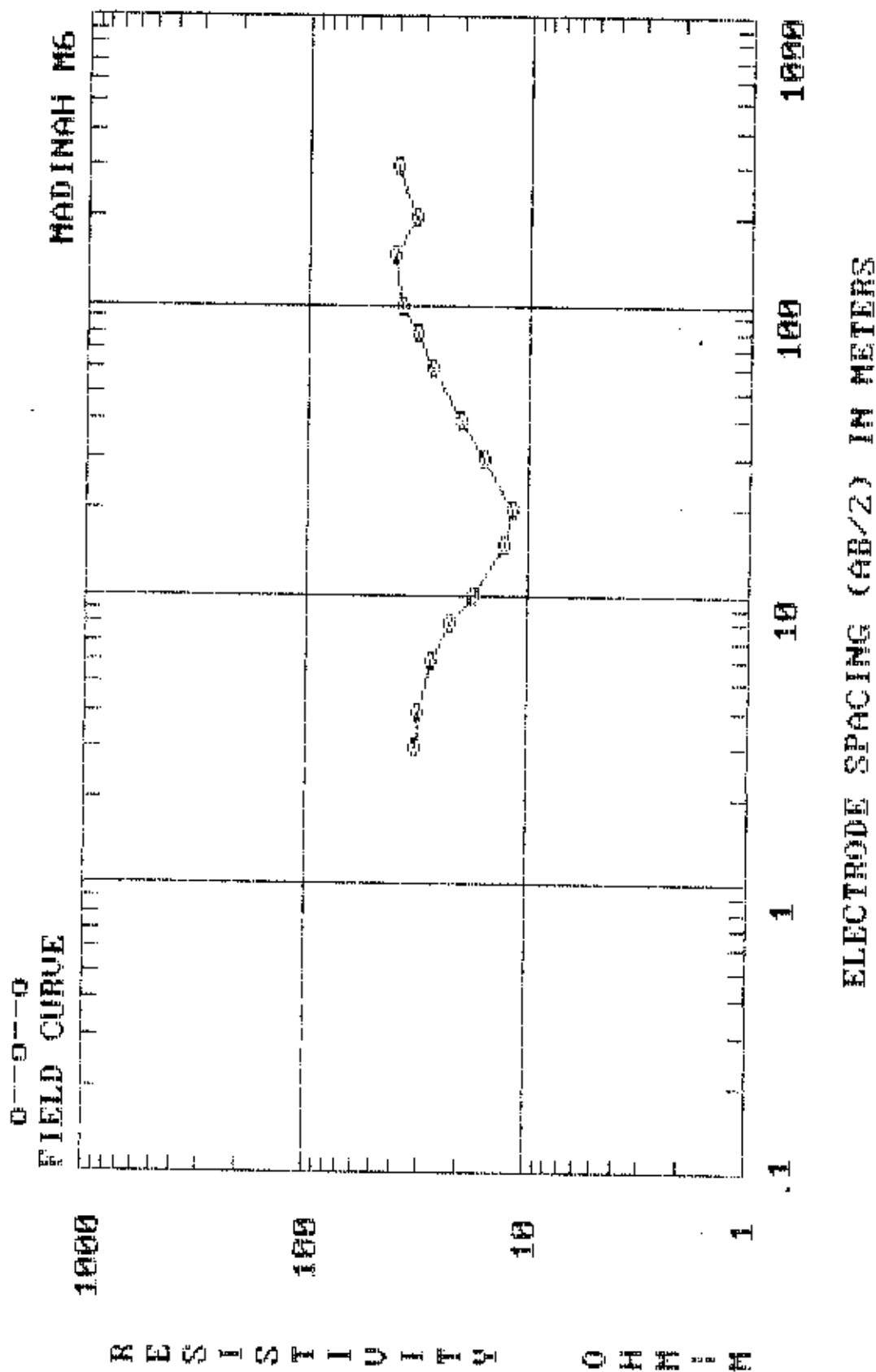


ELECTRODE SPACING (AB/2), OR DEPTH, IN METERS

M34

MADINAH # (FIELD DATA)

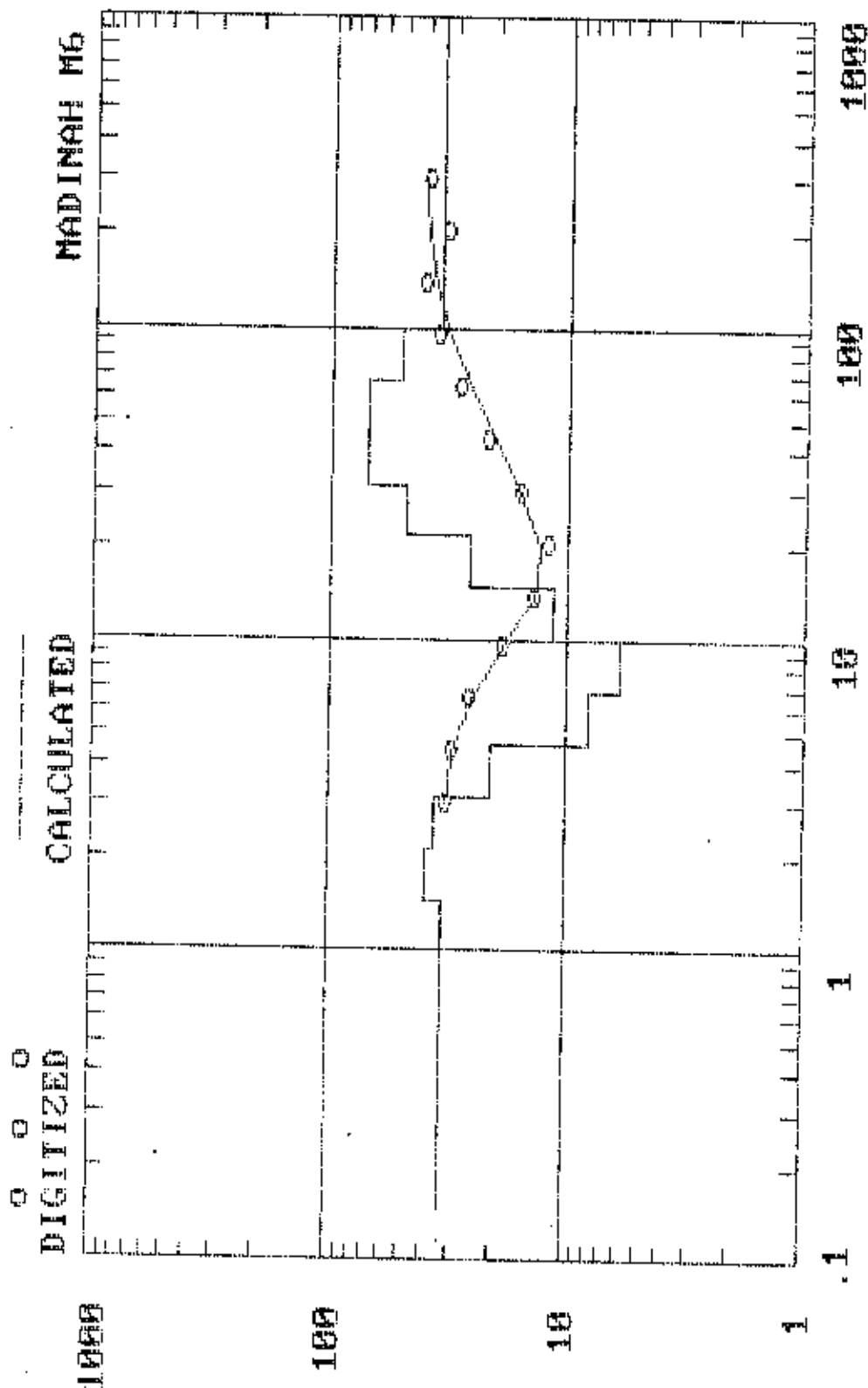
AB/2	App. Res.	AB/2	App. Res.
3	31.8	30	16
4	30.8	40	20.5
6	27.1	60	27.1
8	22.8	80	32
10	17.6	100	37.3
15	12.9	150	41.4
20	11.9	200	33.2
		300	39.4



M34

NADINAH M6 (INTERPRETATION)

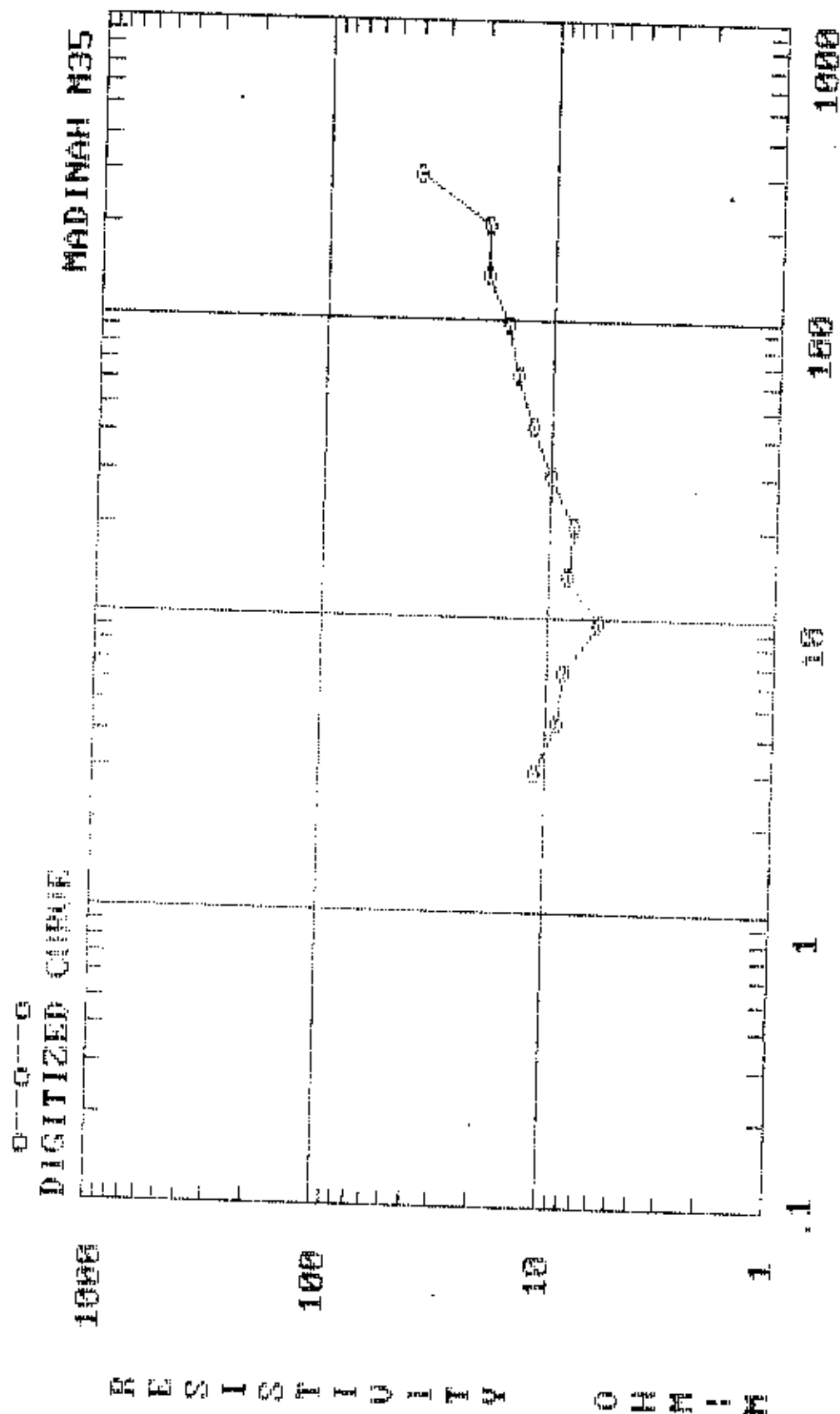
DEPTH	RESIS.	DEPTH	RESIS.
1.458	32.71424	14.58	11.4053
2.140051	38.76193	21.40052	25.81329
3.141166	36.17609	31.41167	48.39599
4.610601	20.71434	46.10602	69.51374
6.767437	8.03611	67.67439	69.95693
9.93324	5.977089	99.33241	51.06752
		99999	34.66684



ELECTRODE SPACING (AB/2), OR DEPTH, IN METERS

MADINAH M35 (DIGITIZED DATA)

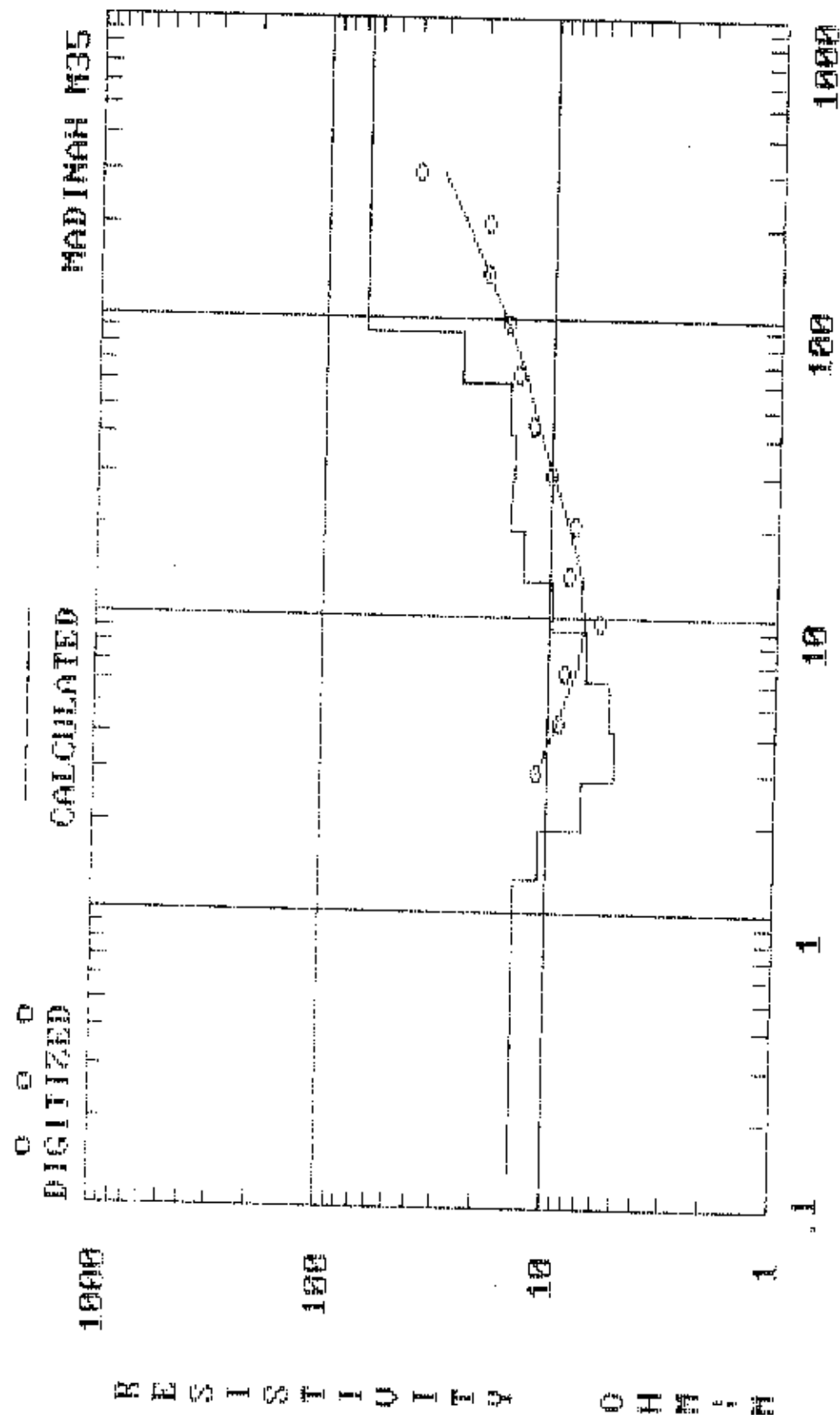
AB/2	App. Res.	AB/2	App. Res.
3	11.1	30.00001	10
4.403399	9.080715	44.03399	12.10334
6.463305	8.551976	64.63304	14.16253
9.486834	5.93777	94.86835	16.02694
13.92477	8.17527	139.2477	19.8276
20.43876	7.842549	204.3876	19.75887
		300.0001	39.40001



MADINAH M35 (INTERPRETATION)

DEPTH	RESIS.	DEPTH	RESIS.
1.3122	13.966	13.122	9.778317
1.926046	10.94778	19.26047	13.21929
2.827049	6.957577	28.2705	15.07867
4.149541	5.020549	41.49542	14.58778
6.090694	5.336439	60.90695	15.37655
8.939917	6.904987	89.39919	25.32334
		99999	65.99423

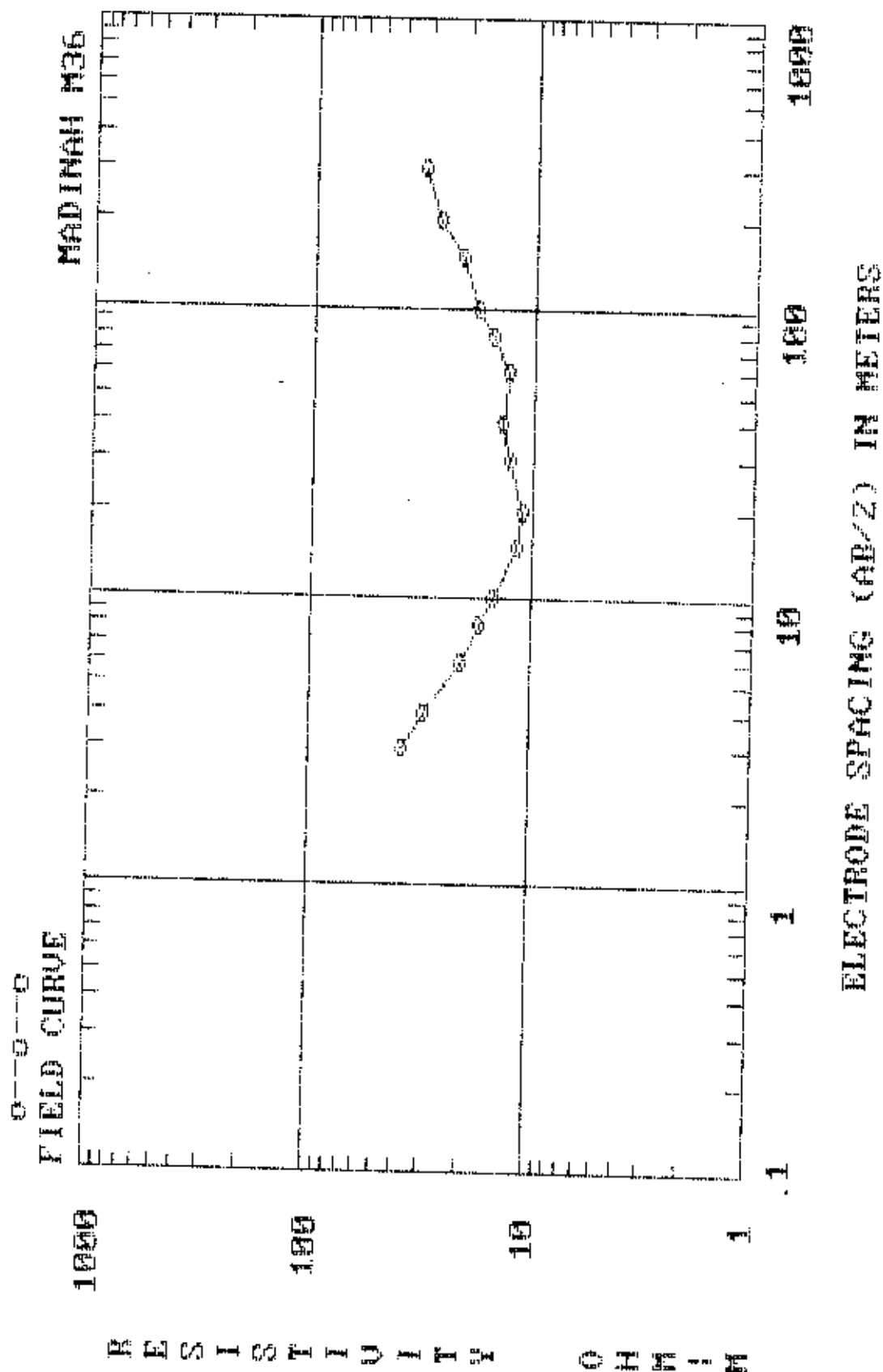
C:V



ELECTRODE SPACING (AB/2), OR DEPTH, IN METERS

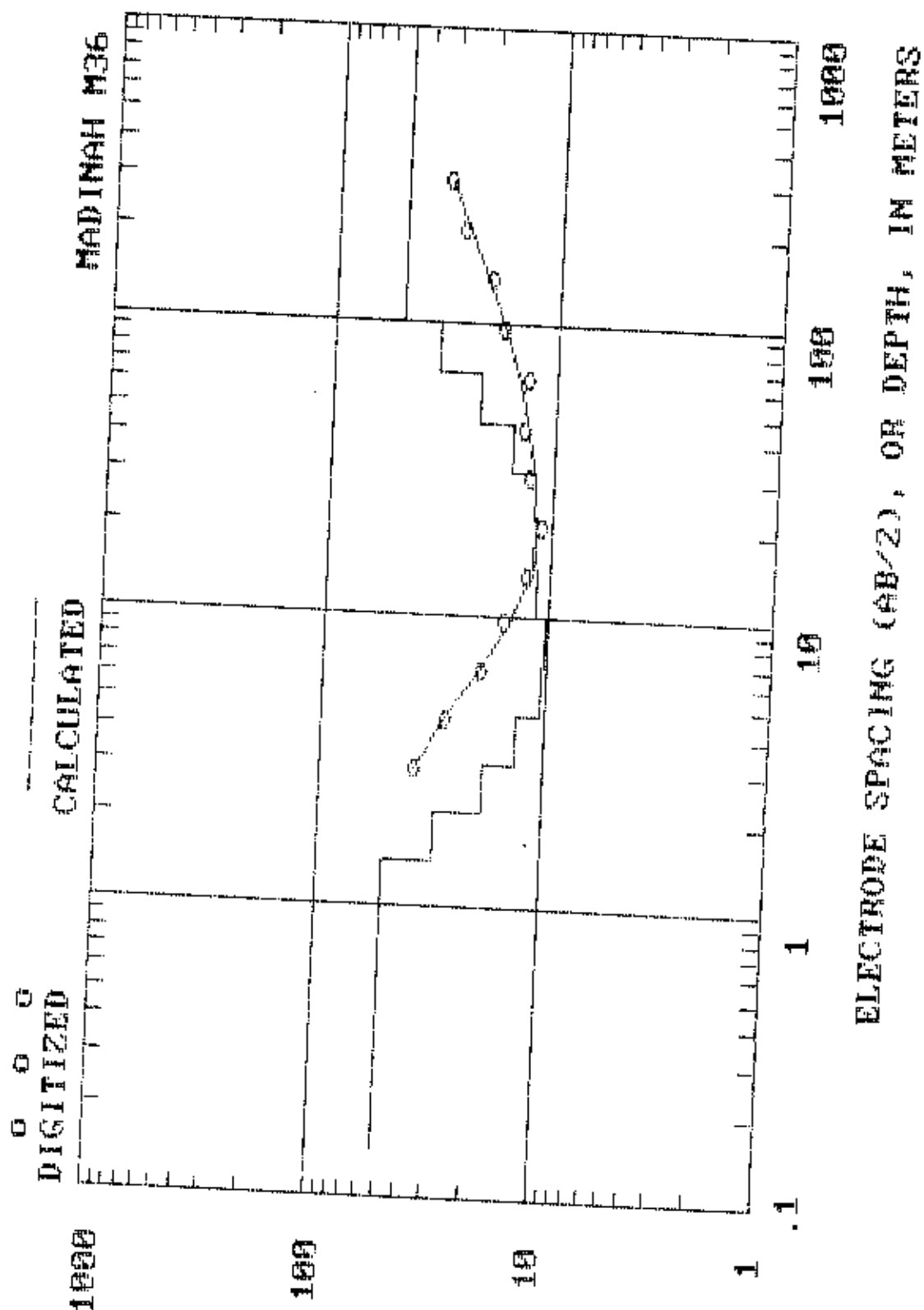
MADINAH M36 (FIELD DATA)

AB/2	App. Res.	AB/2	App. Res.
3	38.1	30	12.65
4	30.1	40	14
6	20.8	60	13.2
8	17.3	80	15.5
10	15.1	100	18.2
15	11.8	150	21.2
20	11.1	200	27
		300	32



MADINAH M36 (INTERPRETATION)

DEPTH	RESIS.	DEPTH	RESIS.
1.458	51.09698	14.58	11.3618
2.140051	30.02487	21.40052	11.68149
3.141166	18.6457	31.41167	12.23651
4.610601	13.50508	46.10602	15.27525
6.767437	10.50679	67.67439	22.16934
9.93324	10.16872	99.33241	33.64334
		99999	49.51752

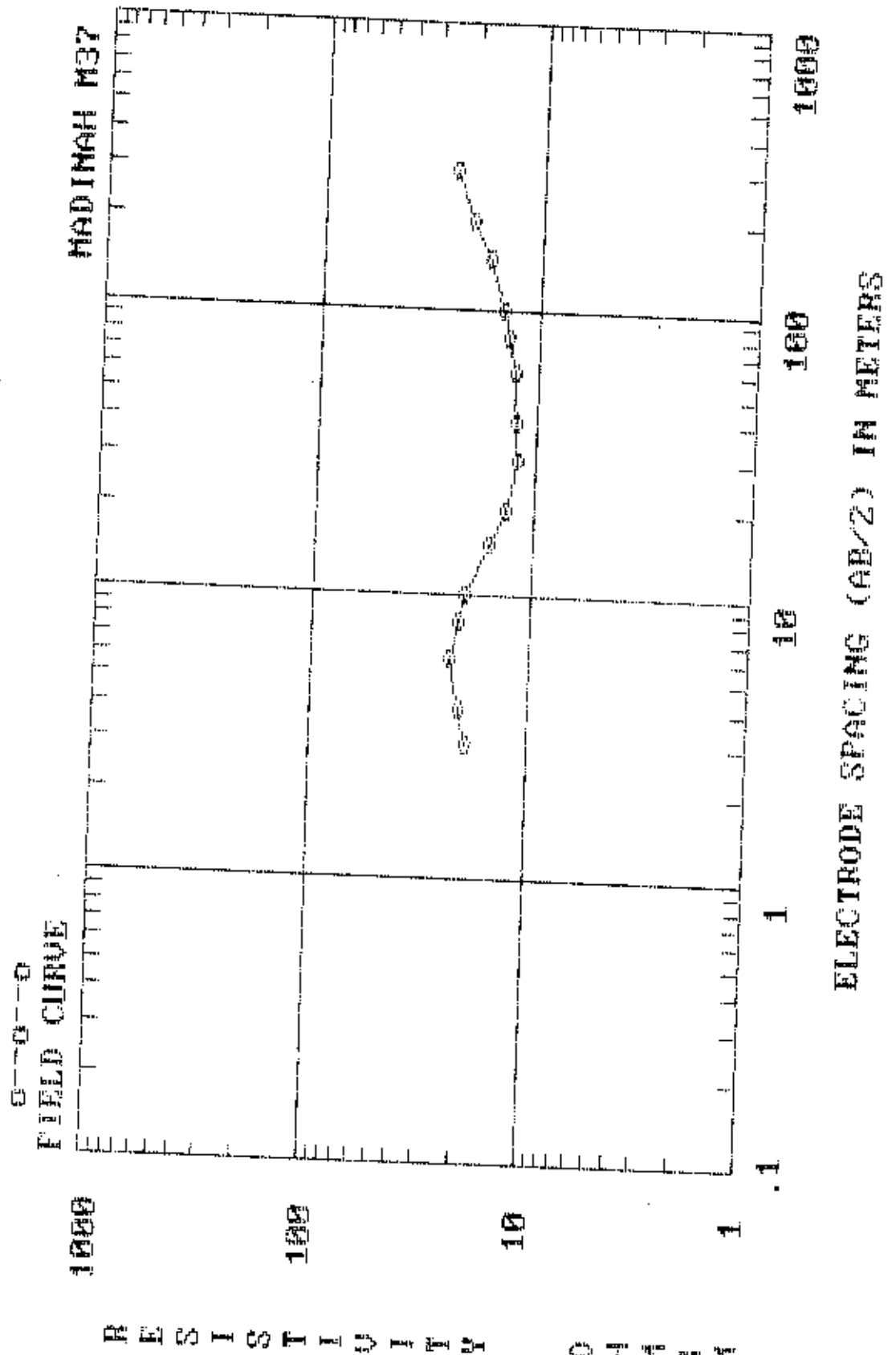


RESISTIVITY

M 3-7

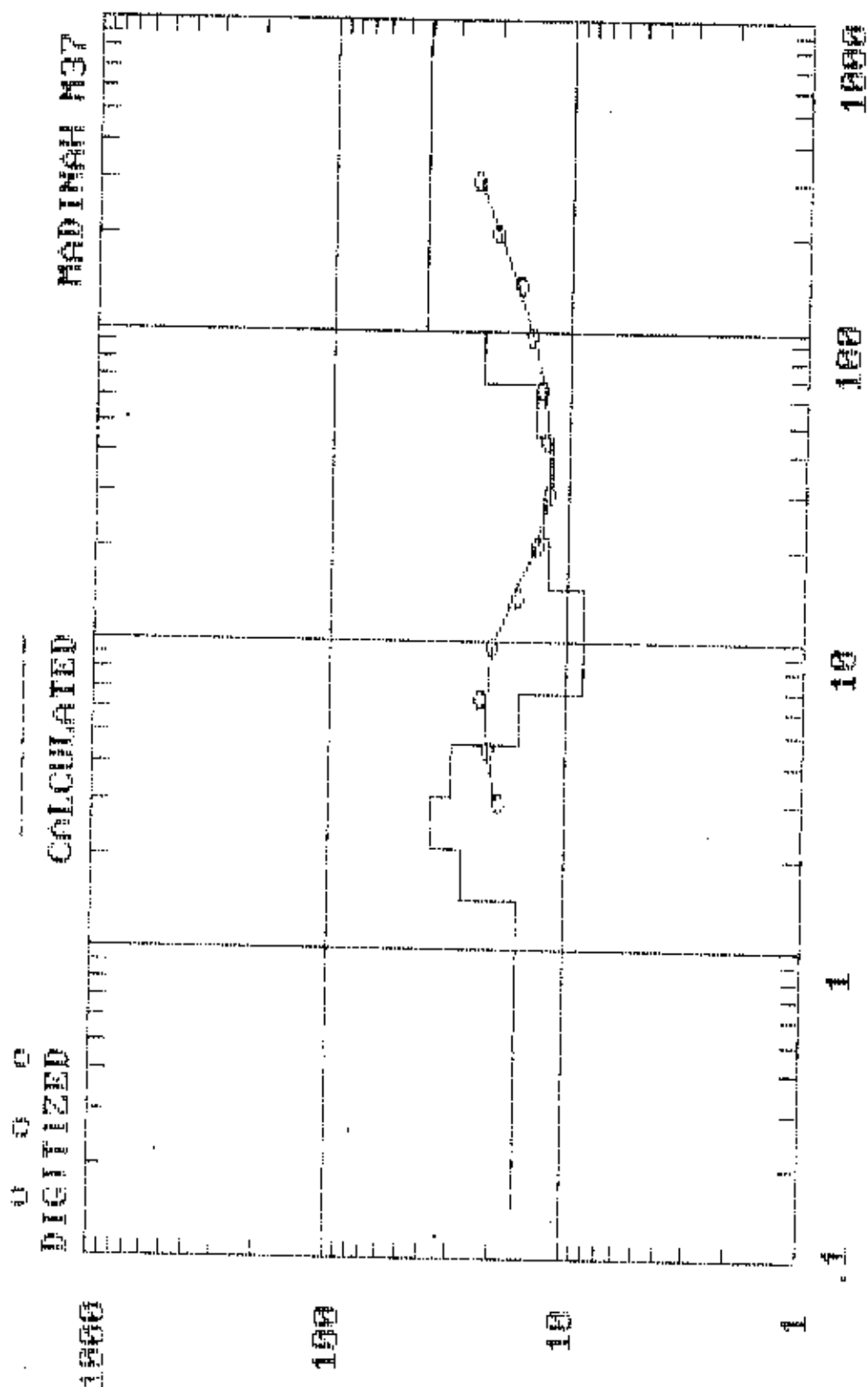
MADINAH M37 (FIELD DATA)

AB/2	App. Res.	AB/2	App. Res.
3	19.3	30	12
4	20.6	40	12.5
6	23.4	60	12.9
8	21.5	80	14
10	20.5	100	14.6
15	15.8	150	17
20	13.6	200	20.7
		300	25



MADINAH M37 (INTERPRETATION)

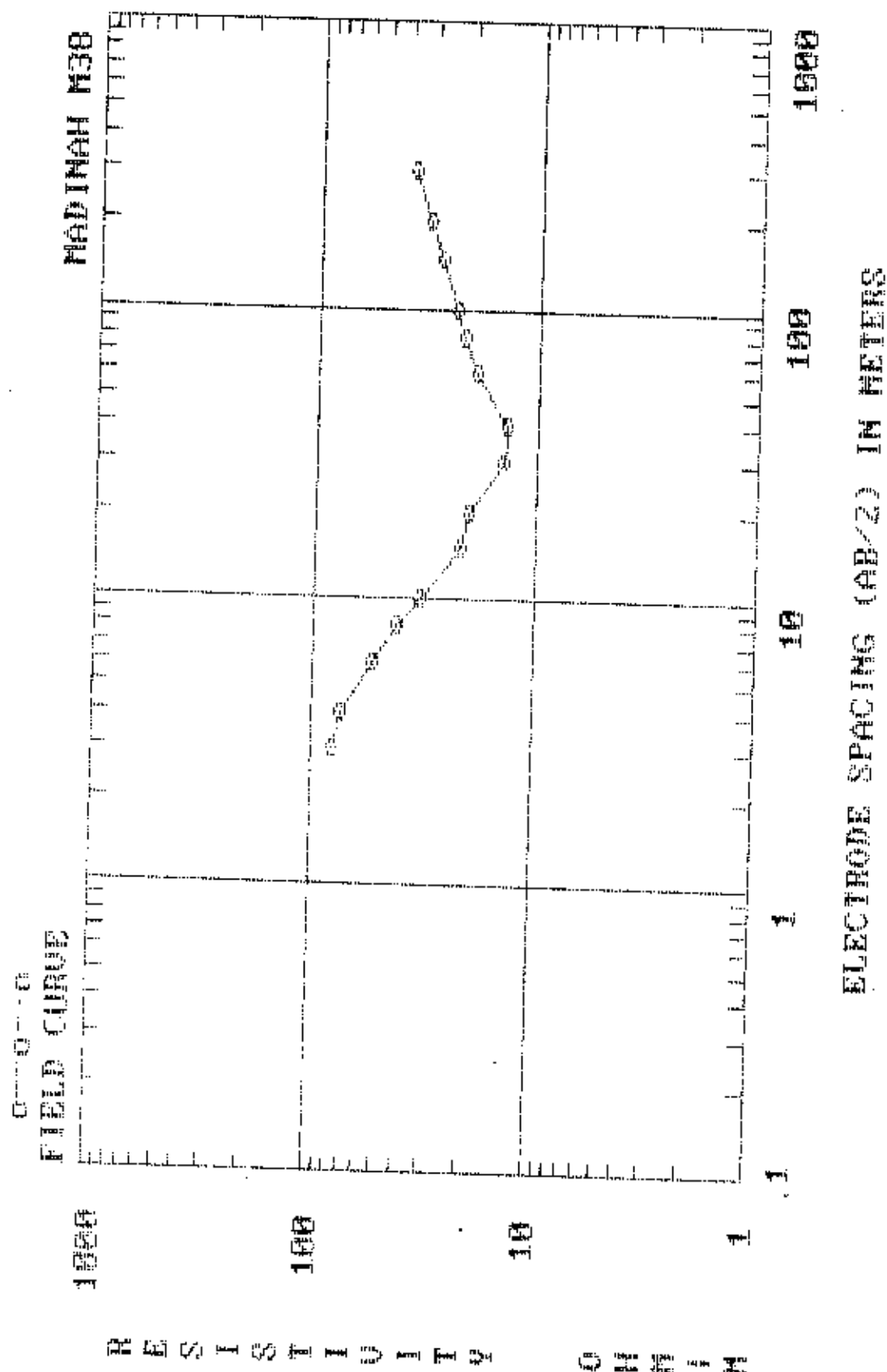
DEPTH	RESIS.	DEPTH	RESIS.
1.458	15.90088	14.58	8.575862
2.140051	27.40899	21.40052	12.16526
3.141166	36.44255	31.41167	12.91501
4.610601	30.021	46.10602	11.72189
6.767437	15.72575	67.67439	13.95432
9.93324	8.396084	99.33241	22.8555
		99999	40.35641



ELECTRODE SPACING (AB/2), OR DEPTH, IN METERS

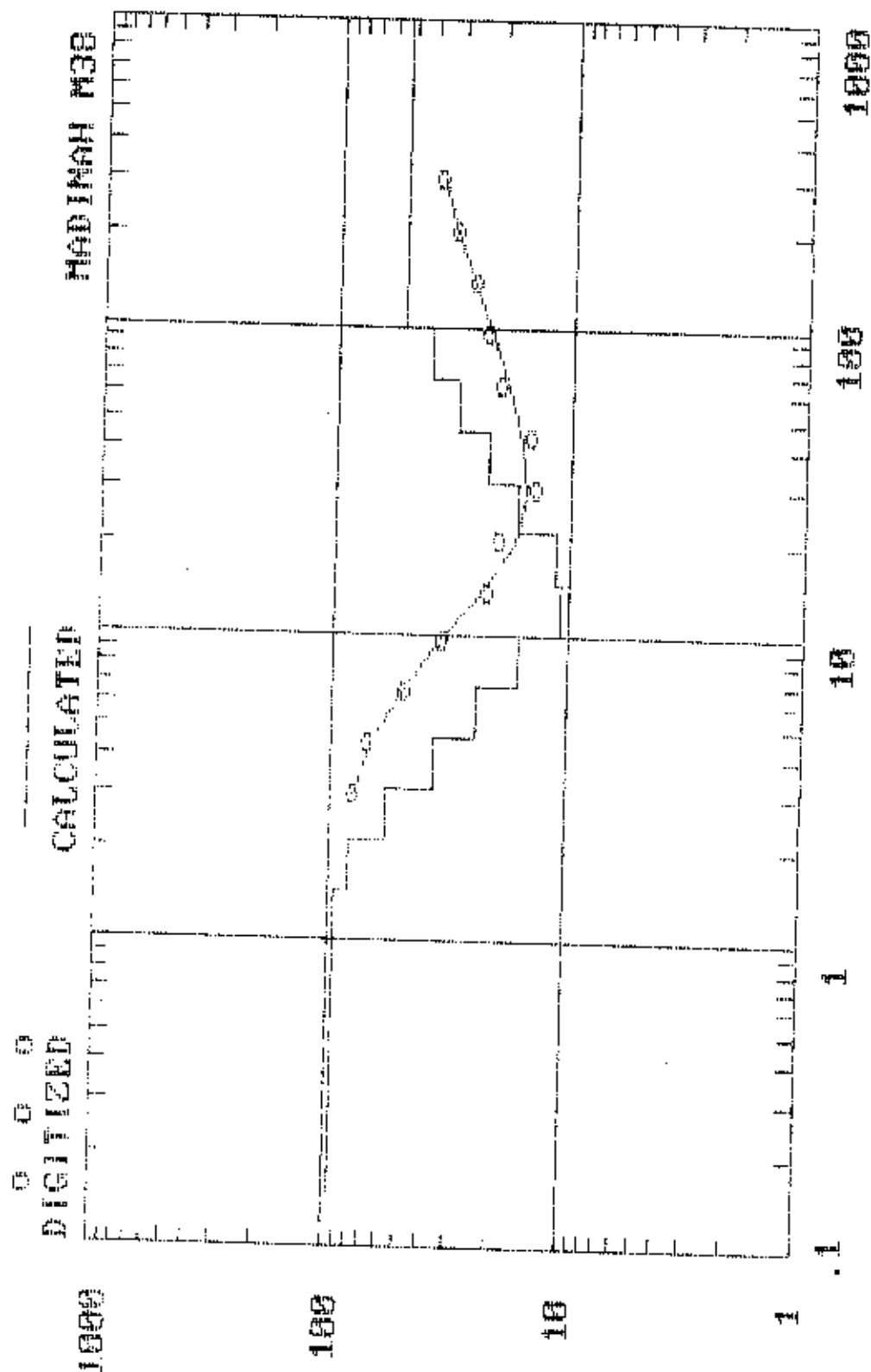
MADINAH M38 (FIELD DATA)

AB/2	App. Res.	AB/2	App. Res.
3	79.8	30	14.2
4	73.7	40	13.9
6	53.7	60	19.3
8	42.1	80	21.9
10	32.7	100	23.7
15	21.7	150	28
20	20.2	200	32
		300	38



HADINAH M38 (INTERPRETATION)

DEPTH	RESIS.	DEPTH	RESIS.
1.458	94.88171	14.58	10.78869
2.140051	81.98153	21.40052	11.55042
3.141166	57.92394	31.41167	16.51611
4.610601	36.36139	46.10602	22.68327
6.767437	24.76564	67.67439	29.97899
9.93324	16.48928	99.33241	39.83847
		99999	52.78296



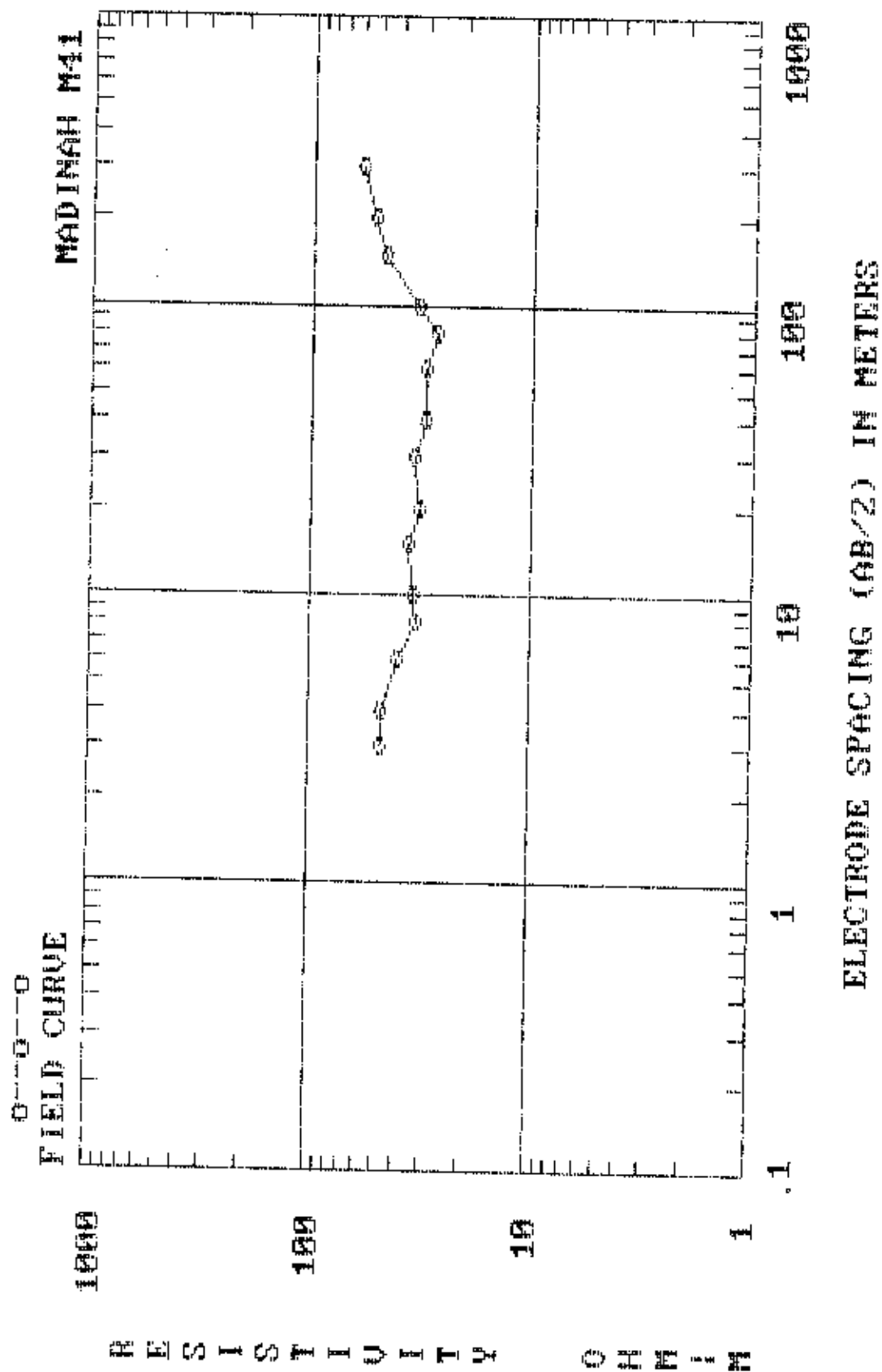
ELECTRODE SPACING (AB/2), OR DEPTH, IN METERS

RESISTIVITY

OHM-M

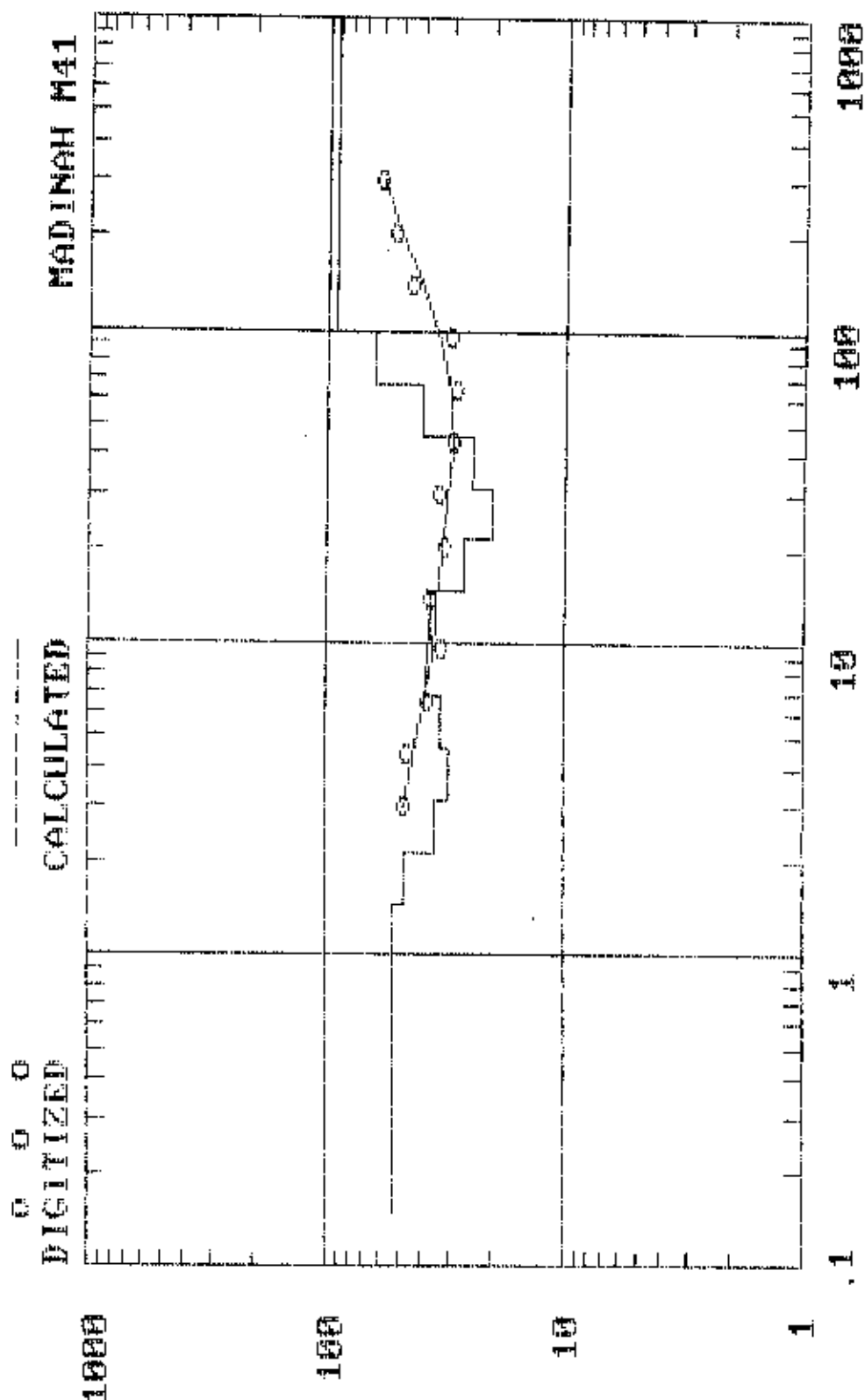
MADINAH M41 (FIELD DATA)

AB/2	App. Res.	AB/2	App. Res.
3	46.8	30	34.2
4	46.4	40	30.1
6	40.1	60	30
8	33.1	80	27.3
10	33.9	100	32.6
15	35.3	150	47
20	31.8	200	52
		300	60



MADINAH M41 (INTERPRETATION)

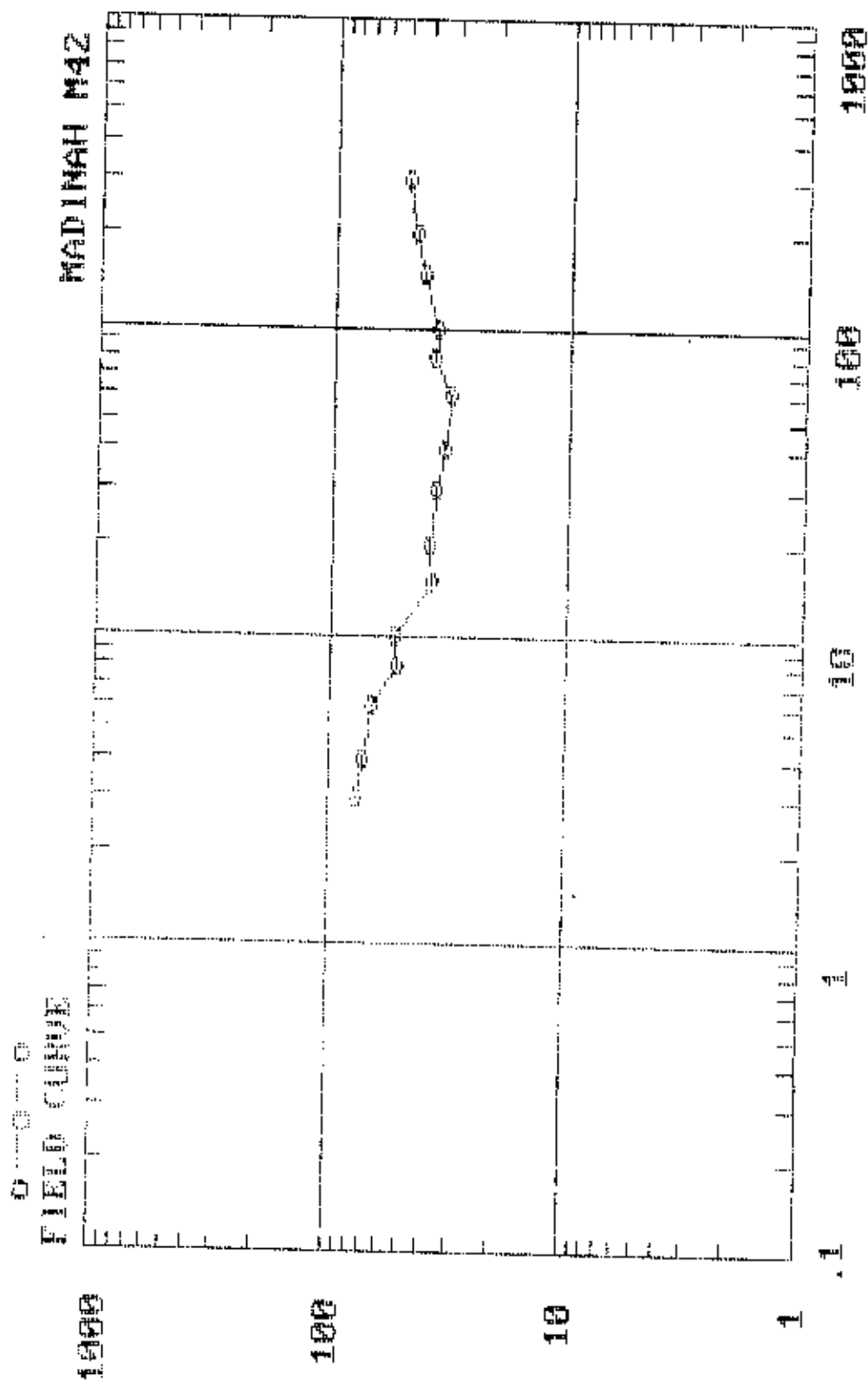
DEPTH	RESIS.	DEPTH	RESIS.
1.458	52.42733	14.58	36.3744
2.140051	46.59575	21.40052	26.81986
3.141166	34.9755	31.41167	20.34091
4.610601	30.16369	46.10602	24.50323
6.767437	33.32325	67.67439	40.23381
9.93324	37.91266	99.33241	63.80075
		99999	91.01215



ELECTRODE SPACING (AB/2), OR DEPTH, IN METERS

MADINAH M42 (FIELD DATA)

AB/2	App. Res.	AB/2	App. Res.
3	75.8	30	36.5
4	71.3	40	33.6
6	65.8	60	31.8
8	52.5	80	37.9
10	53.3	100	36.9
15	37.9	150	42.2
20	38.5	200	45
		300	50

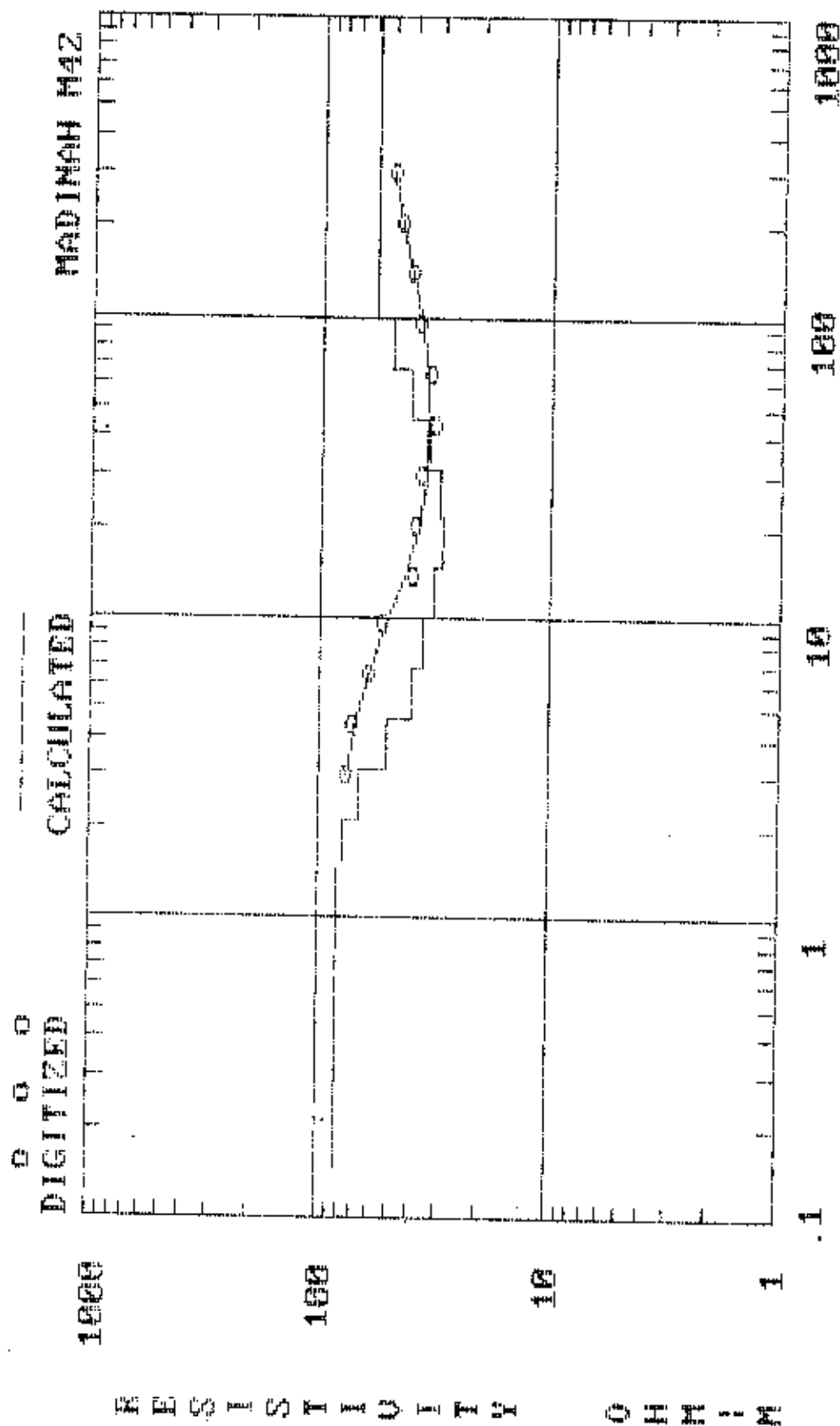


RESISTIVITY

OHM : M

MADINAH M42 (INTERPRETATION)

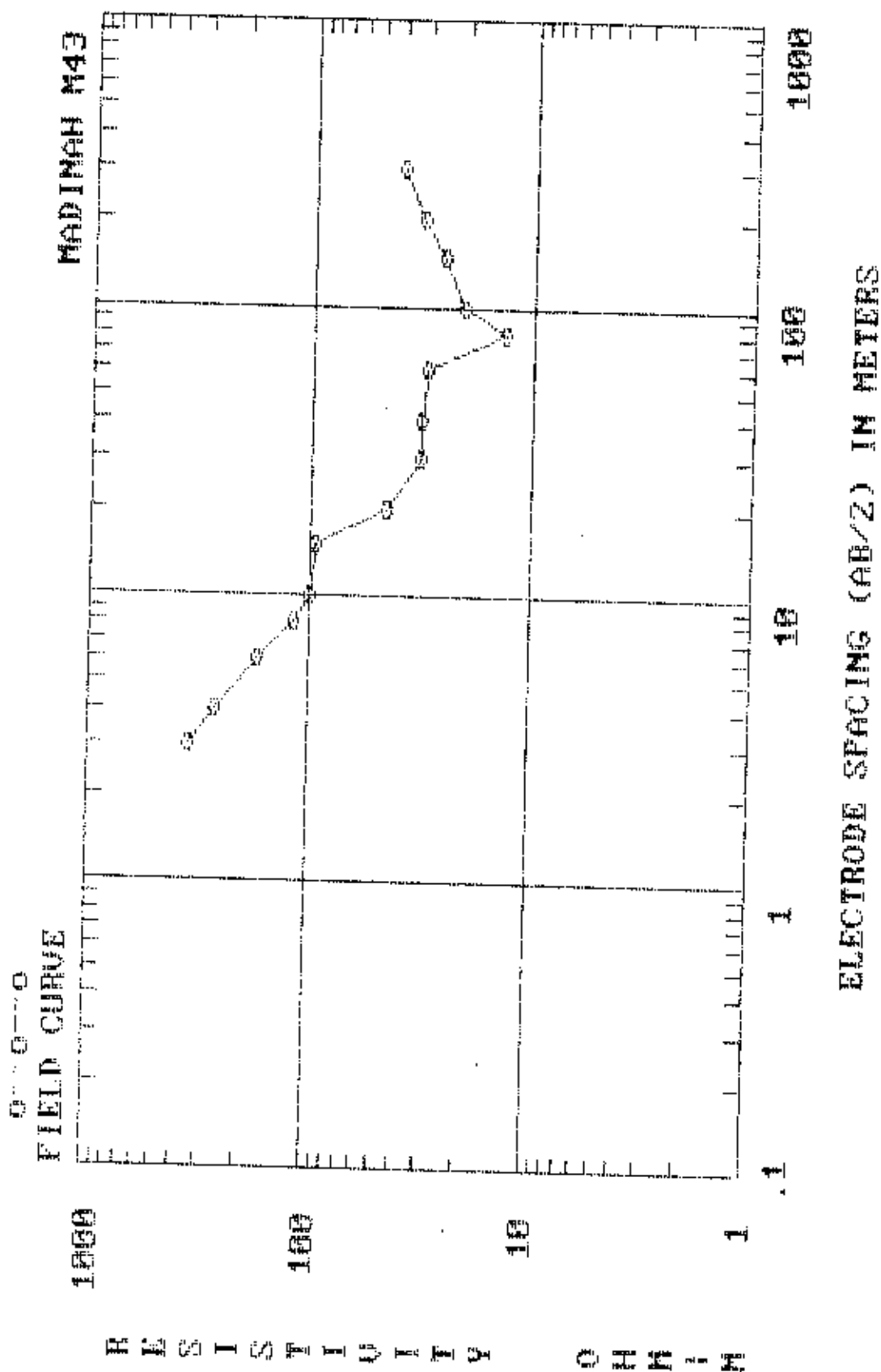
DEPTH	RESIS.	DEPTH	RESIS.
1.458	82.78201	14.58	32.02525
2.140051	78.0798	21.40052	29.22506
3.141166	66.78441	31.41167	29.98623
4.610601	51.35102	46.10602	34.45418
6.767437	39.95715	67.67439	41.0994
9.93324	35.26711	99.33241	49.04857
		99999	57.57236



ELECTRODE SPACING (AB/2), OR DEPTH, IN METERS

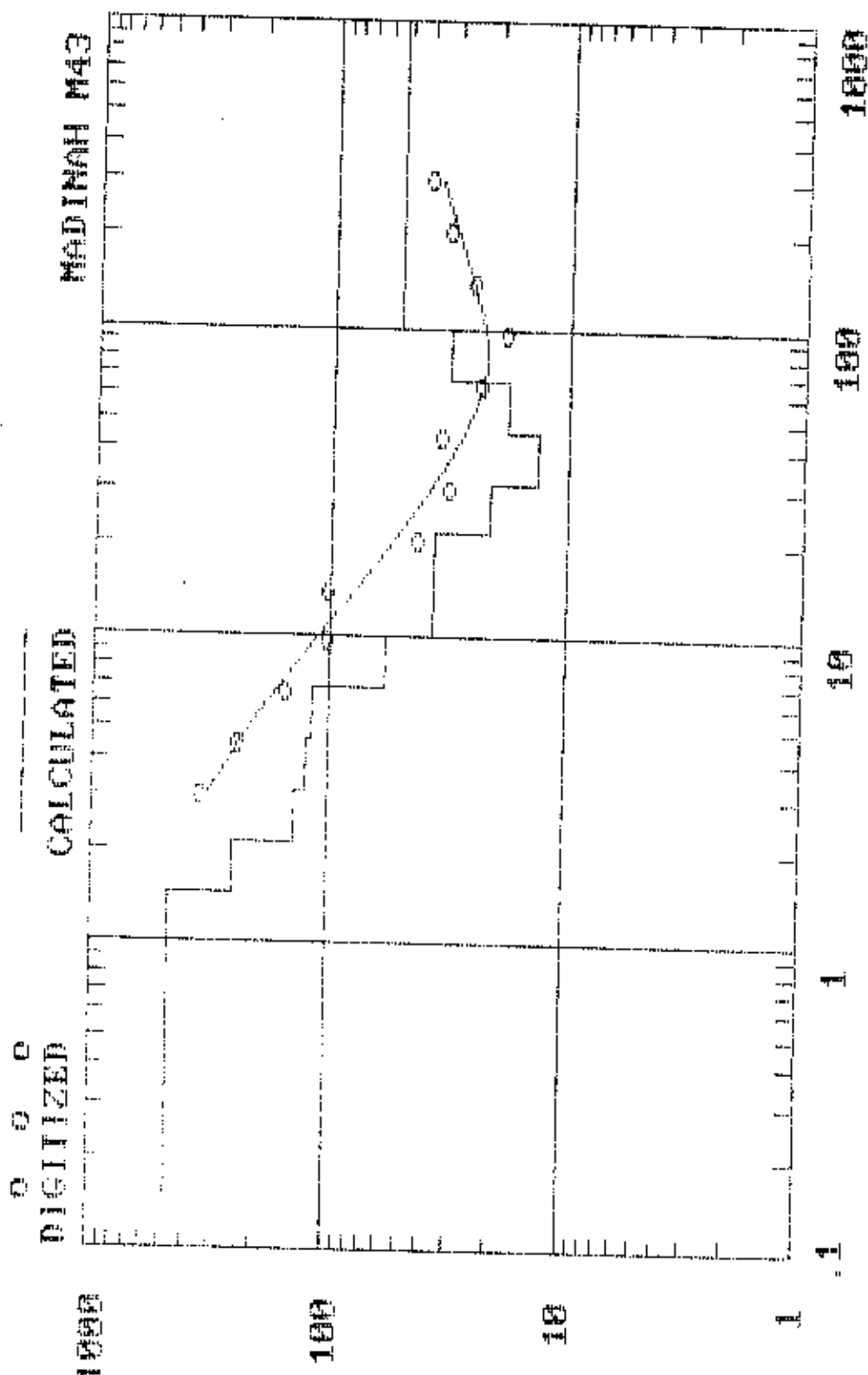
MADINAH M43 (FIELD DATA)

AB/2	App. Res.	AB/2	App. Res.
3	344	30	32.3
4	264.6	40	31.8
6	172	60	30.6
8	118.7	80	13.6
10	99.8	100	21
15	95.7	150	26
20	45.3	200	32
		300	40



MADINAH M43 (INTERPRETATION)

DEPTH	RESIS.	DEPTH	RESIS.
1.458	469.2645	14.58	36.48017
2.140051	254.4098	21.40052	36.98125
3.141166	138.8478	31.41167	21.58573
4.610601	125.183	46.10602	13.64913
6.767437	117.0794	67.67439	18.34864
9.93324	57.70455	99.33241	31.6333
		99999	52.47502

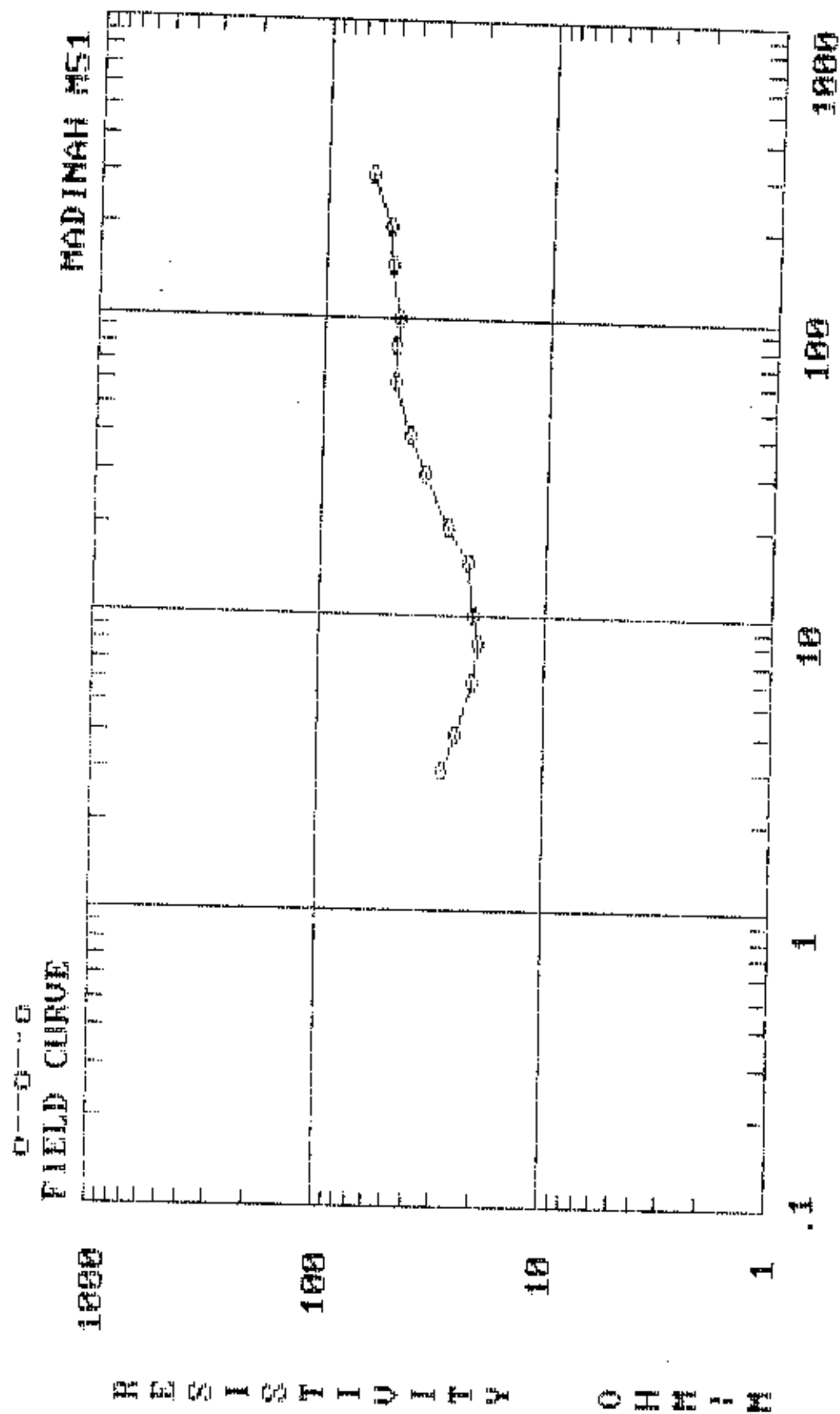


RESISTIVITY

OHM-M

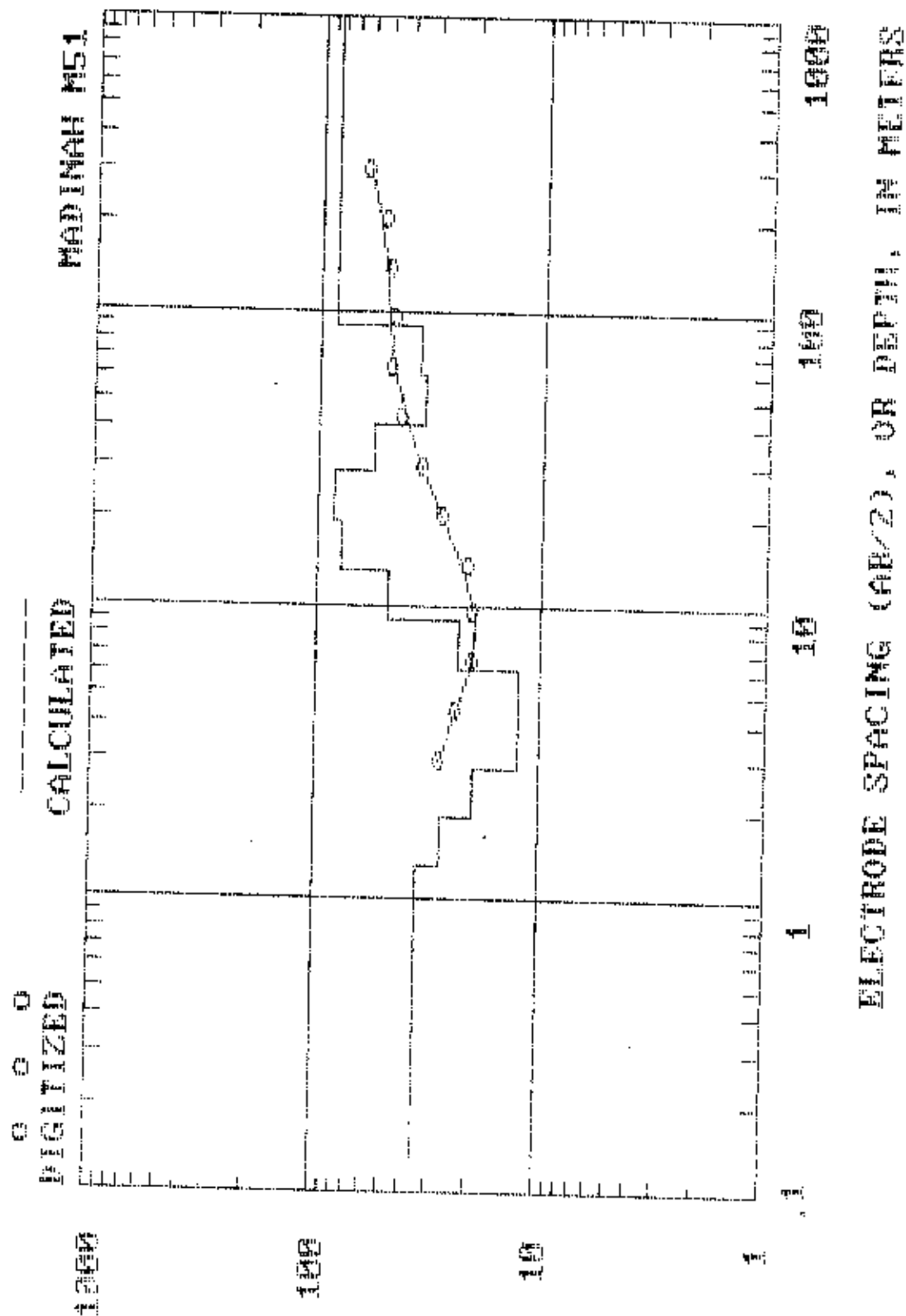
MADINAH M51 (FIELD DATA)

AB/2	App. Res.	AB/2	App. Res.
3	27.8	30	35.1
4	24.4	40	41.2
6	20.9	60	48.3
8	19.5	80	47.5
10	20.6	100	47.1
15	22.2	150	51.4
20	27.2	200	51.5
		300	63.6



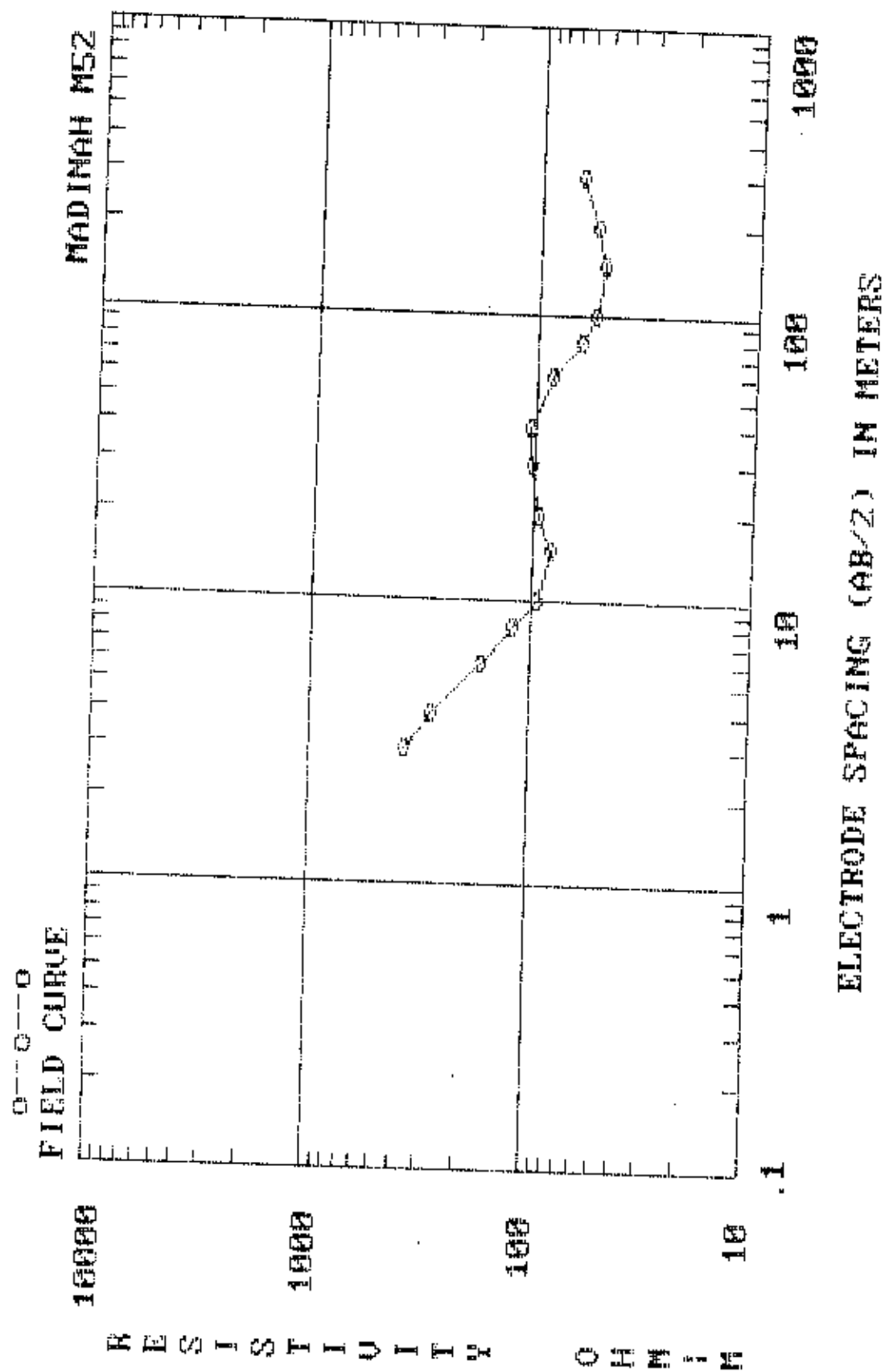
MADINAH M51 (INTERPRETATION)

DEPTH	RESIS.	DEPTH	RESIS.
1.3122	34.65198	13.122	48.77747
1.926046	27.09792	19.26047	79.08587
2.827049	19.62737	28.2705	83.8554
4.149541	12.40745	41.49542	57.21189
6.090694	12.37241	60.90695	34.28916
8.939917	23.29604	89.39919	35.6478
		99999	84.18612



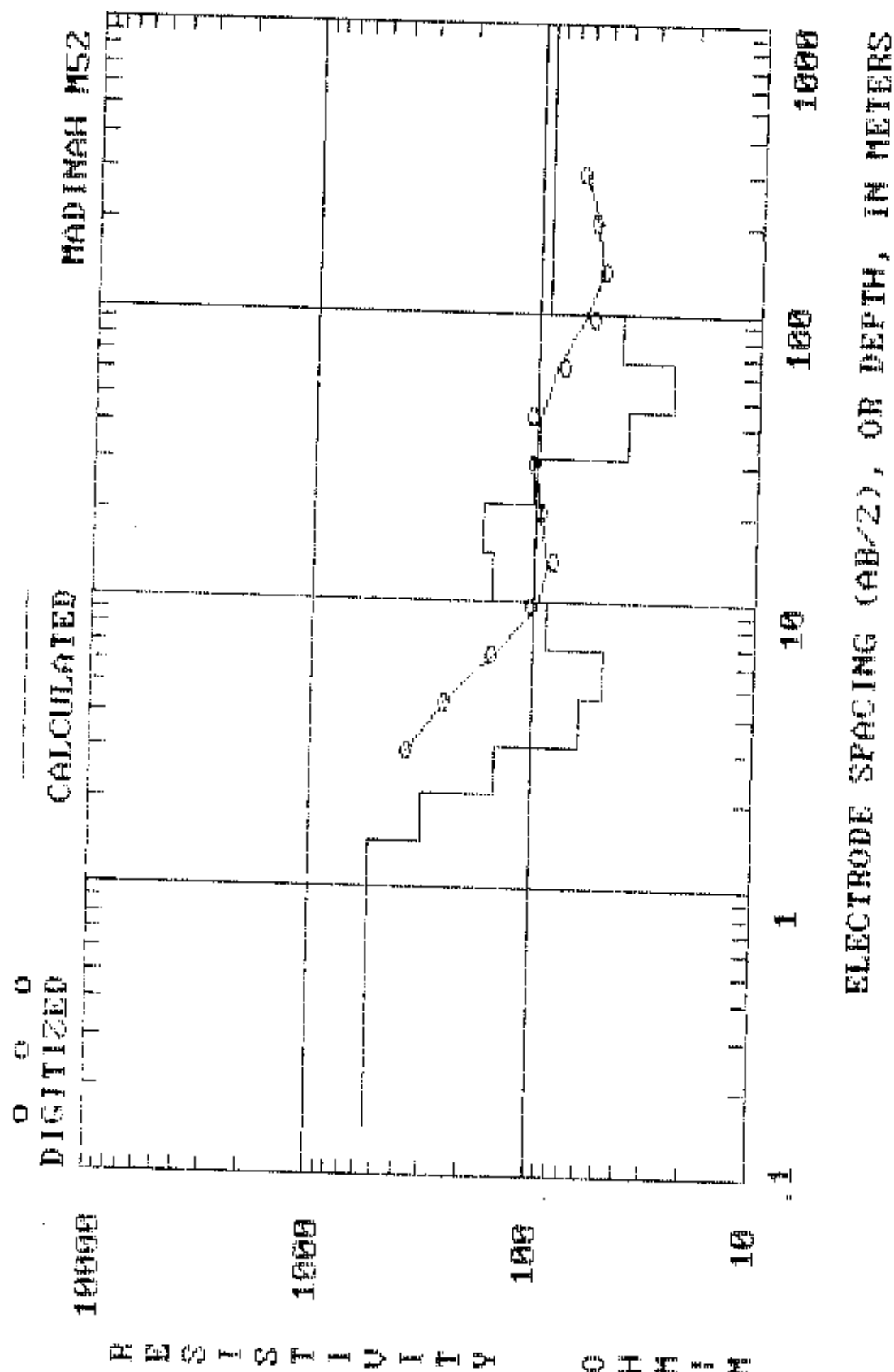
MADINAH M52 (FIELD DATA)

AB/2	App. Res.	AB/2	App. Res.
3	367.3	30	103
4	277.5	40	105.9
6	168.5	60	84.6
8	121.7	80	62.3
10	95.9	100	55.2
15	82.6	150	51.1
20	93.7	200	55.6
		300	65.3



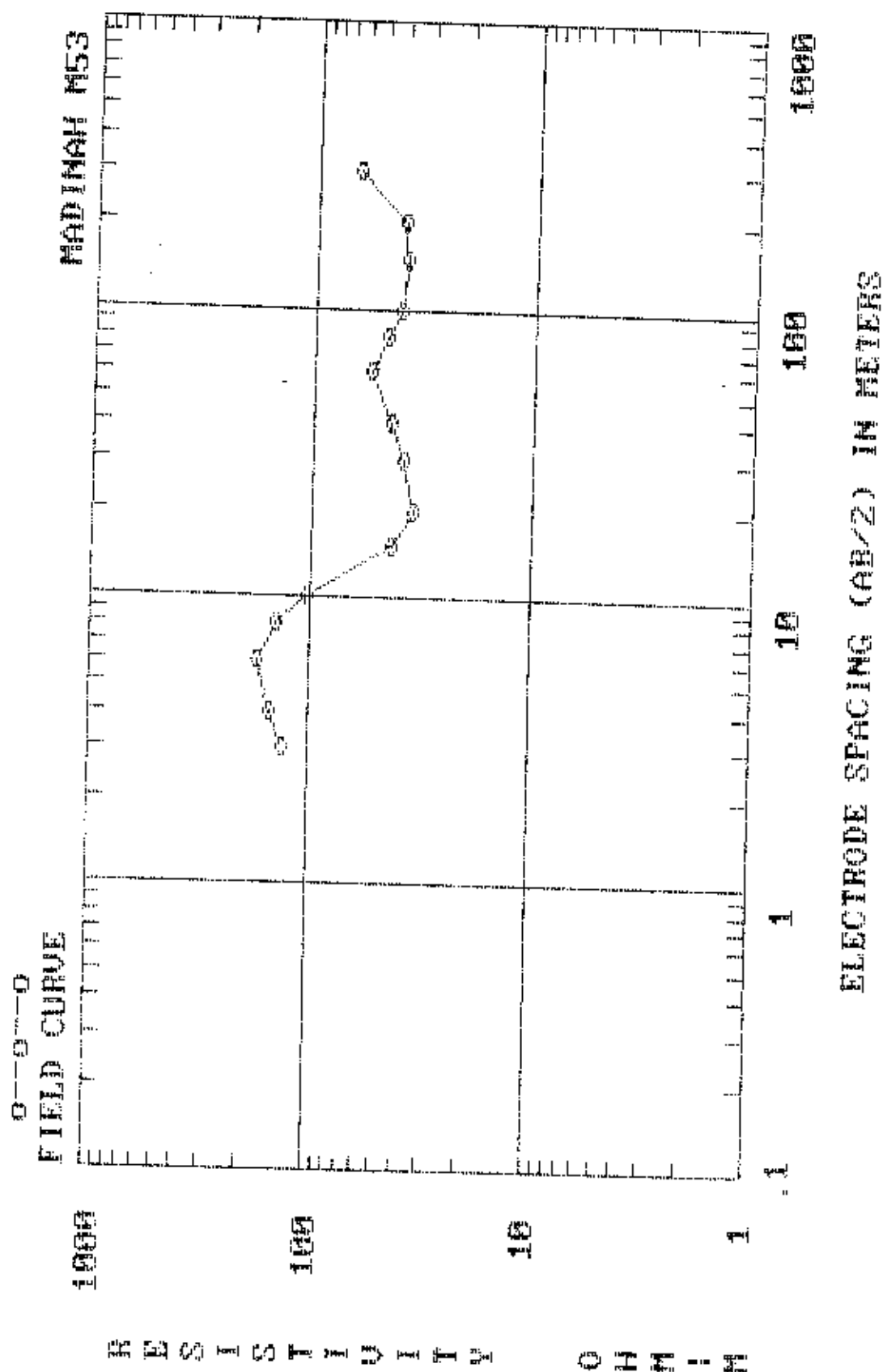
MADINAH M52 (INTERPRETATION)

DEPTH	RESIS.	DEPTH	RESIS.
1.458	537.3914	14.58	153.108
2.140051	308.8828	21.40052	171.6525
3.141166	145.5718	31.41167	101.9708
4.610601	61.05559	46.10602	38.97037
6.767437	48.77863	67.67439	24.67672
9.93324	87.04803	99.33241	41.56671
		99999	89.18443



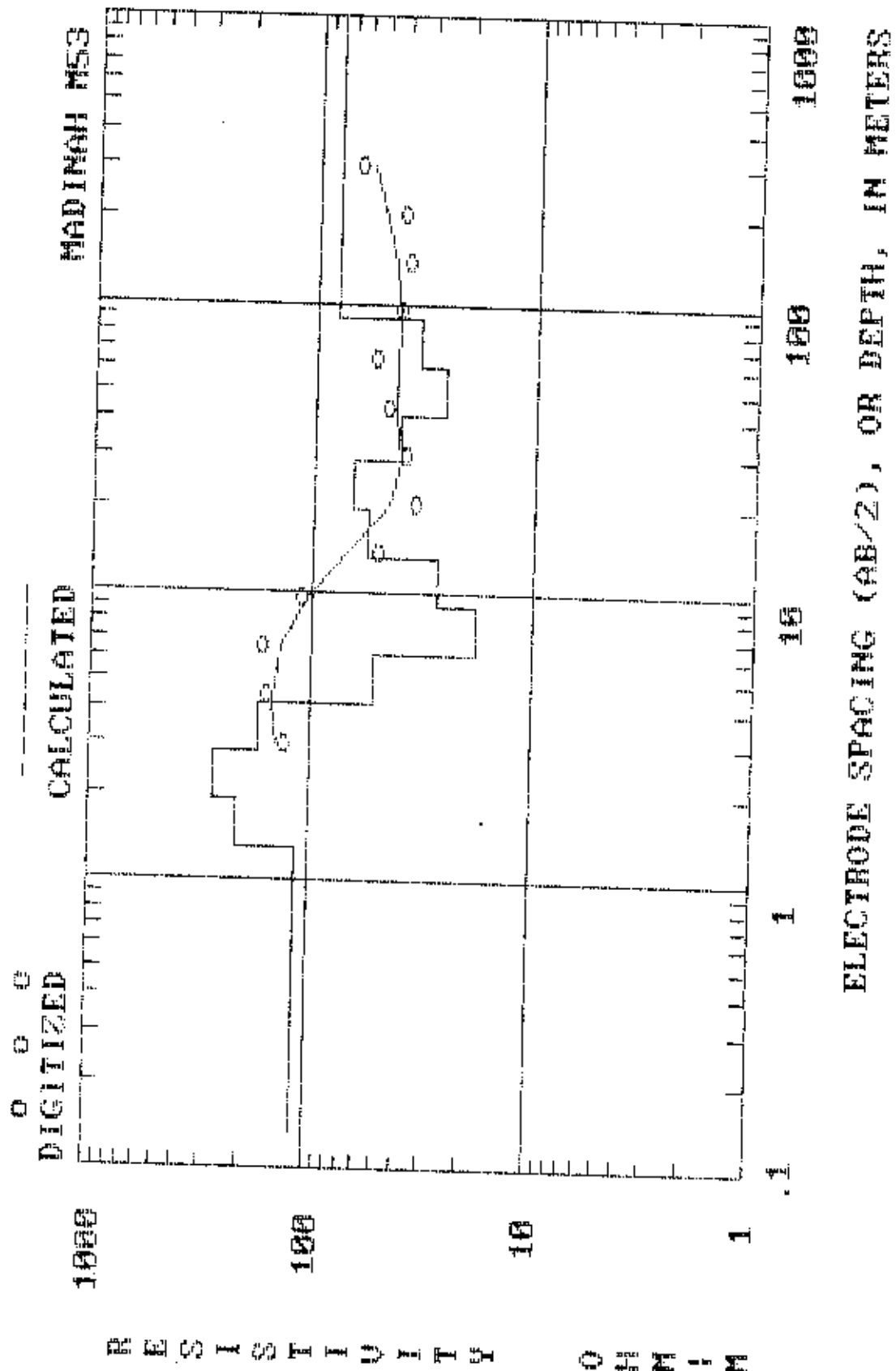
MADINAH M53 (FIELD DATA)

AB/2	App. Res.	AB/2	App. Res.
3	130.2	30	38.9
4	150.1	40	44.1
6	170.1	60	55.6
8	141.7	80	46.9
10	103.1	100	41.3
15	43.2	150	38.6
20	34.6	200	40.1
		300	65.2



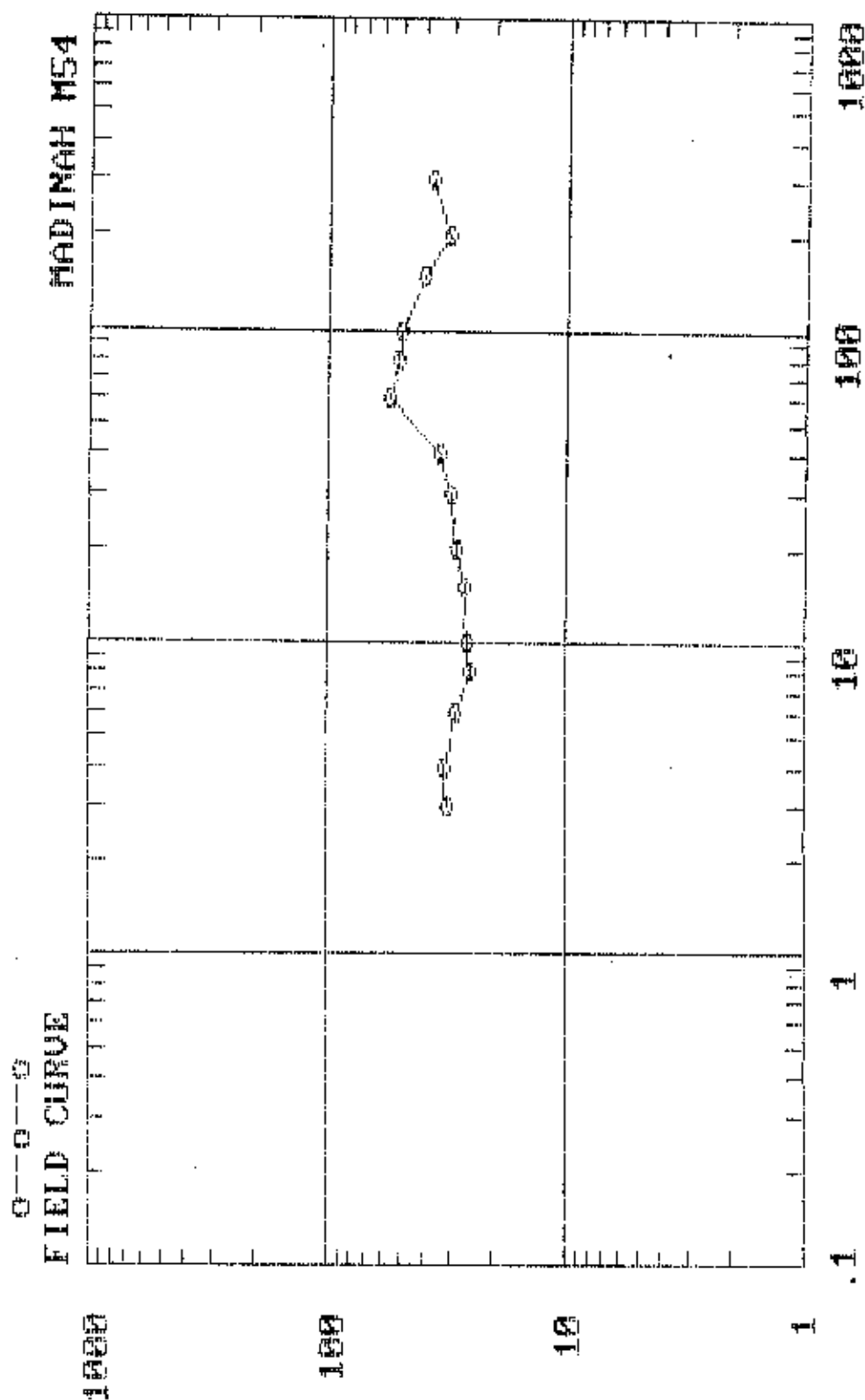
MADINAH M53 (INTERPRETATION)

DEPTH	RESIS.	DEPTH	RESIS.
1.3122	115.6636	13.122	26.94301
1.926046	214.7167	19.26047	57.08423
2.827049	270.312	28.2705	66.55521
4.149541	173.6193	41.49542	41.45418
6.090694	52.10108	60.90695	25.72845
8.939917	18.21843	89.39919	33.89528
		99999	80.97527



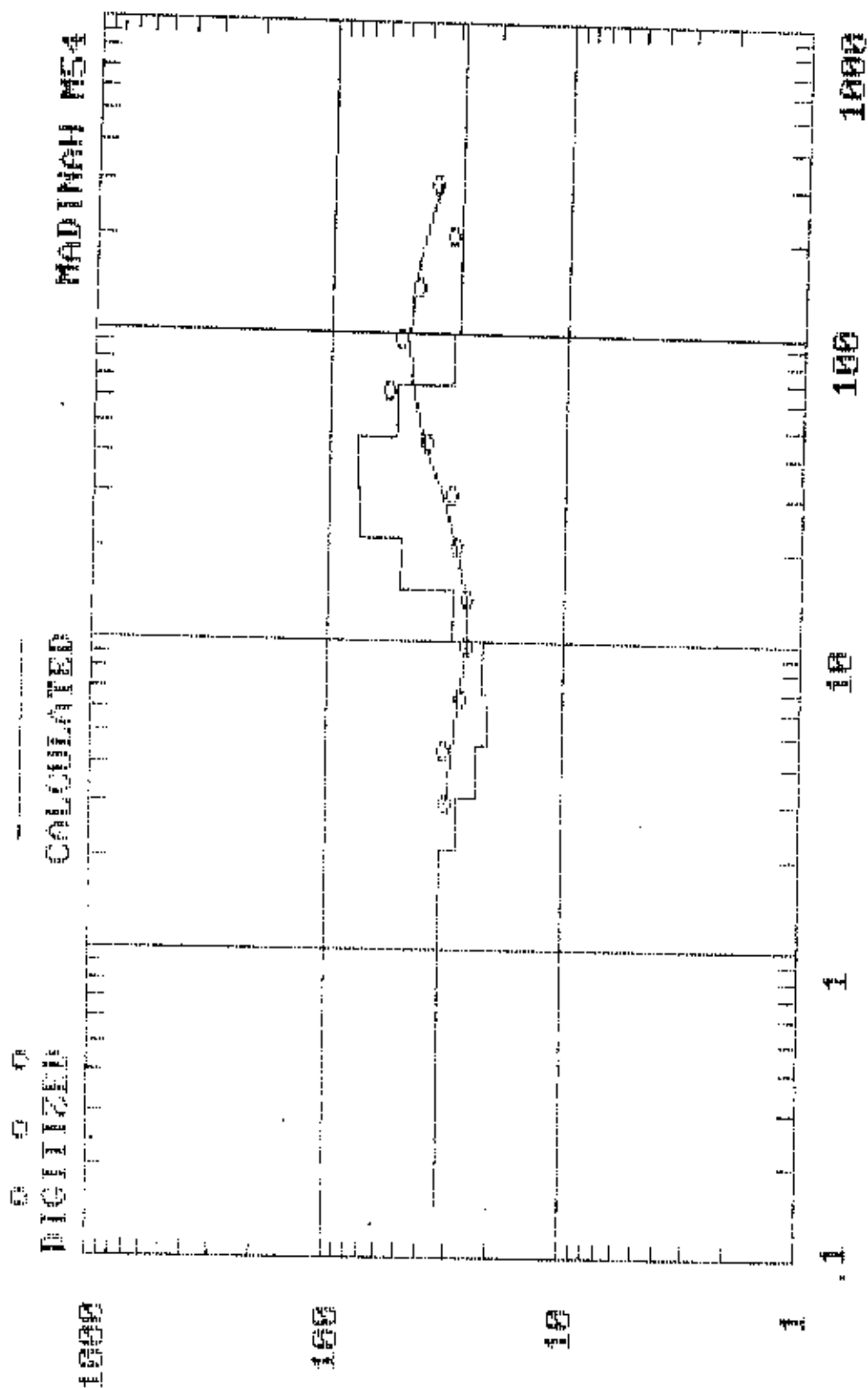
MADINAH M54 (FIELD DATA)

AB/2	App. Res.	AB/2	App. Res.
3	30.9	30	30.1
4	32.1	40	34.2
6	28.5	60	55.6
8	25	80	51.2
10	26.1	100	50.1
15	26.2	150	40.3
20	28.9	200	31.2
		300	36.6



MADINAH M54 (INTERPRETATION)

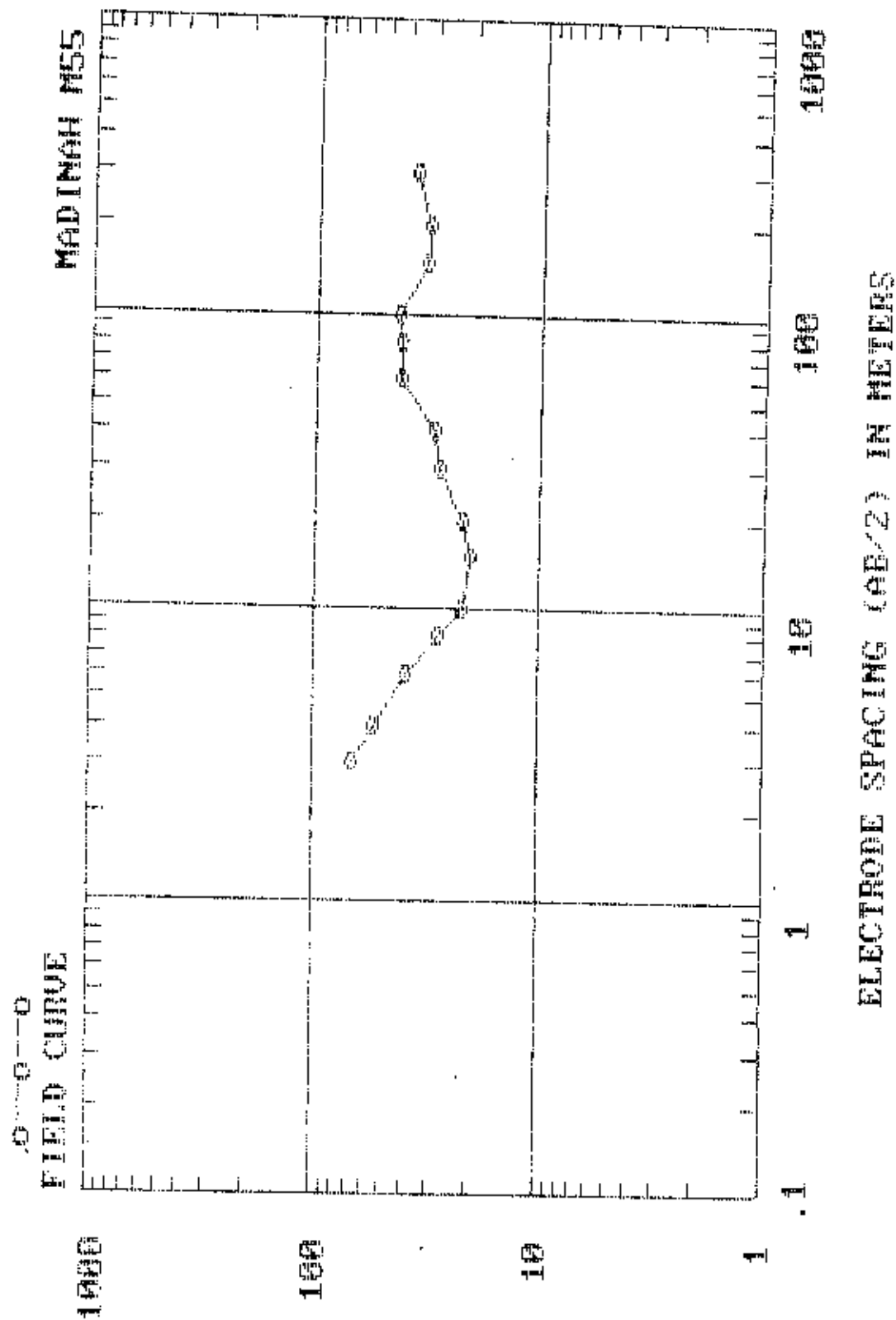
DEPTH	RESIS.	DEPTH	RESIS.
1.458	32.74864	14.58	29.36041
2.140051	32.97722	21.40052	49.6399
3.141166	27.84488	31.41167	74.83958
4.610601	22.9709	46.10602	77.19121
6.767437	20.88445	67.67439	51.84529
9.93324	21.66855	99.33241	30.2525
		99999	28.90185



ELECTRODE SPACING (AB/2), OR DEPTH, IN METERS

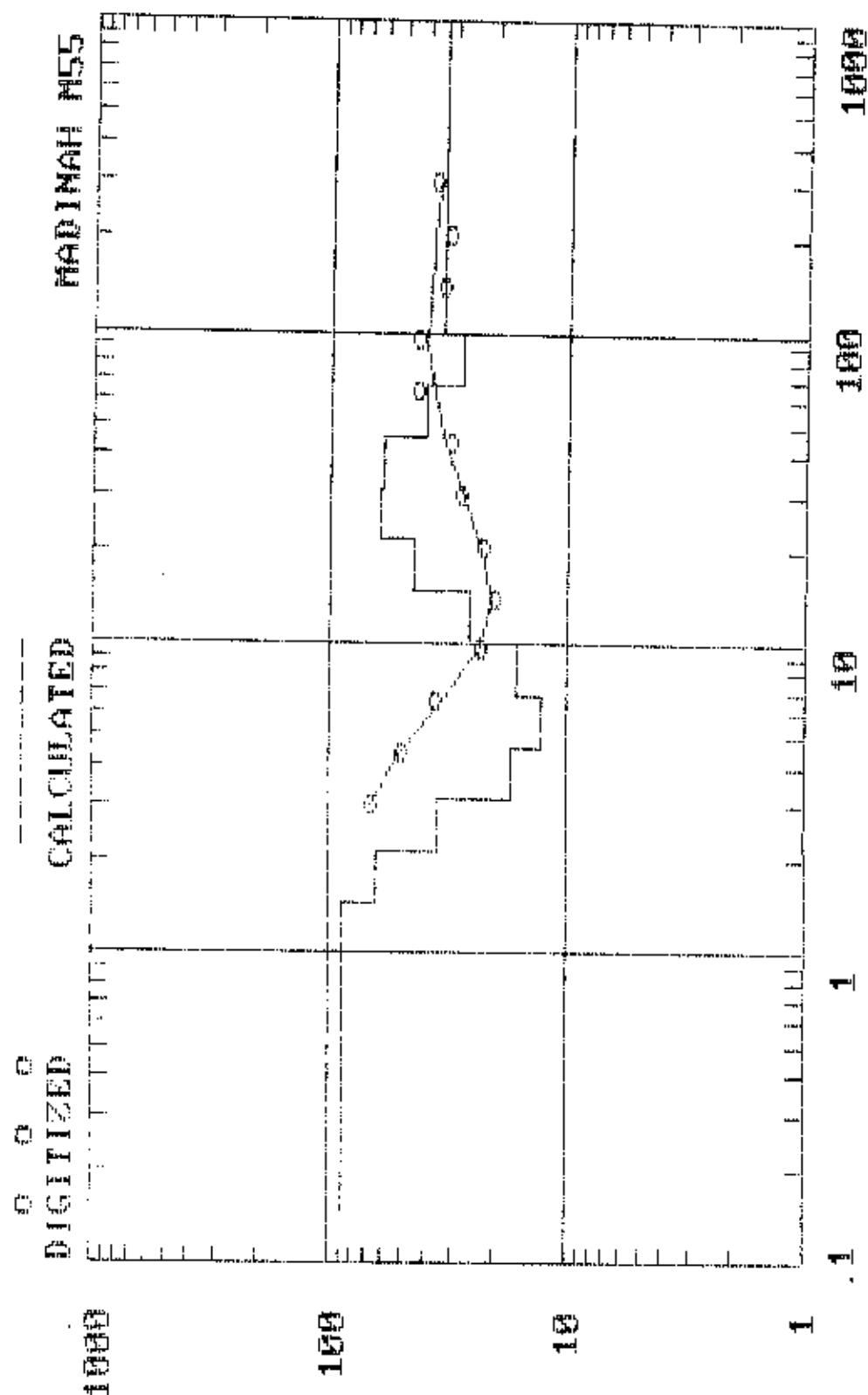
MADINAH M55 (FIELD DATA)

AB/2	App. Res.	AB/2	App. Res.
3	66.6	30	27.9
4	53.1	40	29.2
6	38.9	60	42.5
8	28	80	41.9
10	22.2	100	42.8
15	20.2	150	32.8
20	22	200	31.9
		300	36.9



MADINAH M55 (INTERPRETATION)

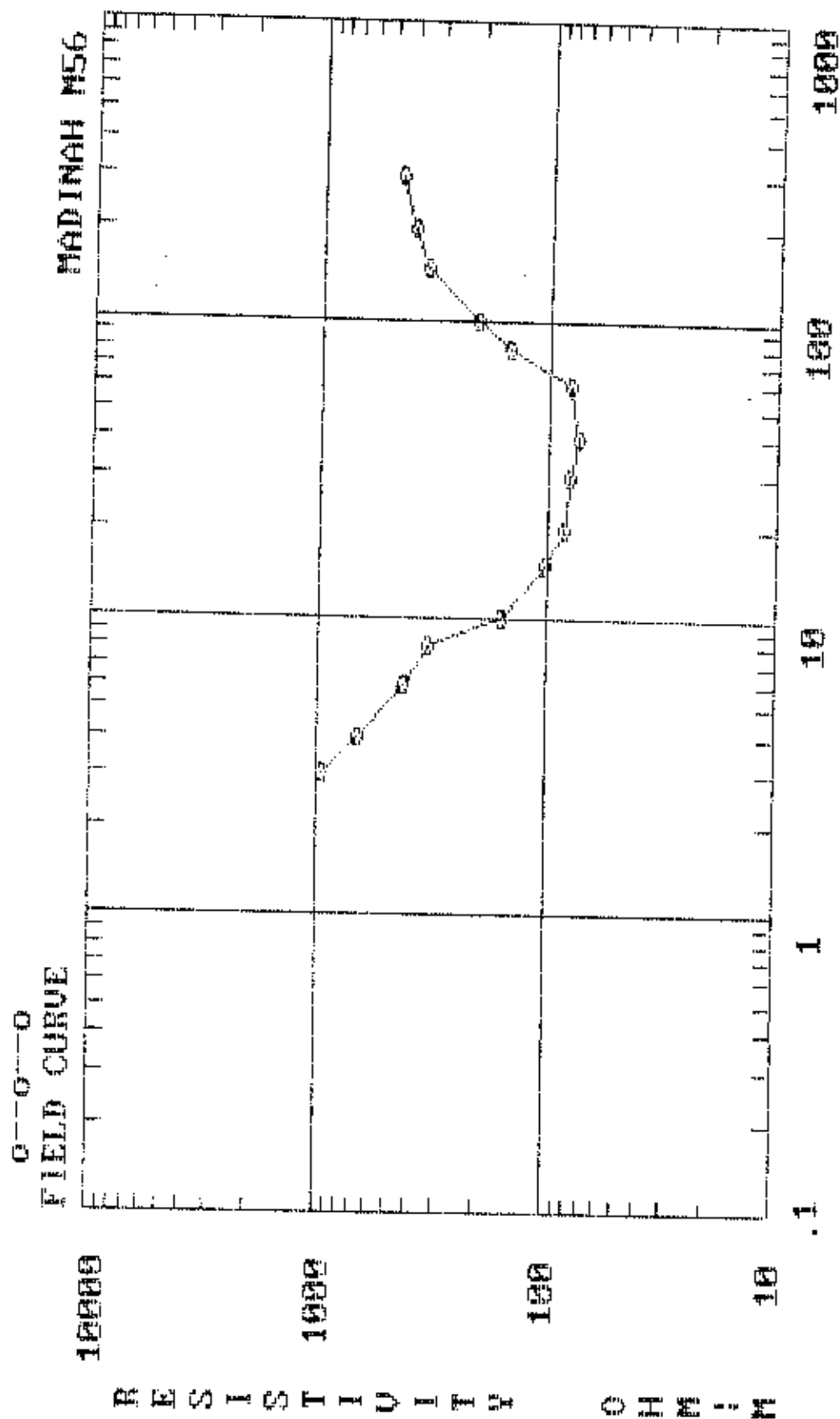
DEPTH	RESIS.	DEPTH	RESIS.
1.458	88.38923	14.58	26.00017
2.140051	62.55786	21.40052	43.87099
3.141166	35.08829	31.41167	61.93848
4.610601	17.17066	46.10602	59.28506
6.767437	12.67133	67.67439	39.56691
9.93324	16.18516	99.33241	27.65998
		99999	33.62548



ELECTRODE SPACING (AB/2), OR DEPTH, IN METERS

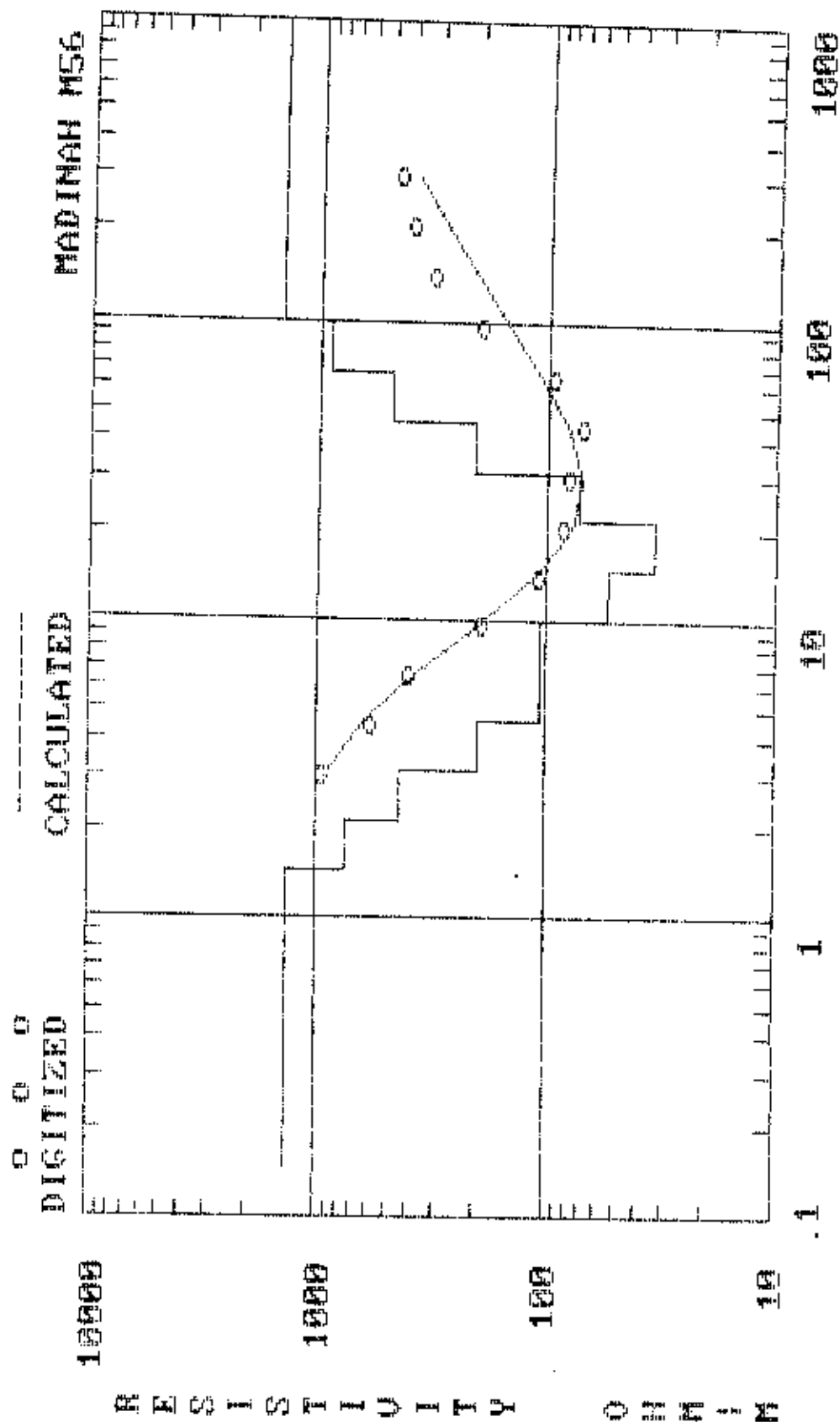
MADINAH M56 (FIELD DATA)

AB/2	App. Res.	AB/2	App. Res.
3	950	30	80
4	670	40	75
6	420	60	80
8	330	80	150
10	160	100	210
15	103	150	350
20	85	200	400
		300	460



MADINAH M56 (INTERPRETATION)

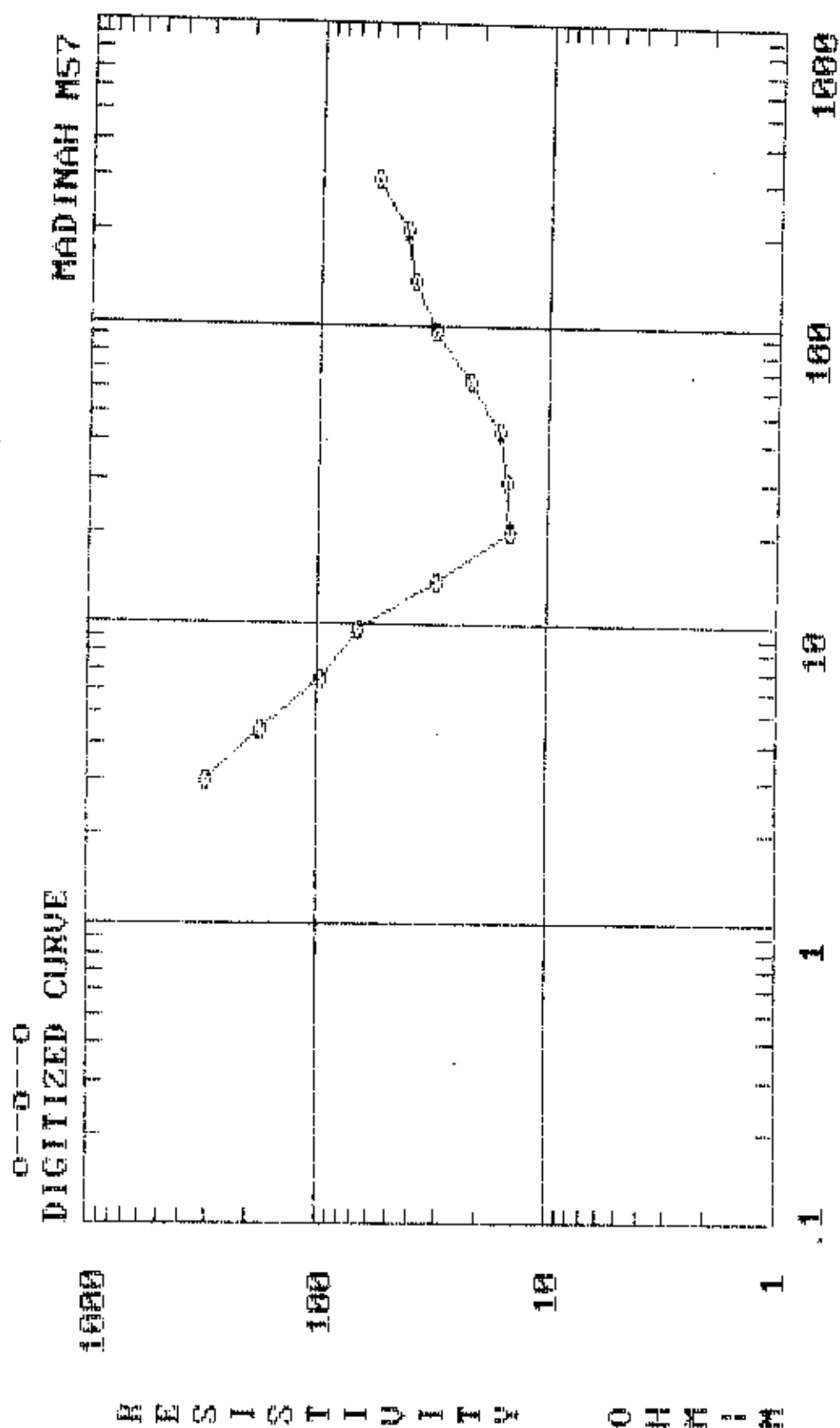
DEPTH	RESIS.	DEPTH	RESIS.
1.458	1352.971	14.58	52.94995
2.140051	742.0034	21.40052	34.01099
3.141166	435.2038	31.41167	73.19828
4.610601	198.246	46.10602	207.8685
6.767437	105.2389	67.67439	478.4003
9.93324	105.4877	99.33241	899.5823
		99999	1479.826



ELECTRODE SPACING (AB/2), OR DEPTH, IN METERS

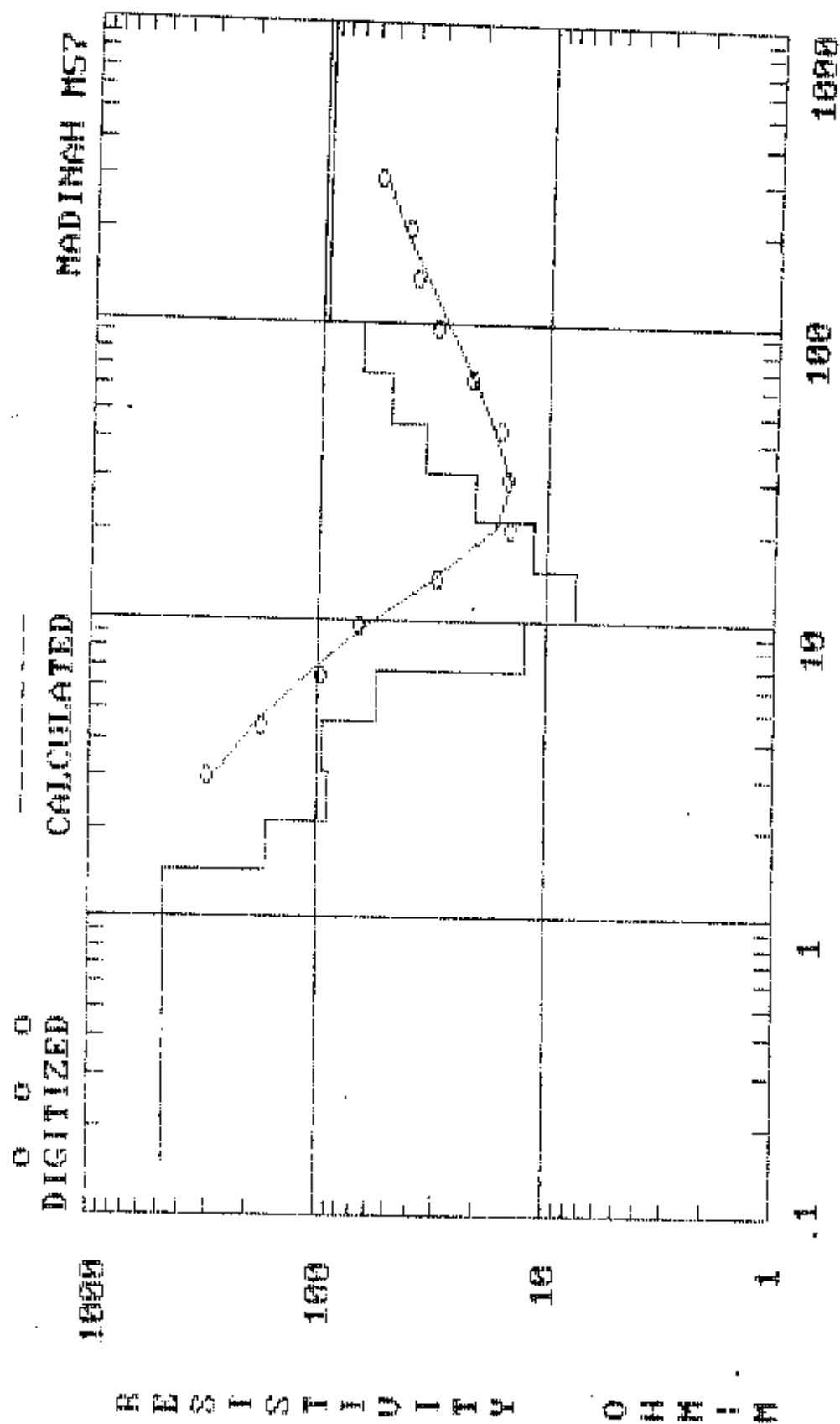
MADINAH M57 (DIGITIZED DATA)

AB/2	App. Res.	AB/2	App. Res.
3	300.0001	30.00001	15
4.403399	176.0787	44.03399	16.29329
6.463305	96.50369	64.63304	22.01596
9.486834	66.79147	94.86835	30.98438
13.92477	30.67178	139.2477	38.38533
20.43876	14.74398	204.3876	42.24401
		300.0001	56



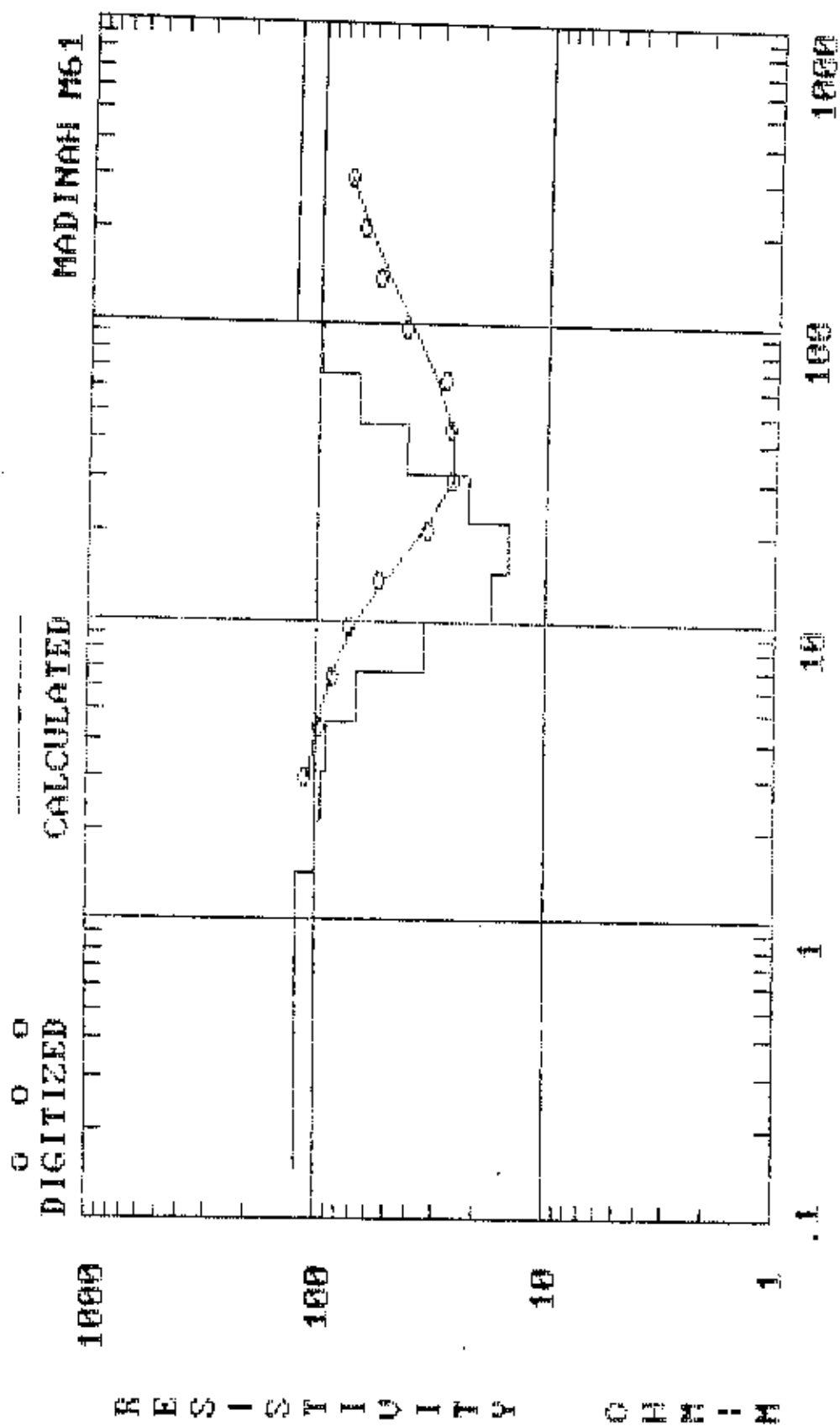
MADINAH M57 (INTERPRETATION)

DEPTH	RESIS.	DEPTH	RESIS.
1.458	468.8432	14.58	7.405501
2.140051	168.2267	21.40052	11.81562
3.141166	89.20263	31.41167	20.818
4.610601	94.08543	46.10602	34.42104
6.767437	55.30275	67.67439	49.25519
9.93324	12.55185	99.33241	67.35815
		99999	95.26546



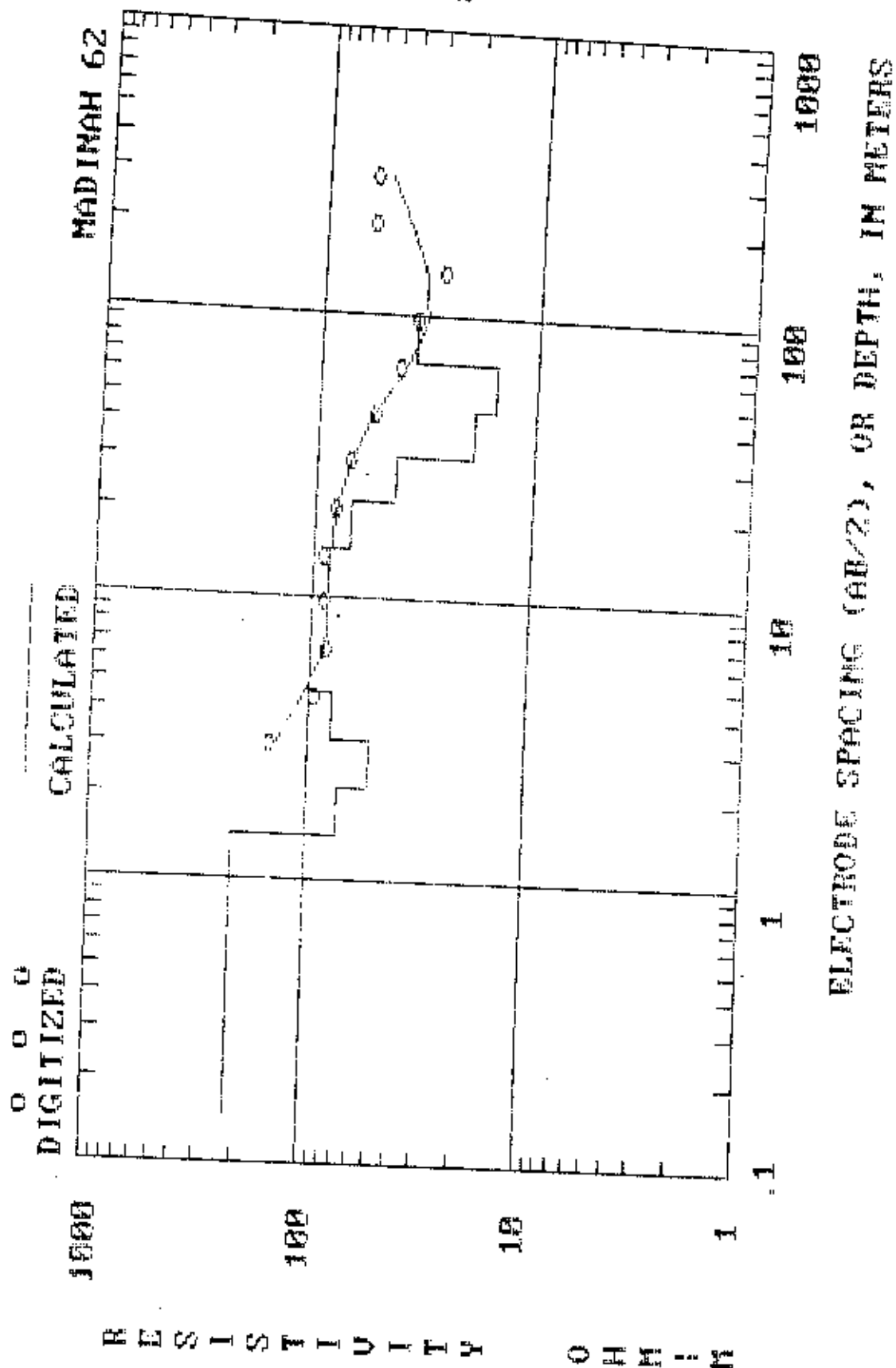
MADINAH M61 (INTERPRETATION)

DEPTH	RESIS.	DEPTH	RESIS.
1.46	119.75	14.58	17.31
2.14	100.69	21.40	14.76
3.14	93.73	31.41	22.08
4.61	89.52	46.11	40.38
6.77	66.30	67.67	67.44
9.93	33.77	99.33	97.96
		99999.00	127.14



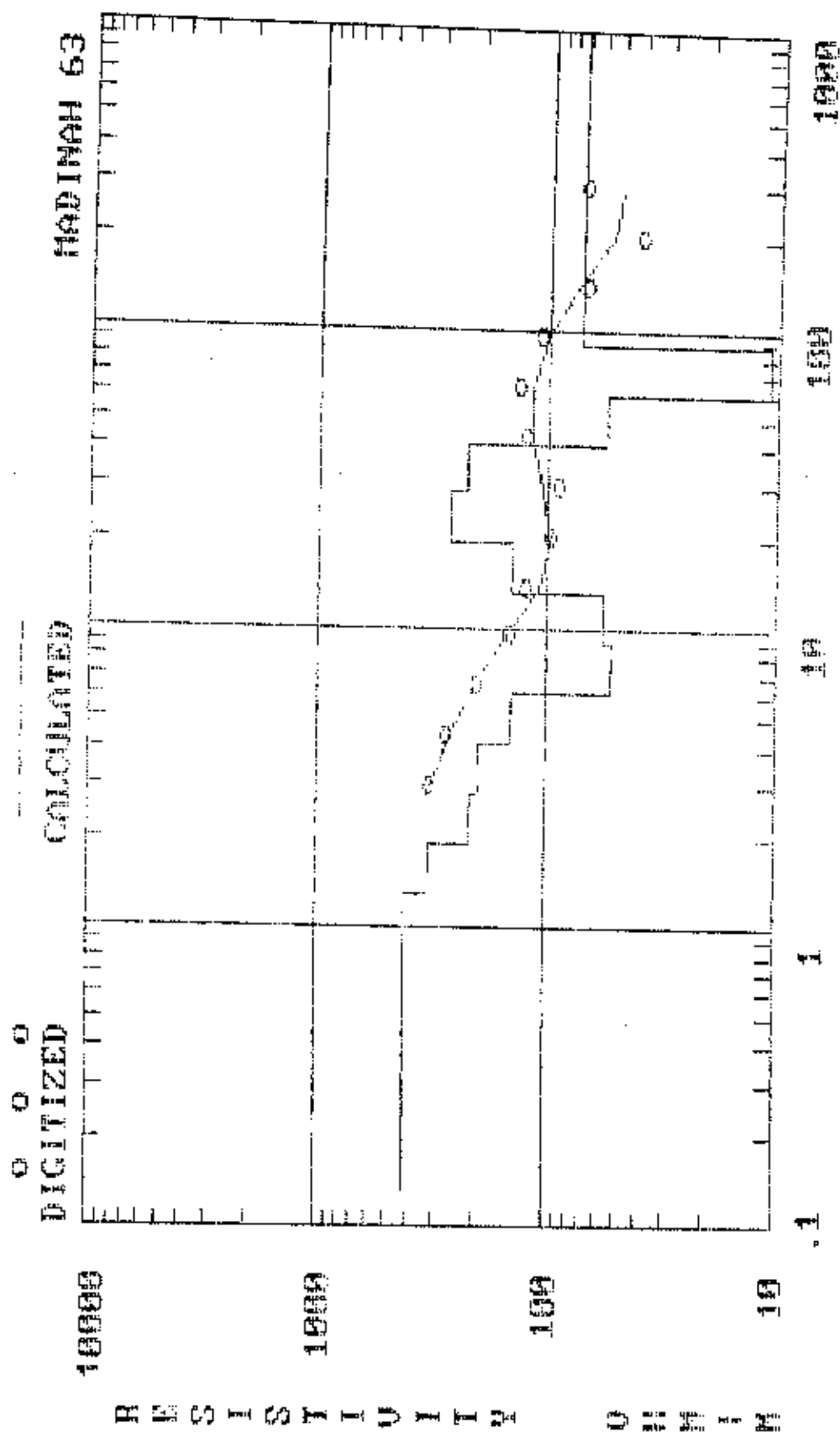
MADINAH 62 (INTERPRETATION)

DEPTH	RESIS.	DEPTH	RESIS.
1.46	218.78	14.58	86.12
2.14	71.58	21.40	68.40
3.14	52.71	31.41	43.70
4.61	78.14	46.11	19.06
6.77	100.99	67.67	15.55
9.93	100.10	99.33	36.41
		99999.00	99.03



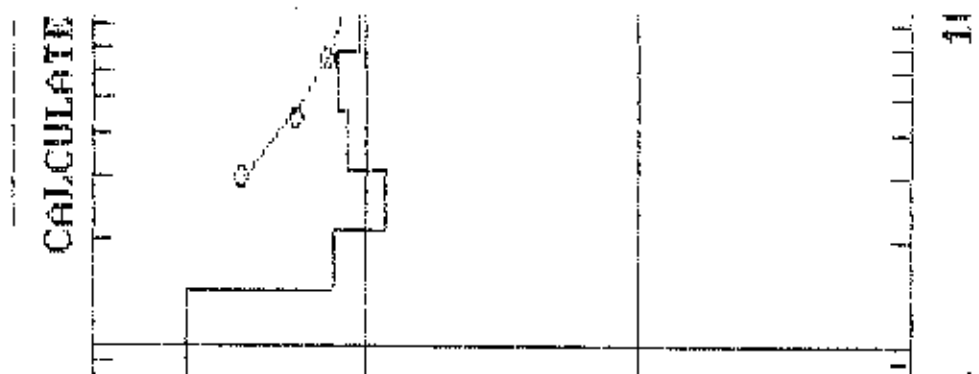
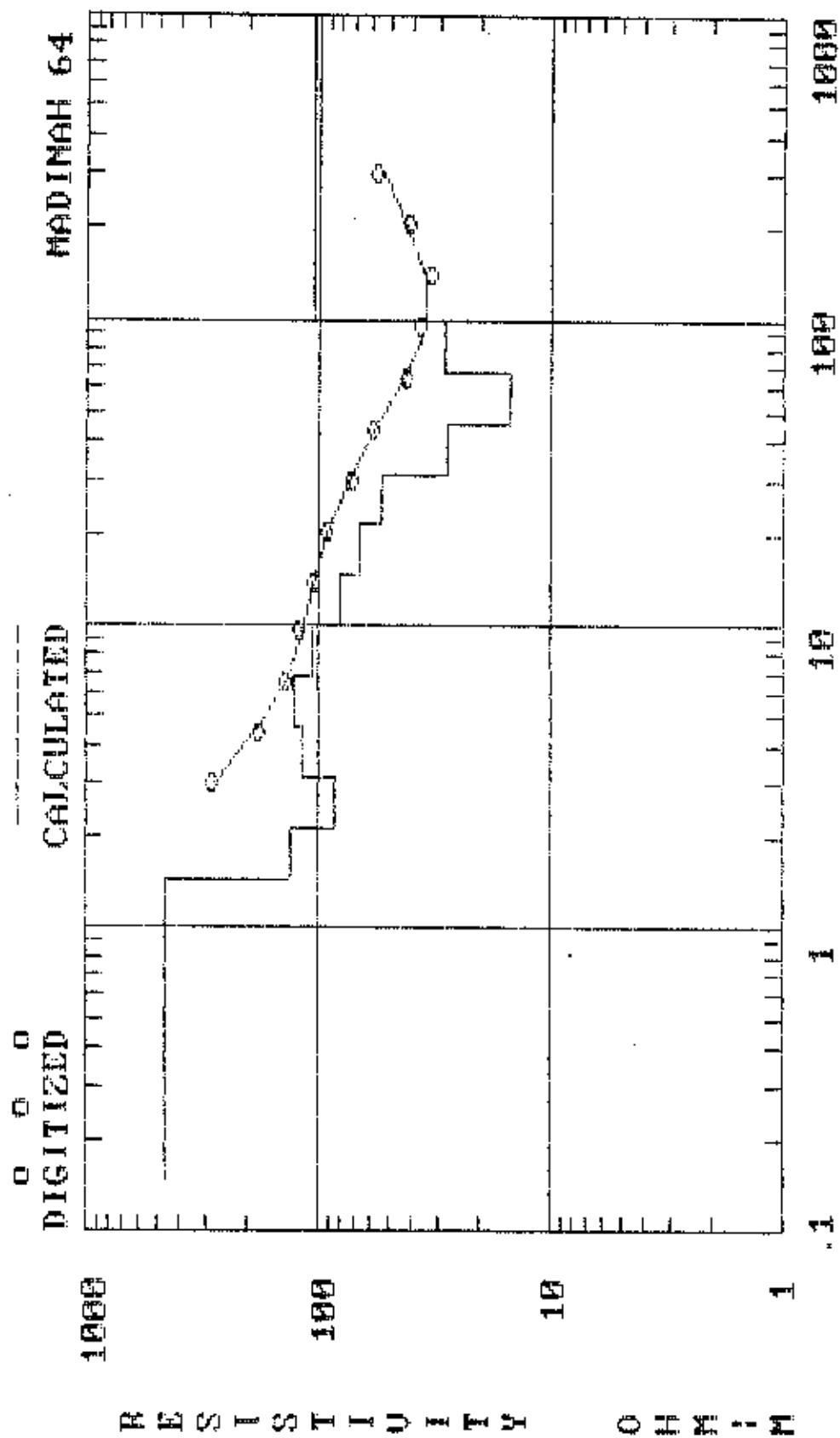
MADINAH 63 (INTERPRETATION)

DEPTH	RESIS.	DEPTH	RESIS.
1.31	404.00	13.12	56.45
1.93	320.69	19.26	141.13
2.83	213.20	28.27	264.34
4.15	195.22	41.50	222.66
6.09	140.72	60.91	55.21
8.94	52.09	89.40	10.86
		99999.00	71.86



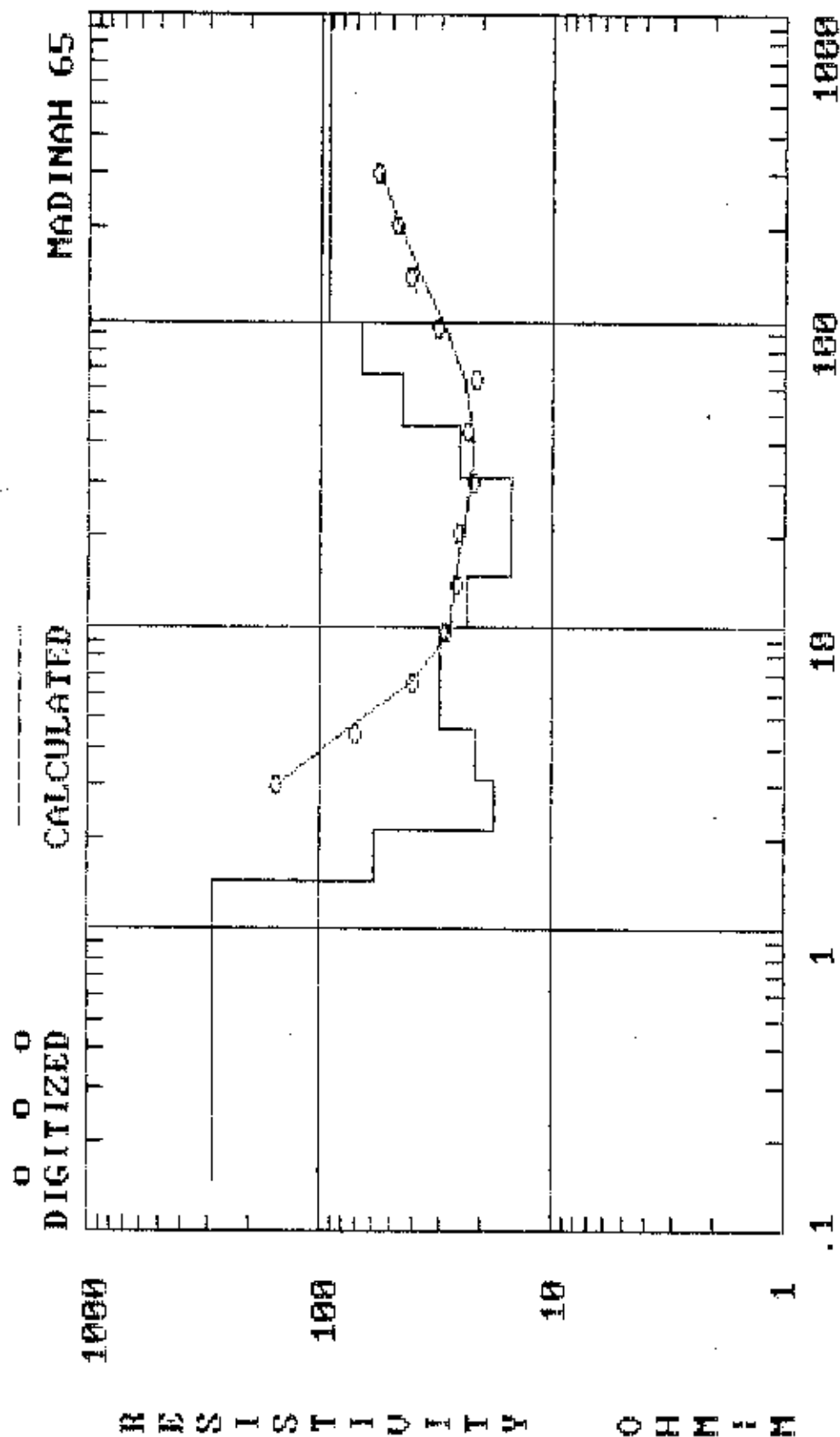
ELECTRODE SPACING (CM/2). OR DEPTH, IN METERS

DEPTH	RESIS.	DEPTH	RESIS.
1.46	459.61	14.58	80.34
2.14	130.26	21.40	65.80
3.14	85.11	31.41	53.34
4.61	116.27	46.11	27.63
6.77	127.08	67.67	15.16
9.93	104.73	99.33	28.55
		99999.00	105.09



MADINAH 65 (INTERPRETATION)

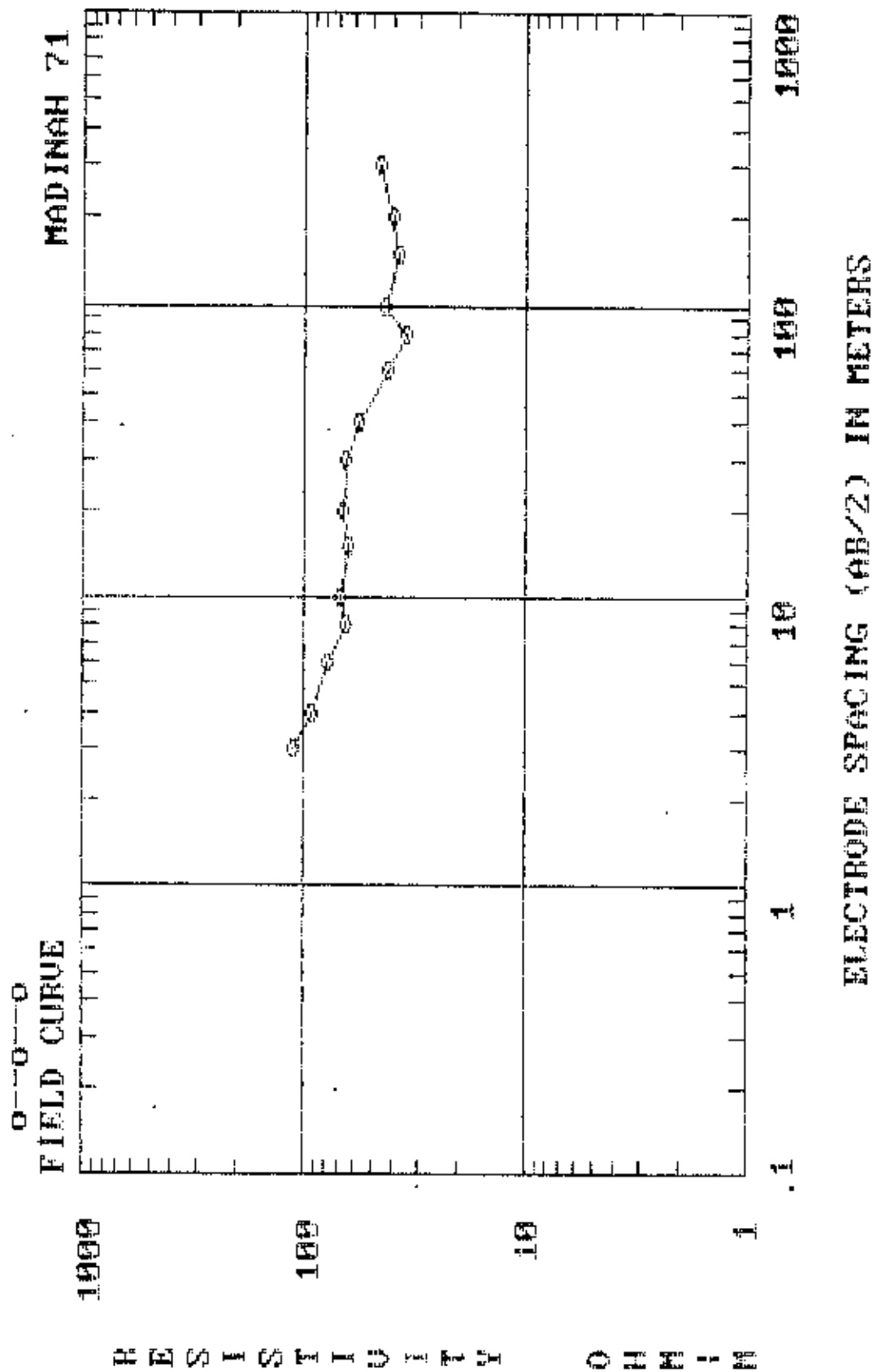
DEPTH	RESIS.	DEPTH	RESIS.
1.46	290.11	14.58	22.96
2.14	58.26	21.40	15.10
3.14	17.61	31.41	14.98
4.61	21.52	46.11	25.40
6.77	30.55	67.67	44.64
9.93	30.72	99.33	67.52
		99999.00	93.14



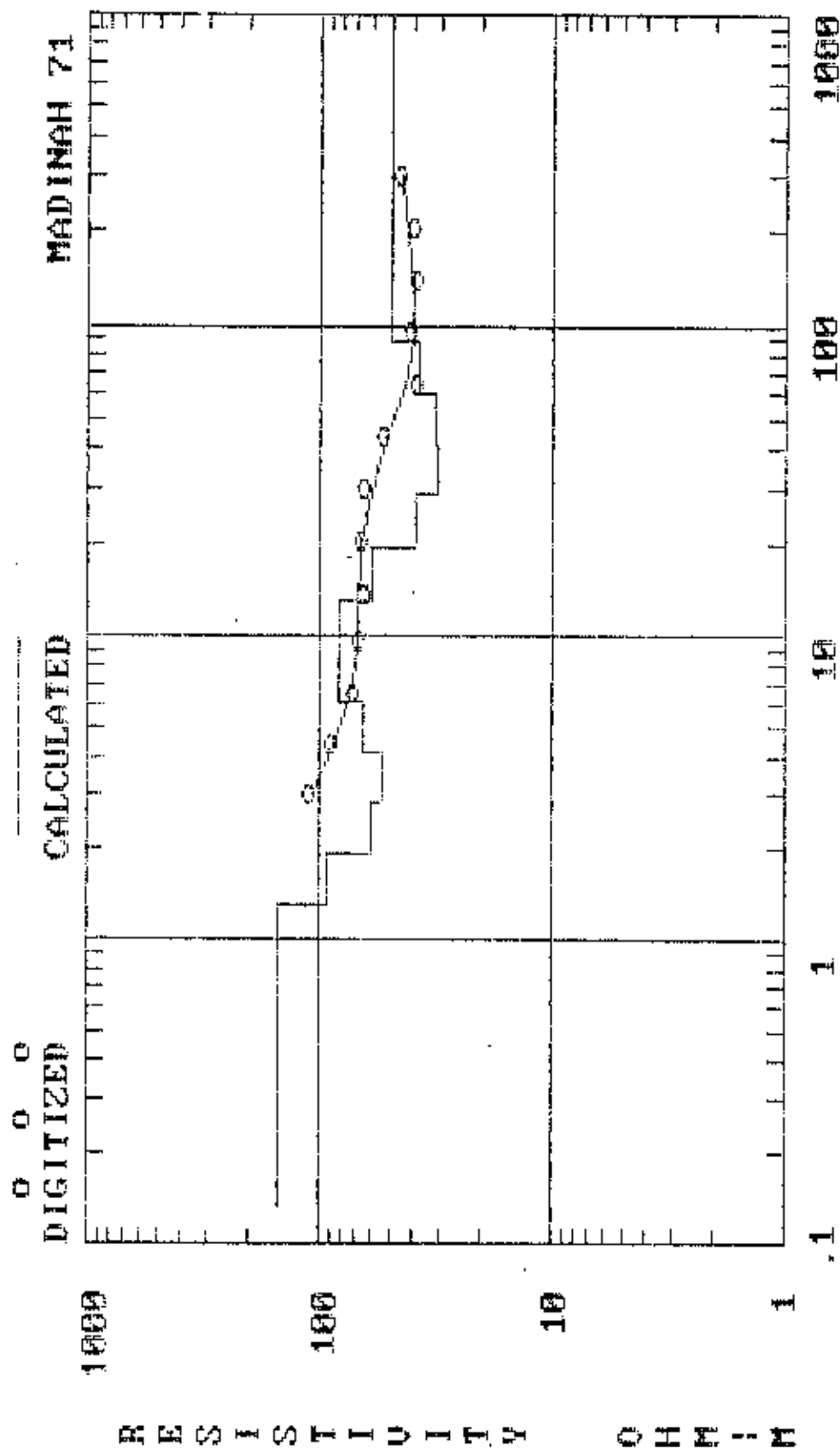
ELECTRODE SPACING (AB/2), OR DEPTH, IN METERS

MADINAH 71 (FIELD DATA)

AB/2	App. Res.	AB/2	App. Res.
3.00	111.00	30.00	64.00
4.00	93.40	40.00	57.00
6.00	77.70	60.00	42.00
8.00	65.00	80.00	35.00
10.00	69.00	100.00	43.00
15.00	63.00	150.00	38.00
20.00	66.00	200.00	40.00
		300.00	45.00

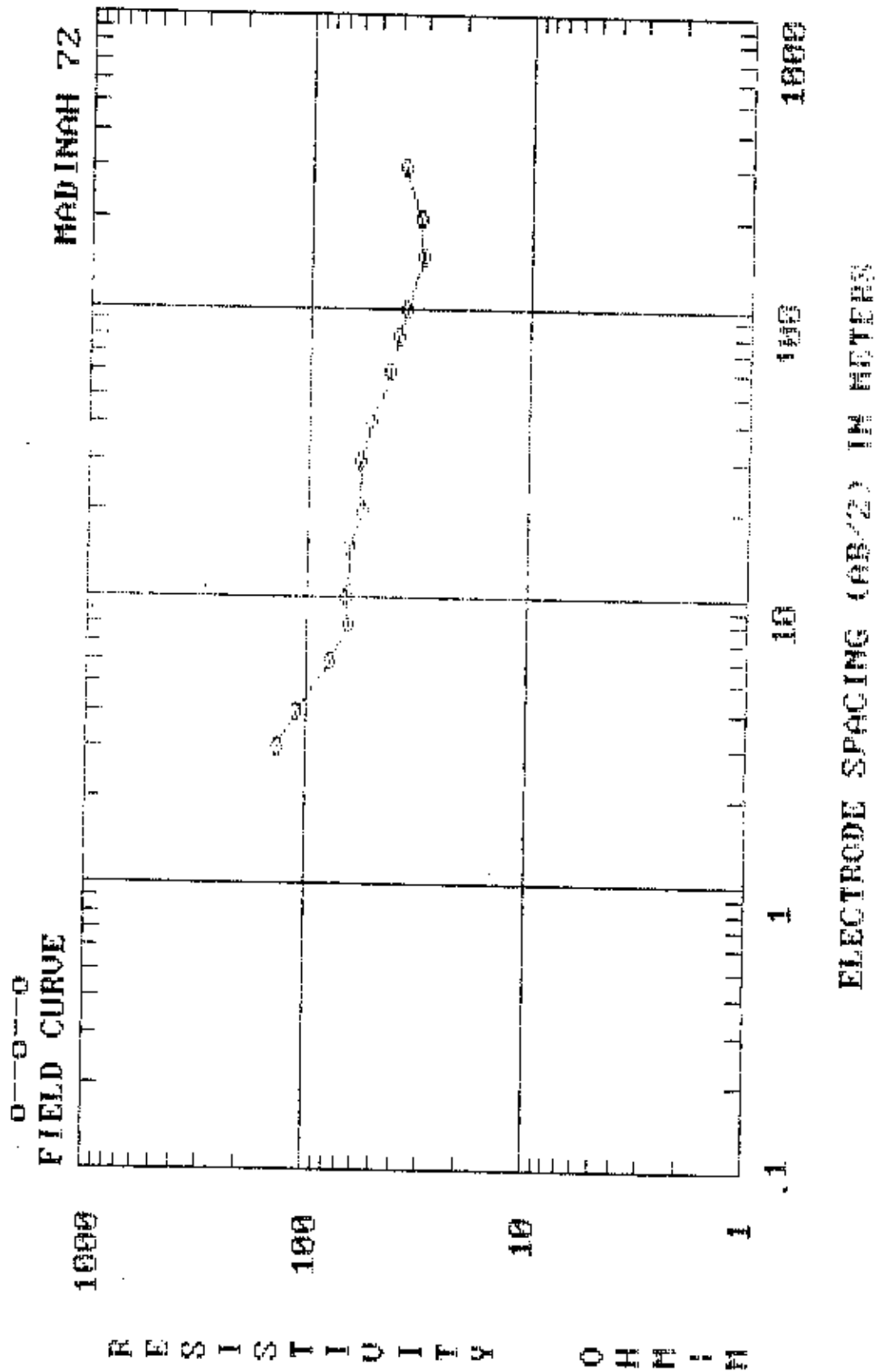


DEPTH	RESIS.	DEPTH	RESIS.
1.31	149.71	13.12	83.29
1.93	91.20	19.26	59.49
2.83	59.65	28.27	38.37
4.15	53.02	41.50	31.13
6.09	63.98	60.91	31.80
8.94	82.14	89.40	38.14
		99999.00	49.16



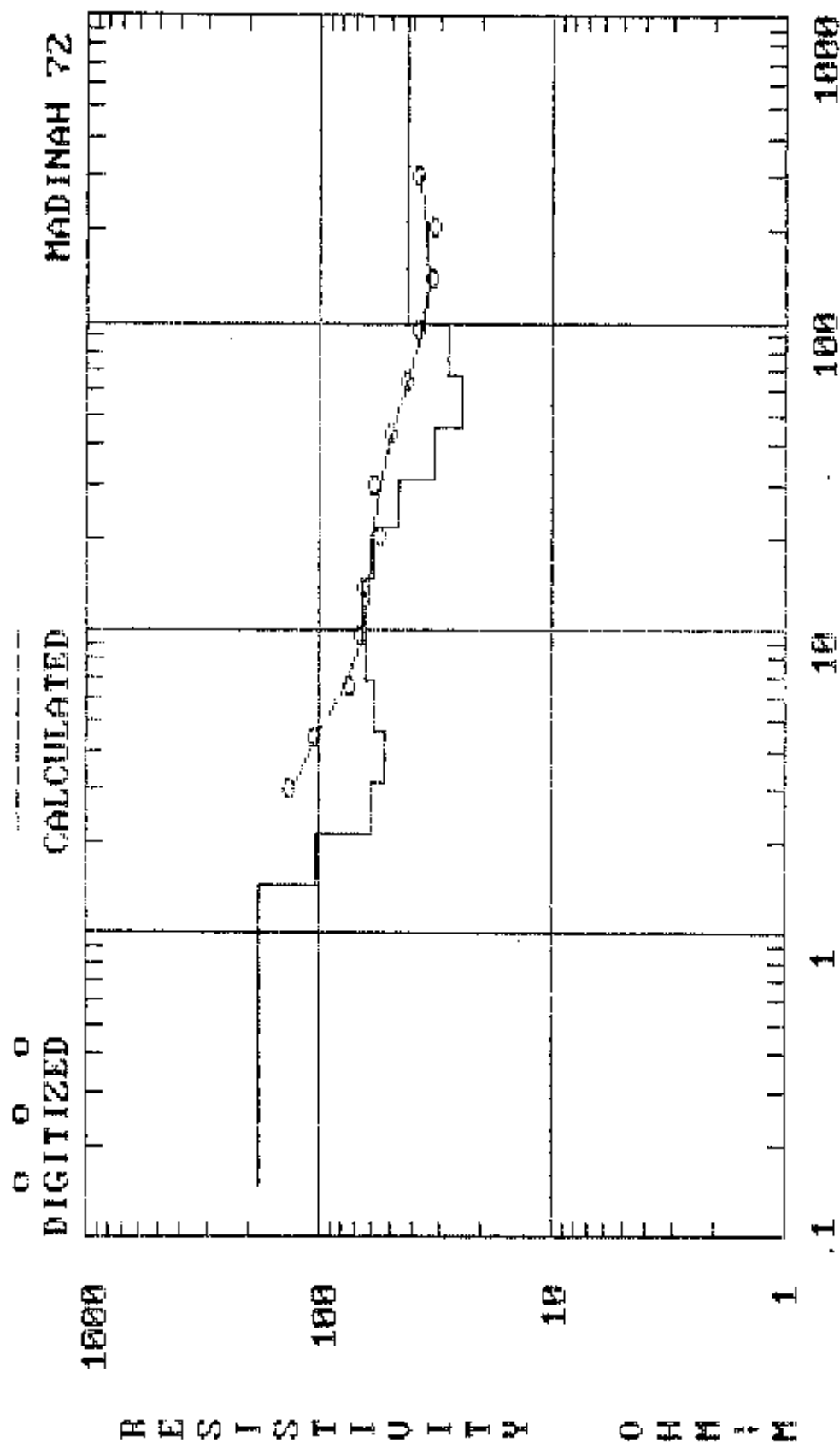
MADINAH 72 (FIELD DATA)

AB/2	App. Res.	AB/2	App. Res.
3.00	134.00	30.00	58.00
4.00	112.00	40.00	51.90
6.00	79.00	60.00	43.00
8.00	65.00	80.00	40.00
10.00	67.00	100.00	37.00
15.00	64.00	150.00	31.00
20.00	56.00	200.00	32.00
		300.00	38.00



MADINAH 72 (INTERPRETATION)

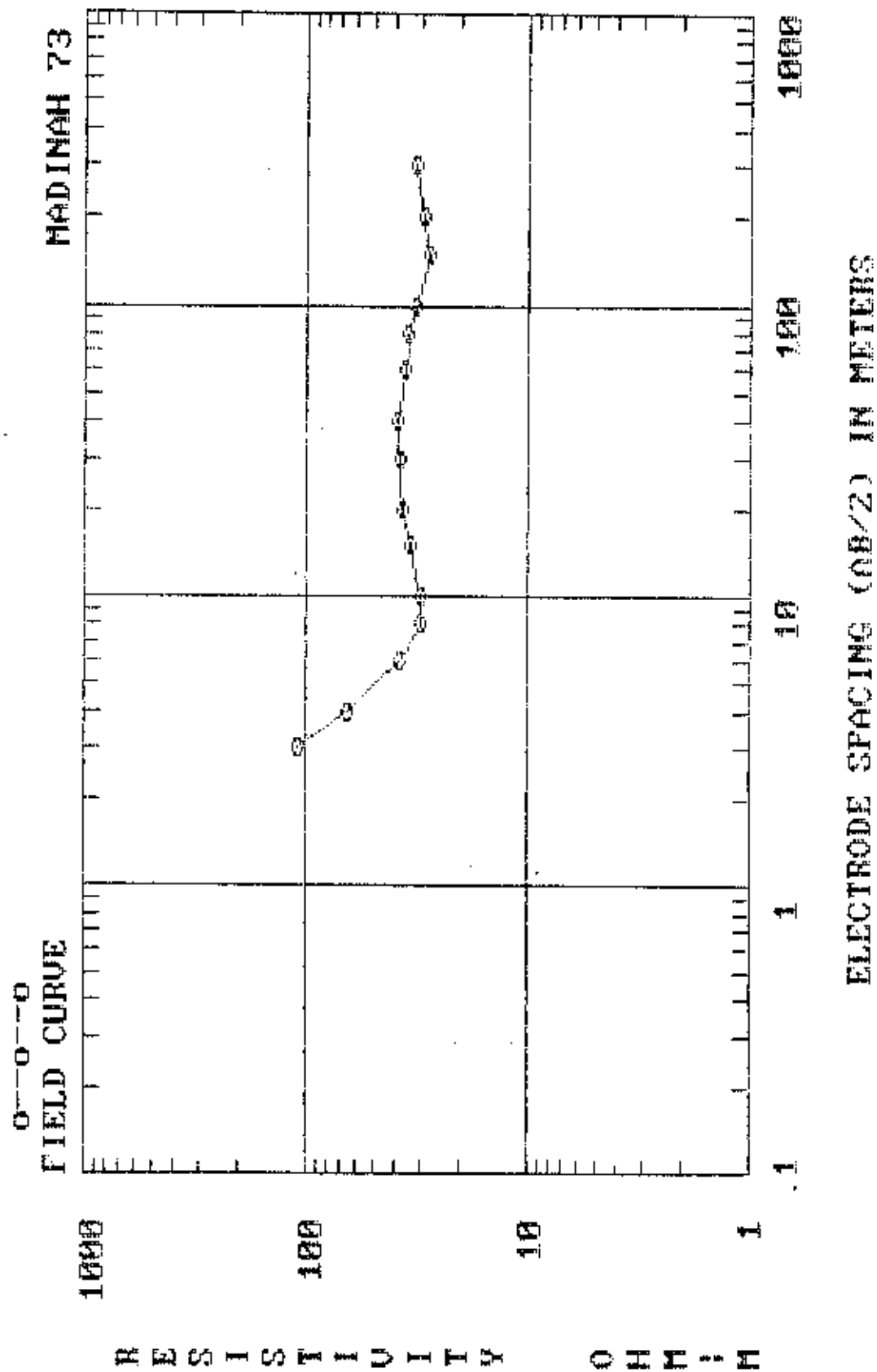
DEPTH	RESIS.	DEPTH	RESIS.
1.46	182.22	14.58	64.08
2.14	101.91	21.40	57.83
3.14	59.42	31.41	45.37
4.61	52.81	46.11	31.86
6.77	57.96	67.67	24.28
9.93	62.37	99.33	27.68
		99999.00	42.54



ELECTRODE SPACING (AB/2), OR DEPTH, IN METERS

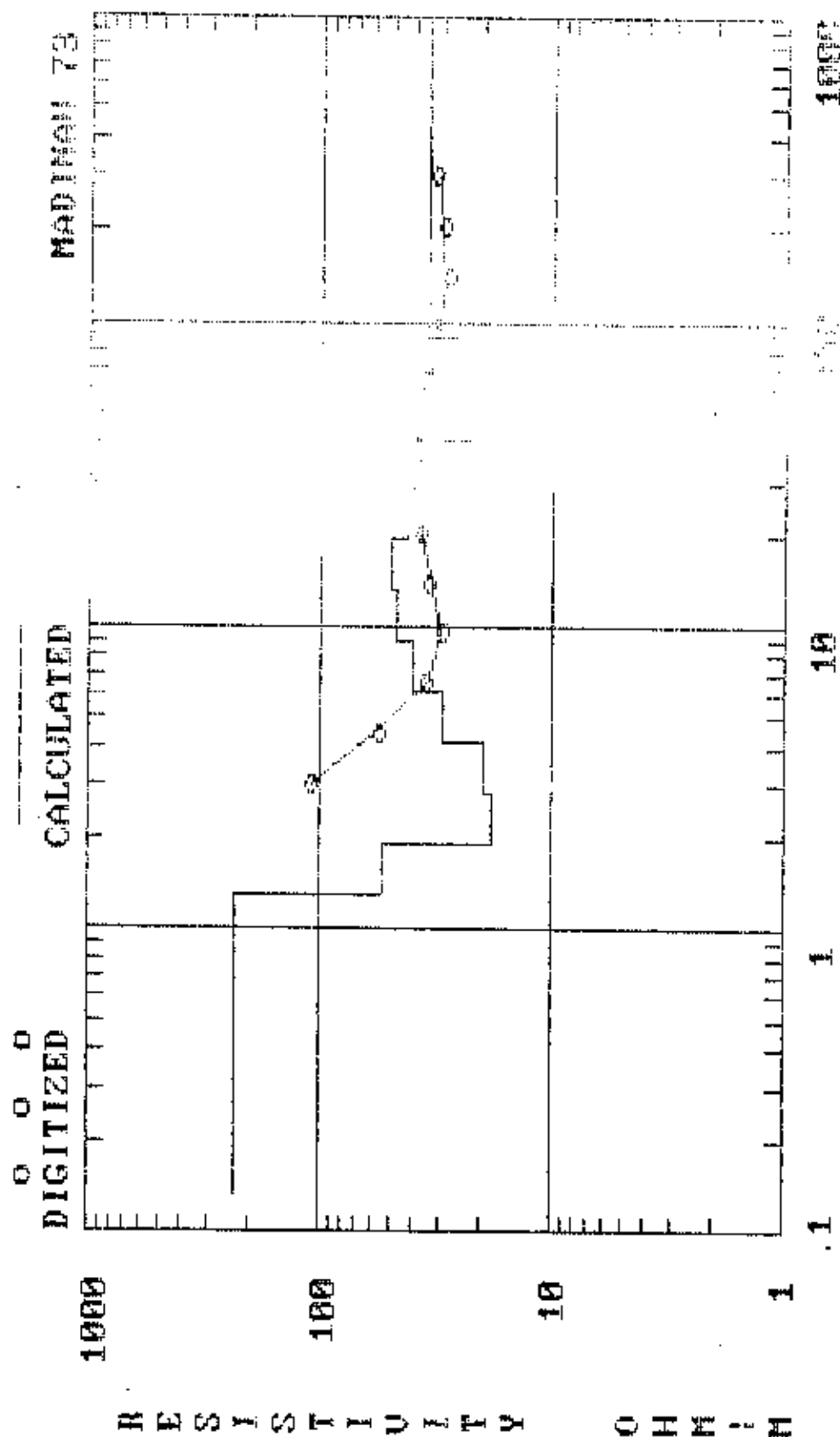
MADINAH 73 (FIELD DATA)

AB/2	App. Res.	AB/2	App. Res.
3.00	109.00	30.00	38.00
4.00	64.00	40.00	38.50
6.00	38.00	60.00	35.60
8.00	30.00	80.00	35.00
10.00	30.00	100.00	32.20
15.00	34.00	150.00	28.30
20.00	37.00	200.00	29.60
		300.00	32.00



MADINAH 73 (INTERPRETATION)

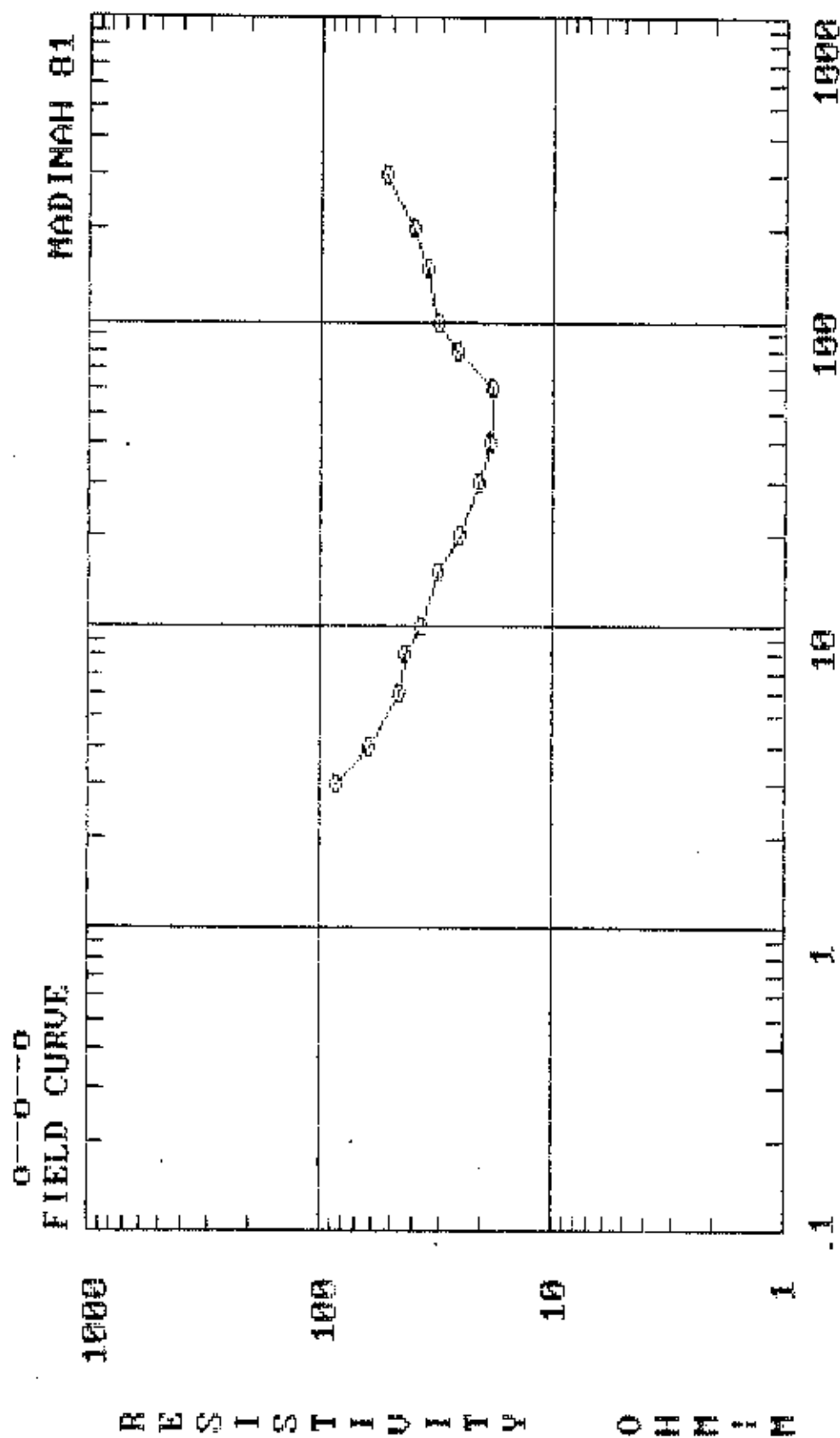
DEPTH	RESIS.	DEPTH	RESIS.
1.31	228.48	13.12	46.91
1.93	53.71	19.26	49.66
2.83	17.93	28.27	42.11
4.15	19.56	41.50	29.17
6.09	29.60	60.91	22.09
8.94	39.66	89.40	24.82
		99.99	34.65



ELECTRODE SPACING (AB/2), METERS

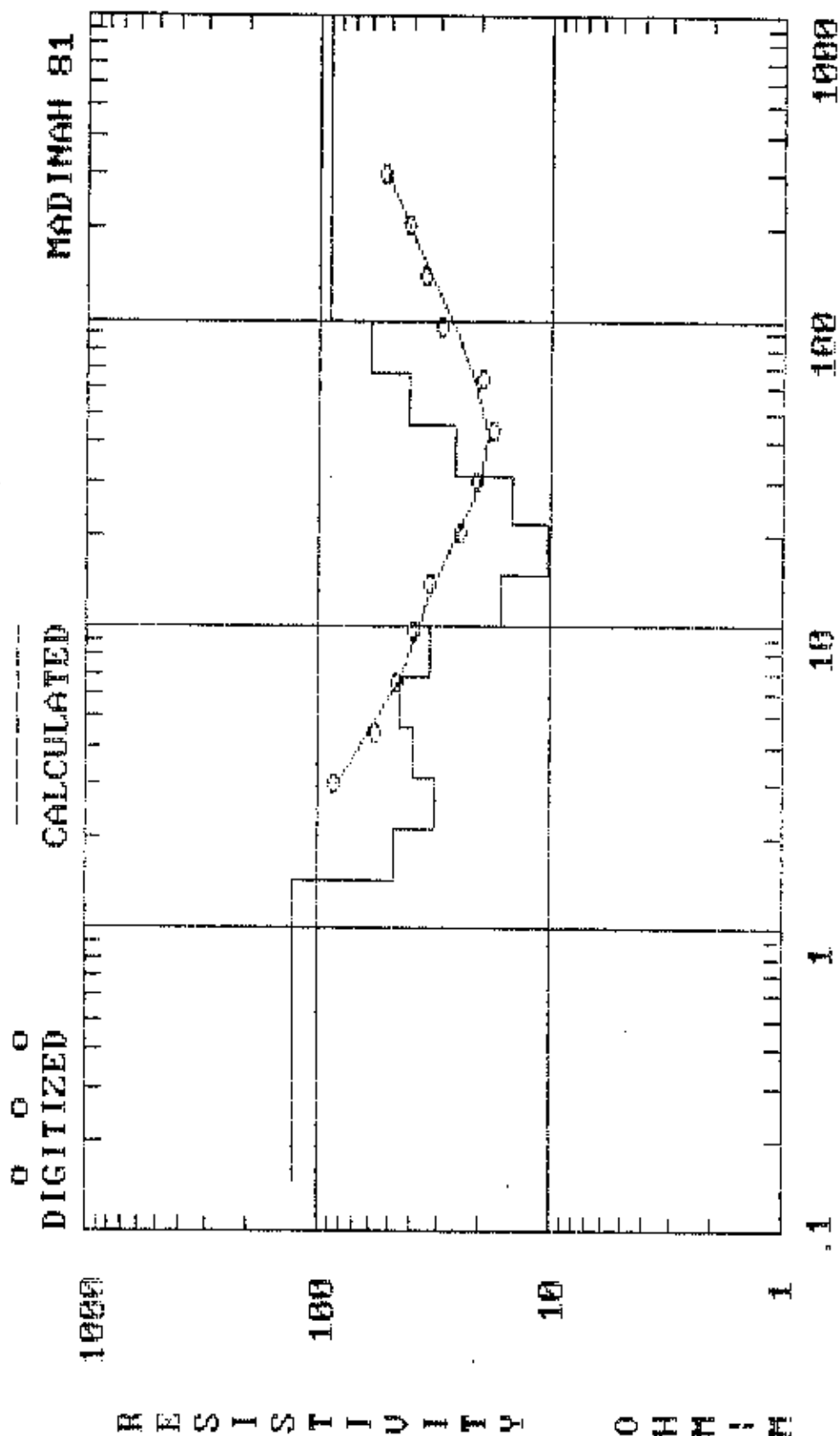
MADINAH 81 (FIELD DATA)

AB/2	App. Res.	AB/2	App. Res.
3.00	85.70	30.00	21.00
4.00	62.00	40.00	18.60
6.00	46.00	60.00	18.20
8.00	43.00	80.00	26.00
10.00	37.00	100.00	31.00
15.00	31.00	150.00	35.00
20.00	25.00	200.00	40.00
		300.00	52.00



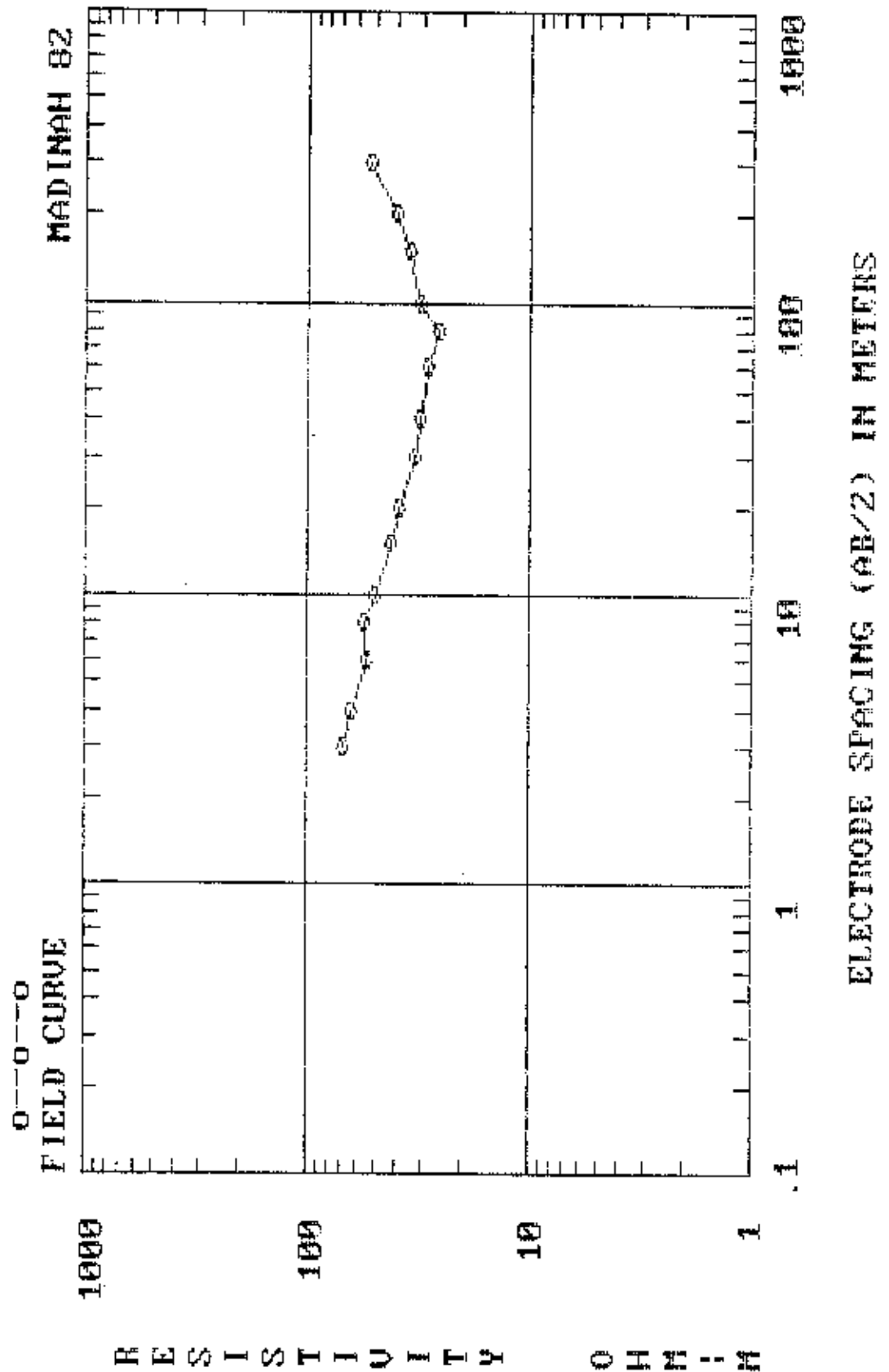
MADINAH 81 (INTERPRETATION)

DEPTH	RESIS.	DEPTH	RESIS.
1.46	125.90	14.58	16.31
2.14	46.95	21.40	10.17
3.14	31.22	31.41	14.42
4.61	39.12	46.11	26.12
6.77	44.08	67.67	40.54
9.93	32.49	99.33	59.13
		99999.00	89.07



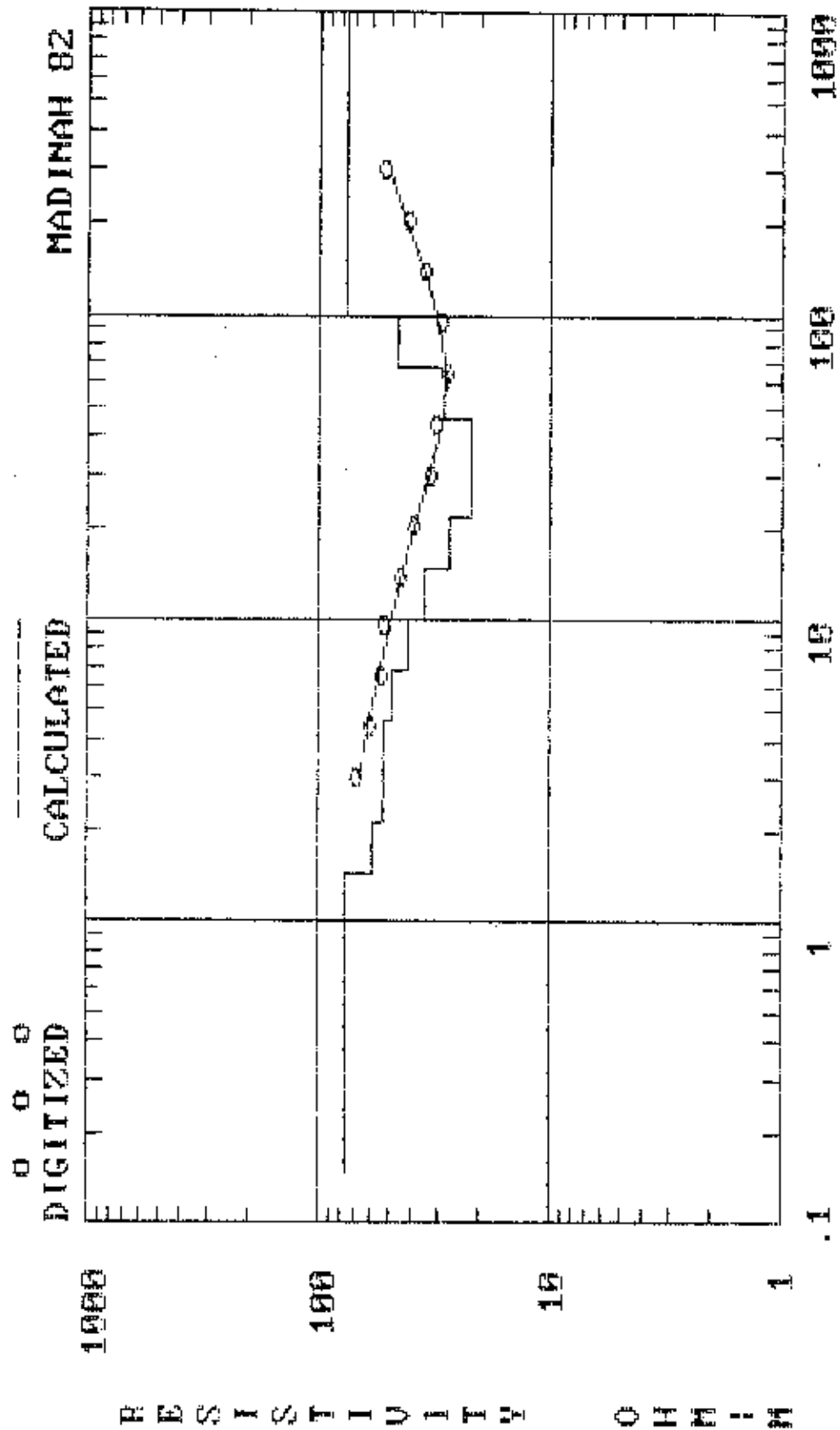
MADINAH 82 (FIELD DATA)

AB/2	App. Res.	AB/2	App. Res.
3.00	68.00	30.00	33.00
4.00	63.00	40.00	31.00
6.00	53.00	60.00	29.00
8.00	55.00	80.00	26.00
10.00	50.00	100.00	31.00
15.00	42.00	150.00	35.00
20.00	39.00	200.00	40.00
		300.00	52.00



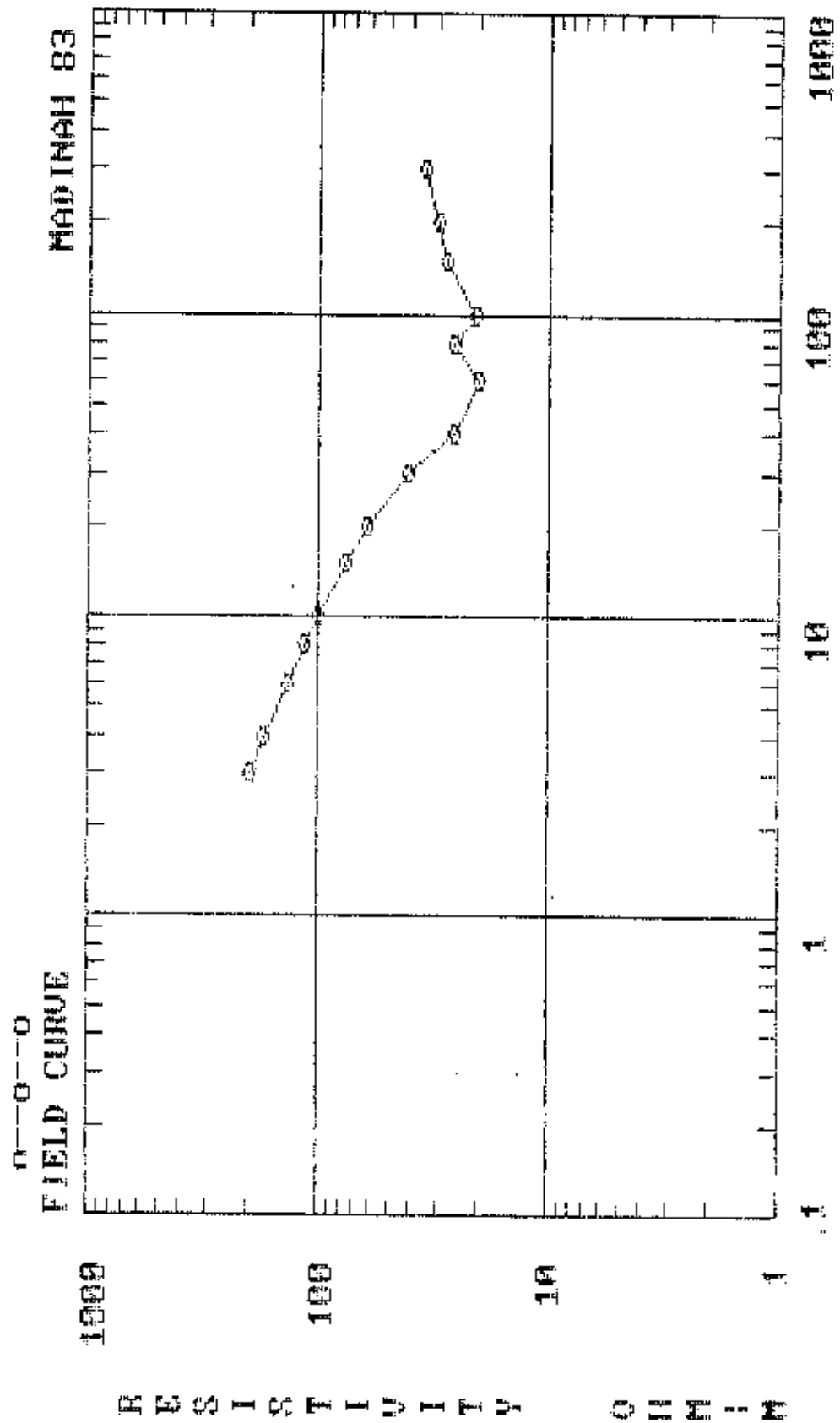
MADINAH 82 (INTERPRETATION)

DEPTH	RESIS.	DEPTH	RESIS.
1.46	76.35	14.58	34.36
2.14	58.11	21.40	27.21
3.14	51.67	31.41	21.69
4.61	51.55	46.11	21.96
6.77	47.96	67.67	29.11
9.93	41.00	99.33	45.68
		99999.00	76.88



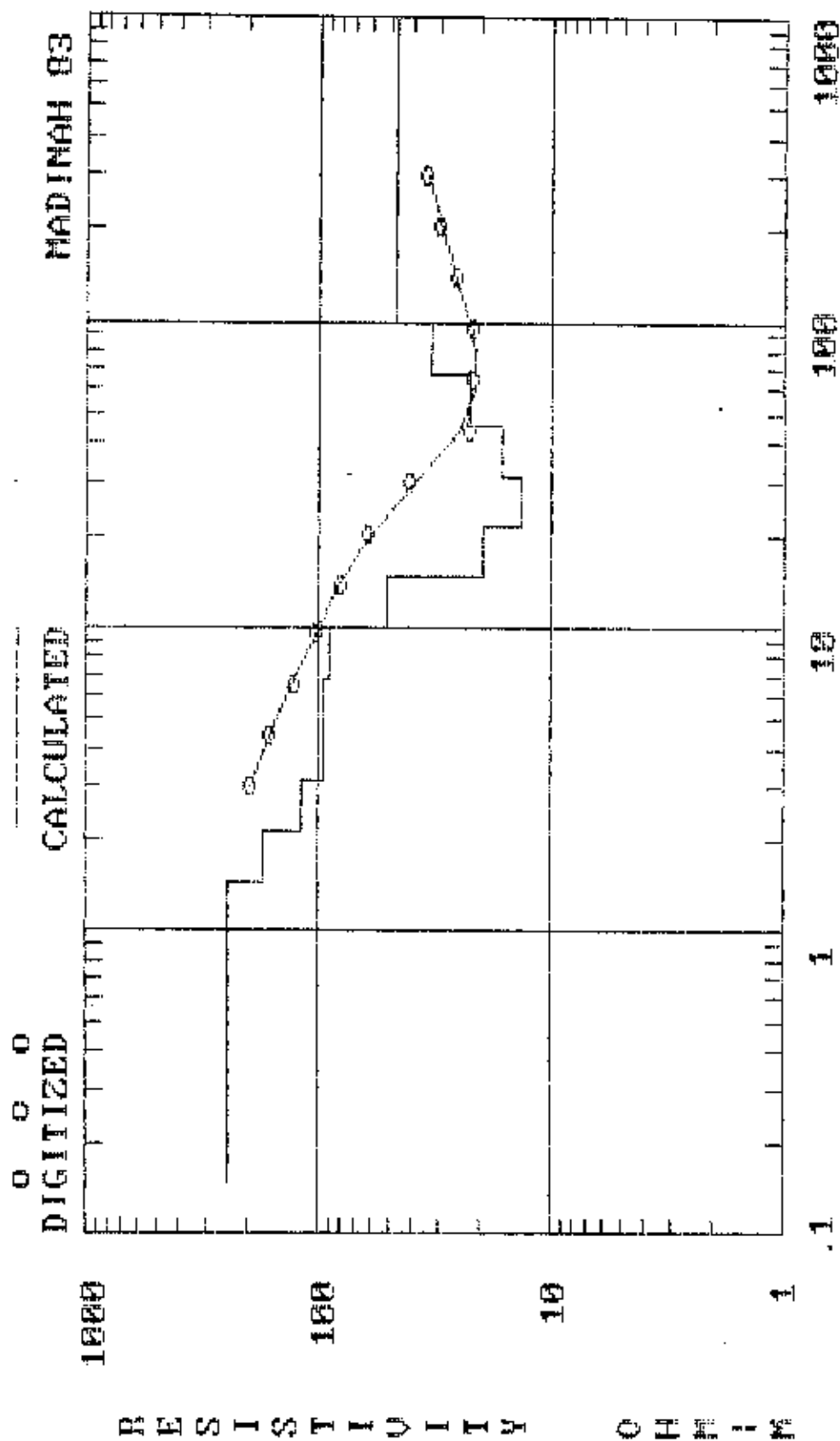
MADINAH B3 (FIELD DATA)

AB/2	App. Res.	AB/2	App. Res.
3.00	198.00	30.00	41.00
4.00	172.00	40.00	26.00
6.00	135.00	60.00	20.00
8.00	113.00	80.00	26.00
10.00	100.00	100.00	21.00
15.00	77.00	150.00	28.00
20.00	62.00	200.00	30.00
		300.00	35.00



MADINAH 83 (INTERPRETATION)

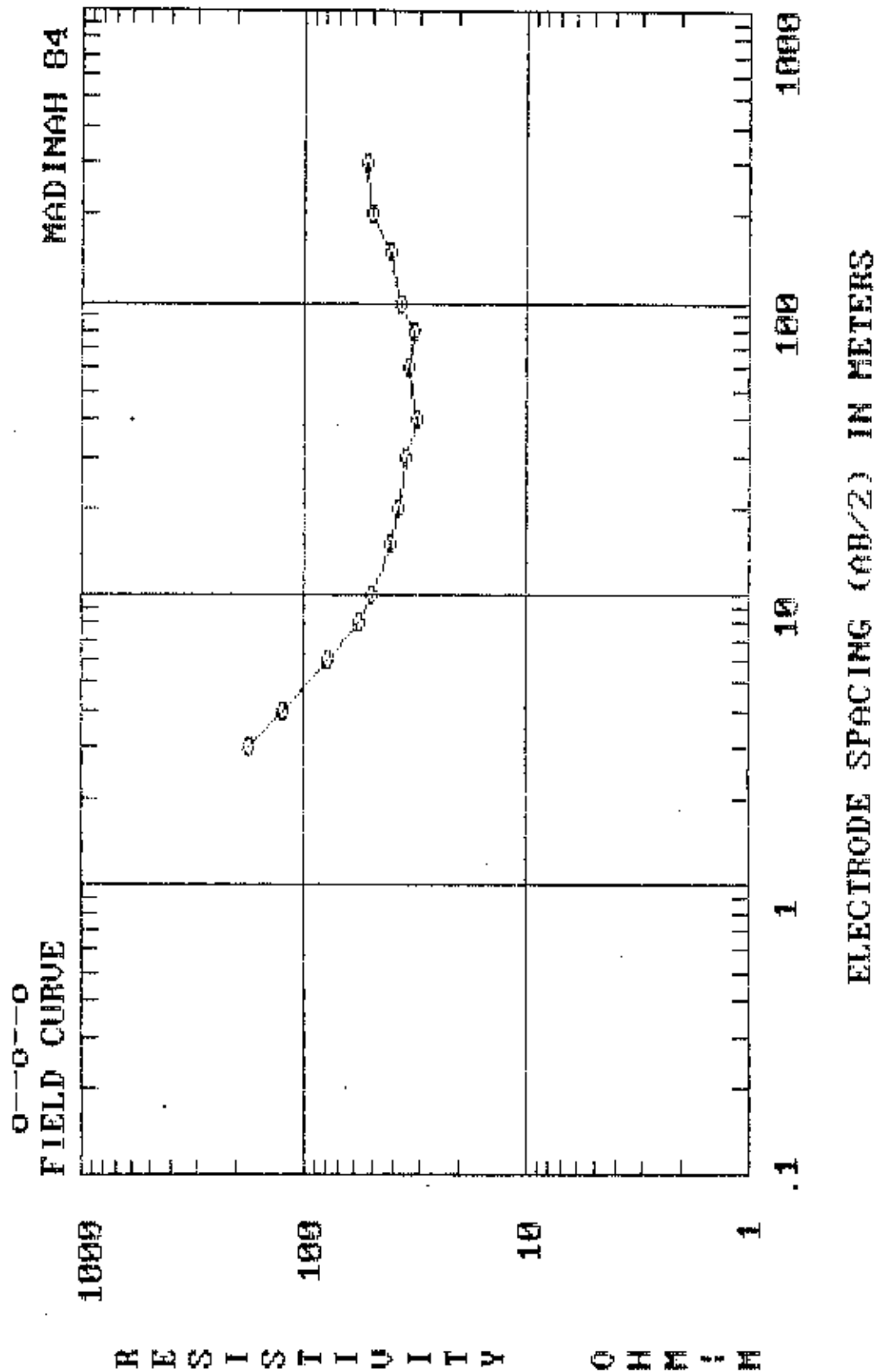
DEPTH	RESIS.	DEPTH	RESIS.
1.46	244.27	14.58	50.20
2.14	172.05	21.40	19.50
3.14	117.98	31.41	13.32
4.61	95.46	46.11	16.31
6.77	95.42	67.67	22.82
9.93	88.76	99.33	32.77
		99999.00	46.35



ELECTRODE SPACING (AB/2), OR DEPTH, IN METERS

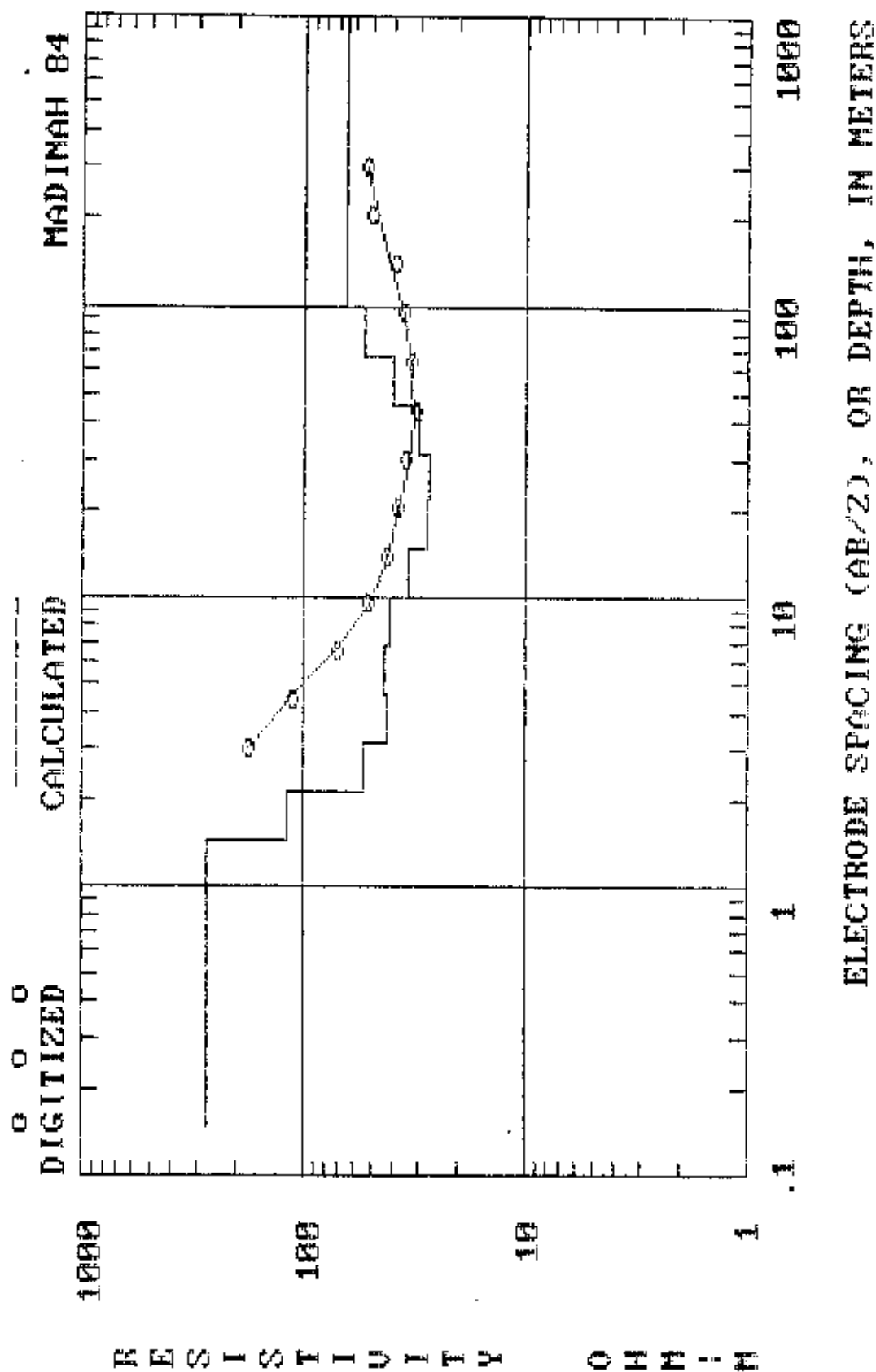
MADINAH 84 (FIELD DATA)

AB/2	App. Res.	AB/2	App. Res.
3.00	179.00	30.00	35.00
4.00	124.00	40.00	31.00
6.00	78.00	60.00	34.00
8.00	56.00	80.00	32.00
10.00	50.00	100.00	37.00
15.00	41.00	150.00	41.00
20.00	38.00	200.00	49.00
		300.00	52.00



MADINAH 84 (INTERPRETATION)

DEPTH	RESIS.	DEPTH	RESIS.
1.46	274.03	14.58	33.51
2.14	117.46	21.40	27.90
3.14	54.28	31.41	26.92
4.61	41.78	46.11	30.53
6.77	42.68	67.67	39.81
9.93	40.56	99.33	53.01
		99999.00	64.86



APPENDIX 5 B

**Magnetic field data (M3 - M7) collected in Wadi Malal
using Envi-Mag instrument. Data were corrected for
solar diurnal variations**

3	2200	41290.2	0.23	12.442222	0
3	2200	41294.4	0.19	12.447500	0
3	2200	41298.4	0.18	12.453056	0
3	2200	41298.4	0.18	12.453056	0
3	2200	41297.0	0.43	12.458056	0
3	2200	41301.0	0.28	12.462778	0
3	2200	41301.6	0.18	12.470556	0
3	2200	41298.7	0.23	12.476389	0
3	2200	41306.4	0.21	12.481667	0
3	2200	41309.4	0.23	12.486667	0
3	2200	41309.7	0.19	12.491667	0
3	2200	41311.4	0.23	12.496389	0
3	2200	41311.0	0.24	12.501111	0
3	2200	41313.6	0.21	12.506111	0
3	2200	41313.9	0.24	12.511389	0
3	2200	41317.4	0.18	12.516944	0
3	2200	41319.6	0.20	12.521111	0
3	2200	41321.6	0.22	12.526389	0
3	2200	41322.7	0.17	12.531389	0
3	2200	41323.2	0.22	12.537778	0
3	2200	41325.0	0.21	12.543056	0
3	2200	41328.0	0.22	12.547500	0
3	2200	41331.6	0.21	12.552500	0
3	2200	41332.3	0.25	12.558611	0
3	2200	41333.2	0.19	12.564444	0

14:43:54 17560.7 7.21

14:44:02 16822.4 7.47

14:44:30 17057.7 7.17

14:44:57 20390.2 8.09

?? ?

3	2200	41087.2	0.14	11.891944	0
3	2200	41070.1	0.16	11.903611	0
3	2200	41111.2	0.15	11.911389	0
3	2200	41122.3	0.15	11.921667	0
3	2200	41136.9	0.17	11.971944	0
3	2200	41141.3	0.20	11.977778	0
3	2200	41143.0	0.19	11.982500	0
3	2200	41144.0	0.19	11.987500	0
3	2200	41146.3	0.17	12.005000	0
3	2200	41147.7	0.17	12.023889	0
3	2200	41150.4	0.18	12.036667	0
3	2200	41145.0	0.17	12.052500	0
3	2200	41148.9	0.17	12.059167	0
3	2200	41148.4	0.18	12.064722	0
3	2200	41148.7	0.18	12.069444	0
3	2200	41146.5	0.21	12.075833	0
3	2200	41148.8	0.21	12.080556	0
3	2200	41151.2	0.15	12.094444	0
3	2200	41142.1	0.19	12.103333	0
3	2200	41138.6	0.20	12.108889	0
3	2200	41142.9	0.22	12.113889	0
3	2200	41146.3	0.19	12.119167	0
3	2200	41149.4	0.17	12.124444	0
3	2200	41156.9	0.17	12.130000	0
3	2200	41157.5	0.22	12.135833	0
3	2200	41160.4	0.21	12.143889	0
3	2200	41160.0	0.19	12.155000	0
3	2200	41163.1	0.19	12.160278	0
3	2200	41168.0	0.17	12.170556	0
3	2200	41167.3	0.21	12.178056	0
3	2200	41172.3	0.24	12.182500	0
3	2200	41173.7	0.27	12.188889	0

3	2200	41178.9	0.26	12.194444	0
3	2200	41182.8	0.17	12.199167	0
3	2200	41185.7	0.23	12.204167	0
3	2200	41189.4	0.21	12.208611	0
3	2200	41191.8	0.19	12.214722	0
3	2200	41197.7	0.17	12.220000	0
3	2200	41200.0	0.21	12.225000	0
3	2200	41201.1	0.18	12.230833	0
3	2200	41203.5	0.19	12.235556	0
3	2200	41207.5	0.20	12.240833	0
3	2200	41213.1	0.18	12.246389	0
3	2200	41216.4	0.22	12.251667	0
3	2200	41219.5	0.20	12.256944	0
3	2200	41224.0	0.20	12.264167	0
3	2200	41225.6	0.21	12.270556	0
3	2200	41227.6	0.21	12.275833	0
3	2200	41232.7	0.21	12.280278	0
3	2200	41235.2	0.19	12.285833	0
3	2200	41240.8	0.21	12.290556	0
3	2200	41245.1	0.23	12.295278	0
3	2200	41249.6	0.21	12.300278	0
3	2200	41250.9	0.22	12.305556	0
3	2200	41249.1	0.18	12.311111	0
3	2200	41249.1	0.19	12.316111	0
3	2200	41254.8	0.19	12.322222	0
3	2200	41258.9	0.18	12.329444	0
3	2200	41260.7	0.26	12.334444	0
3	2200	41262.5	0.17	12.339722	0
3	2200	41263.7	0.25	12.344167	0
3	2200	41265.5	0.20	12.349722	0
3	2200	41270.4	0.22	12.354167	0
3	2200	41269.2	0.24	12.359167	0
3	2200	41269.2	0.20	12.364722	0
3	2200	41272.6	0.24	12.370556	0
3	2200	41272.3	0.18	12.376389	0
3	2200	41274.6	0.19	12.380833	0
3	2200	41274.4	0.21	12.385000	0
3	2200	41277.0	0.21	12.390556	0
3	2200	41281.7	0.20	12.396667	0
3	2200	41281.8	0.20	12.401667	0
3	2200	41284.0	0.21	12.406667	0
3	2200	41287.0	0.18	12.411667	0
3	2200	41287.2	0.23	12.416944	0
3	2200	41287.7	0.22	12.421111	0
3	2200	41285.1	0.19	12.425833	0
3	2200	41288.7	0.23	12.431111	0
3	2200	41289.8	0.20	12.436389	0
3	2200	41290.2	0.23	12.442222	0
3	2200	41294.4	0.19	12.447500	0
3	2200	41298.4	0.18	12.453056	0
3	2200	41297.0	0.43	12.458056	0
3	2200	41301.0	0.28	12.462778	0
3	2200	41301.6	0.18	12.470556	0
3	2200	41298.7	0.23	12.476389	0
3	2200	41306.4	0.21	12.481667	0
3	2200	41309.4	0.23	12.486667	0
3	2200	41309.7	0.19	12.491667	0
3	2200	41311.4	0.23	12.496389	0
3	2200	41311.0	0.24	12.501111	0
3	2200	41313.6	0.21	12.506111	0
3	2200	41313.9	0.24	12.511389	0
3	2200	41317.4	0.18	12.516944	0
3	2200	41319.6	0.20	12.521111	0
3	2200	41321.6	0.22	12.526389	0

3	2200	41322.7	0.17	12.531389	0
3	2200	41323.2	0.22	12.537778	0
3	2200	41325.0	0.21	12.543056	0
3	2200	41328.0	0.22	12.547500	0
3	2200	41331.6	0.21	12.552500	0
3	2200	41332.3	0.25	12.558611	0
3	2200	41333.2	0.19	12.564444	0
3	2200	41337.4	0.21	12.569722	0
3	2200	41339.6	0.22	12.576389	0
3	2200	41339.0	0.18	12.581667	0
3	2200	41337.2	0.22	12.586667	0
3	2200	41336.8	0.22	12.591389	0
3	2200	41338.9	0.20	12.595556	0
3	2200	41338.5	0.22	12.600278	0
3	2200	41341.0	0.26	12.605000	0
3	2200	41341.7	0.25	12.610278	0
3	2200	41343.9	0.22	12.615278	0
3	2200	41341.7	0.24	12.620278	0
3	2200	41339.5	0.21	12.625556	0
3	2200	41341.2	0.20	12.631111	0
3	2200	41341.4	0.21	12.636944	0
3	2200	41341.7	0.20	12.642778	0
3	2200	41341.7	0.23	12.648333	0
3	2200	41340.8	0.18	12.654444	0
3	2200	41342.1	0.18	12.660000	0
3	2200	41340.1	0.19	12.665833	0
3	2200	41340.1	0.19	12.671111	0
3	2200	41339.2	0.22	12.676111	0
3	2200	41342.0	0.18	12.698056	0
3	2200	41339.2	0.18	12.709444	0
3	2200	41338.6	0.19	12.714722	0
3	2200	41339.8	0.21	12.720278	0
3	2200	41337.3	0.21	12.725556	0
3	2200	41337.5	0.19	12.731111	0
3	2200	41343.8	0.20	12.736111	0
3	2200	41345.4	0.20	12.742500	0
3	2200	41349.1	0.18	12.749167	0
3	2200	41348.9	0.18	12.755833	0
3	2200	41350.2	0.25	12.760833	0
3	2200	41347.6	0.18	12.765833	0
3	2200	41349.9	0.18	12.770556	0
3	2200	41348.5	0.19	12.776111	0
3	2200	41349.7	0.20	12.781111	0
3	2200	41353.5	0.18	12.786667	0
3	2200	41352.3	0.21	12.792500	0
3	2200	41353.2	0.22	12.798333	0
3	2200	41353.1	0.19	12.811111	0
3	2200	41356.7	0.20	12.819444	0
3	2200	41358.2	0.20	12.828611	0
3	2200	41359.9	0.24	12.833889	0
3	2200	41361.2	0.19	12.839722	0
3	2200	41362.8	0.25	12.845278	0
3	2200	41364.4	0.18	12.850833	0
3	2200	41368.0	0.19	12.856389	0
3	2200	41368.7	0.18	12.861667	0
3	2200	41370.9	0.18	12.875833	0
3	2200	41371.3	0.19	12.884444	0
3	2200	41371.2	0.20	12.892778	0
3	2200	41372.0	0.20	12.897500	0
3	2200	41377.8	0.20	12.901944	0
3	2200	41379.6	0.19	12.906944	0
3	2200	41377.6	0.21	12.913056	0
3	2200	41380.3	0.20	12.918056	0
3	2200	41380.4	0.17	12.923333	0

3	2200	41382.8	0.19	12.928333	0
3	2200	41380.9	0.25	12.933056	0
3	2200	41381.4	0.21	12.938889	0
3	2200	41377.1	0.23	12.944722	0
3	2200	41380.4	0.19	12.950278	0
3	2200	41378.8	0.21	12.957222	0
3	2200	41379.0	0.17	12.968333	0
3	2200	41380.0	0.20	12.973611	0
3	2200	41380.5	0.19	12.979722	0
3	2200	41382.5	0.21	12.987222	0
3	2200	41382.9	0.19	12.993056	0
3	2200	41382.4	0.19	12.998056	0
3	2200	41380.8	0.18	13.002778	0
3	2200	41380.6	0.20	13.008056	0
3	2200	41382.1	0.20	13.012778	0
3	2200	41381.8	0.19	13.017778	0
3	2200	41381.3	0.20	13.022500	0
3	2200	41382.9	0.17	13.027222	0
3	2200	41383.9	0.21	13.032500	0
3	2200	41383.9	0.18	13.042778	0
3	2200	41383.4	0.22	13.048889	0
3	2200	41382.5	0.22	13.053611	0
3	2200	41383.9	0.22	13.058611	0
3	2200	41384.1	0.18	13.064444	0
3	2200	41382.4	0.19	13.069722	0
3	2200	41380.9	0.17	13.074167	0
3	2200	41383.4	0.20	13.079444	0
3	2200	41386.0	0.18	13.085556	0
3	2200	41388.0	0.17	13.090833	0
3	2200	41389.0	0.19	13.096944	0
3	2200	41384.4	0.16	13.125278	0
3	2200	41383.4	0.19	13.137778	0
3	2200	41381.7	0.17	13.143611	0
3	2200	41386.6	0.19	13.149444	0
3	2200	41381.4	0.20	13.156389	0
3	2200	41381.6	0.21	13.161111	0
3	2200	41380.9	0.19	13.165833	0
3	2200	41383.1	0.18	13.171667	0
3	2200	41381.7	0.19	13.177778	0
3	2200	41383.0	0.19	13.184444	0
3	2200	41381.2	0.19	13.194722	0
3	2200	41381.2	0.22	13.200000	0
3	2200	41382.5	0.22	13.208333	0
3	2200	41385.8	0.18	13.213056	0
3	2200	41384.1	0.17	13.220556	0
3	2200	41380.3	0.17	13.225833	0
3	2200	41381.1	0.17	13.231111	0
3	2200	41380.1	0.19	13.235833	0
3	2200	41381.2	0.18	13.240833	0
3	2200	41381.9	0.20	13.245833	0
3	2200	41379.8	0.19	13.250833	0
3	2200	41377.7	0.18	13.255556	0
3	2200	41377.8	0.18	13.261111	0
3	2200	41380.2	0.21	13.265833	0
3	2200	41380.0	0.18	13.270833	0
3	2200	41381.7	0.18	13.275556	0
3	2200	41378.9	0.18	13.280000	0
3	2200	41378.3	0.17	13.285000	0
3	2200	41378.3	0.17	13.289444	0
3	2200	41377.6	0.20	13.294444	0
3	2200	41374.5	0.19	13.300278	0
3	2200	41371.4	0.20	13.305278	0
3	2200	41371.5	0.19	13.310278	0
3	2200	41370.3	0.19	13.315278	0

3	2200	41370.0	0.19	13.320556	0
3	2200	41368.6	0.18	13.325278	0
3	2200	41366.8	0.18	13.330000	0
3	2200	41364.7	0.19	13.335278	0
3	2200	41365.0	0.17	13.348056	0
3	2200	41369.5	0.18	13.354444	0
3	2200	41368.4	0.19	13.361389	0
3	2200	41372.1	0.18	13.366111	0
3	2200	41371.3	0.18	13.370833	0
3	2200	41370.0	0.20	13.375278	0
3	2200	41372.0	0.19	13.380833	0
3	2200	41374.3	0.16	13.385000	0
3	2200	41375.4	0.18	13.389722	0
3	2200	41378.7	0.18	13.394167	0
3	2200	41377.1	0.17	13.398889	0
3	2200	41375.8	0.16	13.403333	0
3	2200	41383.8	0.17	13.408056	0
3	2200	41382.4	0.17	13.415000	0
3	2200	41380.3	0.16	13.420000	0
3	2200	41381.3	0.18	13.425278	0
3	2200	41387.8	0.17	13.430000	0
3	2200	41377.5	0.18	13.447778	0
3	2200	41381.4	0.20	13.453611	0
3	2200	41381.1	0.18	13.458056	0
3	2200	41385.9	0.17	13.463056	0
3	2200	41380.0	0.19	13.467500	0
3	2200	41377.3	0.17	13.471667	0
3	2200	41378.8	0.17	13.476944	0
3	2200	41374.5	0.17	13.481667	0
3	2200	41369.7	0.19	13.487778	0
3	2200	41369.2	0.19	13.493611	0
3	2200	41370.2	0.18	13.498611	0
3	2200	41368.1	0.17	13.504722	0
3	2200	41364.6	0.19	13.509722	0
3	2200	41364.7	0.17	13.515000	0
3	2200	41361.9	0.18	13.519722	0
3	2200	41362.5	0.17	13.525000	0
3	2200	41361.7	0.17	13.529722	0
3	2200	41359.6	0.16	13.535000	0
3	2200	41360.2	0.19	13.540278	0
3	2200	41358.8	0.17	13.545000	0
3	2200	41356.3	0.17	13.550833	0
3	2200	41354.9	0.17	13.555278	0
3	2200	41354.6	0.17	13.560278	0
3	2200	41352.3	0.18	13.565000	0
3	2200	41352.1	0.17	13.569722	0
3	2200	41354.2	0.17	13.573889	0
3	2200	41350.8	0.17	13.578333	0
3	2200	41348.0	0.17	13.582778	0
3	2200	41347.1	0.19	13.586944	0
3	2200	41345.0	0.17	13.591667	0
3	2200	41345.1	0.18	13.623889	0
3	2200	41345.4	0.18	13.629444	0
3	2200	41346.6	0.16	13.634167	0
3	2200	41347.7	0.20	13.639167	0
3	2200	41344.6	0.18	13.643889	0
3	2200	41342.8	0.18	13.648889	0
3	2200	41345.0	0.19	13.653333	0
3	2200	41345.5	0.16	13.657500	0
3	2200	41346.1	0.16	13.662222	0
3	2200	41347.0	0.17	13.666389	0
3	2200	41349.1	0.16	13.670833	0
3	2200	41349.0	0.17	13.676944	0
3	2200	41352.9	0.18	13.681389	0

3	2200	41358.4	0.20	13.685833	0
3	2200	41361.7	0.21	13.690278	0
3	2200	41363.9	0.17	13.698889	0
3	2200	41358.5	0.21	13.703611	0
3	2200	41350.0	0.20	13.708889	0
3	2200	41348.0	0.18	13.713056	0
3	2200	41344.2	0.17	13.717778	0
3	2200	41342.8	0.18	13.721944	0
3	2200	41343.5	0.20	13.726667	0
3	2200	41347.3	0.18	13.731389	0
3	2200	41342.5	0.19	13.735833	0
3	2200	41341.1	0.20	13.740556	0
3	2200	41343.6	0.18	13.745278	0
3	2200	41343.8	0.18	13.750278	0
3	2200	41346.8	0.18	13.754722	0
3	2200	41343.9	0.18	13.760000	0
3	2200	41345.0	0.20	13.764722	0
3	2200	41348.3	0.17	13.768889	0
3	2200	41347.5	0.16	13.774167	0
3	2200	41349.1	0.17	13.779167	0
3	2200	41348.2	0.18	13.784167	0
3	2200	41348.5	0.18	13.788889	0
3	2200	41351.0	0.20	13.793611	0
3	2200	41348.9	0.18	13.798056	0
3	2200	41347.9	0.17	13.803056	0
3	2200	41350.6	0.18	13.807778	0
3	2200	41351.8	0.19	13.812500	0
3	2200	41350.1	0.19	13.817222	0
3	2200	41354.3	0.18	13.821667	0
3	2200	41354.5	0.17	13.826111	0
3	2200	41352.5	0.17	13.830556	0
3	2200	41353.9	0.17	13.835278	0
3	2200	41351.6	0.17	13.840000	0
3	2200	41354.6	0.17	13.844722	0
3	2200	41353.8	0.18	13.849444	0
3	2200	41352.9	0.19	13.853611	0
3	2200	41356.9	0.19	13.858056	0
3	2200	41358.4	0.19	13.862500	0
3	2200	41355.4	0.17	13.867778	0
3	2200	41357.2	0.17	13.872500	0
3	2200	41356.0	0.17	13.878056	0
3	2200	41355.5	0.17	13.887500	0
3	2200	41360.1	0.18	13.896111	0
3	2200	41359.9	0.16	13.902500	0
3	2200	41358.8	0.18	13.908056	0
3	2200	41358.9	0.19	13.913333	0
3	2200	41358.2	0.17	13.917778	0
3	2200	41357.6	0.20	13.922500	0
3	2200	41357.5	0.21	13.927500	0
3	2200	41358.9	0.19	13.931667	0
3	2200	41359.8	0.23	13.936667	0
3	2200	41362.9	0.18	13.941667	0
3	2200	41362.7	0.18	13.945833	0
3	2200	41362.6	0.18	13.950833	0
3	2200	41361.3	0.19	13.955833	0
3	2200	41361.3	0.18	13.960556	0
3	2200	41364.4	0.19	13.965000	0
3	2200	41364.2	0.17	13.969722	0
3	2200	41365.2	0.17	13.973889	0
3	2200	41362.9	0.19	13.978889	0
3	2200	41363.6	0.18	13.983889	0
3	2200	41370.6	0.18	13.989167	0
3	2200	41370.2	0.17	13.993889	0
3	2200	41368.3	0.17	13.998611	0

3	2200	41367.3	0.19	14.003056	0
3	2200	41368.2	0.18	14.007500	0
3	2200	41367.8	0.19	14.011389	0
3	2200	41368.3	0.16	14.016111	0
3	2200	41366.8	0.18	14.020278	0
3	2200	41368.7	0.19	14.025000	0
3	2200	41369.1	0.17	14.030000	0
3	2200	41365.9	0.20	14.034444	0
3	2200	41366.8	0.19	14.040833	0
3	2200	41371.8	0.18	14.045000	0
3	2200	41369.3	0.18	14.049444	0
3	2200	41366.9	0.17	14.053611	0
3	2200	41364.8	0.18	14.058056	0
3	2200	41365.3	0.18	14.062500	0
3	2200	41366.2	0.19	14.067778	0
3	2200	41365.4	0.19	14.072222	0
3	2200	41366.1	0.17	14.077500	0
3	2200	41376.4	0.19	14.085556	0
3	2200	41370.9	0.17	14.092222	0
3	2200	41366.6	0.18	14.103333	0
3	2200	41370.7	0.17	14.108056	0
3	2200	41370.8	0.17	14.112778	0
3	2200	41377.3	0.18	14.117222	0
3	2200	41377.0	0.21	14.121944	0
3	2200	41379.3	0.17	14.128333	0
3	2200	41382.8	0.18	14.134167	0
3	2200	41380.4	0.17	14.138889	0
3	2200	41377.2	0.19	14.143611	0
3	2200	41378.4	0.18	14.148056	0
3	2200	41378.7	0.17	14.152222	0
3	2200	41377.9	0.17	14.157500	0
3	2200	41374.8	0.17	14.163333	0
3	2200	41375.1	0.18	14.168611	0
3	2200	41376.4	0.17	14.173056	0
3	2200	41374.5	0.17	14.177778	0
3	2200	41373.1	0.19	14.182778	0
3	2200	41369.8	0.19	14.188056	0
3	2200	41370.4	0.22	14.193333	0
3	2200	41369.4	0.18	14.198056	0
3	2200	41366.5	0.19	14.203333	0
3	2200	41365.0	0.24	14.207778	0
3	2200	41361.6	0.19	14.212500	0
3	2200	41357.6	0.22	14.216667	0
3	2200	41357.3	0.20	14.221667	0
3	2200	41353.3	0.21	14.226667	0
3	2200	41351.9	0.20	14.231667	0
3	2200	41350.0	0.19	14.236389	0
3	2200	41349.8	0.19	14.246944	0
3	2200	41346.4	0.19	14.251944	0
3	2200	41340.5	0.19	14.256944	0
3	2200	41334.4	0.18	14.267222	0
3	2200	41332.4	0.17	14.275833	0
3	2200	41335.5	0.20	14.284722	0
3	2200	41352.6	0.21	14.291667	0
3	2200	41349.5	0.19	14.299444	0
3	2200	41349.0	0.19	14.305278	0
3	2200	41341.0	0.18	14.309722	0
3	2200	41349.1	0.20	14.316667	0
5	1	41309.3	0.14	6.779722	0
5	1	41322.6	0.14	6.808889	0
5	1	41319.5	0.15	6.828333	0
5	1	41319.4	0.15	6.844167	0
5	1	41315.6	0.16	6.860278	0
5	1	41319.0	0.16	6.878056	0

5	1	41320.2	0.21	6.899722	0
5	1	41318.9	0.15	6.915833	0
5	1	41322.1	0.14	6.937222	0
5	1	41321.2	0.16	6.956944	0
5	1	41318.4	0.15	6.975000	0
5	1	41322.0	0.14	7.008611	0
5	1	41321.5	0.14	7.022500	0
5	1	41317.2	0.18	7.035000	0
5	1	41315.7	0.20	7.056944	0
5	1	41315.9	0.18	7.071944	0
5	1	41316.3	0.15	7.086111	0
5	1	41313.9	0.16	7.100278	0
5	1	41310.8	0.15	7.112778	0
5	1	41308.5	0.16	7.127778	0
5	1	41306.9	0.14	7.140833	0
5	1	41299.0	0.13	7.164444	0
5	1	41294.6	0.13	7.181944	0
5	1	41296.7	0.15	7.203889	0
5	1	41292.0	0.13	7.219444	0
5	1	41290.9	0.15	7.243611	0
5	1	41293.0	0.14	7.260556	0
5	1	41290.2	0.16	7.276111	0
5	1	41285.6	0.15	7.288333	0
5	1	41285.4	0.16	7.297778	0
5	1	41285.4	0.13	7.310278	0
5	1	41282.8	0.15	7.328611	0
5	1	41277.2	0.15	7.343333	0
5	1	41273.6	0.14	7.360556	0
5	1	41273.7	0.15	7.375556	0
5	1	41274.0	0.16	7.393889	0
5	1	41270.2	0.16	7.404722	0
5	1	41270.4	0.18	7.418056	0
5	1	41268.8	0.16	7.433889	0
5	1	41267.8	0.14	7.446111	0
5	1	41267.8	0.18	7.457222	0
5	1	41265.4	0.15	7.471389	0
5	1	41264.7	0.16	7.485833	0
5	1	41263.9	0.18	7.501111	0
5	1	41262.3	0.16	7.516111	0
5	1	41262.3	0.17	7.528611	0
5	1	41259.4	0.17	7.539167	0
5	1	41259.4	0.17	7.569722	0
5	1	41256.5	0.19	7.583611	0
5	1	41255.1	0.16	7.611111	0
5	1	41253.8	0.16	7.623333	0
5	1	41248.1	0.15	7.633889	0
5	1	41238.4	0.19	7.643611	0
5	1	41242.5	0.18	7.660833	0
5	1	41237.1	0.17	7.677500	0
5	1	41229.7	0.15	7.691111	0
5	1	41228.6	0.17	7.705000	0
5	1	41226.0	0.21	7.720000	0
5	1	41223.9	0.15	7.730833	0
5	1	41218.3	0.16	7.744167	0
5	1	41213.0	0.16	7.758056	0
5	1	41210.7	0.15	7.768056	0
5	1	41205.7	0.19	7.785000	0
5	1	41196.2	0.18	7.806667	0
5	1	41190.8	0.17	7.821111	0
5	1	41184.7	0.24	7.834722	0
5	1	41176.4	0.17	7.846111	0
5	1	41170.6	0.20	7.857778	0
5	1	41166.3	0.21	7.873889	0
5	1	41161.8	0.15	7.898333	0

5	1	41159.6	0.16	7.913333	0
5	1	41155.8	0.15	7.936389	0
5	1	41153.5	0.19	7.952778	0
5	1	41154.2	0.19	7.965000	0
5	1	41155.0	0.16	7.978056	0
5	1	41159.7	0.16	7.992500	0
5	1	41160.4	0.17	8.010556	0
5	1	41169.8	0.16	8.022778	0
5	1	41173.6	0.21	8.038889	0
5	1	41184.4	0.21	8.050000	0
5	1	41195.9	0.18	8.066111	0
5	1	41204.6	0.16	8.078333	0
5	1	41212.4	0.18	8.088889	0
5	1	41220.6	0.17	8.099722	0
5	1	41243.5	0.16	8.110278	0
5	1	41285.2	0.16	8.136667	0
5	1	41340.5	0.18	8.150556	0
5	1	41330.9	0.22	8.160556	0
5	1	41359.8	0.18	8.171111	0
5	1	41408.8	0.15	8.184722	0
5	1	41398.2	0.21	8.197778	0
5	1	41377.0	0.19	8.208333	0
5	1	41313.4	0.20	8.233056	0
5	1	41549.0	0.24	8.247778	0
6	1	41178.8	0.22	9.443611	0
6	1	41140.0	0.23	9.460833	0
6	1	41109.5	0.27	9.472222	0
6	1	41057.6	0.33	9.481111	0
6	1	41093.7	0.33	9.490556	0
6	1	41193.6	0.16	9.518889	0
6	1	41142.5	0.17	9.530833	0
6	1	41128.0	0.16	9.536667	0
6	1	41118.6	0.17	9.543056	0
6	1	41106.6	0.17	9.550556	0
6	1	41103.2	0.16	9.557500	0
6	1	41100.9	0.15	9.563333	0
6	1	41102.0	0.16	9.569722	0
6	1	41095.5	0.17	9.576944	0
6	1	41096.0	0.15	9.583889	0
6	1	41091.6	0.16	9.589167	0
6	1	41098.6	0.18	9.594722	0
6	1	41101.8	0.16	9.600556	0
6	1	41100.3	0.21	9.606111	0
6	1	41102.8	0.19	9.611944	0
6	1	41101.3	0.17	9.617500	0
6	1	41095.4	0.17	9.622500	0
6	1	41093.5	0.15	9.628333	0
6	1	41093.4	0.21	9.642500	0
6	1	41089.1	0.17	9.647778	0
6	1	41081.2	0.16	9.653056	0
6	1	41076.2	0.16	9.658611	0
6	1	41071.4	0.16	9.663889	0
6	1	41068.2	0.16	9.669167	0
6	1	41054.2	0.16	9.674722	0
6	1	41059.8	0.16	9.680833	0
6	1	41062.9	0.16	9.686111	0
6	1	41057.5	0.27	9.691944	0
6	1	41056.6	0.19	9.696667	0
6	1	41058.2	0.18	9.701389	0
6	1	41056.3	0.17	9.705833	0
6	1	41052.3	0.17	9.710556	0
6	1	41051.8	0.16	9.715278	0
6	1	41049.7	0.18	9.720556	0
6	1	41049.1	0.15	9.726944	0

6	1	41048.0	0.17	9.734167	0
6	1	41047.2	0.18	9.738889	0
6	1	41048.6	0.17	9.745833	0
6	1	41048.6	0.18	9.751667	0
6	1	41045.9	0.17	9.756667	0
6	1	41044.9	0.17	9.761944	0
6	1	41043.5	0.18	9.767500	0
6	1	41044.4	0.17	9.773889	0
6	1	41045.1	0.18	9.779444	0
6	1	41048.1	0.17	9.784167	0
6	1	41045.1	0.15	9.790000	0
6	1	41047.6	0.16	9.794167	0
6	1	41041.2	0.18	9.798889	0
6	1	41041.6	0.16	9.804167	0
6	1	41047.6	0.17	9.808889	0
6	1	41048.0	0.16	9.815000	0
6	1	41048.8	0.15	9.819444	0
6	1	41044.8	0.20	9.824167	0
6	1	41050.5	0.16	9.829167	0
6	1	41047.8	0.17	9.834167	0
6	1	41047.9	0.17	9.838889	0
6	1	41047.0	0.18	9.844444	0
6	1	41048.5	0.16	9.849444	0
6	1	41047.7	0.18	9.854444	0
6	1	41048.5	0.18	9.858889	0
6	1	41046.1	0.17	9.865833	0
6	1	41043.2	0.18	9.871667	0
6	1	41039.8	0.18	9.876667	0
6	1	41042.9	0.17	9.883056	0
6	1	41039.2	0.17	9.890833	0
6	1	41040.6	0.17	9.895000	0
6	1	41046.5	0.17	9.901667	0
6	1	41037.9	0.16	9.906667	0
6	1	41036.0	0.16	9.911389	0
6	1	41036.5	0.17	9.916389	0
6	1	41033.3	0.18	9.921944	0
6	1	41033.9	0.16	9.926389	0
6	1	41030.9	0.17	9.931944	0
6	1	41030.0	0.18	9.936389	0
6	1	41025.9	0.19	9.941111	0
6	1	41026.7	0.19	9.946389	0
6	1	41030.3	0.19	9.950833	0
6	1	41020.7	0.17	9.955833	0
6	1	41019.9	0.17	9.960556	0
6	1	41017.4	0.17	9.966111	0
6	1	41014.9	0.17	9.970556	0
6	1	41017.1	0.18	9.975833	0
6	1	41012.8	0.18	9.980556	0
6	1	41011.6	0.18	9.984722	0
6	1	41007.0	0.17	9.988889	0
6	1	41006.4	0.16	9.993056	0
6	1	41009.1	0.22	9.997778	0
6	1	41007.6	0.19	10.004722	0
6	1	41007.6	0.23	10.009167	0
6	1	41005.0	0.18	10.013889	0
6	1	41002.6	0.18	10.021667	0
6	1	41002.8	0.20	10.026389	0
6	1	40997.8	0.18	10.031389	0
6	1	40998.5	0.19	10.041111	0
6	1	41002.9	0.19	10.046944	0
6	1	40999.1	0.21	10.054444	0
6	1	40996.0	0.20	10.059444	0
6	1	40998.4	0.21	10.067222	0
6	1	40996.6	0.17	10.074444	0

6	1	40995.5	0.17	10.079444	0
6	1	41001.1	0.20	10.084167	0
6	1	40998.3	0.20	10.089722	0
6	1	40996.6	0.22	10.096389	0
6	1	40999.4	0.22	10.101389	0
6	1	40991.3	0.20	10.106111	0
6	1	40994.5	0.18	10.111111	0
6	1	40996.5	0.19	10.116389	0
6	1	40999.9	0.20	10.121111	0
6	1	41005.2	0.21	10.125556	0
6	1	40980.6	0.21	10.133056	0
6	1	41023.8	0.31	10.140000	0
6	1	41028.5	0.21	10.147500	0
6	1	41028.9	0.25	10.153333	0
6	1	41052.9	0.24	10.159444	0
6	1	41071.4	0.20	10.165833	0
6	1	41096.1	0.19	10.172222	0
6	1	41114.9	0.20	10.178333	0
6	1	41137.4	0.17	10.185556	0
6	1	41163.3	0.17	10.191389	0
6	1	41196.3	0.18	10.197500	0
6	1	41224.6	0.18	10.203889	0
6	1	41256.0	0.19	10.210833	0
6	1	41286.9	0.18	10.222222	0
6	1	41316.0	0.19	10.230278	0
6	1	41344.2	0.20	10.235000	0
6	1	41369.0	0.21	10.240000	0
6	1	41398.7	0.17	10.245556	0
6	1	41419.2	0.20	10.251111	0
6	1	41437.6	0.21	10.259167	0
6	1	41448.6	0.21	10.264722	0
6	1	41455.0	0.20	10.273056	0
6	1	41462.2	0.20	10.280000	0
6	1	41468.2	0.21	10.285278	0
6	1	41462.0	0.23	10.291111	0
6	1	41462.7	0.22	10.295556	0
6	1	41458.1	0.23	10.300278	0
6	1	41452.4	0.24	10.304722	0
6	1	41447.4	0.22	10.310556	0
6	1	41441.1	0.24	10.316944	0
6	1	41441.8	0.19	10.324167	0
6	1	41433.7	0.18	10.329722	0
6	1	41430.5	0.18	10.334444	0
6	1	41424.2	0.24	10.339167	0
6	1	41417.5	0.26	10.343611	0
6	1	41413.5	0.19	10.347778	0
6	1	41407.5	0.19	10.352222	0
6	1	41405.2	0.20	10.356667	0
6	1	41397.0	0.20	10.362222	0
6	1	41394.8	0.27	10.367500	0
6	1	41391.2	0.30	10.372222	0
6	1	41386.6	0.17	10.376389	0
6	1	41380.3	0.19	10.381111	0
6	1	41375.0	0.19	10.386667	0
6	1	41374.6	0.18	10.391667	0
6	1	41383.9	0.26	10.396389	0
6	1	41365.5	0.19	10.401667	0
6	1	41373.4	0.19	10.407778	0
6	1	41366.3	0.18	10.421667	0
6	1	41361.5	0.20	10.427500	0
6	1	41359.6	0.19	10.434722	0
6	1	41356.4	0.19	10.440278	0
6	1	41354.6	0.18	10.446111	0
6	1	41351.6	0.18	10.456944	0

6	1	41347.9	0.18	10.462500	0
6	1	41343.6	0.18	10.467778	0
6	1	41337.8	0.19	10.472500	0
6	1	41334.2	0.19	10.478333	0
6	1	41329.5	0.18	10.483611	0
6	1	41327.5	0.18	10.489167	0
6	1	41353.6	0.24	10.493611	0
6	1	41320.4	0.21	10.498889	0
6	1	41317.2	0.19	10.505556	0
6	1	41311.2	0.18	10.513056	0
6	1	41305.6	0.18	10.523889	0
6	1	41306.8	0.21	10.529444	0
6	1	41299.3	0.20	10.534722	0
6	1	41296.4	0.18	10.541389	0
6	1	41295.9	0.18	10.546944	0
6	1	41290.1	0.21	10.552778	0
6	1	41287.9	0.21	10.557778	0
6	1	41288.7	0.18	10.563056	0
6	1	41288.4	0.19	10.567778	0
6	1	41287.7	0.17	10.572778	0
6	1	41287.0	0.19	10.577500	0
6	1	41286.6	0.19	10.582222	0
6	1	41280.7	0.18	10.586667	0
6	1	41280.2	0.17	10.591667	0
6	1	41280.6	0.18	10.596667	0
6	1	41285.0	0.18	10.601667	0
6	1	41278.0	0.18	10.606389	0
6	1	41283.9	0.18	10.611389	0
6	1	41282.3	0.18	10.615556	0
6	1	41281.9	0.20	10.621111	0
6	1	41282.5	0.22	10.625833	0
6	1	41277.4	0.21	10.630556	0
6	1	41277.6	0.22	10.635278	0
6	1	41275.1	0.21	10.640556	0
6	1	41270.1	0.19	10.645833	0
6	1	41275.4	0.21	10.650278	0
6	1	41252.3	0.19	10.655278	0
6	1	41261.9	0.18	10.661111	0
6	1	41264.4	0.23	10.665000	0
6	1	41259.4	0.17	10.670556	0
6	1	41254.2	0.18	10.675833	0
6	1	41247.6	0.21	10.680000	0
6	1	41243.8	0.19	10.684722	0
6	1	41240.0	0.20	10.690000	0
6	1	41237.8	0.22	10.693889	0
6	1	41229.5	0.21	10.698611	0
6	1	41267.4	0.29	10.704167	0
6	1	41238.1	0.19	10.711389	0
6	1	41241.2	0.17	10.716111	0
6	1	41217.8	0.18	10.720556	0
6	1	41221.1	0.19	10.724444	0
6	1	41223.5	0.18	10.728889	0
6	1	41220.1	0.19	10.733889	0
6	1	41255.6	0.20	10.737778	0
6	1	41232.6	0.18	10.742222	0
6	1	41235.1	0.20	10.747222	0
6	1	41242.7	0.18	10.751111	0
6	1	41241.8	0.21	10.756389	0
6	1	41247.0	0.21	10.760833	0
6	1	41253.4	0.20	10.765556	0
6	1	41255.0	0.19	10.770833	0
6	1	41257.8	0.18	10.776111	0
6	1	41259.1	0.21	10.781667	0
6	1	41246.8	0.18	10.785556	0

6	1	41251.8	0.19	10.789722	0
6	1	41255.2	0.19	10.794444	0
6	1	41254.8	0.17	10.798611	0
6	1	41254.0	0.22	10.803056	0
6	1	41256.4	0.18	10.807222	0
6	1	41258.0	0.30	10.811111	0
6	1	41261.7	0.19	10.815833	0
6	1	41258.6	0.19	10.820000	0
6	1	41249.7	0.20	10.824722	0
6	1	41252.5	0.21	10.829167	0
6	1	41251.0	0.20	10.833889	0
6	1	41252.9	0.17	10.838333	0
6	1	41255.9	0.18	10.842778	0
6	1	41248.8	0.24	10.846944	0
6	1	41246.8	0.19	10.851667	0
6	1	41243.0	0.23	10.857222	0
6	1	41242.5	0.17	10.862222	0
6	1	41237.0	0.19	10.867500	0
6	1	41237.7	0.21	10.873056	0
6	1	41235.4	0.24	10.878611	0
6	1	41228.2	0.18	10.883611	0
6	1	41225.3	0.18	10.891944	0
6	1	41220.8	0.17	10.897778	0
6	1	41209.0	0.18	10.902500	0
6	1	41191.7	0.21	10.910556	0
6	1	41184.1	0.19	10.916389	0
6	1	41206.1	0.17	10.922222	0
6	1	41260.0	0.19	10.926389	0
6	1	41298.2	0.20	10.931667	0
6	1	41409.9	0.21	10.936944	0
7	1	40847.7	0.17	12.127500	0
7	1	40856.9	0.20	12.147500	0
7	1	40895.3	0.21	12.158056	0
7	1	40908.4	0.23	12.166389	0
7	1	40916.3	0.22	12.174167	0
7	1	40903.2	0.19	12.180000	0
7	1	40916.8	0.21	12.186667	0
7	1	40915.7	0.17	12.192778	0
7	1	40898.0	0.19	12.199167	0
7	1	40832.4	0.22	12.207222	0
7	1	40914.7	0.19	12.214444	0
7	1	40975.1	0.17	12.222778	0
7	1	40974.4	0.18	12.229722	0
7	1	40982.1	0.27	12.236389	0
7	1	40990.2	0.25	12.242222	0
7	1	41000.4	0.18	12.247222	0
7	1	41011.9	0.17	12.255278	0
7	1	41019.8	0.17	12.261389	0
7	1	41025.4	0.18	12.268889	0
7	1	41033.5	0.18	12.275556	0
7	1	41042.3	0.18	12.281111	0
7	1	41053.0	0.18	12.288611	0
7	1	41063.3	0.17	12.295278	0
7	1	41068.4	0.19	12.302500	0
7	1	41070.8	0.21	12.310278	0
7	1	41062.1	0.20	12.315278	0
7	1	41066.2	0.17	12.320833	0
7	1	41066.6	0.20	12.325833	0
7	1	41067.1	0.24	12.330000	0
7	1	41061.5	0.19	12.334722	0
7	1	41059.2	0.18	12.340000	0
7	1	41062.6	0.18	12.345000	0
7	1	41059.3	0.18	12.351944	0
7	1	41043.5	0.16	12.357222	0

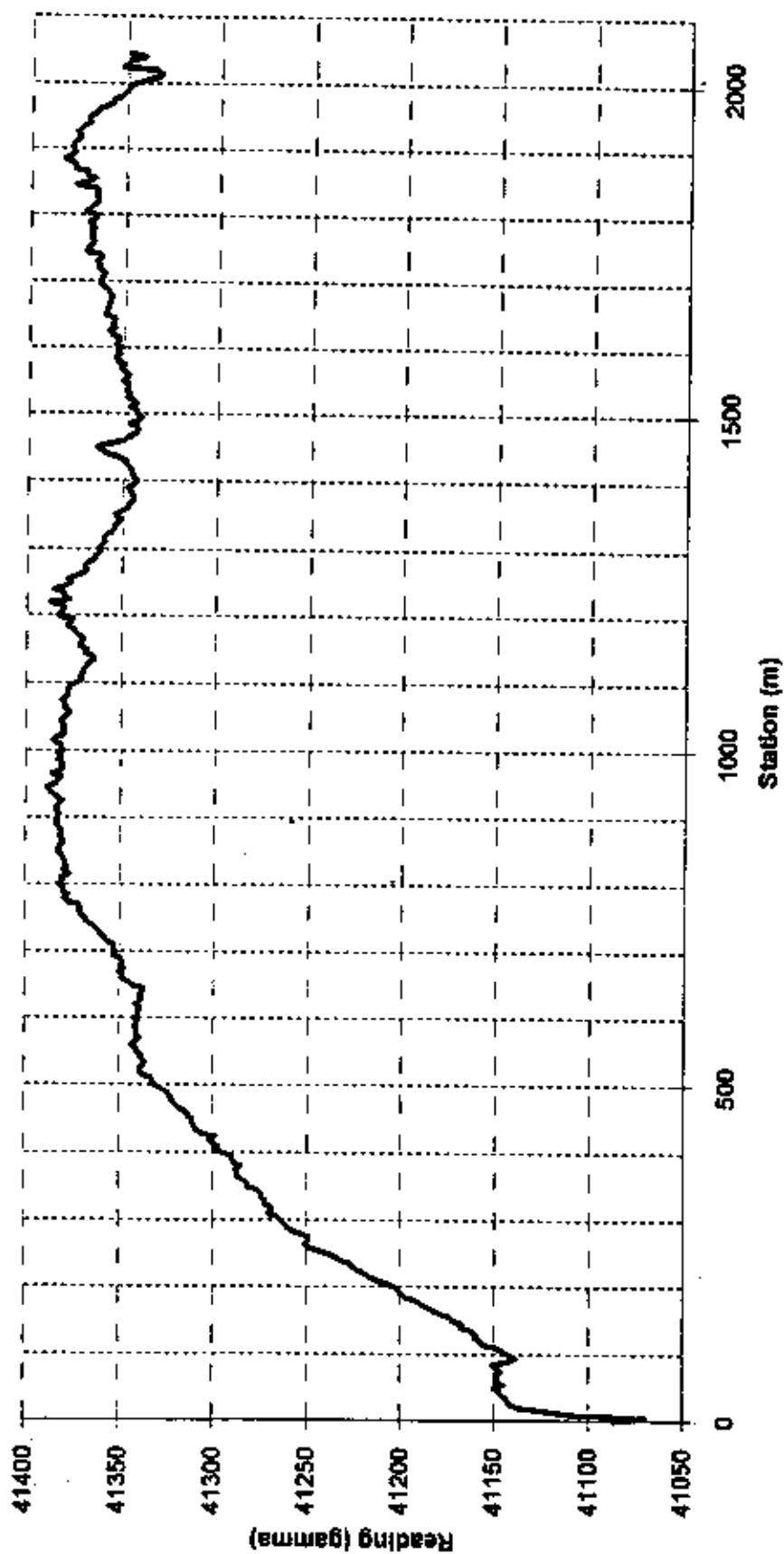
7	1	41035.4	0.31	12.363333	0
7	1	41028.8	0.18	12.368611	0
7	1	41020.2	0.17	12.375278	0
7	1	41021.9	0.18	12.380278	0
7	1	41013.8	0.17	12.387778	0
7	1	41011.1	0.17	12.393889	0
7	1	41007.8	0.17	12.399444	0
7	1	41004.0	0.17	12.405000	0
7	1	41006.6	0.19	12.410833	0
7	1	41004.3	0.24	12.419444	0
7	1	41004.7	0.19	12.424722	0
7	1	41005.5	0.19	12.431389	0
7	1	41007.5	0.19	12.439444	0
7	1	41016.0	0.17	12.445833	0
7	1	41014.3	0.18	12.450556	0
7	1	41006.2	0.17	12.459167	0
7	1	41009.1	0.18	12.465556	0
7	1	41009.7	0.16	12.470556	0
7	1	41017.5	0.17	12.475833	0
7	1	41018.1	0.18	12.481667	0
7	1	41018.3	0.18	12.488056	0
7	1	41018.4	0.21	12.493889	0
7	1	41028.0	0.19	12.500000	0
7	1	41032.3	0.18	12.507778	0
7	1	41039.7	0.19	12.513056	0
7	1	41044.6	0.17	12.519722	0
7	1	41048.6	0.19	12.530278	0
7	1	41056.1	0.23	12.535278	0
7	1	41059.9	0.20	12.539722	0
7	1	41061.7	0.18	12.546111	0
7	1	41067.2	0.21	12.550833	0
7	1	41069.8	0.21	12.555556	0
7	1	41071.1	0.19	12.560000	0
7	1	41076.8	0.17	12.563611	0
7	1	41076.3	0.17	12.567500	0
7	1	41095.2	0.17	12.574167	0
7	1	41093.9	0.20	12.578611	0
7	1	41091.1	0.19	12.586944	0
7	1	41097.1	0.19	12.594167	0
7	1	41098.6	0.18	12.599722	0
7	1	41098.7	0.17	12.604444	0
7	1	41102.1	0.19	12.609444	0
7	1	41105.0	0.43	12.613889	0
7	1	41101.5	0.18	12.619444	0
7	1	41098.8	0.22	12.624722	0
7	1	41108.8	0.21	12.630278	0
7	1	41104.7	0.23	12.636389	0
7	1	41097.8	0.19	12.641389	0
7	1	41093.7	0.19	12.645556	0
7	1	41092.7	0.18	12.650556	0
7	1	41094.4	0.19	12.655556	0
7	1	41093.6	0.19	12.661111	0
7	1	41091.5	0.21	12.666944	0
7	1	41088.7	0.20	12.671944	0
7	1	41085.8	0.20	12.678889	0
7	1	41087.0	0.20	12.684167	0
7	1	41083.0	0.19	12.689444	0
7	1	41078.0	0.29	12.695278	0
7	1	41080.9	0.18	12.701111	0
7	1	41078.8	0.19	12.706389	0
7	1	41069.5	0.21	12.712222	0
7	1	41066.4	0.22	12.718056	0
7	1	41063.9	0.19	12.723611	0
7	1	41063.3	0.20	12.728611	0

7	1	41066.2	0.17	12.733611	0
7	1	41062.3	0.17	12.740556	0
7	1	41063.9	0.18	12.745000	0
7	1	41060.5	0.17	12.749444	0
7	1	41066.3	0.18	12.753611	0
7	1	41064.4	0.19	12.758333	0
7	1	41063.9	0.17	12.763333	0
7	1	41068.9	0.18	12.769167	0
7	1	41070.8	0.17	12.774167	0
7	1	41074.3	0.19	12.778611	0
7	1	41079.0	0.18	12.783333	0
7	1	41088.0	0.18	12.788889	0
7	1	41089.6	0.18	12.793056	0
7	1	41095.5	0.16	12.797500	0
7	1	41100.4	0.17	12.801667	0
7	1	41105.5	0.17	12.806667	0
7	1	41115.0	0.19	12.812222	0
7	1	41117.5	0.17	12.816389	0
7	1	41120.1	0.17	12.820833	0
7	1	41120.7	0.17	12.825833	0
7	1	41122.5	0.18	12.830833	0
7	1	41126.7	0.18	12.837222	0
7	1	41132.6	0.21	12.841944	0
7	1	41144.5	0.20	12.847778	0
7	1	41151.6	0.19	12.852778	0
7	1	41141.5	0.20	12.858056	0
7	1	41163.7	0.18	12.864722	0
7	1	41158.0	0.18	12.878333	0

?

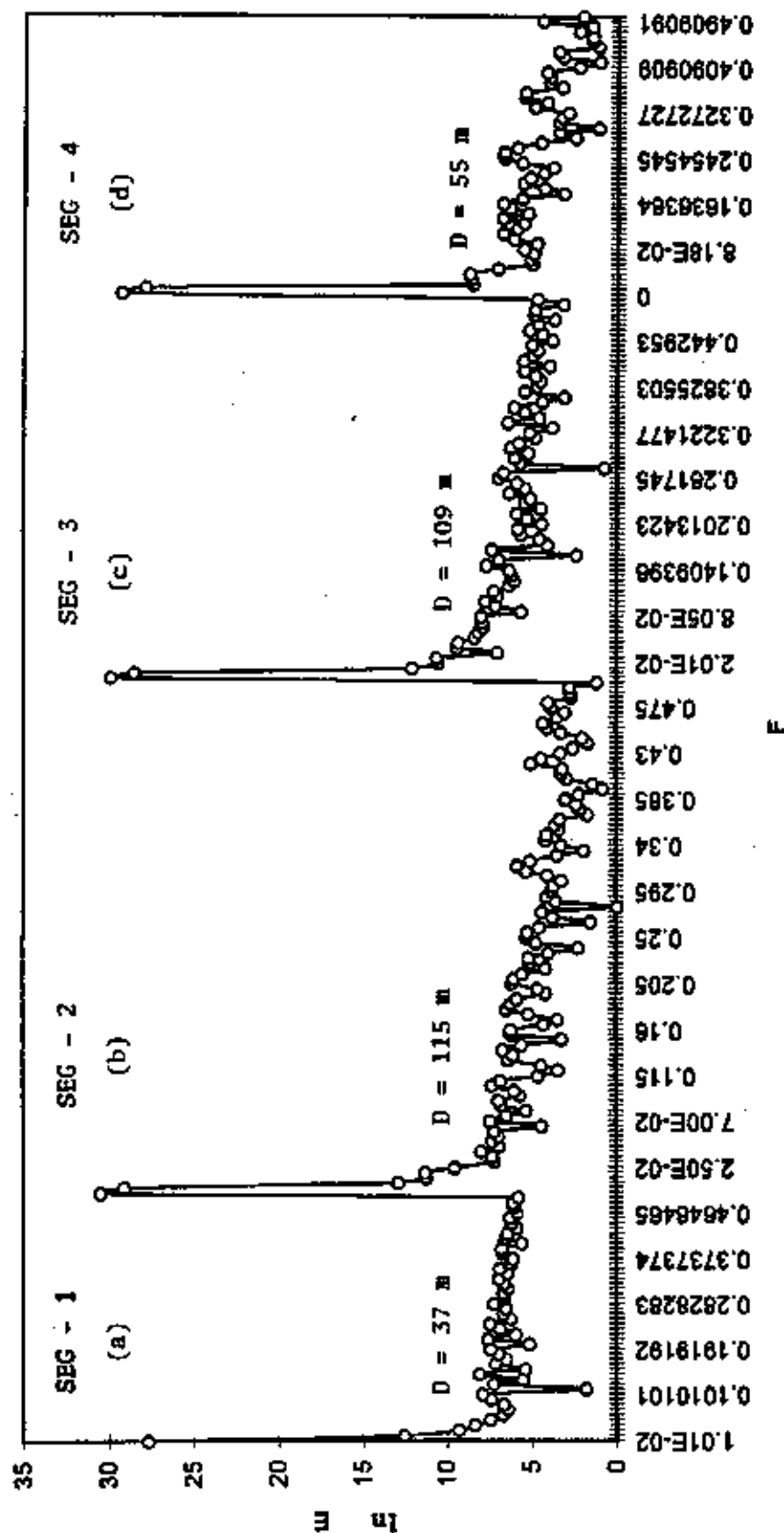
APPENDIX 5 C

**The energy spectrum decay curve (ln energy Vs.
frequency) of total intensity magnetic profiles**



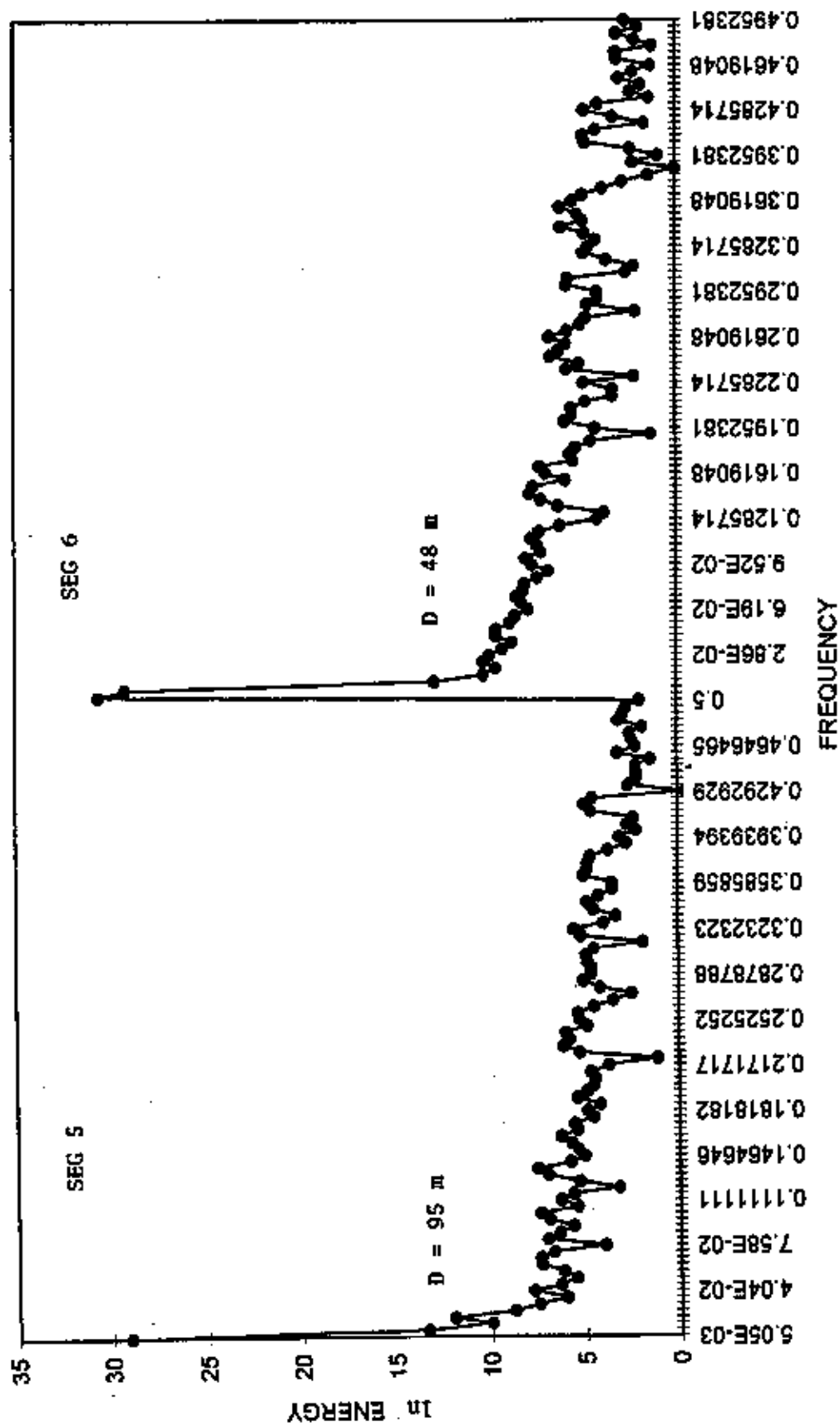
The total intensity magnetic profile (Readings in gamma Vs. station) measured
at the line of M3 with station spacing of 5m.

LINE (3) NSM

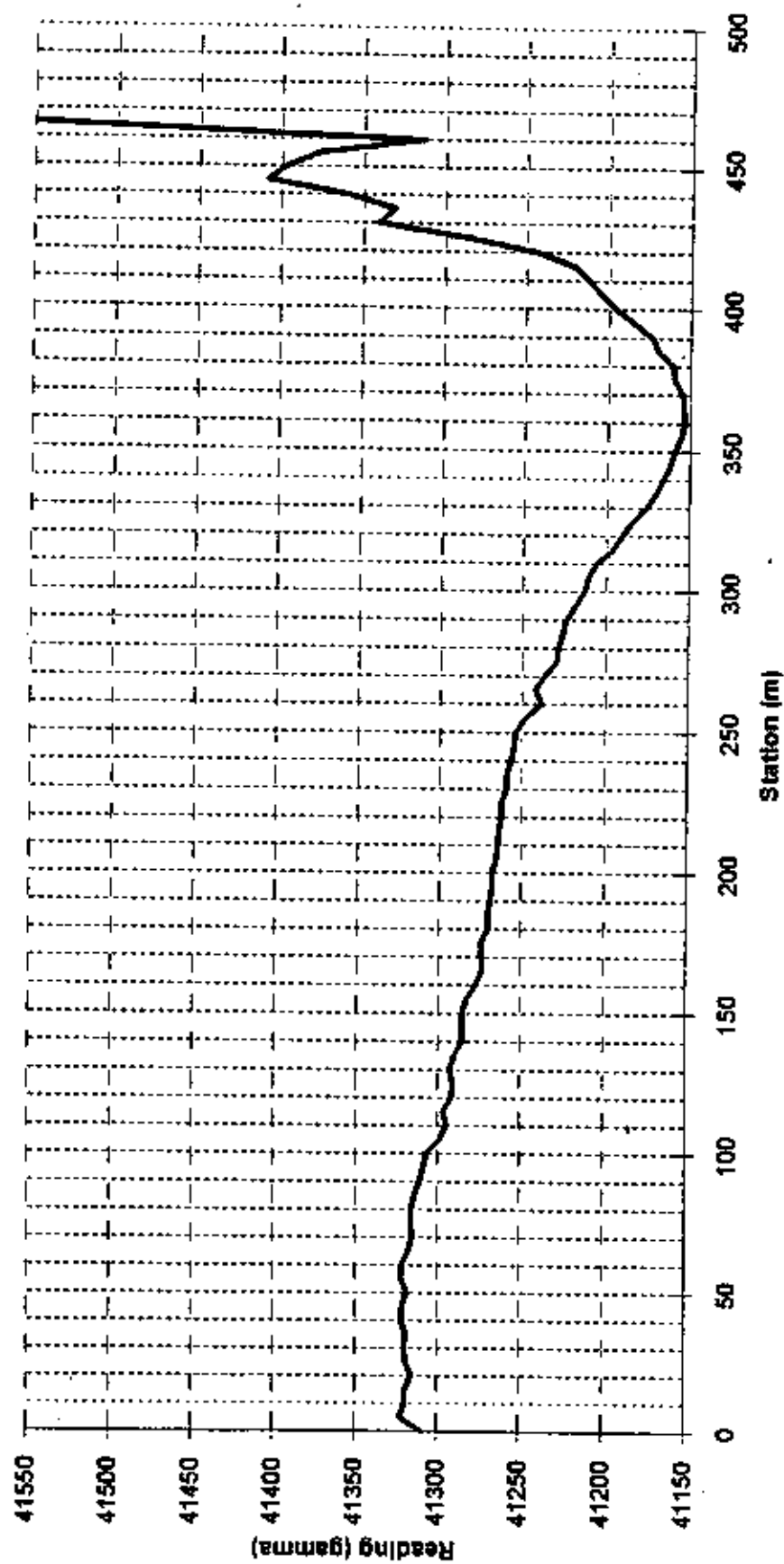


The energy spectrum decay curve (in energy Vs. frequency) of 4 segments of the total intensity magnetic profile M3. The depth to the basement (D) at the center of each segment is calculated and fixed at the linear part of the curve.

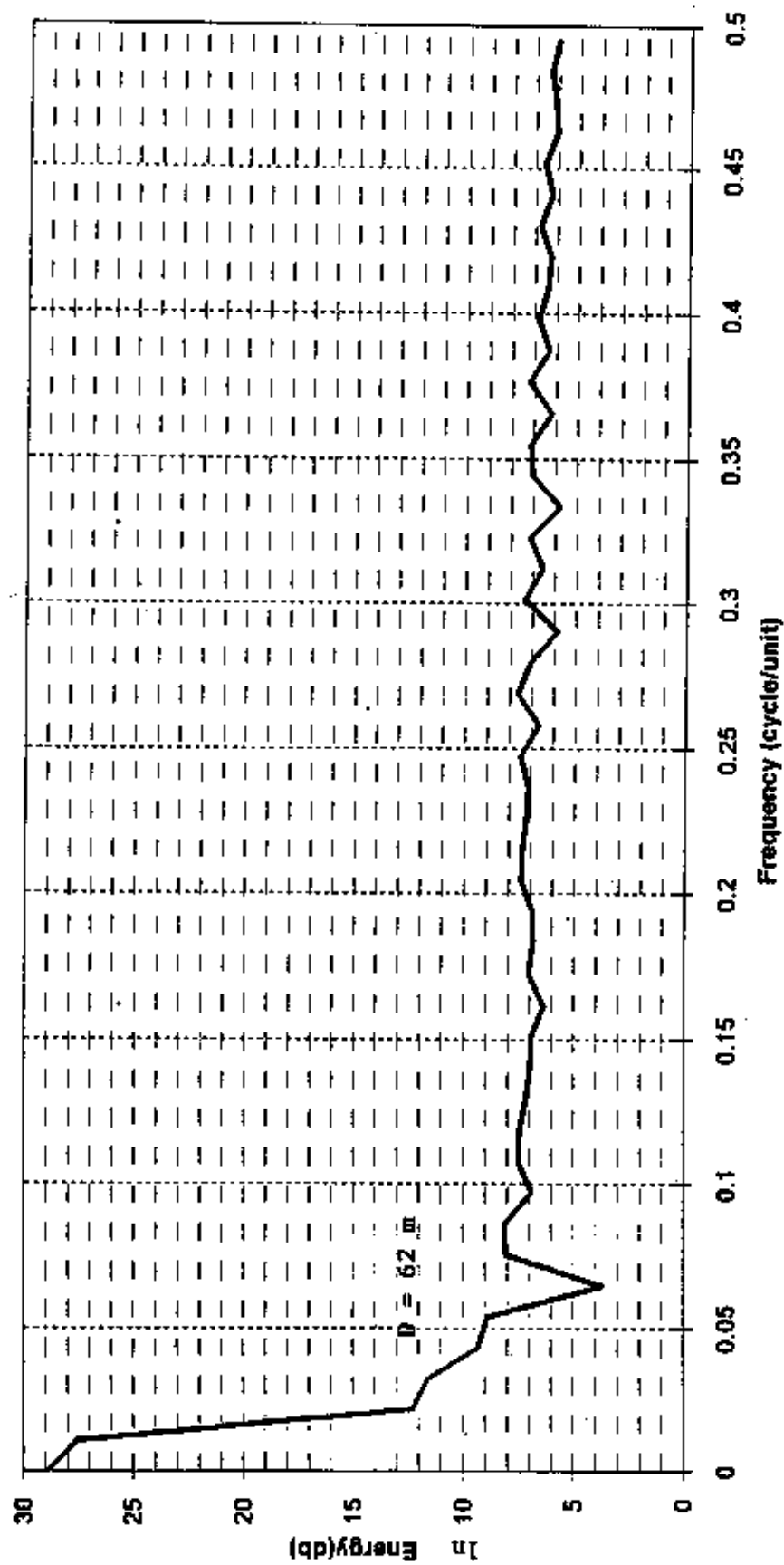
LINE (3) NOT SMOOTHED



The energy spectrum decay curve (in energy vs. frequency) of 2 segments of the total intensity magnetic profile M3.

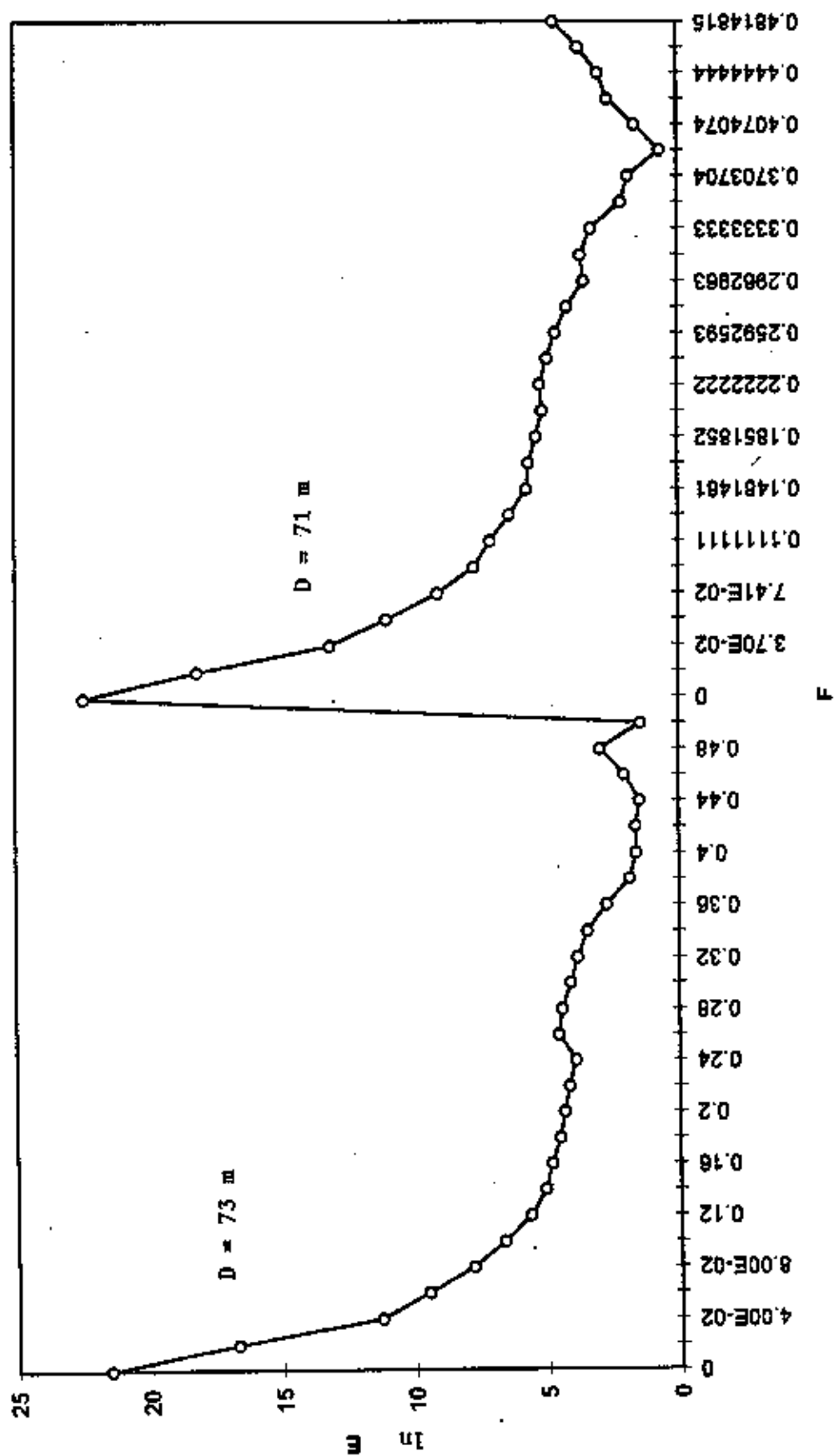


The total intensity magnetic profile (Readings in gamma Vs. station) measured at the line of M5 with station spacing of 5m.

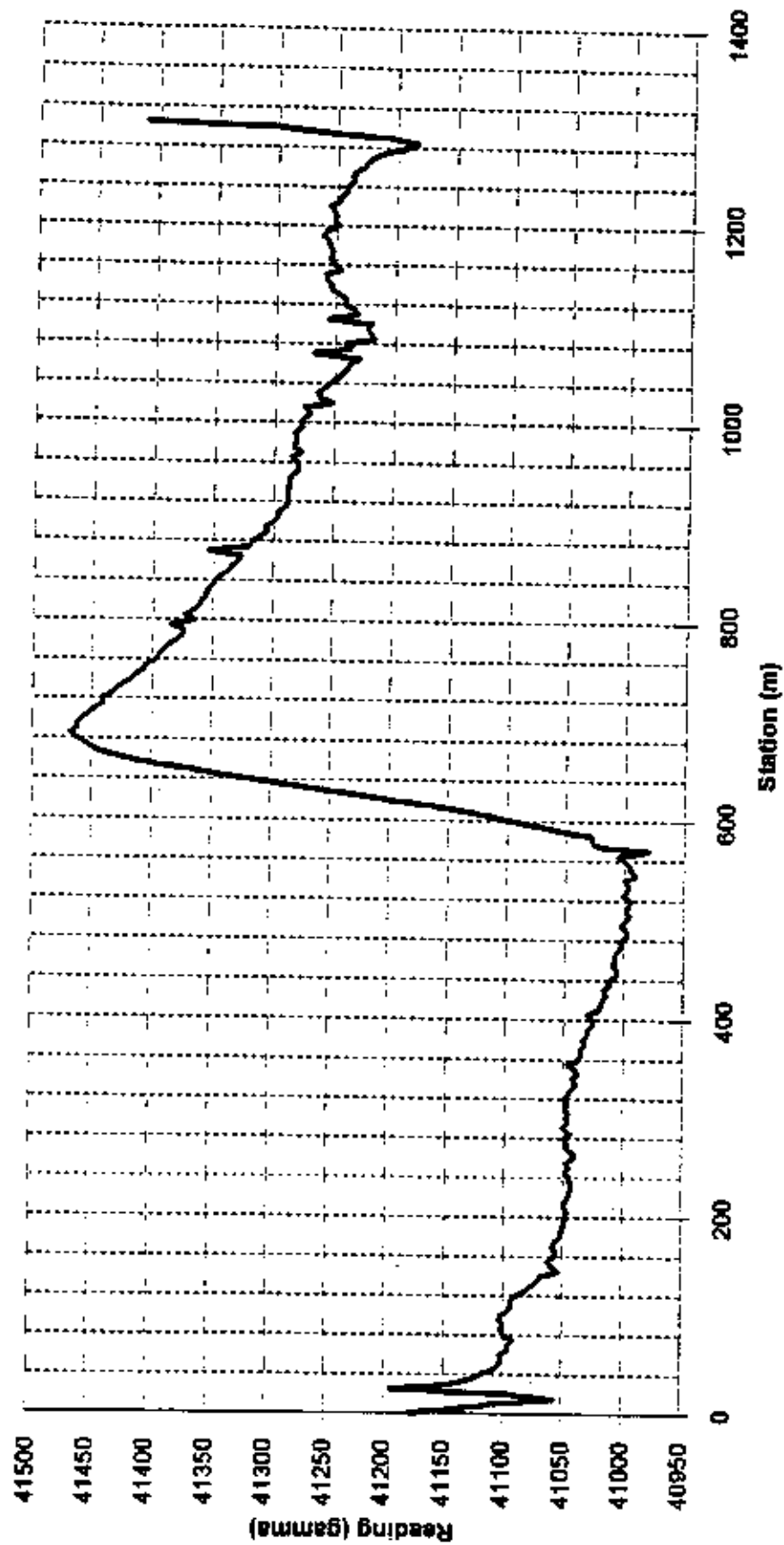


The energy spectrum decay curve (in energy Vs. frequency) of the total intensity magnetic profile M5. The depth to the basement (D) at the center of each segment is calculated and fixed at the linear part of the curve.

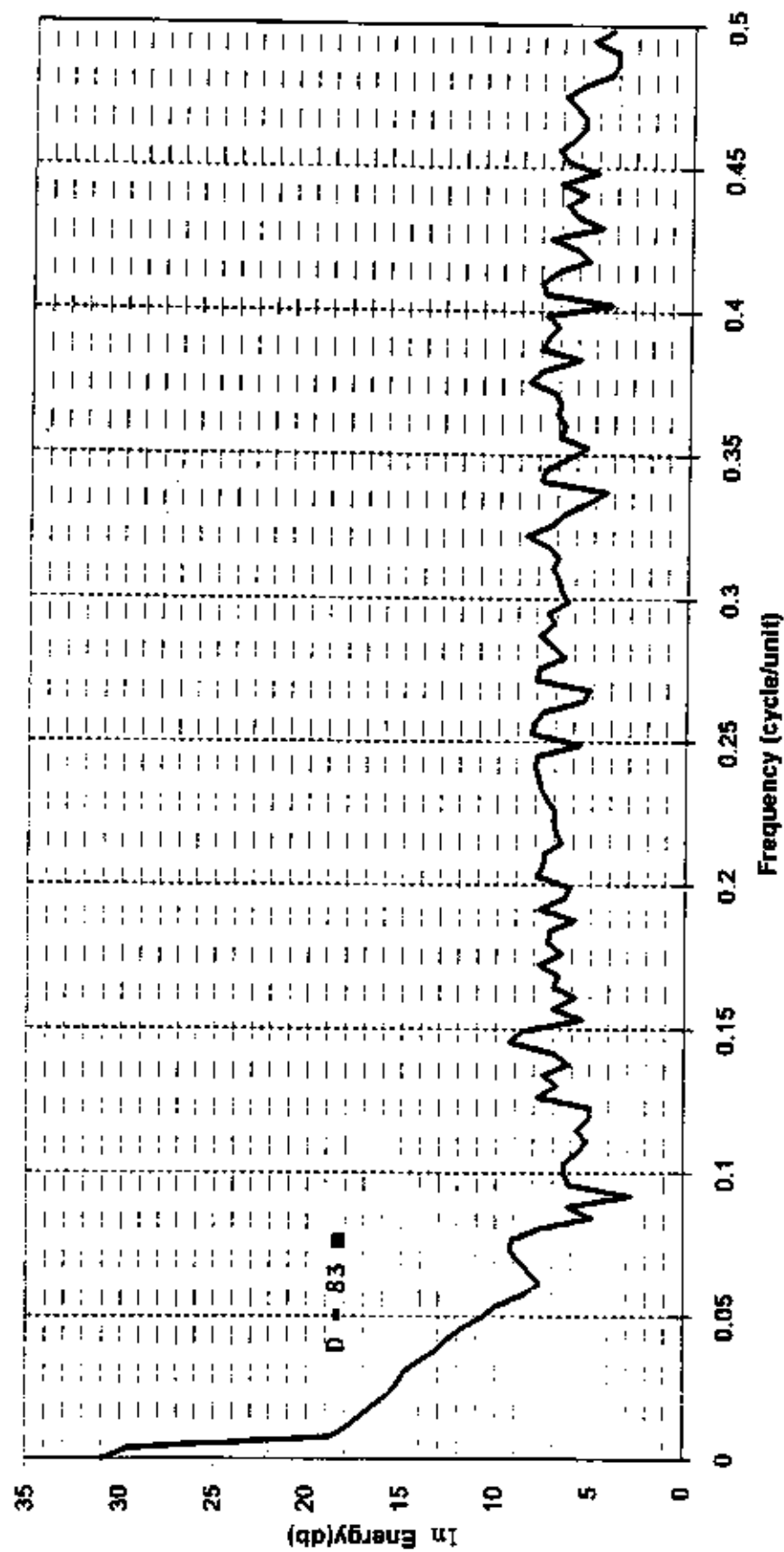
LINE (5) SM



The energy spectrum decay curve (in energy Vs. frequency) of 2 segments of the total intensity magnetic profile M5.

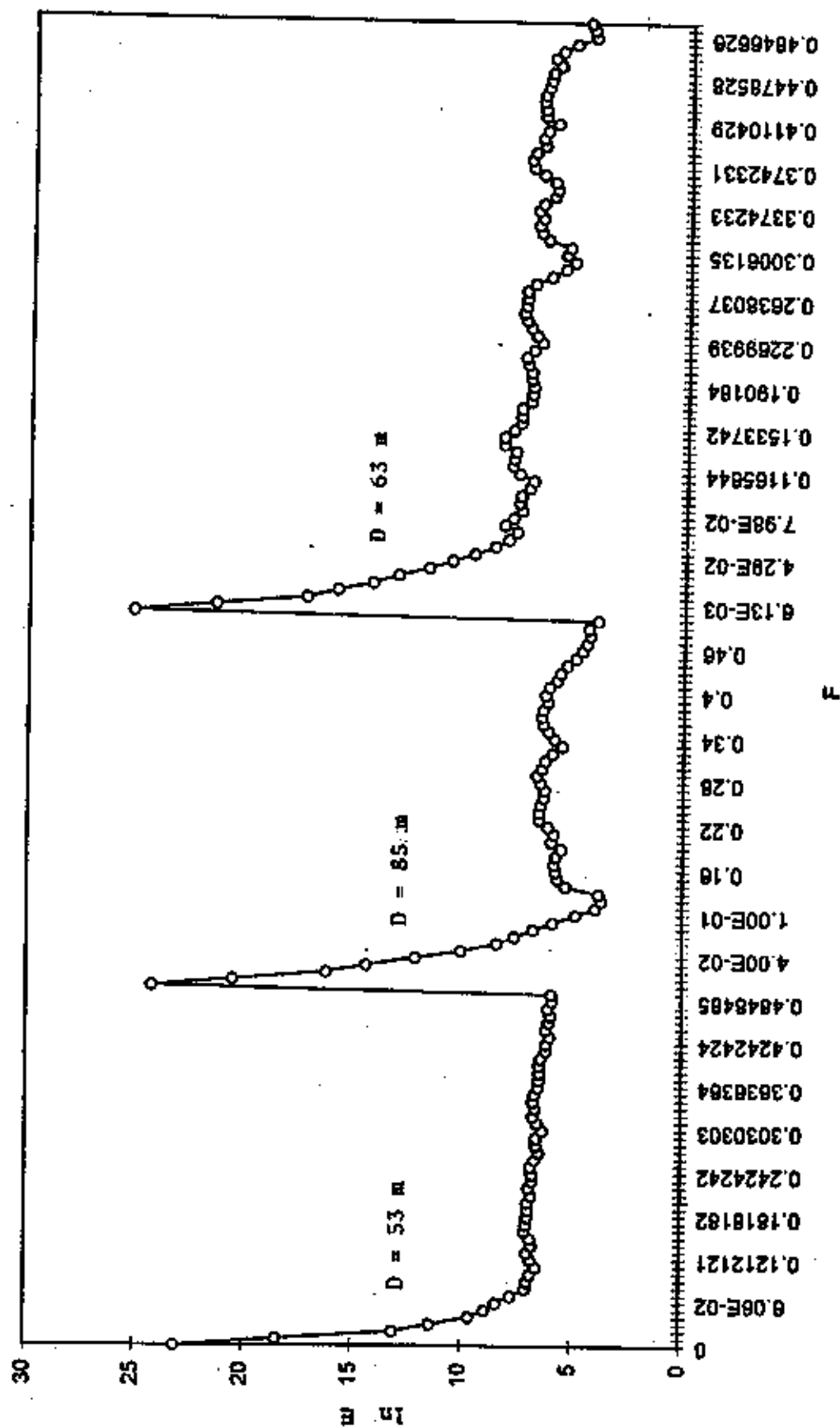


The total intensity magnetic profile (Readings in gamma vs. station) measured at the line of M6 with station spacing of 5m.

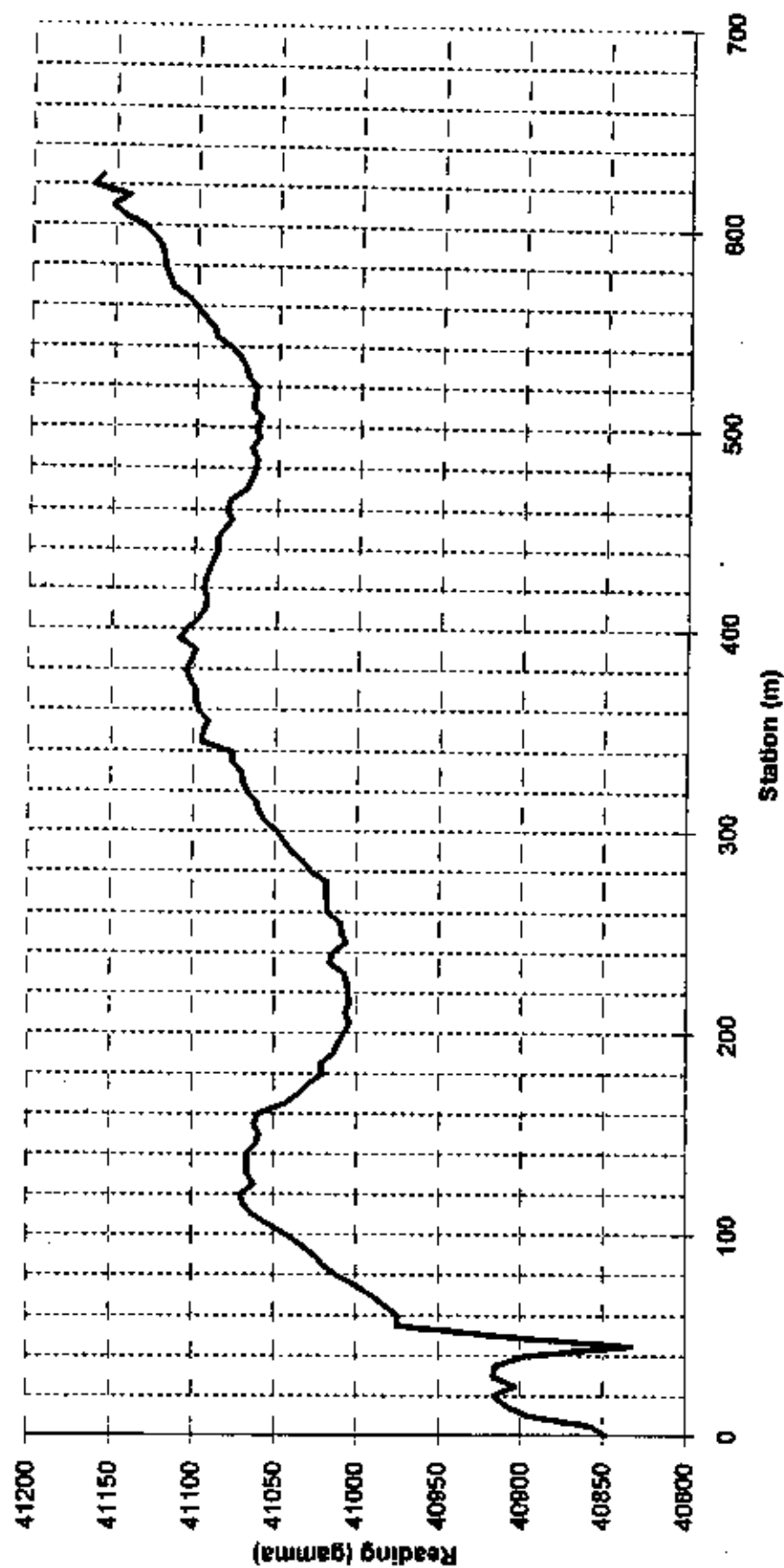


The energy spectrum decay curve (ln energy Vs. frequency) of the total intensity magnetic profile M6. The depth to the basement (D) at the center of each segment is calculated and fixed at the linear part of the curve.

LINE (6) SMO

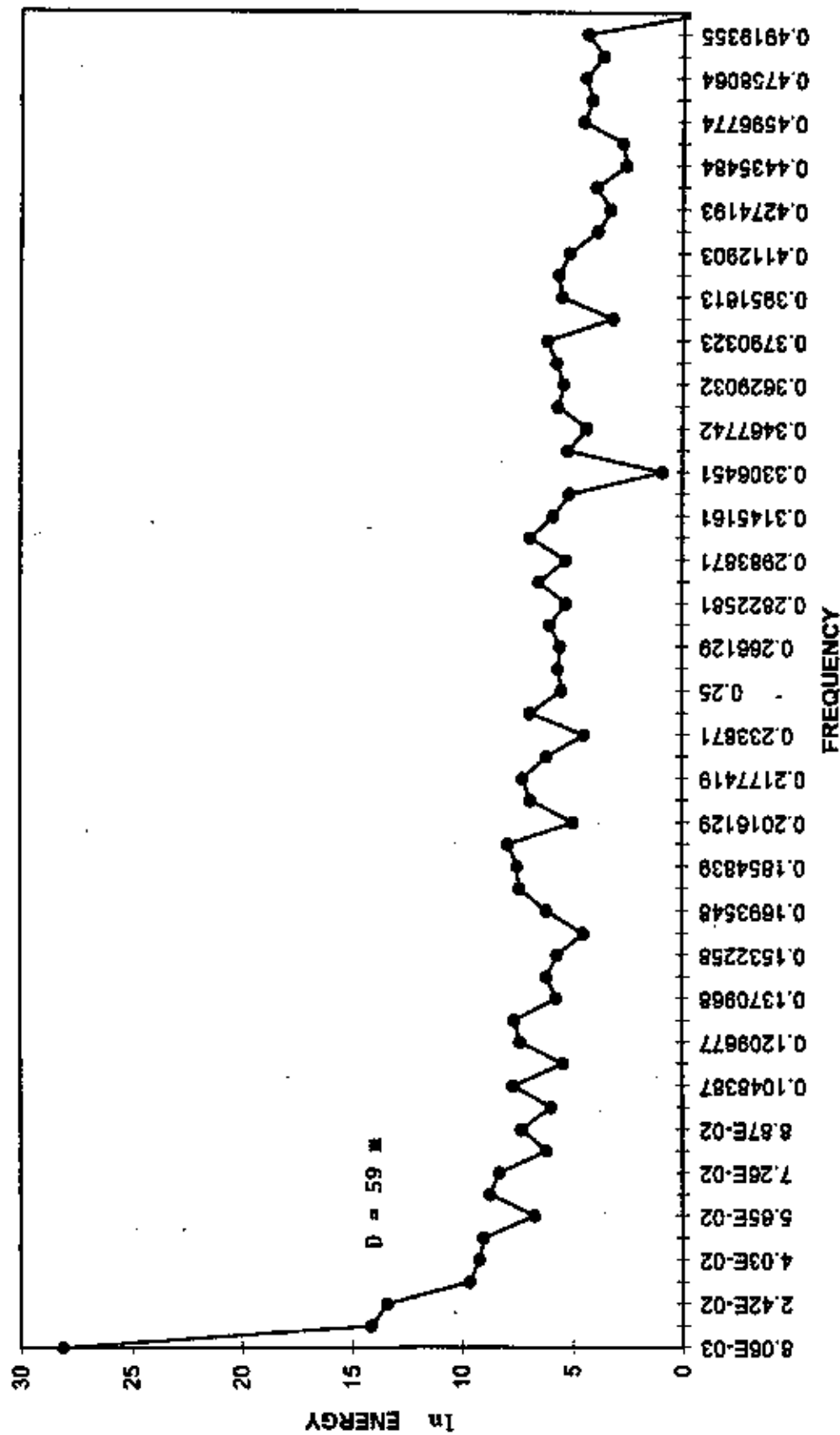


The energy spectrum decay curve (in energy Vs. frequency) of 3 segments of the total intensity magnetic profile M6.



The total intensity magnetic profile (Readings in gamma Vs. station) measured at the line of M7 with station spacing of 5m.

LINE (7) NSM



The energy spectrum decay curve (in energy Vs. frequency) of 1 segments of the total intensity magnetic profile M7. The depth to the basement (D) at the center of each segment is calculated and fixed at the linear part of the curve.

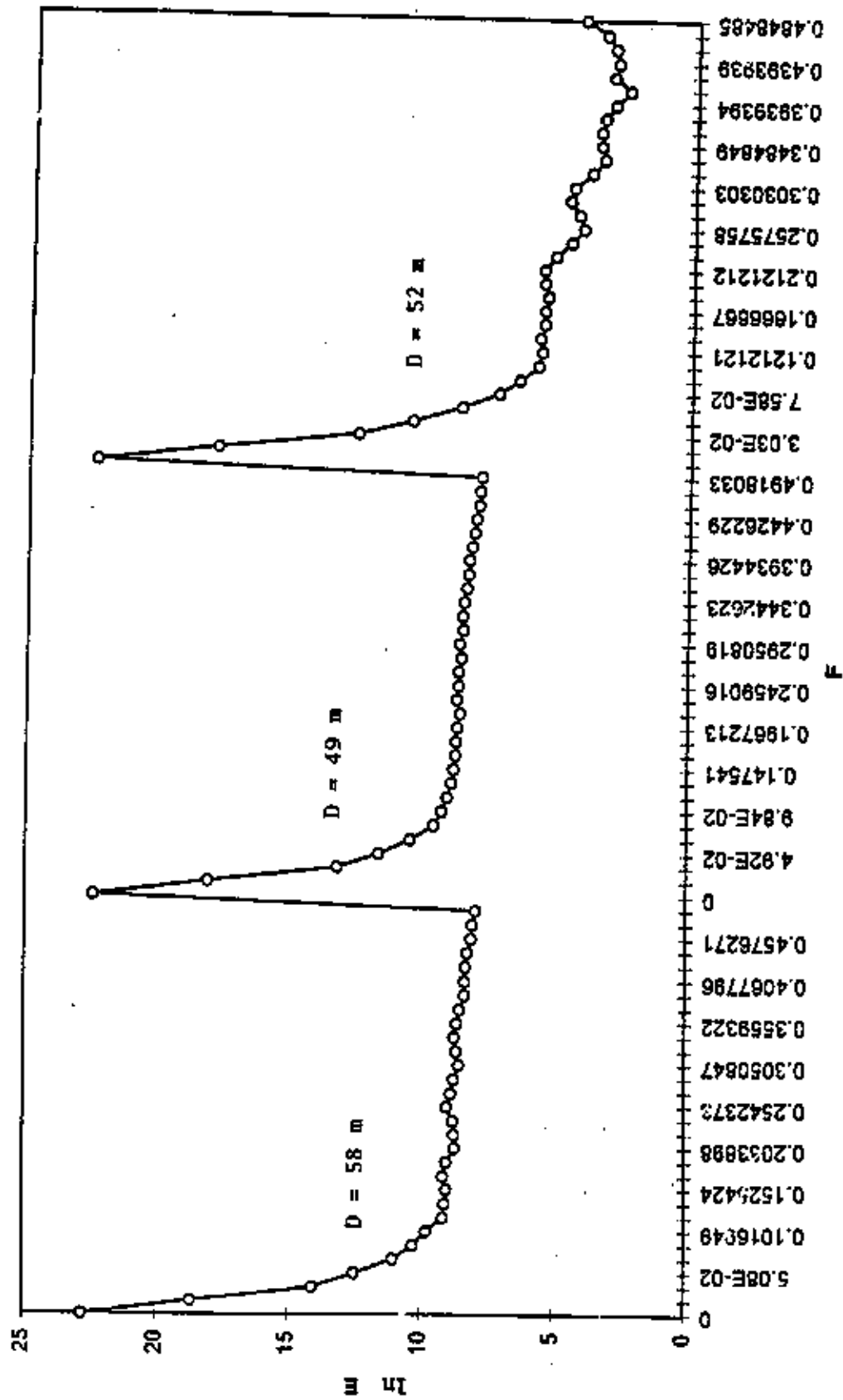


Figure 3 The energy spectrum decay curve (in energy Vs. frequency) of 3 segments of the total intensity magnetic profile M7.



المملكة العربية السعودية
مدينة الملك عبدالعزيز للعلوم والتقنية
الإدارة العامة لبرامج المنح

أت-١٥-٥

(التقرير النهائي)

دراسة الخواص الجيوفيزيائية والهيدروجيولوجية لشمال غرب المدينة المنورة (وادي ملل)

د. عمر بن عساف الحربي
د. عبدالرحمن بن إبراهيم العبدالعالي
د. عبدالله بن محمد العمري
د. عبدالعزيز بن سليمان الطرباق
د. كامل بن محمد شيخو

مدينة الملك عبدالعزيز للعلوم والتقنية